



Terms and Conditions of Use of Digitised Theses from Trinity College Library Dublin

Copyright statement

All material supplied by Trinity College Library is protected by copyright (under the Copyright and Related Rights Act, 2000 as amended) and other relevant Intellectual Property Rights. By accessing and using a Digitised Thesis from Trinity College Library you acknowledge that all Intellectual Property Rights in any Works supplied are the sole and exclusive property of the copyright and/or other IPR holder. Specific copyright holders may not be explicitly identified. Use of materials from other sources within a thesis should not be construed as a claim over them.

A non-exclusive, non-transferable licence is hereby granted to those using or reproducing, in whole or in part, the material for valid purposes, providing the copyright owners are acknowledged using the normal conventions. Where specific permission to use material is required, this is identified and such permission must be sought from the copyright holder or agency cited.

Liability statement

By using a Digitised Thesis, I accept that Trinity College Dublin bears no legal responsibility for the accuracy, legality or comprehensiveness of materials contained within the thesis, and that Trinity College Dublin accepts no liability for indirect, consequential, or incidental, damages or losses arising from use of the thesis for whatever reason. Information located in a thesis may be subject to specific use constraints, details of which may not be explicitly described. It is the responsibility of potential and actual users to be aware of such constraints and to abide by them. By making use of material from a digitised thesis, you accept these copyright and disclaimer provisions. Where it is brought to the attention of Trinity College Library that there may be a breach of copyright or other restraint, it is the policy to withdraw or take down access to a thesis while the issue is being resolved.

Access Agreement

By using a Digitised Thesis from Trinity College Library you are bound by the following Terms & Conditions. Please read them carefully.

I have read and I understand the following statement: All material supplied via a Digitised Thesis from Trinity College Library is protected by copyright and other intellectual property rights, and duplication or sale of all or part of any of a thesis is not permitted, except that material may be duplicated by you for your research use or for educational purposes in electronic or print form providing the copyright owners are acknowledged using the normal conventions. You must obtain permission for any other use. Electronic or print copies may not be offered, whether for sale or otherwise to anyone. This copy has been supplied on the understanding that it is copyright material and that no quotation from the thesis may be published without proper acknowledgement.

The Rational Design and Synthesis of Novel α_2 Adrenoceptor Antagonists as Potential Antidepressants



**A thesis presented to Trinity College Dublin
for the degree of Doctor of Philosophy**

by

Daniel Hillebrand O' Donovan, B. A. (Mod.)

Under the supervision of Prof. Isabel Rozas

September 2011

Trinity College Dublin

Declaration

This work comprises a doctoral thesis submitted for the consideration of Trinity College Dublin.

I declare that this thesis has not been submitted as an exercise for a degree at this or any other university and it is entirely my own work, with due acknowledgement and reference given to the work of others, where appropriate.

I agree to deposit this thesis in the University's open access institutional repository or allow the library to do so on my behalf, subject to Irish Copyright Legislation and Trinity College Library conditions of use and acknowledgement.

Thesis 9667

Acknowledgements

First and foremost, I offer my sincere thanks to my supervisor Prof. Isabel Rozas, whose support and encouragement has always been a source of solace and inspiration. Thank you for having faith in me, and for being a mentor and a friend.

I offer my thanks too to my fellow researchers, especially the other members of my research group. There have been many times during the past few years when I needed your help and your kindness, and you have always been there for me. I will sorely miss writing reaction mechanisms on whatever surface we could find, and our friendship both inside and outside of the laboratory.

To all the other research groups I am sincerely thankful; especially to the laboratories of Prof. Thorri Gunnlaugsson and Prof. Stephen J. Connon, who have always been willing to donate their material, expertise and equipment in times of need. Very special thanks are due to Cormac Quigley for his assistance and advice in performing several experiments in the field of organocatalysis; I also thank Sean Tallon and Oliver Gleeson for generously donating their catalysts to the project.

To all the other academics, especially Dr. John O' Brien and Dr. Manuel Ruether for their help with all the NMR work, Dr. Tom McCabe for his help with X-ray crystallography experiments, Dr. Mike Southern, Dr. Stephen Connon and Dr. Eoin Scanlan for advising me in organic synthesis, Dr. J. Bernard Jean-Denis and Dr. Martin Feeney for their help with mass spectrometry, Prof. David H. Grayson for his mentorship, and everyone who has helped me over the past few years, I offer my gratitude.

I also thank the Cocker laboratory and all of the staff for their help. To our pharmacological colleagues in Spain; particularly Prof. Koldo Callado and Carolina Muguruza Millan, I am also very thankful. My sincere gratitude goes out to the people at IRCSET who have generously supported my research career. To my friend Patrick Keating and all of the other people who I am proud to call my friends, I offer my thanks.

To the support of my family I am also forever indebted. Finally I am grateful to Aisling, who has always been there when I needed her kindness and support.

-Daniel Hillebrand O' Donovan

Summary

Depression is one of the leading causes of illness worldwide and has been closely linked to low concentrations of monoaminergic neurotransmitters in the brain. Activation of presynaptic alpha-2 adrenoceptors (α_2 -AR) by the endogenous ligands noradrenaline (NA) and adrenaline (AD) results in a decrease in the release of monoaminergic neurotransmitters. Therefore, the administration of α_2 -AR antagonists leads to increased concentrations of brain monoamines and constitutes a viable strategy for the treatment for depression.

The rational design and synthesis of guanidine and 2-iminoimidazolidine derivatives as α_2 -AR antagonists is presented. In order to establish structure-activity relationships for these classes of α_2 -AR ligands, a comparative molecular field analysis (CoMFA) study has been carried out. The results of this analysis have been combined with literature studies of α_2 -AR antagonist pharmacology in order to design a new series of compounds as potential antagonists, fulfilling two general structures: *N,N'*-disubstituted guanidines and 4-substituted-2-iminoimidazolidines.

A novel and expedient synthesis of *N,N'*-disubstituted guanidines, and new methods for the preparation of 4-substituted-2-iminoimidazolidine derivatives are described. Given that the 4 position of 4-substituted-2-iminoimidazolidines incorporates a chiral centre, asymmetric methods for the preparation of optically active 4-substituted-2-iminoimidazolidine derivatives were explored using both chiral pool and organocatalytic strategies. The chiral pool strategy, starting from an optically active amino acid, was evaluated using a chiral derivatization approach and found to produce a racemate. The organocatalytic strategy was evaluated using chiral stationary phase high-pressure liquid chromatography (CSP-HPLC) and showed promising early results; however this strategy was terminated at an investigative stage.

These synthetic studies produced a total of 32 compounds for pharmacological evaluation as α_2 -AR antagonists. The affinity of these compounds for the α_2 -AR was evaluated using competitive radioligand binding assays, followed by [35 S]GTP γ S functional assays to determine whether they act as agonists or antagonists of the α_2 -AR. Generally, the transition from an unsubstituted guanidine or 2-iminoimidazolidine motif to a substituted compound led to a reduction in affinity for the α_2 -AR, but greatly improved the likelihood of the resulting compound possessing antagonistic rather than agonistic properties at the α_2 -AR.

Abbreviations

| | |
|--------------------|---|
| 5-HT | 5-Hydroxytryptamine, Serotonin |
| α_2 -AR | Alpha 2 Adrenergic Receptor |
| Ar. | Aromatic |
| Arom | Aromatic |
| AD | Adrenaline |
| BBB | Blood-Brain Barrier |
| Boc | <i>tert</i> -Butyl carbonyl |
| Boc ₂ O | Di- <i>tert</i> -butyl dicarbonate |
| CDCl ₃ | Deuterated Chloroform |
| CNS | Central Nervous System |
| CoMFA | Comparative Molecular Field Analysis |
| Conc. | Concentrated |
| D ₂ O | Deuterated Water |
| DA | Dopamine |
| D ₂ O | Deuterated Water |
| DA | Dopamine |
| DCM | Dichloromethane |
| DFT | Density Functional Theory |
| DMSO | Dimethylsulfoxide, Deuterated |
| EDCI | 1-Ethyl-3-(3-dimethylaminopropyl)carbodiimide |
| EEG | Electroencephalogram |
| Et | Ethyl |
| EtOAc | Ethyl Acetate |
| Fur. | Furanyl |
| GPCR | G-Protein Coupled Receptor |
| GTP | Guanosine Triphosphate |
| H ₂ O | Water |
| HCl | Hydrochloric Acid |
| HgCl ₂ | Mercury (II) Chloride |
| HPLC | High-Performance Liquid Chromatography |
| HRMS | High Resolution Mass Spectrometry |

| | |
|--------------------|--|
| IMHB | Intramolecular Hydrogen Bond |
| IR | Infrared |
| MAOI | Monoamine Oxidase Inhibitor |
| MDD | Major Depressive Disorder |
| Me | Methyl |
| MgSO ₄ | Magnesium Sulfate |
| MMFF94 | Merck Molecular Force Field 1994 |
| MS | Mass Spectrometry |
| NA | Noradrenaline |
| NaH | Sodium Hydride |
| NaHCO ₃ | Sodium Bicarbonate |
| NMR | Nuclear Magnetic Resonance |
| NOE | Nuclear Overhauser Effect |
| PDB | Protein Data Bank |
| Ph | Phenyl |
| QSAR | Quantitative Structure-Activity Relationship |
| RBF | Round Bottomed Flask |
| SNRI | Serotonin and Noradrenaline Reuptake Inhibitor |
| SSRI | Selective Serotonin Reuptake Inhibitor |
| SDM | Site-Directed Mutagenesis |
| TCA | Tricyclic Antidepressant |
| TEA | Triethylamine |
| TFA | Trifluoroacetic Acid |
| TFAA | Trifluoroacetic Anhydride |
| TLC | Thin-Layer Chromatography |
| THF | Tetrahydrofuran |

Table of Contents

| | |
|--|----------|
| Chapter 1 - Introduction | 1 |
| 1.1 Depression..... | 1 |
| 1.1.1 Depression: Symptoms and Prognosis..... | 1 |
| 1.1.2 The Burden of Depression | 1 |
| 1.1.3 Antidepressants: Their Role and Limitations | 3 |
| 1.1.4 History of Depression | 4 |
| 1.2 Theories of Depression..... | 6 |
| 1.2.1 Synaptic Neurotransmission | 6 |
| 1.2.2 Neurotransmitters in the Central Nervous System..... | 8 |
| 1.2.3 The Monoamine Hypothesis | 18 |
| 1.2.4 Neuroplasticity Theories..... | 19 |
| 1.2.5 The Cytokine Hypothesis..... | 22 |
| 1.2.6 Theories of Depression: Application to New Treatments..... | 23 |
| 1.3 Clinical Antidepressants..... | 25 |
| 1.3.1 Early Antidepressants: The MAOIs and TCAs | 25 |
| 1.3.2 The Rise of the SSRIs | 27 |
| 1.3.3 Current and Future Antidepressants..... | 28 |
| 1.4 The Alpha 2 Adrenoceptor..... | 30 |
| 1.4.1 Adrenoceptor Structure and Function | 30 |
| 1.4.2 Alpha 2 Adrenoceptor Antagonists..... | 33 |
| 1.4.3 Previous Work within our Group..... | 37 |
| 1.5 Comparative Molecular Field Analysis | 40 |

| | |
|--|-----------|
| Chapter 2 - Objectives | 44 |
| 2.1 CoMFA and Rational Design..... | 44 |
| 2.2 Chemical Synthesis | 44 |
| 2.3 Pharmacology..... | 45 |
| | |
| Chapter 3 - CoMFA and Rational Design | 46 |
| 3.1 Data Selection and Alignment..... | 46 |
| 3.2 CoMFA Model: Results and Discussion..... | 50 |
| 3.3 Molecular Design | 53 |
| 3.4 Context and Discussion..... | 56 |
| 3.5 Conclusions | 59 |
| | |
| Chapter 4 - Chemical Synthesis..... | 62 |
| 4.1 Modifications to Existing Lead Compounds..... | 62 |
| 4.1.1 Analogues of <i>N</i> -(4-ethylaminophenyl)guanidine dihydrochloride | 62 |
| 4.1.2 Conformational aspects of <i>bis</i> -Boc protected guanidine derivatives..... | 63 |
| 4.1.3 Reactivity of <i>bis</i> -Boc protected 2-iminoimidazolidine derivatives | 65 |
| 4.1.4 Mechanistic aspects of guanidylation using thiourea derivatives..... | 67 |
| 4.2 <i>N,N'</i> -Disubstituted Guanidines | 70 |
| 4.2.1 Literature methods for preparing <i>N,N'</i> -disubstituted guanidines | 70 |
| 4.2.2 A concise synthesis of <i>N,N'</i> -disubstituted guanidines..... | 74 |
| 4.2.3 Conformational aspects of <i>N,N'</i> -disubstituted guanidines..... | 82 |
| 4.3 4-Substituted-2-Aryliminoimidazolidines..... | 87 |
| 4.3.1 Literature methods for the preparation of 2-aryliminoimidazolidines..... | 87 |
| 4.3.2 Literature reports of 4-substituted 2-aryliminoimidazolidines | 89 |
| 4.3.3 Early strategies towards 4-substituted-2-aryliminoimidazolidines..... | 93 |
| 4.3.4 1-Acetyl-2-thiohydantoins in the synthesis of 2-iminoimidazolidines..... | 96 |

| | | |
|--|---|------------|
| 4.3.5 | Determining the enantiomeric excess of 2-iminoimidazolidine precursors | 100 |
| 4.3.6 | Method for the synthesis of 4-(2-furyl)-2-aryliminoimidazolidines..... | 107 |
| 4.3.7 | Towards an asymmetric synthesis of 4-substituted 2-iminoimidazolidines | 109 |
| Chapter 5 - Pharmacology | | 114 |
| 5.1 | Introduction | 114 |
| 5.2 | Pharmacological Methods | 116 |
| 5.2.1 | Determining receptor affinity: competitive radioligand binding assays..... | 116 |
| 5.2.2 | Agonism versus antagonism: [³⁵ S]GTP γ S binding functional assays | 117 |
| 5.2.3 | Confirming activity <i>in vivo</i> : microdialysis experiments..... | 119 |
| 5.3 | Results and Discussion..... | 120 |
| 5.3.1 | Affinity of the <i>N,N'</i> -disubstituted guanidine hydrochloride salts..... | 120 |
| 5.3.2 | Affinity of the 4-substituted-2-iminoimidazolidine hydrochloride salts | 122 |
| 5.3.3 | [³⁵ S]GTP γ S binding functional assays..... | 124 |
| 5.4 | Conclusions..... | 127 |
| Chapter 6 - Future Work | | 130 |
| Chapter 7 - Experimental..... | | 133 |
| 7.1 | General Procedures: Pharmacology | 133 |
| 7.2 | General Procedures: Chemical Synthesis..... | 135 |
| 7.3 | Synthesis and Characterisation..... | 140 |
| References | | 216 |
| Appendices | | i |
| Appendix A: Compounds prepared previously in our group..... | | i |
| Appendix B: NMR spectra of diastereomeric mixture 96r and 96s..... | | iii |

Chapter 1 - Introduction

1.1 Depression

1.1.1 Depression: Symptoms and Prognosis

The fourth edition of the Diagnostic and Statistical Manual of Mental Disorders (DSM-IV) describes depression as a mood disorder characterised by long-term feelings of sadness, anhedonia, irritability, anxiety, cognitive disturbances, and the sensation of physical and psychic pain. Adverse behavioural symptoms include disturbances to sleeping patterns and personal motivation, difficulties with social interactions and sexual functioning, and diminished occupational or academic performance.¹ Panic attacks and substance abuse problems may also develop. Sadly, self-medication through alcohol and drug abuse only worsens the prognosis, as addiction often results in a deepening of the patient's depression.²

Suicide comprises the most serious danger for depressed individuals, with up to 56% of patients attempting to take their own lives.³ Although the severity of depression is closely tied to the emergence of suicidal ideation, other causative factors such as environmental stress, mania, and psychopathology may also play a role.⁴ While in some instances a suicide attempt may be intended as an expression of despair rather than a genuine wish to die, the probability of death is greatly increased with each repeat attempt.⁵ Nonetheless, the reduction in life expectancy associated with depression is only partly explicable by suicide risk alone. Co-morbidity of depression with such diseases as heart failure, hypertension, arthritis, and diabetes has a vastly negative effect upon the outcome of the illness.⁶ The associated health risks imply that the issue of mortality and morbidity in depression transcends the psychological affliction alone.

1.1.2 The Burden of Depression

In 2004, the World Health Organization (WHO) commissioned a report titled "The Global Burden of Disease" in which multinational health data was assembled to assess the loss of health from the 135 leading causes of illness worldwide.⁷ Among the conclusions published in this report, it was found that mental health issues ranked second only to cardiovascular illness as the world's leading cause of disability, with depression as a single diagnostic

category outranking all other sources of illness.⁸ The WHO has predicted that by the year 2020, depression will constitute the single largest contributor to morbidity and disability in the developed world.⁹

Although the prevalence of depression is subject to international variations, accurate estimates are available for many developed nations, where as many as 17% of people will suffer from depression during their lifetime.¹⁰ In Ireland, approximately 7% of the population suffers from depression at any given time, and 2% of the population is considered disabled due to the illness.¹¹ Figures for the developing world are more difficult to determine, as the symptoms of depression often go unrecognised; cultural differences result in a vast discrepancy between epidemiological estimates and the end diagnoses actually stated by health workers. Often, a patient will present somatic symptoms such as tiredness and headache which, upon inquiry, are revealed to be rooted in depression.¹² In one Zimbabwean study, it was estimated that up to 25% of patients attending either primary care institutions or a traditional healer exhibit symptoms of depression.¹³ However, only 1% of clinical patients actually receive a psychiatric diagnosis.¹⁴

Within the adult population, women are almost twice as likely as men to suffer from depression, however the risk of suicide is greater among males than females; this discrepancy is partly explained by the decreased likelihood in men to seek medical help with depression.¹⁵ In childhood the occurrence is equal across both genders, with the gender imbalance emerging around the onset of puberty. The risk for depression peaks between the ages of 15 to 30, with suicide constituting the second highest cause of death among this age group;⁹ persons over the age of 65 may also be particularly affected. Sadly, there remains a common misconception that geriatric depression is simply “a natural part of ageing” which results in the disease being underreported in a population especially vulnerable to the risks of co-morbidity and mortality. Widowed, separated or unhappily married persons are also at risk, although the negative impact of depression upon interpersonal relationships blurs the line of causation in such instances.¹⁶ In common with many other diseases, socioeconomic deprivation ranks among the most important risk factors for depression.¹⁷ Although several studies have attempted to decouple economic considerations from ethnicity, conflicting evidence makes it difficult to determine whether race plays a significant role.^{18,19} Other genetic considerations such as a familial history of psychiatric disorders may be more predictive in terms of patient vulnerability.²⁰

To illustrate the societal burden of depression, mental health problems are estimated to account for some 35-45% of absenteeism from work.⁹ Economic costs from the loss of labour alone are estimated to be within the tens to the hundreds of billions of dollars within the U.S.A.²¹ European studies have estimated the direct expenses of outpatient care, drug costs and hospitalization within the E.U. at 42 billion euro, a figure which neglects to account for the fact that only 43% of those affected actually seek treatment.²² When indirect costs due to morbidity and mortality are also taken into account, the total annual expense soars to 118 billion euro; thus, the aggregate costs of depression consume as much as 3-4% of the total gross national product of Europe.²³ Hospitalisation accounts for the majority of this economic burden, while the use of antidepressant drugs constitutes only 2-11% of healthcare expenditure.²⁴ This implies that early pharmacotherapeutic intervention may provide an efficient means of alleviating depression before the need for hospitalisation arises.

1.1.3 Antidepressants: Their Role and Limitations

The argument for antidepressant drug treatment is supported by the correlation of an increase in antidepressant prescriptions since the 1970s with a fall in the incidence of suicide.²⁵ In adults, increased availability of antidepressants has been linked to a 19-25% reduction in suicide rates in Scandinavia and the U.S.A. (Fig. 1.1).²⁶

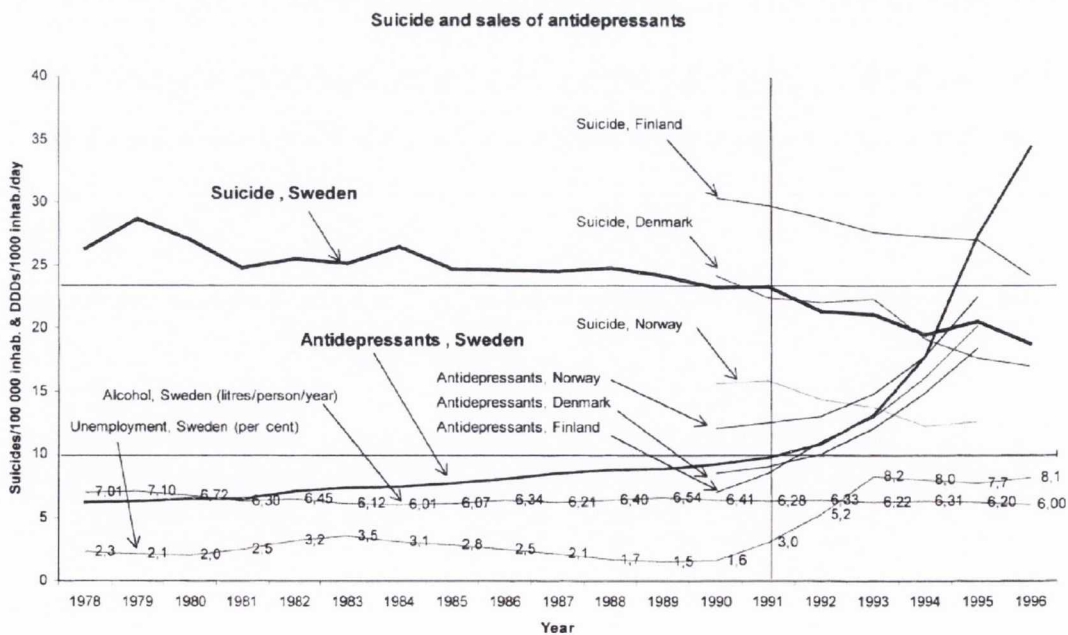


Fig. 1.1. The relationship between suicide in Scandinavia and antidepressant sales. Alcohol consumption and unemployment rates are also shown. Reproduced from G. Isaacson, 2000.²⁶

The use of antidepressants in children and adolescents warrants further discussion, as there has been controversy linking antidepressants to suicidal ideation in younger patients. Although early studies prompted the U. S. Food and Drug Administration (FDA) to introduce labels warning of increased suicidal thoughts, an extensive study recently concluded that the anti-suicidal benefits of antidepressants far outweigh any such risk.²⁷ Sadly, some authors have concluded that the FDA warning labels resulted in a drop in prescription rates correlating to an overall increase in suicide rates in the wake of the controversy.²⁸ Nonetheless, the need for caution remains in prescribing psychiatric medication to younger patients still undergoing neural development.

In conclusion, the development of effective antidepressant drugs provides an invaluable means of ameliorating the burden of depression. The application of antidepressant drugs can alleviate suffering in 43-70% of patients,²⁹ circumventing the need for hospitalisation and the consequent increase in morbidity in later life. When properly used, antidepressant drugs also provide a means of reducing the incidence of suicide. It follows that antidepressant drugs remain critical in the effort to reduce the burden of depression, not only in societal and economic terms, but also in regard to the loss of human life.

1.1.4 History of Depression

Although depression has been associated with illness since antiquity,³⁰ the pathophysiological mechanisms underlying the disease remain poorly understood. Symptoms and causes present in one instance may be absent in another, and patient responses to antidepressant and psychotherapeutic therapies are often inconsistent and difficult to predict.³¹ Each individual case of depression might therefore be thought of an illness unique to that patient, the symptoms of which overlap with the broader clinical definition. Given the heterogeneous nature of the disease, it follows that many disparate theories have been put forward regarding its causes and treatment throughout history.

According to Hippocrates (c. 460 BC), depression fell under the broader definition of *melancholia*; a condition which also included phobias, delusions and certain physical symptoms.³² Following his humoral theory of disease, *melancholia* was associated with an excess of black bile within the body, and the term is derived from the Ancient Greek words *melas* (black) and *kholé* (bile). Although the Persian physician Avicenna (c. 980 AD) redefined *melancholia* to more closely describe a psychological illness evidenced by a

lowered emotional state,³³ the coetaneous European world viewed depression as a sinful indulgence and a spiritual ailment termed ‘acedia’ (Fig. 1.2).³⁴



Fig. 1.2. The 16th century engraving ‘Acedia’ by Flemish artist Jerome Wierix.

In 1763, the Frenchman Pierre Pomme popularised a condition termed ‘vapeurs’ (“the vapours”) with symptoms closely matching clinical depression; he prescribed chicken soup and cold baths for the treatment of this malaise, and would serve as medical advisor to King Louis XV.³⁵ However, the modern definition of depression only entered the medical lexicon in the 19th century with the advent of medical psychiatry. Early psychiatry made little distinction between the various forms of mental illness, and Emil Kraepelin became the first to distinguish between *manic depression* and *dementia praecox* in the second edition of his *Psychiatrie* (1899); conditions which we now recognise as mood disorders and schizophrenia, respectively.³⁶ By the 20th century, Karl Leonhard had drawn a distinction between bipolar and unipolar depression (major depressive disorder).³⁷ Around the same time, the link between chemistry and the nervous system was confirmed by the pharmacologist Otto Loewi, who discovered the first neurotransmitter (NT) in acetylcholine (ACh), and received the 1936 Nobel Prize in Physiology or Medicine for his work.

Since the establishment of chemical neurotransmission, theorists from many different disciplines have sought to understand the biochemical origins of depression. Although experiments have uncovered a myriad of links between physical changes to the nervous system and depressive disorder, a ‘general theory of depression’ has yet to be found. Nonetheless, many theories have provided useful predictions regarding the causes and treatment of depression, and the development of antidepressant drugs remains closely tied to the ongoing evolution of our understanding of depression.

1.2 Theories of Depression

1.2.1 Synaptic Neurotransmission

The key functional unit of the central nervous system (CNS) is the neuron, a highly specialised cell capable of receiving, processing and transmitting information in the form of electrical and chemical signals (called action potentials). The morphology of a neuron comprises a central nucleus from which several long, wire-like structures called dendrites and axons protrude (Fig. 1.3). The dendrite's role is to receive action potentials from other cells, while the axon functions as a transmitter. Typically, a nerve cell has only one axon, but the axon termini are highly branched allowing for information to be transmitted simultaneously to the dendrites of many neighbouring neurons.

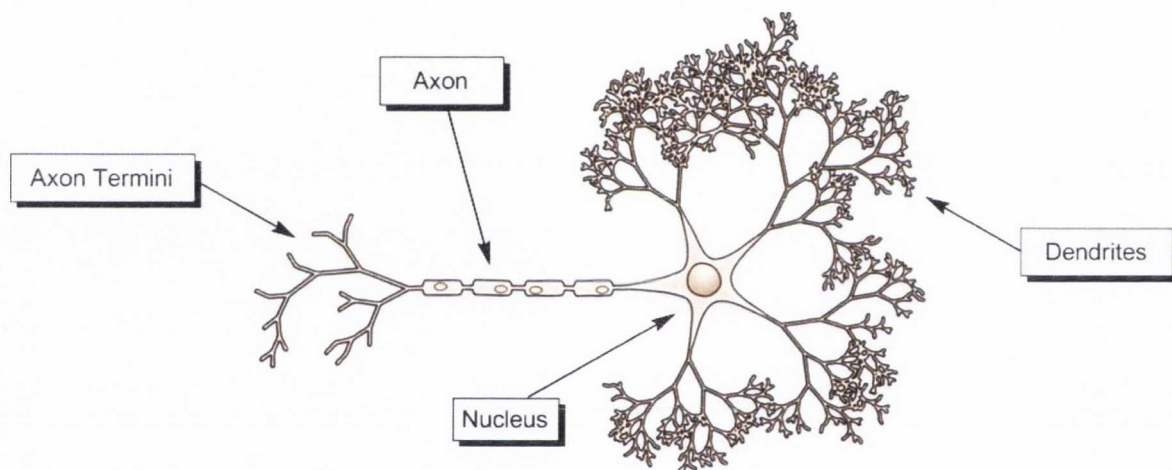


Fig. 1.3. Morphological features of a typical neuron. The axon and dendrites are much longer than this diagram can accurately depict.³⁸

In the resting state, a neuron maintains a voltage gradient between the cell contents and its surrounding environment. If the level of electrical input to the neuron exceeds a certain threshold (around -55 mV), the voltage gradient collapses and a wave of depolarisation sweeps along the cell body from dendrite to axon; the neuron then repolarises in preparation for the next action potential. Thus, an action potential can traverse the neuron in the form of an electrical impulse at a velocity of 30 – 120 m/s.

When the action potential reaches the axon terminus, depolarisation gives rise to an influx of Ca^{2+} ions which induces NT storage vesicles to fuse with the cell membrane (Fig. 1.4). The newly released NT diffuses towards the dendrite of a neighbouring cell through a gap called

the synapse, which includes both the presynaptic terminus (which releases the NT) and the postsynaptic terminus (which receives the chemical signal). A variety of receptor types on the postsynaptic neuron respond to NT activation in different ways; ligand-gated ion channels (ionotropic receptors) respond by transporting ions such as K^+ and Cl^- into the cell, while G-protein coupled receptors (GPCRs; metabotropic receptors) modulate the production of intracellular second messengers such as cyclic AMP (cAMP), which may indirectly modify the influx of ions. In this way, some NTs induce the cell to produce an action potential of its own, while others may suppress the cell from firing. This interplay of inhibitory and excitatory postsynaptic potentials is fundamental to the complex signal processing ability of neurons.

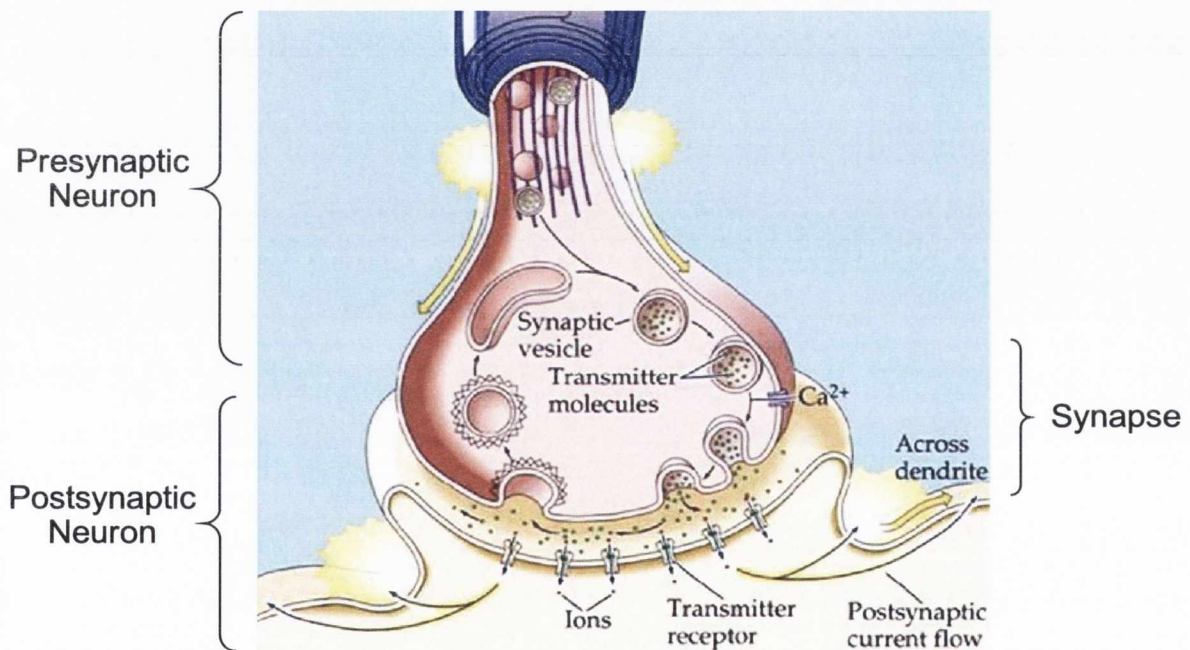


Fig. 1.4. A schematic depiction of synaptic neurotransmission.³⁹

NTs in the synapse may also interact with receptors on the presynaptic terminus, which fall into two general categories: autoreceptors and heteroreceptors. Activation of an autoreceptor results in a reduction in the release of further NT; thus, an autoreceptor forms part of a negative feedback loop which limits the level of NT released by the cell. In the case of heteroreceptors, activation results in the modulation of NTs other than the NT which binds to that receptor. For example, activation of presynaptic muscarinic heteroreceptors by acetylcholine serves to inhibit the release of noradrenaline in the heart of the rat.⁴⁰

Other proteins located on the presynaptic neuron include reuptake transporters, which reabsorb NTs released into the synapse to terminate the neural impulse. The majority of reuptake proteins are symporters, meaning that they couple the transport of NT molecules with the favourable movement of ions across the cell membrane. By taking advantage of the transport of ions along their concentration gradient, transporter proteins are able to perform the energetically unfavourable task of NT reuptake without the direct consumption of energy. Once the NT has been reabsorbed, it may be repackaged into storage vesicles for later release, or broken down by enzymes such as monoamine oxidase (MAO). In some cases, catabolic enzymes capable of breaking down NTs may also be found on the surface of neurons and nearby cells; catechol O-methyl transferase (COMT) and acetylcholine esterase (AChE) are two common examples.⁴¹

It is important to note that chemical neurotransmission is not the only method of communication between neurons. In some instances neurons may be directly connected via electrical synapses, in which cells are separated by a distance of only 3.5 nm (compared with 20 to 40 nm in a chemical synapse).⁴² In electrical synapses, a series of hydrophilic channels cross the membranes of both the pre- and postsynaptic neuron and allow for the direct transport of ions and small molecules between cells. This allows electrical synapses to communicate at a much greater speed than their chemical counterparts; however, they lack many of the subtleties of the chemical synapse, such as the capacity for inhibitory input. As a result, electrical synapses are most prominent in systems requiring rapid control but little signal processing, such as the retina.⁴³

1.2.2 Neurotransmitters in the Central Nervous System

Chemical neurotransmission relies on a multitude of small molecules (neurotransmitters; NTs), and networks of neurons are often characterised by which neurotransmitter(s) they use to communicate. Broadly speaking, a NT can be classified as excitatory or inhibitory, depending on its effect upon the cell at the receiving end of the chemical synapse. Excitatory NTs induce depolarisation, increasing the likelihood of an action potential; inhibitory NTs reduce this likelihood via hyperpolarisation. However, NTs often carry out functions which defy this categorisation. The full list of chemical entities which could be called NTs is expansive; more than 100 such molecules are known to exist, and new NTs are frequently discovered. However, the most important NTs comprise a short list of molecules, many of

which have been thoroughly studied with regard to not only their biochemistry, pharmacology and metabolism; but also their relevance to human behaviour and cognition.

The Amino Acids

Several amino acids function as NTs, both in an inhibitory and excitatory role. Glutamate (Fig. 1.5) is the principal excitatory NT in the CNS; however, as one of the 20 proteinogenic amino acids it has proven difficult to determine its localisation within the brain. The receptors with which glutamate interacts include both ionotropic receptors of the Kainate and NMDA types, and the metabotropic glutamate receptors (mGluRs). NMDA receptors are closely associated with neuroplasticity and learning, and require both glutamate and glycine to be present for activation. Aspartate and D-serine have also been shown to activate the NMDA receptors.⁴⁴ Kainate receptors are less fully understood, however Kainate-knockout mice exhibit reduced motor function and are resistant to seizure, yet retain the ability to learn maze tasks. As a result, Kainate receptors have been proposed as a target for anti-epileptic drugs. The mGluR receptors fulfil a variety of roles, including nociception, learning and memory. Several subtypes of the mGluR receptor, as well as many of the Kainate receptors, can be localised on either the post- or the presynaptic terminus.⁴⁵

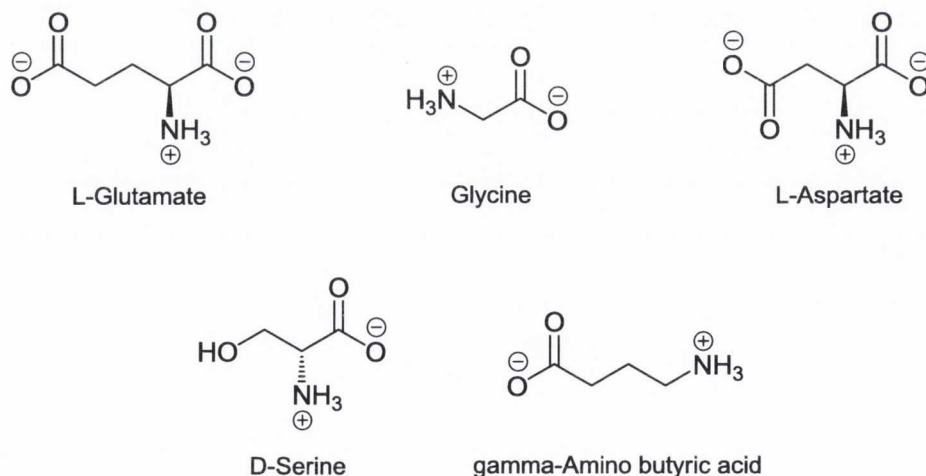


Fig. 1.5. Chemical structures of the principal amino acid NTs at physiological pH.

In addition to its role as a co-agonist for NMDA receptors, glycine also acts as an inhibitory NT, particularly in the caudal part of the brain, the retina and the spinal cord. A genetic defect in the glycine receptor results in hyperekplexia, a disorder characterised by an exaggerated

startle reflex.⁴⁶ The second major inhibitory amino acid is gamma amino-butyric acid (GABA), for which both ionotropic (GABA_A) and metabotropic (GABA_B) receptors are known. GABA_A receptors are the target for tranquilizer drugs such as benzodiazepines, while GABA_B agonists have been investigated as anxiolytics and for the treatment of addiction. A third class of GABA receptor, termed the GABA_A-rho or GABA_C receptor, is highly expressed in the retina, where it may play an important role in retinal signal processing.⁴⁷

Acetylcholine, Neuropeptides, and Other Transmitters

Although acetylcholine (ACh; Fig. 1.6) was the first NT to be discovered, ACh is far less prominent than the amino acid NTs within the CNS. Instead, ACh is the primary NT within the neuromuscular junction and in the peripheral nervous system, where it initiates skeletomuscular contraction. ACh receptors are divided into the nicotinic (ionotropic) and muscarinic (metabotropic) classes, which are localised on the post- and presynaptic sides of the neuromuscular junction, respectively. In the CNS, ACh acts as an excitatory NT and is associated with alertness and arousal.⁴⁸ The reduced function of presynaptic central ACh receptors has been implicated in the onset of Alzheimer's Disease, and several medications currently marketed for the treatment of Alzheimer's Disease act by inhibiting acetylcholine esterase (AChE), the enzyme responsible for catabolising ACh.

Neuropeptides are proteinaceous molecules which may act both as neurotransmitters and as neuromodulators; molecules capable to modifying the metabolism, functioning and gene expression of neurons and their surrounding cells. Neuropeptides are often co-localised with a small molecule neurotransmitter; for instance there are GABAergic neurons which also produce the neuropeptide cholecystokinin-8 (Fig. 1.6).⁴⁹ Many neuropeptides also act as neurohormones, and the physiological and behavioural response to their release may be long-lasting and profound; such as opioid-withdrawal induced hypersensitivity to pain, which has been associated with cholecystokinin-8.⁵⁰

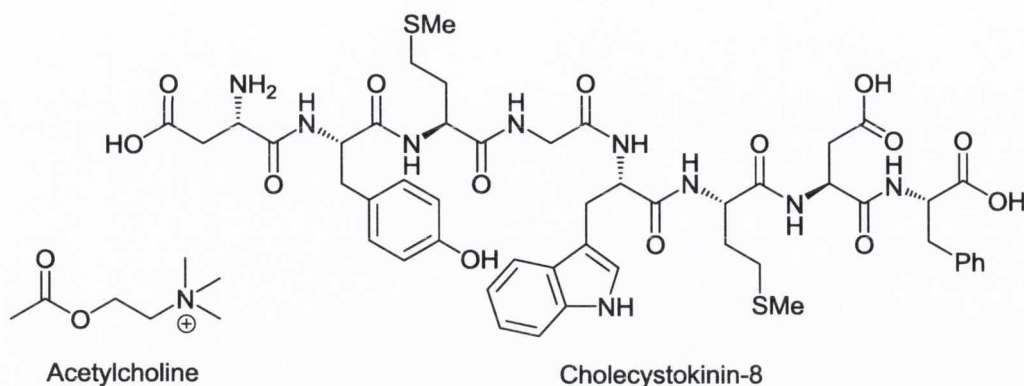


Fig. 1.6. Chemical structures of Acetylcholine and Cholecystokinin-8.

Other entities which function as NTs include histamine (Fig. 1.7), which famously modulates the immune response. It follows that many of the histamine receptor subtypes are localised in immunologically important tissues such as the bone marrow and the vascular smooth muscle, however the H_1 and H_3 receptors are also found in the CNS where they serve to regulate sleep and excitatory NT release, respectively.⁵¹ Several steroids are also released by CNS neurons, such as progesterone (Fig. 1.7). These neuroactive steroids may modulate the activities of nearby neuroglia; cells which support the neurons and maintain the homeostatic environment of the CNS. However, such steroids can also interact with synaptic receptors via allosteric interactions, such as pregnenolone, which modulates the NMDA receptor.⁵² Therapeutic applications for neuroactive steroids are also forthcoming; ganaxolone for example is a synthetic neurosteroid in clinical development for the treatment of epilepsy.⁵³

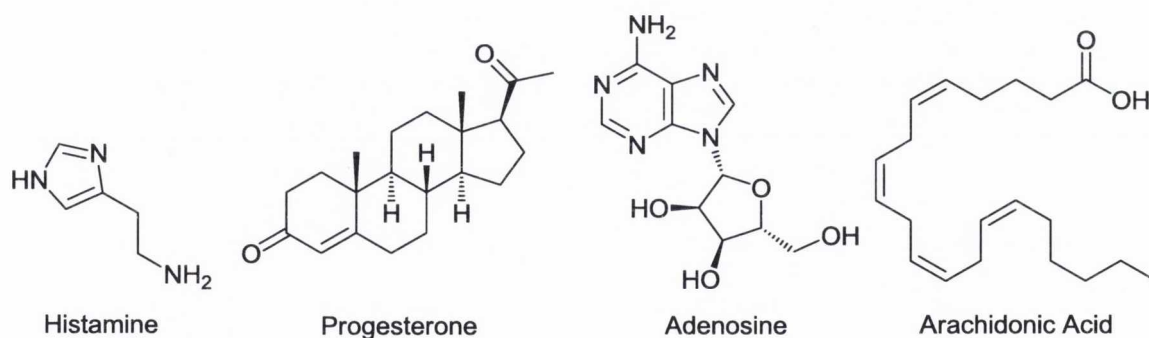


Fig. 1.7. Chemical structures of Histamine, Progesterone, Adeonsine, and Arachidonic Acid.

Several other small molecules might be classified as NTs; including adenosine, nitric oxide and the prostaglandins. In addition to its ubiquitous role in cell metabolism, adenosine is a NT important in the promotion of sleep, and also functions as a neuromodulator. The A_1 and A_{2A} adenosine receptors regulate the release of excitatory NTs and may play an important

role in neuroprotection.⁵⁴ Nitric oxide (NO) is a so-called gasotransmitter; a gaseous signalling molecule which can traverse the cell membrane without the need for transport proteins. NO has been alternately associated with neuroprotection and neurodegeneration, depending on its concentration.⁵⁵ Given that gasotransmitters directly affect the intracellular environment of neighbouring cells without the need for synaptic receptors, they cannot be considered NTs in the classical sense. Other potential gasotransmitters include carbon monoxide and hydrogen sulphide. The prostaglandins and their precursor arachidonic acid (Fig. 1.7) are also present at high concentrations within the brain and are important for signalling between neuroglia. Their role in neurodevelopment and in CNS inflammation makes them a potential target for the treatment of Alzheimer's and Parkinson's disease.⁵⁶

The Monoamines and Trace Amines

Monoamines are NTs fulfilling the general structure (aryl)-(ethyl)-(amine). Broadly speaking, this definition also includes histamine and several trace amines present in the CNS; however the classical monoamine NTs are limited to the catecholamines (namely; dopamine and noradrenaline; Fig. 1.8, top) and the tryptamines (serotonin and melatonin; Fig. 1.8, bottom). The metabolic pathways of the monoamine NTs are closely linked, with every monoamine being ultimately derived from a parent amino acid via enzymatic decarboxylation. In spite of their shared metabolism, each of the monoamines fulfils a very different role within the CNS, and each is associated with its own family of receptors.

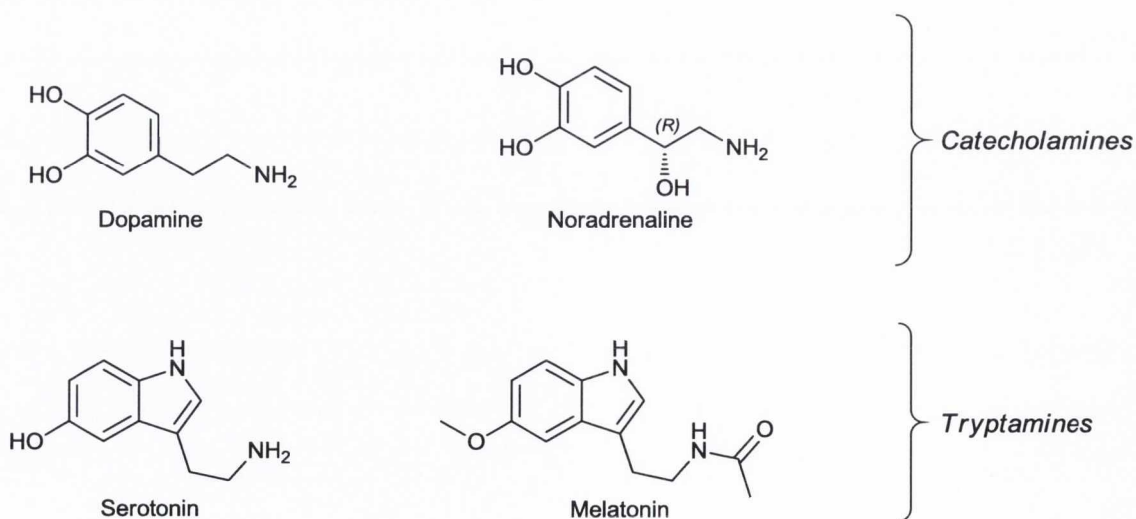


Fig. 1.8. Chemical structures of the classical monoamine NTs.

Dopamine is especially prevalent in the *substantia nigra*, a region of the brain associated with motor control and reward. As a result, dopamine has been closely associated with addiction, Parkinson's disease, spatial memory, mood and learning. The dopamine receptors are GPCRs, and are divided into the D₁ family (which increases intracellular cAMP) and the D₂ family (which reduces intracellular cAMP). Thus, dopamine can function as either an excitatory or an inhibitory NT. Although dopaminergic receptors are widespread within the CNS, subtype concentrations differ from one region to another; reflecting the functional diversity of dopamine in different parts of the brain.⁴⁷

Dopamine shares a common metabolic pathway with the other catecholamines, beginning with non-essential amino acid tyrosine. Tyrosine hydroxylase introduces a hydroxyl group in the *meta* position to generate L-dihydroxyphenylalanine (L-DOPA), an entity which is administered for the treatment of parkinsonian symptoms in order to elevate dopamine concentrations within the CNS and improve motor control. L-DOPA is the substrate for aromatic amino acid decarboxylase, which produces dopamine (Fig. 1.9).

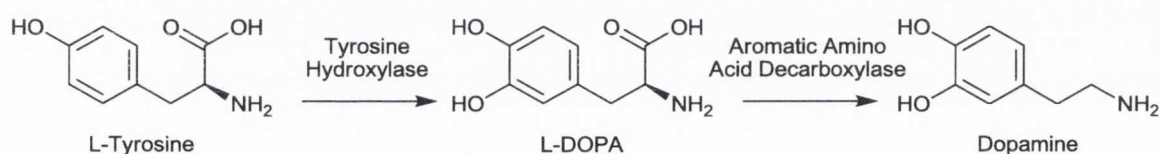


Fig. 1.9. Biosynthetic pathway of dopamine.

Several possible metabolic fates exist for the dopamine molecule; in dopaminergic neurons, DA is released as a NT and reabsorbed via the dopamine reuptake transporter (DAT1). In neurons lacking the DAT1 transporter, the noradrenaline reuptake transporter (NERT) can perform this task. Within the cell, dopamine may be repackaged into vesicles or broken down by the combined action of MAO and COMT. Although two subtypes of MAO exist (A and B), both subtypes can catabolise DA. Either MAO or COMT may act first; in the case of MAO, the terminal amine is converted to a carboxylic acid moiety to produce 3,4-dihydroxyphenylacetic acid; COMT then introduces a methyl group in the *meta* hydroxyl group to produce homovanillic acid, which is excreted via the plasma. Alternatively, COMT can introduce this methyl group prior to the oxidative action of MAO, producing 3-methoxytyramine enroute to homovanillic acid (Fig. 1.10).

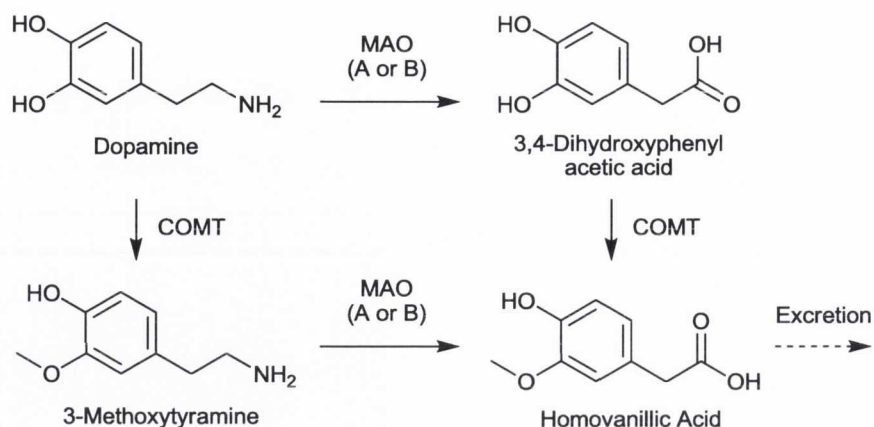


Fig. 1.10. Catabolic pathways of dopamine.

In noradrenergic neurons, dopamine is produced via this same pathway as an intermediate in the synthesis of noradrenaline (NA). Dopamine β -hydroxylase introduces the requisite hydroxyl group in a stereospecific sense to produce L-(R)-noradrenaline (Fig. 1.11).



Fig. 1.11. Biosynthetic pathways of noradrenaline and adrenaline.

Although noradrenergic neurons are widespread throughout the CNS, their distribution is diffuse making it difficult to define a singular role for NA. It is generally understood, however, that NA is important in the control of arousal and alertness. There is also evidence that NA is important in modulating both mood and the stress response; in particular the ability of an individual to ‘cope’ with stressful stimuli.⁴⁷ A direct interpretation of NA within the CNS is further complicated by its relation to adrenaline (AD), an important hormone for which it comprises the biosynthetic precursor (Fig. 1.11). NA and AD share a family of receptors (adrenoceptors; ARs) of which there are two major types, the α and β ARs, both of which are GPCRs. Generally, AD exhibits a stronger affinity for the β ARs, while NA is preferred by the α ARs. The β ARs are principally located in the heart, kidney and stomach (β_1 subtype); and in the smooth muscles and lungs (β_2 subtype). Medications acting on the β ARs have been useful in the treatment of cardiac illness and asthma. The α ARs are also

divided into two subtypes. In the periphery, they are associated with cardiovascular, urinary and bronchial contraction (α_1), as well as insulin release and gastrointestinal smooth muscle contraction (α_2). Both subtypes are also widespread within the CNS, where their role is to modulate the release of monoaminergic NTs. This function makes these receptors a key target for CNS drugs, and is further discussed in section 1.4.

Following synaptic release, NA may be reabsorbed through the action of a reuptake protein (NERT), and broken down by the action of catabolic enzymes. Inhibitors of the NERT transport protein find clinical usage as decongestants and antihypertensive agents (in the periphery), and as stimulants and antidepressants (in the CNS). The catabolism of NA is somewhat complex (Fig. 1.12), involving the combined action of MAO, COMT, aldehyde reductase, and aldehyde dehydrogenase. As with DA, either COMT or MAO can initiate the process. This pathway gives rise to two possible end-products, namely 3-methoxy-4-hydroxyphenylglycol (MHPG), and vanillylmandelic acid.⁴⁷ In the CNS, MHPG is the principal metabolite; while in the periphery, vanillylmandelic acid is the major product.

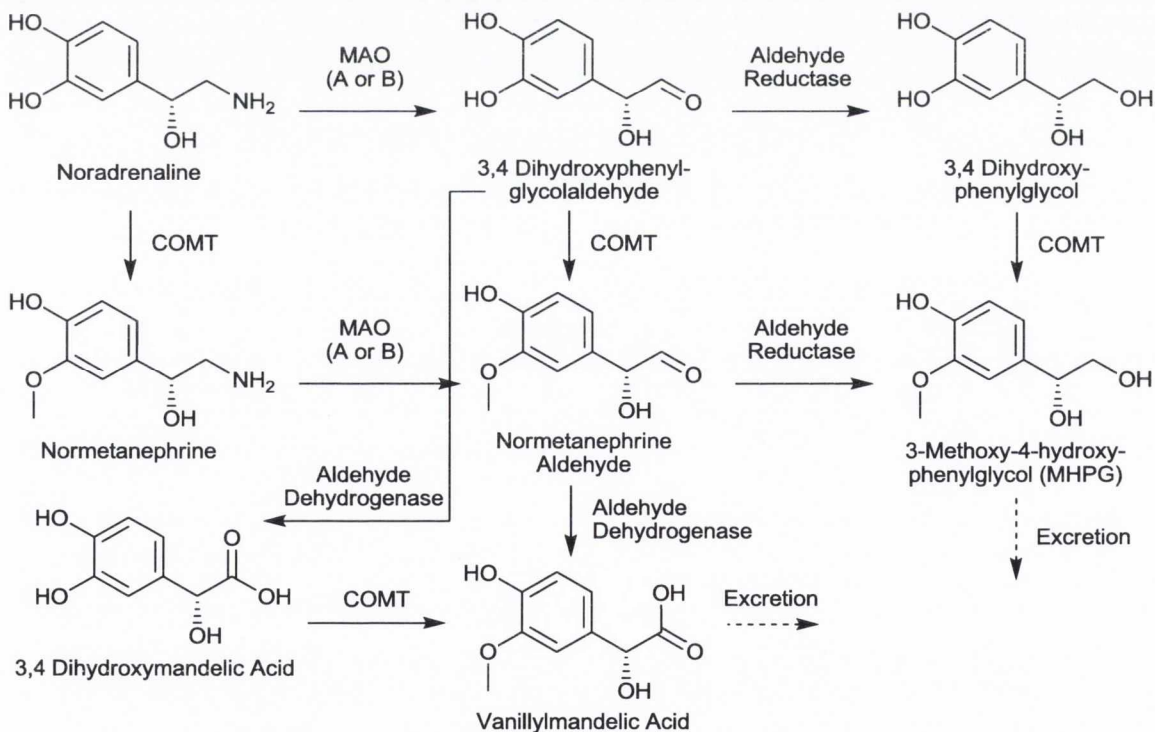


Fig. 1.12. The catabolic pathways of noradrenaline.

As with the catecholamines, the tryptamine NTs also share a biosynthetic pathway, starting with the hydroxylation of L-tryptophan by tryptophan hydroxylase to produce 5-

hydroxytryptophan (5-HTP). Aromatic amino acid decarboxylase converts 5-HTP to 5-hydroxytryptamine (5-HT), also known as serotonin (Fig. 1.13). While 5-HT is thought to be the more important of the tryptamine NTs, it is also an intermediate in the biosynthesis of the NT melatonin. In this case, serotonin N-acetyltransferase produces N-acetylserotonin, which is converted to melatonin through the action of hydroxyindole-O-methyltransferase (HIOMT).

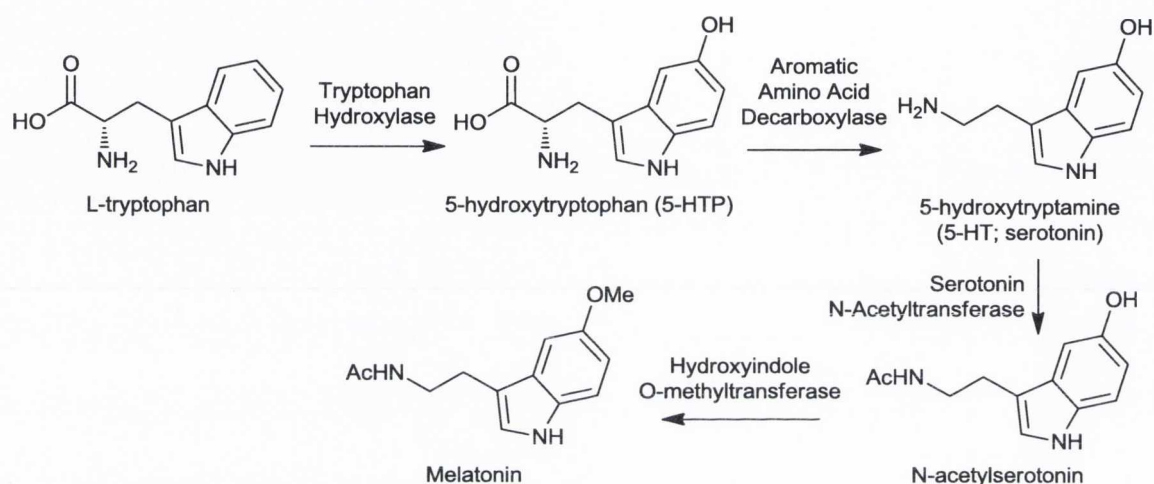


Fig. 1.13. Biosynthetic pathways of the tryptamine NTs serotonin and melatonin.

Serotonin (5-HT) is a complex NT associated with a wide spectrum of physiological and behavioural responses; including mood, anxiety, appetite, sexual arousal, sleep and nociception. There are seven families of 5-HT receptor designated 5-HT₁₋₇, each of which has several subtypes. These receptors are variably excitatory and inhibitory in nature, and only the 5-HT₃ receptor acts as an ion channel (ionotropic); all other receptors being metabotropic (GPCRs). The diverse effects of 5-HT may stem from the capability of the 5-HT receptors to modulate the release of other NTs; many of the 5-HT receptors are heteroreceptors, and are found both pre- and postsynaptically. By tuning the selectivity for various receptors, 5-HT ligands have found many clinical applications; agonists have been used as anxiolytics, antiemetics and appetite suppressants, while antagonists have been used as antipsychotics and antidepressants. In spite of its many important central effects, most 5-HT is found in the periphery, where it regulates gastric motility, bladder control, and cardiovascular function.⁵⁷

The serotonin reuptake transporter (SERT) provides another pharmacological target. Inhibitors of SERT have been widely used as antidepressants and are generally referred to as selective serotonin reuptake inhibitors (SSRIs), a class of drugs which is discussed at length

in section 1.3.2. Similar to the use of L-DOPA to increase central concentrations of DA, dietary 5-HTP is also used to supplement the feedstock available for 5-HT biosynthesis in order to treat depression. The efficacy of this approach, however, is debated.⁵⁸

Serotonin is broken down by the action of MAO-A and aldehyde dehydrogenase (Fig. 1.14). The principal metabolite is 5-hydroxyindoleacetic acid (5-HIAA), and elevated levels of 5-HIAA in the urine may be indicative of bowel cancer in healthy individuals owing to the prevalence of 5-HT in the gut. Excess 5-HIAA has also been associated with CNS disorders such as autism, while diminished 5-HIAA is associated with violent behaviour.⁵⁹

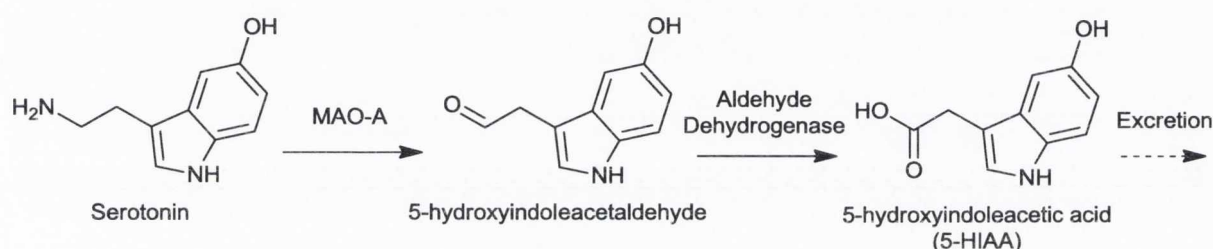


Fig. 1.14. Catabolic pathway of serotonin.

Melatonin is generally regarded as less important than 5-HT within the CNS; however, it does play an important role in the regulation of circadian rhythms, sleep, memory and mood. Two melatonin receptors have been identified, dubbed Mel_{1A} and Mel_{1B}. Both are found throughout the CNS, however the Mel_{1B} receptor is also found in the retina, where it may regulate the light-dependent nature of circadian rhythms. Melatonin agonists, such as agomelatine (Fig.1.23, section 1.3.3), have recently been developed for the treatment of sleep disorders and as antidepressants.⁶⁰ Unlike 5-HT, melatonin is broken down by cytochrome enzymes, and several of the metabolites produced in this way exhibit pharmacological activity at the Mel and 5-HT receptors. The catabolic pathway of melatonin clearly diverges from the MAO and COMT mediated pathways utilised for 5-HT and the catecholamine NTs, and research into the reason behind melatonin's unique mode of metabolism is ongoing.⁶¹

The trace amines are a class of NTs closely related to the monoamines which includes phenethylamine, octopamine, tyramine and tryptamine (Fig. 1.15). Although their central concentrations account for only 1% of biogenic amines, the trace amines have been extensively studied in light of their unique behavioural and physiological effects. Their biosynthesis stems from the action of amino acid decarboxylase on the same amino acids used in the production of the monoamines, and they exhibit affinity for many of the

monoaminergic receptors. However, their effects are sometimes contrary to that of the monoamine NTs; for instance, while tryptamine is a 5-HT agonist,⁶² intra-hypothalamic injection of tryptamine produces hyperthermia while administration of 5-HT causes hypothermia in rats.⁴⁷ In 2001, a family of receptors was identified which appeared to bind preferentially to the trace amines.⁶³ While these trace amine associated receptors (TAARs) are increasingly recognised as important modulators of NT release within the CNS,⁶⁴ further research is needed to establish their full biochemical significance.

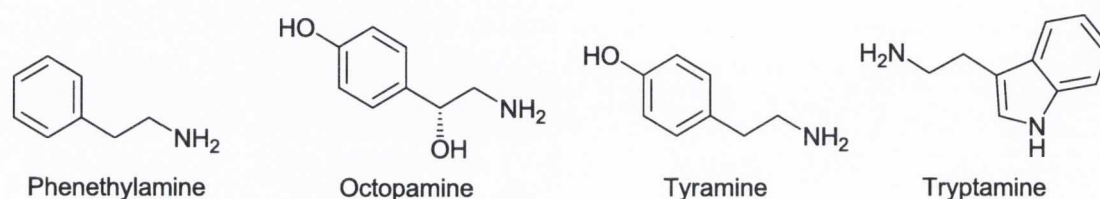


Fig. 1.15. Chemical structures of several of the trace amine NTs.

1.2.3 The Monoamine Hypothesis

In 1965 Schildkraut,⁶⁵ Bunney and Davis⁶⁶ formulated the ‘Catecholamine Hypothesis of Affective Disorders’ in order to explain the effectiveness of the monoamine oxidase inhibitor (MAOI) and tricyclic (TCA) classes of antidepressants. Experiments had shown that the MAOIs obstructed the breakdown of NTs, while the TCAs prevented their reuptake. The antidepressant effect, they argued, is concomitant with an increase in catecholamines in the synapse; therefore depression must be caused by a depletion of catecholaminergic NTs. Further evidence for their seminal hypothesis came in the form of the antipsychotic drug reserpine. Pharmacological studies had shown that the administration of reserpine led to a depletion of catecholamine NTs within the brain, and in accordance with their hypothesis, depression was commonly associated with its usage.⁶⁷

The catecholamine hypothesis was challenged in 1969 when Carlsson showed that certain mood-elevating drugs actually led to a decrease in catecholamine NTs and suggested that these drugs might act instead via 5-HT receptors.⁶⁸ In the same year, Glassman demonstrated the clinical effectiveness of combining MAOIs with the 5-HT precursor L-tryptophan.⁶⁹ It was theorised that depression might stem from a reduction in indoleamine NTs, and soon thereafter 5-HT became the target for intensive antidepressant research. To this day, 5-HT remains the NT most closely associated with depression, and a large volume of research continues to investigate the relationship between the indoleamine NTs and mood.^{70,71}

In its modern formulation, the monoamine hypothesis states that neither the indoleamines nor the catecholamines are exclusively responsible for depression, and that depletion in either might bring about symptoms of the illness. Some researchers argue that each NT is associated with a characteristic symptomology; thus, reduced 5-HT levels might lead to a depressed mood; reduced NA would lead to diminished energy and alertness, while a reduction in DA would lead to anhedonia.⁷² Indeed, virtually every clinically used antidepressant drug can be shown to act upon monoamine systems within the CNS.⁷³ Therefore, impairment in central monoaminergic function has found broad acceptance as a working aetiology of depression.

While most researchers would agree that a simple deficit in monoaminergic NT function constitutes an incomplete description of the disease,^{74,75} in the face of the startling complexity of the CNS the monoamine hypothesis provides such testable indicators as monoaminergic NT concentrations and drug-receptor affinities. Therefore, while the capability of the monoamine theory to describe the underlying mechanics of depression may remain in doubt, there can be little question of its utility in the development of safer and more effective antidepressant drugs.

1.2.4 Neuroplasticity Theories

For a large part of its history, there existed a consensus within neuroscience that brain development ceased after childhood. However, over the past twenty years research has revealed that neurogenesis and changes to brain structure continue throughout a person's life, and that such changes are essential to the proper functioning of the brain.⁷⁶ The term 'neuroplasticity' refers to the structural and functional adaptations that take place within the brain in response to stresses and the outside environment.

Accordingly, one major structural change observed in the brains of depressed patients is atrophy of the hippocampus. In the early 2000's, Sapolsky showed that increased levels of stress-related glucocorticoids within the CNS can bring about a reduction in hippocampal volume, and suggested that this mechanism may be responsible for the onset of depression.⁷⁷ Treatment with antidepressants has been shown to stimulate neurogenesis in the hippocampus, and the fact that antidepressants often require several weeks to take effect might be explained by the time taken for hippocampal neurons to regrow.⁷⁸ However, the hippocampus remains more closely associated with learning and memory than with emotion,

casting doubt on the causative effect of hippocampal atrophy on depressed mood.⁷⁹ Nonetheless, as a central component of the working memory, atrophy of the hippocampus provides a cogent explanation for the cognitive deficit associated with depression.

As the biochemistry of neuroplasticity began to be elucidated, some researchers shifted their attention to neurotrophic factors; small protein signalling molecules which regulate the growth, repair and differentiation of neurons. Reduced levels of brain-derived neurotrophic factor (BDNF) and vascular endothelial growth factor (VEGF) are associated with hippocampal atrophy and depression, and administration of BDNF has been shown to exhibit antidepressant-like effects in animal models.⁸⁰ The administration of both clinical antidepressants such as fluoxetine and electroconvulsive therapy has been shown to elevate levels of BDNF, suggesting that antidepressants may work by upregulating the expression of BDNF and promoting neuroplasticity in the brain.⁸¹ In a 2008 study, Parada demonstrated that neither antidepressant drugs nor exercise were effective in alleviating depression in the absence of the tyrosine kinase receptor responsive to BDNF (TrkB) using an animal model, providing further evidence that BDNF-promoted neurogenesis is an essential component of the antidepressant effect.⁸²

Given that synaptic NT concentrations are rapidly affected by antidepressant drugs and yet their positive effects upon mood, behaviour and cognition can take weeks to emerge; a growing body of evidence suggests that their effectiveness stems from slower, neurobiological changes rather than an immediate biochemical response. This hypothesis is supported by the effectiveness of tianeptine, an antidepressant similar in structure to the TCAs which has little effect upon monoaminergic NTs, but with significant effects upon neuronal plasticity (Fig. 1.16).

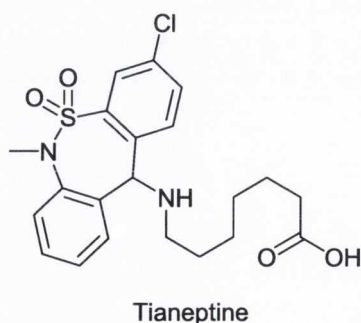


Fig. 1.16. Chemical structure of the atypical antidepressant tianeptine.

As with the monoaminergic antidepressants, chronic rather than acute treatment with tianeptine is needed to produce any antidepressant effect.⁸³ However, unlike other antidepressants, administration actually reduces concentrations of 5-HT within the synapse. Tianeptine nonetheless behaves as an antidepressant *in vivo*, and this activity has been attributed to its capacity to diminish hippocampal apoptosis and to promote the release of BDNF,^{84,85} potentially via interactions with excitatory glutamate receptors.⁸⁶

It has been postulated that the monoaminergic antidepressants, tianeptine and BDNF ultimately exert their effects through the phosphorylation of cAMP response element-binding (CREB) transcription factor. The binding of NTs to metabotropic receptors gives rise to increased concentrations of second messengers, while BDNF initiates the MAPK/ERK pathway. These biochemical cascades activate the phosphorylation enzymes Protein kinase A (PKA), CREB kinase and calmodulin-dependent protein kinase (CAM) to bring about the phosphorylation of CREB. Phosphate-bound CREB-P then binds to DNA to upregulate the expression of the BDNF gene and the anti-apoptotic protein B-cell lymphoma 2 (BCL-2) gene. BDNF-promoted neuroplasticity, coupled with reduced apoptosis from BCL-2, then gives rise to increased neurogenesis, thereby ameliorating depression (Fig. 1.17).⁸⁷

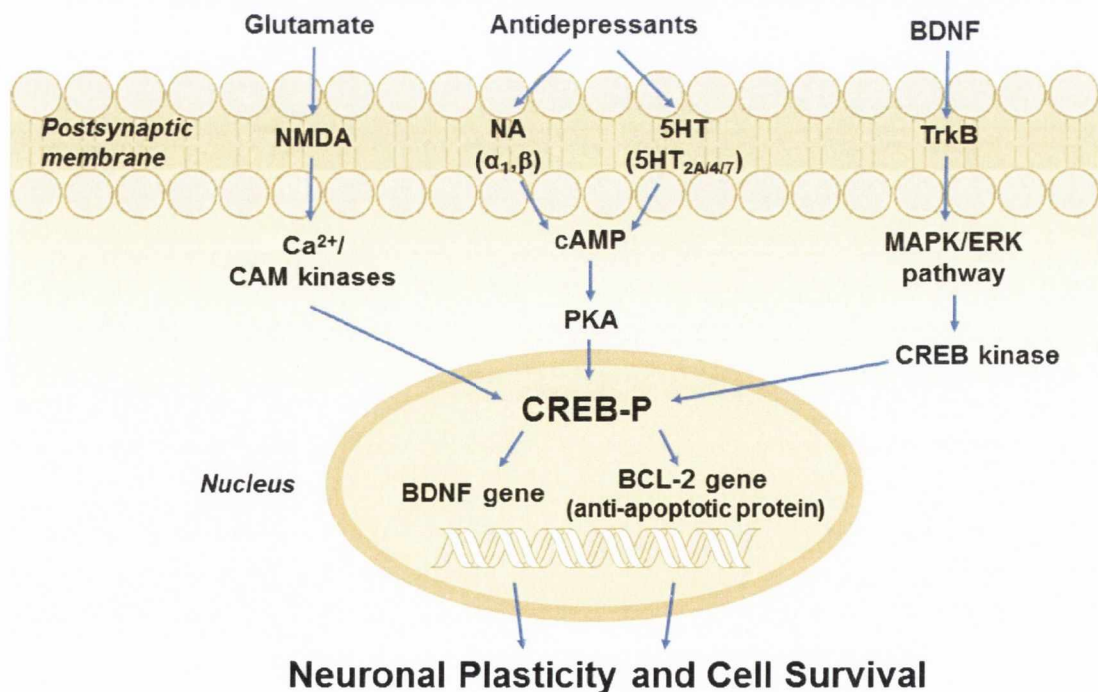


Fig. 1.17. Biochemical pathways linking neuroplasticity and antidepressants.

Adapted from B. Leonard, 2010 and R. C. Duman and C. D'Sa, 2002.^{87,88}

1.2.5 The Cytokine Hypothesis

Although neuroplasticity theories represent a significant development since the monoamine hypothesis, the insights they provide are linked mainly to the neuropathology of depression with fewer details regarding initiation of the illness. Moreover, there is no explanation as to the concurrent health issues of comorbidity; such as increased mortality due to heart disease, diabetes, cancers and autoimmune diseases.

Recognising that both stress and depression are associated with a reduction in immune function, the cytokine theory posits that the hypersecretion of cytokines may be responsible for the initial onset of depression.⁸⁹ In times of stress, pro-inflammatory cytokine production increases and the blood-brain barrier becomes more permeable, allowing peripheral cytokines to cross into the CNS⁹⁰ where microglia provide a further source of cytokines.⁹¹ The acute response to the elevated presence of cytokines involves an increase in neuronal excitation and neurotransmitter activity;⁹² however, chronic inflammation results in the opposite effect, leading to a long-term decrease in monoaminergic neurotransmission, decreased neurogenesis and an increase in neural apoptosis (Fig. 1.18).

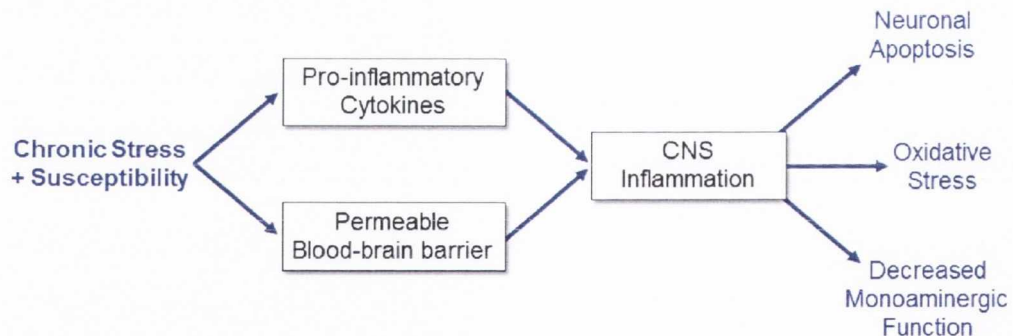


Fig. 1.18. General schema for the onset of depression as per the cytokine hypothesis.

Depressed patients have been shown to exhibit elevated levels of pro-inflammatory cytokines, in line with the cytokine hypothesis. Further evidence comes from the fact that prolonged treatment of patients with interferons (proteins which activate the immune response) is known to induce depression.⁹³ Initially, depression may be a normal behavioural response to stress or sickness; thus, symptoms of depression are commonly observed in patients recovering from long-term illness, or those with arthritis or multiple sclerosis. However, chronic depression is associated with lasting inflammation, resulting in oxidative

stress throughout the CNS and the periphery, increasing the risk of Alzheimer's disease, cardiovascular problems and other comorbidities associated with depression.⁹⁴

Research suggests that many of the antidepressant drugs in clinical use may actually function as immunomodulators in the CNS.⁹⁵ It has been proposed that future antidepressants which induce the production of anti-inflammatory cytokines or block the release of pro-inflammatory cytokines could provide a non-monoaminergic target for the treatment of depression.⁹⁶ However, one recent study showed that treatment with anti-inflammatory drugs actually reduced the overall effectiveness of clinical antidepressants.⁹⁷ While there can be little doubt of a relationship between inflammation and depression, this study suggests that further research is needed to understand the interaction between inflammation and the CNS before effective drugs can be developed using this approach.

1.2.6 Theories of Depression: Application to New Treatments

Clearly, no single theory has yet emerged which can encompass the full aetiology of depression. However, it would be erroneous to conclude that the predominant theories at the time of writing are wholly inaccurate or incompatible. In fact, most theories provide a useful description of possible neurological and biochemical dysfunctions which may give rise to depression. Given that depression is a heterogeneous condition with symptoms varying widely from one patient to another, it is likely that the aetiology of depression is similarly variable and that the underlying biology might differ from patient to patient.

The variable nature of the disease is one reason why antidepressant treatment remains unsuccessful for many patients. Both the cytokine and neuroplasticity theories suggest that more effective treatments might emerge from a deeper consideration of neuronal biochemistry, and indeed the administration of BDNF gives rise to antidepressant-like results in animal models.⁸⁰ However, cessation of treatment with BDNF results in opiate-like withdrawal symptoms, proving the need for caution in the exploitation of novel biochemical pathways.⁹⁸ In spite of this caveat, new treatment options are clearly needed for the successful treatment of the burgeoning problem of depression.

Proponents of the monoamine hypothesis often suggest that antidepressant treatment should be tailored to reflect the symptomatology of the patient; thus, a person experiencing anxiety should be treated with medicines which boost 5-HT concentrations, while a patient suffering

from lethargy might respond better to drugs addressing the noradrenergic system.⁷² Given a wide enough arsenal of drugs targeting the various mechanisms of depression, a tailored approach to treatment might well prove successful.

However, the diagnostician must first identify which medication is suitable for a given patient and at present an ineffective prescription takes up to 14 weeks to be discovered. Encouragingly, recent experiments in the use of electroencephalography (EEG) biomarkers have successfully predicted which antidepressant will succeed for a given patient, with accuracy as high as 74%.⁹⁹ If biomarker technology proves successful and the pharmacopoeia of antidepressants can be expanded to provide as broad a spectrum of treatment options as possible, a vast improvement in the effectiveness of antidepressant treatment becomes a very realistic possibility.

1.3 Clinical Antidepressants

1.3.1 Early Antidepressants: The MAOIs and TCAs

In the early 1950s, the term ‘antidepressant’ was coined to describe the mood-elevating effects of the newly discovered anti-tuberculosis medications isoniazid and iproniazid (Fig. 1.19), with clinical trials suggesting improvements in up to two-thirds of depressive patients.¹⁰⁰ Shortly following this serendipitous discovery, Roland Kuhn identified similar effects using imipramine, the first tricyclic antidepressant (TCA).¹⁰¹



Fig. 1.19. Chemical structures of three early examples of antidepressant drugs.

As antidepressants began to be prescribed to the public, pharmacologists sought to discover their various physiological effects. Iproniazid was determined to be a potent monoamine oxidase inhibitor (MAOI), while imipramine was found to inhibit the proteins responsible for the reuptake of 5-HT, AD, NA, and DA; these discoveries would prove crucial to the development of the monoamine hypothesis. Notably, the antidepressant mode of action of isoniazid remains poorly understood, and in spite of its structural similarity to iproniazid, it does not appear to function as an MAOI.¹⁰²

In 1960, amitriptyline (Fig. 1.20) became the second TCA antidepressant to be developed, and it remains the most commonly prescribed TCA in clinical use today.¹⁰³ Through chemical modification of the tricyclic core and side-chain, a wide range of TCAs have since been discovered. Although many of these drugs exhibit DA reuptake inhibitor and NA/AD reuptake inhibitor (NERT) pharmacology, there are also examples of TCAs devoid of this activity. Trimipramine (Fig. 1.20), for example, is believed to function by strong antagonism of the H₁ histaminergic receptor, alongside some antagonist activity at the 5-HT₂, 5-HT₁, D₂ and α_{2A} receptors.¹⁰⁴

The MAOI class of antidepressants has also evolved to include not only hydrazine-containing structures such as iproniazid, but also drugs mimicking endogenous NTs such as tranlycypromine (a phenethylamine derivative) and etryptamine (a tryptamine derivative).

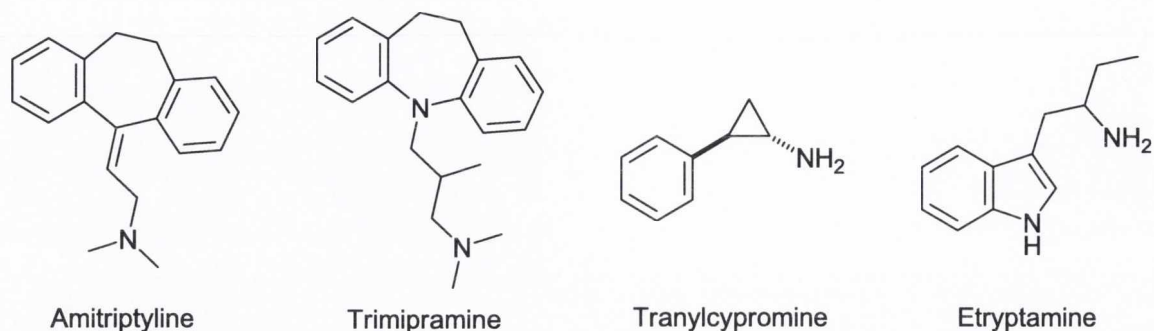


Fig. 1.20. Chemical structures of two TCA (*left*) and two MAOI (*right*) antidepressant drugs.

Today, the TCA and MAOI classes of antidepressants are no longer considered as first-line treatments owing to their propensity for serious and potentially fatal side effects. The TCAs frequently induce peripheral side effects attributed to their pharmacological activity at the muscarinic, histaminergic and α_1 adrenergic receptors. The severity of these effects ranges from dryness of the mucosal membranes and dizziness to seizure, apnea and cardiac arrhythmia. The overdose potential is also high, as there is little difference between the therapeutic and toxic doses.¹⁰⁵

The MAOIs are also problematic, as the action of MAO is required for the breakdown of dietary amines. Tyramine-containing foods such as cheese and interaction with other medications can give rise to hypertensive crisis, a life-threatening condition in which the blood pressure rises suddenly leading to damage to the major organs. Even if these interactions are carefully avoided, the side effects of MAOIs include weight gain, mania and sexual dysfunction. Compounds which selectively target MAO-A (responsible for the breakdown of 5-HT, NA and DA) or MAO-B (which breaks down DA and trace amines) have since been developed in an effort to improve the therapeutic profile of MAOIs. Although some side effects are reduced by selectively targeting MAO-A, many side effects are unaffected and the danger of drug interactions remains high. As a result of these dangers, the MAOI and TCA antidepressants are usually limited to the treatment of atypical and unresponsive depression.¹⁰⁴

1.3.2 The Rise of the SSRIs

For many clinicians, the selective serotonin reuptake inhibitor (SSRI) class of antidepressants now represents the first-line of pharmacotherapy owing to their effectiveness, low overdose potential and comparatively mild side effects. The history of the SSRIs may be traced back to the work of Carlsson in the 1960s, who suggested their development based on clinical observations with the TCA-type antidepressant clomipramine.^{68,106} Unlike other TCAs which were either stimulating or sedating, clomipramine exhibited neither of these symptoms and was primarily an anxiolytic. Pharmacological studies provided a clue to its unique characteristics; while most TCAs inhibited NA reuptake, clomipramine had a striking affinity for the 5-HT reuptake protein SERT.

Around the same time, several antihistamine drugs were also found to have antidepressant effects which correlated to an affinity for SERT, such as brompheniramine. Through chemical modification to its structure, Astra AB (later Astra-Zeneca) worked closely with Carlsson to develop zimelidine (Fig. 1.21), the first drug designed to act as an SSRI.¹⁰⁷ Although zimelidine was launched in 1982, it was soon removed from the market owing to a risk of serious neurological side effects.¹⁰⁸

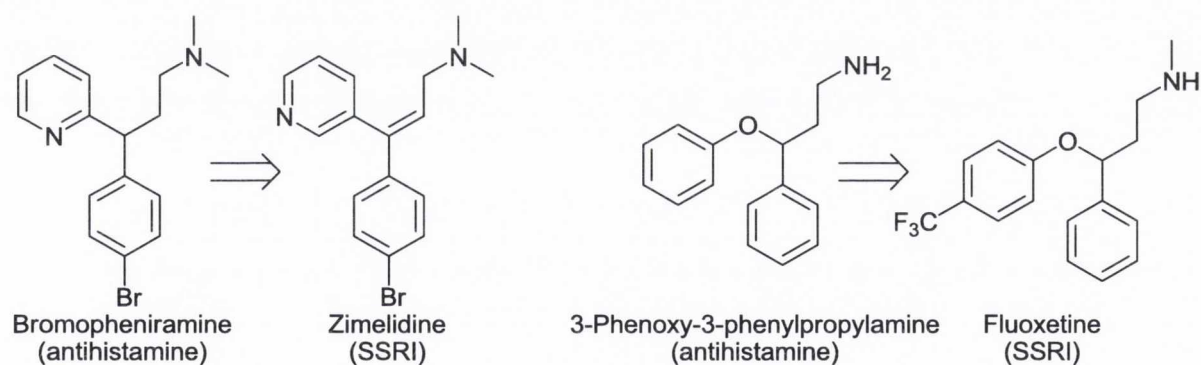


Fig. 1.21. Chemical structures of two SSRI-type antidepressant drugs showing the antihistamines from which they were developed.

In the wake of zimelidine, several other SSRIs were launched including Eli Lilly's blockbuster fluoxetine (Prozac; Fig. 1.21). Following a project examining derivatives of the research antihistamine 3-phenoxy-3-phenylpropylamine, fluoxetine was launched in 1987 and became the first drug to be marketed using the term 'SSRI'. During the 1990s, the SSRI class would go on to supersede the older classes of antidepressants, and their development would mark the beginning of the modern approach to antidepressant drug design.

In contrast with the TCA and MAOI antidepressants, the SSRIs are characterised by an improved therapeutic index and greatly reduced overdose potential, making them safer to use than the older antidepressants. However, the SSRIs still incur many serious side effects. In spite of their being termed 'selective', many SSRIs also interact with other proteins; fluoxetine for example exhibits significant antagonism at the 5-HT_{2C} serotonin receptor.¹⁰⁹ Whether these off-target interactions or the intrinsic mode of action is responsible for their side effects is unknown; these include gastrointestinal and CNS disturbances, as well as the possibility of sexual dysfunction.¹¹⁰ Furthermore, as with the TCAs and MAOIs, SSRIs suffer from a slow onset of effect, which incurs the danger of allowing the patient's depression to deepen before any therapeutic effect can take place.¹¹¹

1.3.3 Current and Future Antidepressants

While the SSRIs maintain a significant market share today, their sales have been overshadowed by the newer non-tricyclic serotonin-noradrenaline reuptake inhibitor class of drugs (SNRIs). These drugs target both SERT and the noradrenaline reuptake transporter (NERT), and appear to be slightly more efficacious than the SSRIs.¹¹² Both of the best-selling drugs at the time of writing, venlafaxine and duloxetine, are SNRIs (Fig. 1.22). The third biggest seller is escitalopram, an SSRI which is a single-enantiomer variant of the racemic SSRI drug citalopram.¹¹³

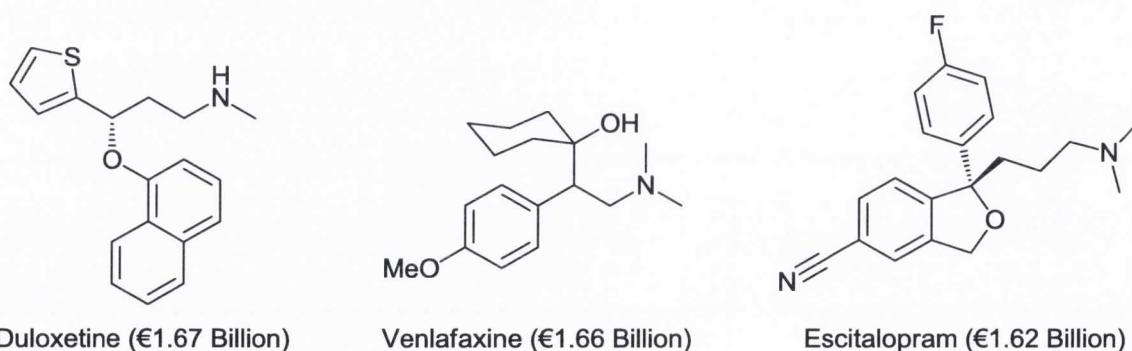


Fig. 1.22. The top three best-selling antidepressants including their sales figures for 2009.

In spite of their improved effectiveness, SNRIs may exhibit an increased risk of suicide¹¹⁴ and suffer from many of the same side effects as the SSRIs. In addition, many patients ceasing treatment with SNRIs suffer from what has been termed 'discontinuation syndrome', a condition whose effects include dizziness, the sensation of electric shocks in the brain, and

severe nausea. Although SSRIs also incur the risk of withdrawal effects, the risk appears to be somewhat worse for the SNRI class of drugs.¹¹⁵

Examining the research pipeline of major pharmaceutical companies provides a picture of the future generation of antidepressants. Compounds in Phase I/II trials include Pfizer's CP-601,927 which is a partial agonist of the $\alpha_4\beta_2$ nicotinic receptor, an excitatory acetylcholine receptor widespread in the CNS. Meanwhile, AstraZeneca are developing a compound called AZD6765 which acts as an NMDA receptor antagonist. GlaxoSmithKline are developing Orvepitant, an antagonist of the Neurokinin-1 neuropeptide-type receptor. It is encouraging to note that many of these compounds exhibit new modes of action, and that the industry is clearly thinking beyond the monoamine hypothesis.

Phase III drugs and compounds awaiting FDA approval lie at the bridge between current and future drugs. Many of these combine traditional modes of action with novel pharmacological profiles. Agomelatine (Servier/Novartis) is a melatonin receptor agonist which incorporates some activity at the 5-HT receptors (Fig. 1.23) while BCI-952 (BrainCells Inc.) is a combination of buspirone (a 5-HT_{1A} agonist) and melatonin. Aripiprazole is a 5-HT_{1A} and D₂ (dopaminergic) agonist. While some companies are testing the waters with combined pharmacological approaches, other drugs are still rooted in the SSRI approach. Forest Labs' vilazodone gained FDA approval in January 2011 and acts as both an SSRI and a 5-HT_{1A} agonist. It is interesting to note the popularity of the aryl piperidine nucleus, a fragment with affinity for several CNS receptors.¹¹⁶ While novel antidepressants are clearly on the horizon, it is likely that monoaminergic drugs may be prevalent for some years to come.

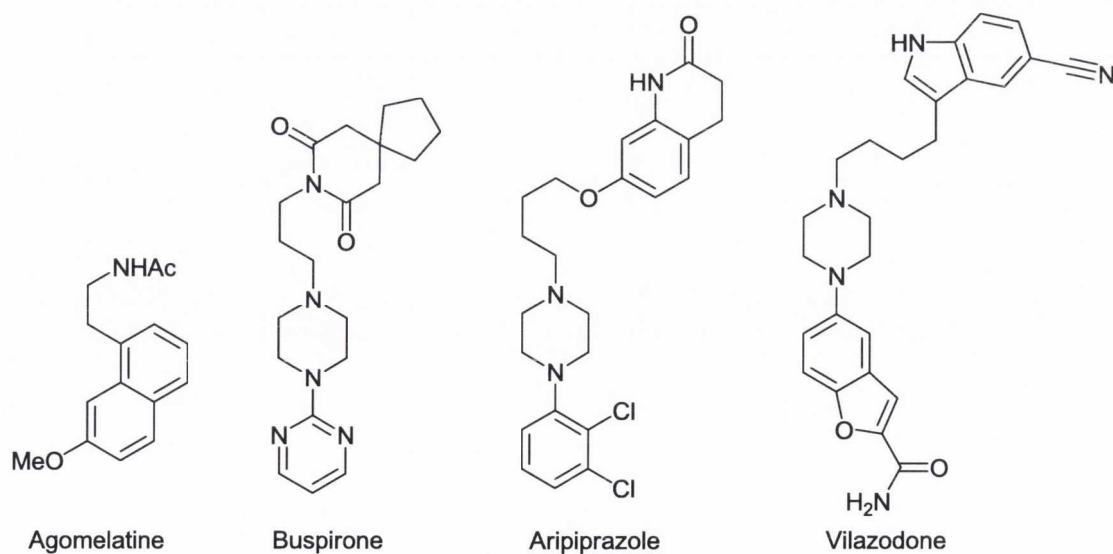


Fig. 1.23. Chemical structures of several forthcoming antidepressants at the time of writing.

1.4 The Alpha 2 Adrenoceptor

1.4.1 Adrenoceptor Structure and Function

Adrenoceptors (ARs) are membrane-bound proteins found throughout the CNS and in the periphery which are activated by the endogenous ligands AD and NA. Their phylogeny places them within the superfamily of rhodopsin-like G-protein coupled receptors (GPCRs), all of which share the common structural motif of seven transmembrane alpha-helices, combined with an intracellular domain to which a G-protein binds when the receptor is in the resting state. The G-proteins associated with rhodopsin-like GPCRs are heterotrimeric proteins made of up three subunits labelled α , β and γ . When an agonist interacts with the GPCR binding site, the receptor takes on a new conformation, causing the G-protein to become phosphorylated and to dissociate from the GPCR. The α subunit and the $\beta\gamma$ dimer also dissociate from each other and proceed to interact with second messenger proteins in order to initiate various biochemical cascades. After a time, the α subunit is dephosphorylated and the G-protein returns to the GPCR and resumes its resting position (Fig. 1.24). Different GPCRs couple to different G-proteins, each of which has its own effects upon second messenger pathways; this allows each GPCR to elicit different physiological responses.

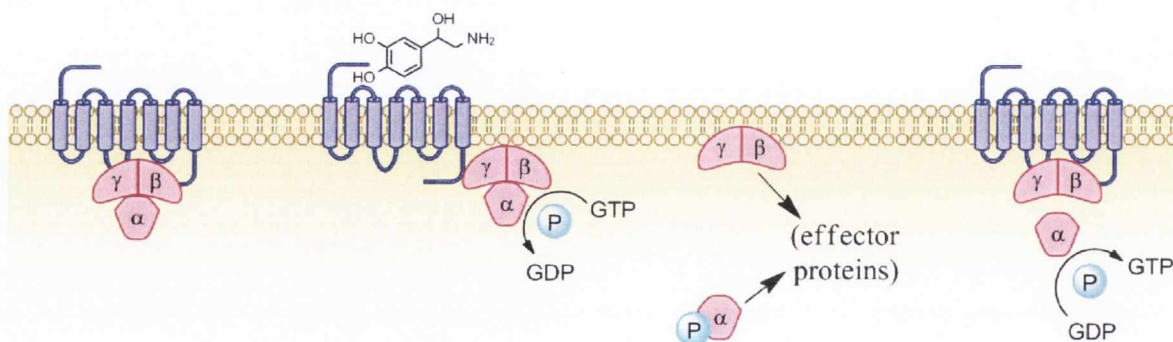


Fig. 1.24. General mechanism of action of GPCRs.

The ARs have been divided into the α_1 , α_2 , and β families according to pharmacological and molecular cloning data.¹¹⁷ While the β -ARs are important in the heart and lungs, the α_1 - and α_2 -ARs are found both in the periphery (see Section 1.2.2) and in the CNS. Of these, the α_2 -ARs are especially significant as a target for antidepressant drugs.

The α_2 -ARs are divided into three subtypes; the α_{2A} , α_{2B} , and α_{2C} subtypes (a fourth subtype termed α_{2D} is found in several species but is absent in man).¹¹⁸ Thus far, the complete

pharmacological and functional evaluation of each subtype has been hindered by a lack of highly subtype-selective ligands; this is possibly a result of the high degree of homology exhibited by the α_2 -AR subtypes.¹¹⁹ Nonetheless, differences in their distribution within the CNS indicate the possibility of differing roles for each subtype; most significantly, the α_{2A} subtype has been closely associated with noradrenergic neurotransmission in the human pre-frontal cerebral cortex.¹²⁰ Increased numbers of α_{2A} -ARs in a high affinity conformation have also been found in the post-mortem brains of suicidal depressive patients while α_{2C} -ARs in the same patients were comparatively unaffected, suggesting that the α_{2A} -AR subtype may play an important role in depression.¹²¹

Although little is known about the α_{2B} receptor, it appears to be the least prevalent of all three subtypes within the brain, where its localisation within the thalamus may contribute to the sedating effects of α -AR agonist drugs such as anti-hypertensives. However, in the periphery the α_{2B} subtype actually appears to increase blood pressure.¹²² As with the α_{2A} subtype, the α_{2C} receptor is also found throughout the pre-frontal cortex in man,¹²³ while in the periphery, the α_{2C} -AR is an important mediator of venous vasoconstriction.¹²⁴

Despite the recent crystallographic structure determination of the β_2 -AR,¹²⁵ the complete structure of the α_2 -AR remains obscure. Although the β_2 and α_2 -AR likely share structural similarity,¹²⁶ a brief examination using the protein sequence alignment tool BLASTP¹²⁷ shows a homology of just 26% to 49% between the α_2 -AR and the β_2 -AR, depending on the subtype chosen for comparison. Therefore, homology studies can provide only an approximate picture of the α_2 -AR. Nonetheless, the β_2 -AR crystal structure highlights structural features likely to be shared by all adrenoceptors (Fig. 1.25).

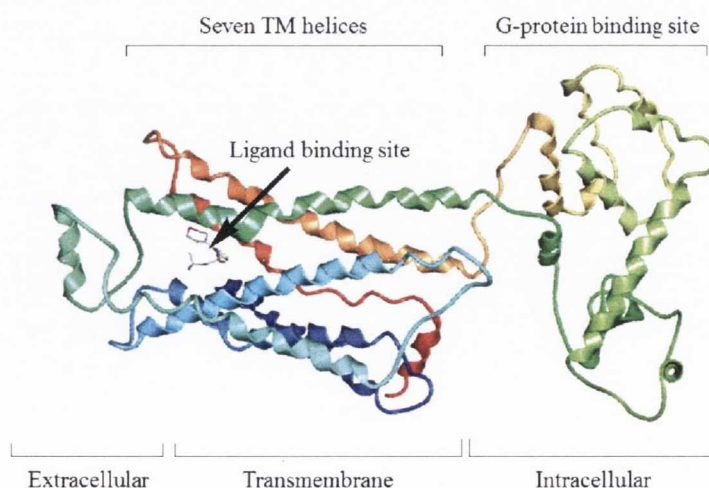


Fig. 1.25. Structural features of adrenoceptors as per β_2 -AR x-ray data (PDB code 3D4S).¹²⁸

In the absence of an X-ray crystal structure, the binding site of the α_2 -AR has been examined using site-directed mutagenesis (SDM) experiments which suggest ligand-receptor interactions for several residues. Homology modelling studies have been combined with SDM data to provide a qualitative model of ligand-receptor binding (Fig. 1.26).

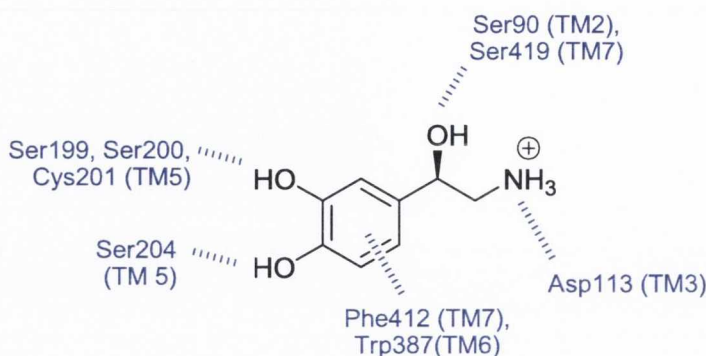


Fig. 1.26. Putative binding interactions of the endogenous α_2 -AR ligand NA as evidenced by combined SDM and homology modelling data.

Foremost among these interactions is the salt bridge formed between the protonated ligand amine and the highly-conserved aspartate residue Asp113; SDM studies with α_{2A} demonstrate that substitution of this residue for arginine reduces agonist binding by a factor of almost 500 eliminates all affinity for the α_2 -AR antagonist yohimbine.¹²⁹ Mutation of the Phe412 residue also results in a 450-fold reduced affinity for yohimbine, and homology models suggest that this residue (and several other residues, depending on the subtype) define the binding pocket around the incumbent ligand, in tandem with Trp387.¹³⁰ Several residues are thought to undergo hydrogen bonding to the catecholic hydroxyl groups, with Ser204 binding the *para* hydroxyl moiety while either Cys201, Ser200 or Ser199 may interact with the *meta* position.¹³¹ SDM studies also support the interaction of Ser90 and/or Ser419 with the *beta*-hydroxyl group of catecholamine-type ligands.¹³²

All three subtypes of the α_2 -AR couple to the G_i heterotrimeric G-protein, the primary function of which is to inhibit adenylyl cyclase. Activation of α_2 -ARs therefore brings about a reduction in the second messenger cAMP. In presynaptic α_2 -ARs, this inhibits the influx of Ca^{2+} needed for vesicle fusion and exocytosis, preventing the release of NT into the synapse. Thus, presynaptic α_2 -ARs function as autoreceptors which react to the presence of NA or AD in the synapse by inhibiting the release of further NT (Fig. 1.27).¹³³

Interestingly, increased numbers of presynaptic α_2 -ARs have been found in the hippocampus and cerebral cortex of patients suffering from major depression.¹³⁴ Moreover antagonism of

presynaptic α_2 -ARs results in increased levels of NA, 5-HT and DA within the synapse.¹³⁵ This makes the α_2 -AR an attractive target for the treatment of not only depression but also of other disease states responding to changes in monoaminergic activity; agonists find clinical use as antihypertensives and analgesics,¹³⁶ while antagonists have been suggested as both antidepressants¹³⁷ and anxiolytics.¹³⁸

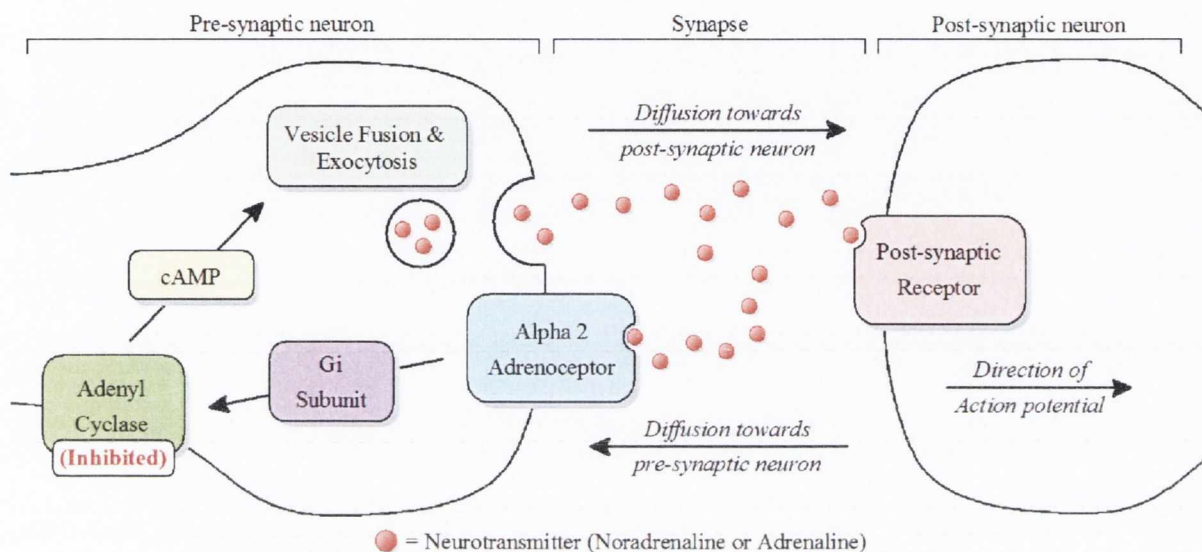


Fig. 1.27. The role of presynaptic α_2 -ARs in the inhibition of neurotransmitter release.

Postsynaptic α_2 -ARs are not so readily understood; as with other postsynaptic receptors they contribute to the complex processing abilities of neuronal networks. However, they may also have distinct functionalities in mood and cognition. One study demonstrated that low-level stimulation of postsynaptic α_2 -ARs improved the memory of ageing primates,¹³⁹ while other researchers conclude that interactions with postsynaptic α_2 -ARs may be necessary for the activity of some antidepressants.¹⁴⁰ While the presynaptic function of α_2 -ARs has historically been the target for antidepressants acting on α_2 -ARs, their postsynaptic role may become increasingly important as the nature of these receptors becomes elucidated.

1.4.2 Alpha 2 Adrenoceptor Antagonists

In the 1960s, research led Organon to the development of a new class of antidepressants exhibiting a novel mode of action. During a research program examining tetracyclic derivatives of the TCA class of drugs, researchers identified a compound (mianserin; Fig.

1.28) whose administration gave rise to antidepressant-like EEG data. At the time, a common pharmacological assay for antidepressant activity was the reserpine reversal test; rodents would be treated with reserpine and the compound under investigation would be administered to determine whether it could ‘reverse’ the effects of reserpine (such as sedation, hypothermia and akinesia).¹⁴¹ Surprisingly, mianserin failed this test. The researchers gradually came to realise that they had uncovered a new type of antidepressant, and subsequent clinical trials proved that mianserin was indeed effective against depression.¹⁴² In the 1970s it became evident that mianserin was a potent antagonist of the α_2 -AR and that its antidepressant effects were likely attributable to this unique pharmacology.¹⁴³



Fig. 1.28. Chemical structures of three tetracyclic α_2 -AR antagonist used as antidepressants.

Unfortunately, mianserin was later found to lower the white blood cell count of some patients, and in the wake of the controversy surrounding this potentially dangerous side effect, sales for the drug collapsed.¹⁰⁷ Today, a close analogue named mirtazepine is prescribed in its place (Fig. 1.28). In the Japanese marketplace, yet another analogue named setiptiline is used,¹⁴⁴ presumably owing to regulatory and marketing differences. As with mianserin, both mirtazepine and setiptiline were originally developed by Organon.

Thus far, these three drugs are the only α_2 -AR antagonists approved for the treatment of depression. Other potential applications of α_2 -AR antagonists include peripherally-acting drugs for cardiovascular illness and obesity, as well as CNS drugs for schizophrenia and neurodegenerative disorders.¹⁴⁵ As antidepressants, recent research has shown that mirtazepine exhibits a level of clinical efficacy similar to that of venlafaxine,¹⁴⁶ which is the best-selling antidepressant by sales at the time of writing. Although mirtazepine incurs such side effects as somnolence, weight-gain and dizziness,¹⁴⁷ these problems appear to be less common when compared with the SNRI class of drugs.^{148,149} Owing to their reduced tendency for side effects, combined with their novel pharmacological profile, the

development of novel α_2 -AR antagonists for use as antidepressants has been of considerable pharmacological interest.

Among the first class of compounds explored in the search for new α_2 -AR antagonists were analogues of the natural product alkaloid yohimbine. Both yohimbine and its epimer rauwolscine (Fig. 1.29) act as α_2 -AR antagonists and have been used clinically and in folk medicine for the treatment of sexual dysfunction. However, both compounds commonly incur such adverse effects as hypertension, anxiety and cognitive disturbances. These complications possibly stem from off-target interactions with both 5-HT receptors and the α_1 -AR,¹⁵⁰ prompting medicinal chemists to explore derivatives in the hope of maintaining the stimulating, α_2 -AR antagonist-like effects of yohimbine while reducing its side effects. In the search for a novel compounds for the treatment of cognitive disorders, Aventis Pharma developed the yohimbine-derived α_2 -AR antagonist RU-52583 as a potential antidepressant. However, this compound is no longer under active development (Fig. 1.29, **1**).¹⁵¹

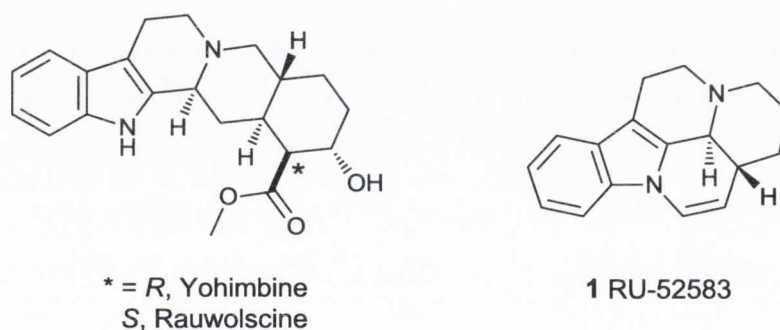


Fig. 1.29. Chemical structures of yohimbine and two closely related derivatives.

A variety of imidazole and imidazoline derivatives also exhibit promising affinity for the α_2 -AR. This motif appears in the α_2 -AR agonist clonidine, which is used clinically as an antihypertensive and anaesthetic (Fig. 1.30). However, the structurally-related clinical vasodilator tolazoline exhibits the opposite activity, acting as a non-selective α_1 -AR/ α_2 -AR antagonist. The phenomenon of small structural changes leading to an inversion of activity appears to be common among these derivatives, as evidenced by the diphenylmethyl-containing α -AR ligands prepared by Cordi *et al.* (Fig. 1.30, **2** and **3**).¹⁵² Our own research efforts also encountered this phenomenon; a topic which will be discussed in further detail in the following section. In a later study, Cordi *et al.* explored the possibility of combining α_2 -AR antagonist activity with 5-HT and NA reuptake inhibition using the imidazoline motif, suggesting that such agents might be potent antidepressants.¹⁵³

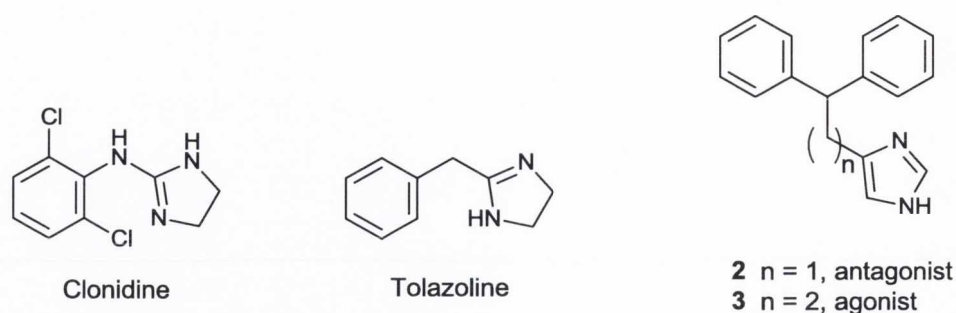


Fig. 1.30. Chemical structures of several imidazoline and imidazole-type α -AR ligands.

Compounds integrating the benzodioxane nucleus have also been explored, although prior to the 1980s, benzodioxane derivatives were widely thought to be non-selective α_1 -AR/ α_2 -AR antagonists, such as piperoxan (Fig. 1.31). Through the combination of the benzodioxane nucleus with the imidazolidine motif, Chapleo *et al.* created idazoxan,¹⁵⁴ a compound with striking affinity and selectivity for the α_2 -AR. Both idazoxan and its 2-methoxy derivative RX 821002¹⁵⁵ are extensively used today in adrenoceptor research.

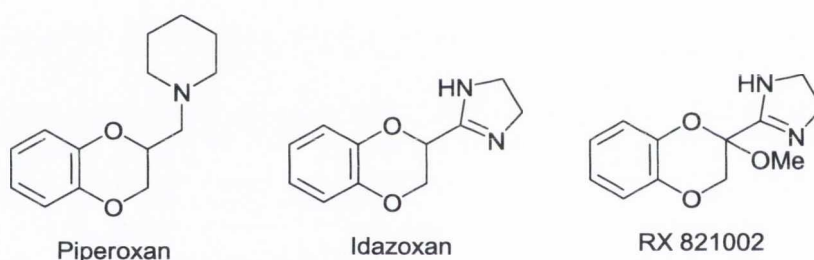


Fig. 1.31. Chemical structures of three benzodioxane-type α -AR antagonists.

A common feature in benzodioxane α_2 -AR ligands is a closely-tethered basic nitrogen atom (*cf.* the piperidine ring in piperoxan; Fig. 1.31). Fluparoxan is a potent benzodioxane-type α_2 -AR antagonist which makes this moiety rigid through cyclisation (Fig. 1.32). Although it was investigated as an antidepressant, fluparoxan is no longer under development.¹⁵⁶ Mayer *et al.* examined ring-opened analogues of fluparoxan and demonstrated that the benzodioxane ring is not essential for α_2 -AR antagonism (Fig. 1.32, **4**).¹⁵⁷

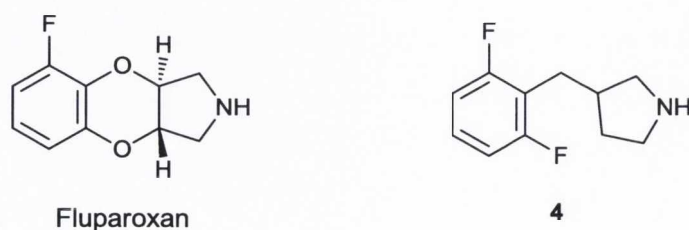


Fig. 1.32. Chemical structures of fluparoxan and a close analogue prepared by Mayer *et al.*¹⁵⁷

1.4.3 Previous Work within our Group

In a series of publications beginning in 2007, our research group has described the preparation and pharmacological evaluation of more than 80 molecules acting as ligands of the α_2 -AR.^{158,159,160} The general chemical structure of these compounds incorporates an aromatic ring directly bonded to either a guanidine or a 2-iminoimidazolidine moiety. Most of the variation within this series stems from different substitutions on the phenyl moiety; however, several dimers were also prepared, containing two aryl guanidine/2-iminoimidazolidine groups connected via a linker in the *para* and/or *meta* position of the aromatic ring (Fig. 1.33).

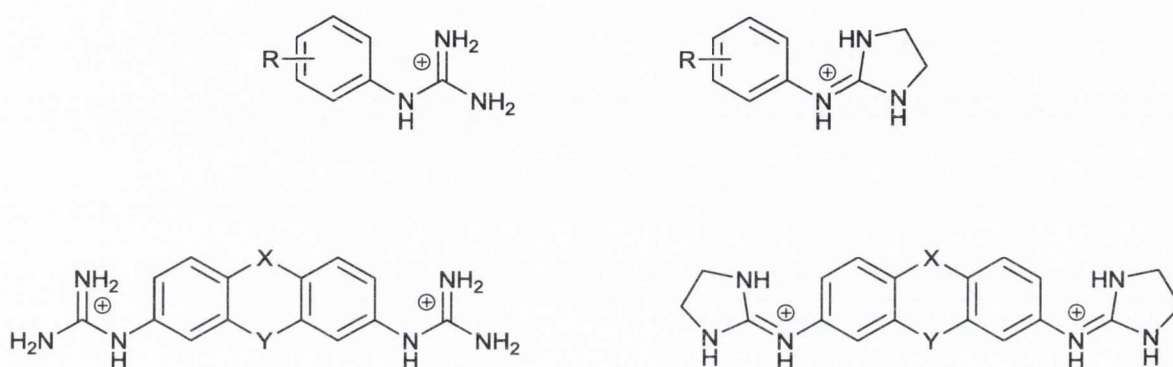


Fig. 1.33. General structures of α_2 -AR ligands prepared previously within our group.

For a complete list of structures, see Appendix A.

Each compound was tested for α_2 -AR affinity by determining the displacement of the α_2 -AR selective radioligand [3 H] RX 821002 (Fig. 1.31) in human prefrontal cortex. Compounds determined to have a high affinity in these experiments were further examined using functional [35 S]GTP γ S binding assay studies, which were also carried out in human prefrontal cortex. The [35 S]GTP γ S assay demonstrates the degree to which a G-protein is displaced upon ligand binding, thereby inferring whether the ligand acts as an agonist or an antagonist. Following this procedure, five compounds exhibiting *in vitro* high affinity and antagonist activity at the α_2 -AR were discovered (Fig. 1.34).

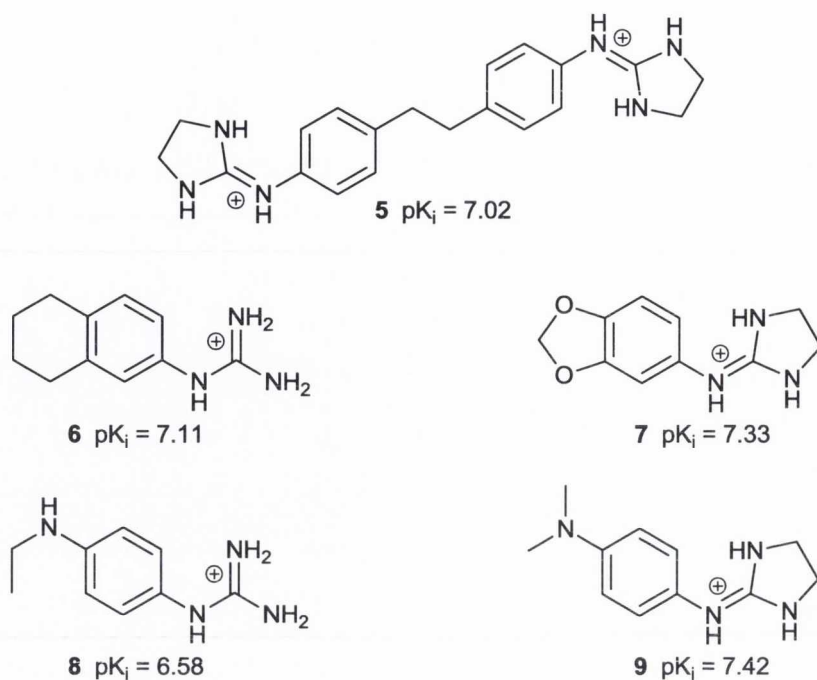


Fig. 1.34. High affinity α_2 -AR antagonists discovered in previous studies within our group.

These five lead compounds were also examined using *in vivo* animal studies. Microdialysis experiments were performed in which the compound is administered to a mouse with a capillary embedded in its brain; the capillary provides real-time information regarding the chemical composition of extracellular fluid in the CNS, typically via HPLC. In this manner it is possible to examine the effects of a given compound on NT release in a live animal. Behavioural experiments were also carried out; thus, in the tail suspension test (TST), a mouse is treated with the compound and held by the tail; the length of time the animal exerts motility while in this position (demonstrating a will to escape) is taken as an indicator of antidepressant activity.¹⁶¹ The forced swim test is another behavioural assay in which the animal is placed in a pool of water from which it cannot escape; the time until the animal retires from swimming is taken as a measure of its emotional state.²⁵⁰

While microdialysis studies confirmed the ability of all five compounds to increase central NA concentrations, only compounds **6** and **8** exhibited antidepressant activity using behavioural assays, in which both compounds exceeded the performance of the SSRI fluoxetine (results awaiting publication).¹⁹³ The use of intraperitoneal administration in some of these experiments also demonstrated the ability of this class of compounds to penetrate the blood-brain barrier (BBB).

In spite of the large quantity of data collected during these experiments, it has thus far proven difficult to establish structure-activity relationships (SAR) for this series of compounds. On average, the aryl-2-iminoimidazolidine species exhibit slightly higher affinities for the α_2 -AR. However, behavioural experiments have thus far found only guanidine derivatives to act as antidepressants *in vivo*. There is also contradictory information regarding the structural features behind antagonist versus agonist activity; in the case of the tetrahydronaphthalene derivative **6**, changing from a guanidine to a 2-iminoimidazolidine moiety inverted the activity to produce agonist **10**. However, in the case of the 2-iminoimidazolidine antagonist **9** the introduction of a guanidine yields the opposite result, producing agonist compound **11** (Fig. 1.35).

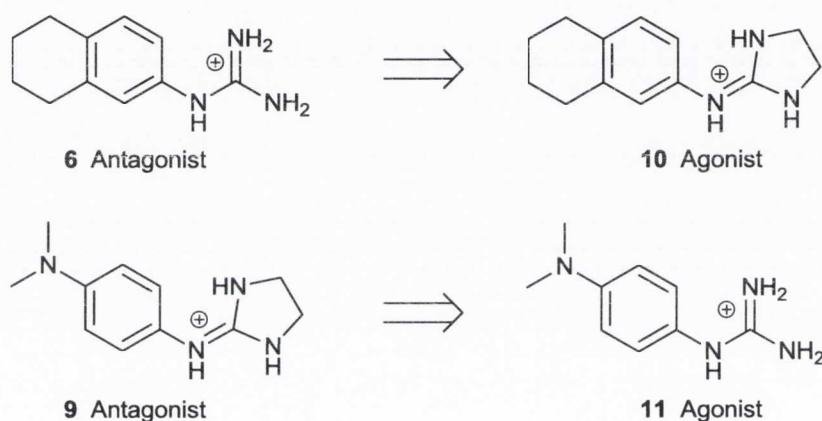


Fig. 1.35. Four compounds which exemplify the difficulties in establishing reliable SAR data regarding the structural origins of agonist versus antagonist activity.

Clearly, deeper analysis is required if these results are to be fully understood. Although our previous studies failed to elucidate exactly which structural features are necessary to construct high affinity α_2 -AR antagonists, they nonetheless produced promising results in the form of compounds **6** and **8**, both of which are under further investigation as potential antidepressants. For future studies, in the absence of X-ray crystallographic data for the α_2 -AR, it will be necessary to adopt a ligand-based drug design approach. Thankfully, our previous work provides a suitable volume of data for the construction of quantitative structure-activity relationships (QSAR).

1.5 Comparative Molecular Field Analysis

The purpose of any SAR study is to relate variations in activity within a series of molecules to variations in their structure; a QSAR study provides a quantitative schema of the relationship between structure and activity. Comparative molecular field analysis (CoMFA) is a QSAR technique which correlates variations in activity to the electrostatic and steric force fields surrounding these molecules. Because these force fields are determined within three-dimensional space, CoMFA provides a 3D picture of which electrostatic and/or steric features correlate to favourable and unfavourable activity. As such, CoMFA is referred to as a 3D-QSAR technique.

The starting point for a CoMFA study is the selection of a set of molecules for which experimental data describing their activity is known (typically, pK_i values are used). This data should be internally consistent - ideally acquired within a single laboratory - and should span across a wide range of activity; a range of at least three pK_i values is often prescribed. A small, representative subset of molecules should be assigned to a test set, and only the remaining molecules (the training set) are used to construct the model. When the model is complete, activity values will be predicted for test set compounds and compared with experimental values in order to validate the model's predictive power.

Three-dimensional structures must be available for every molecule involved; these may be obtained experimentally or generated using molecular or quantum mechanical methods. The training set structures are aligned to maximise the overlap of steric bulk and of analogous functional groups; rotatable torsional angles are adjusted as necessary. This alignment is the single most important factor in assembling a CoMFA model; in studies where the bioactive conformation is known this data may be used to align the structures, however in the absence of receptor data pharmacophoric elements can also be used for alignment.

The energy of interaction between a steric/electronic probe and each molecule in the training set is then calculated at regular intervals (an interval of 2 Å is typical) within a 3D grid surrounding the molecule. Generally, the Coulombic potential is used to describe electrostatic interactions using a positively charged probe atom. These values are produced according to equation 1.1, in which q_i and q_j represent the charges on the probe atom and the electrostatic potential (ESP) at a given point in the space surrounding the molecule, respectively. The distance between the two point charges is d_{ij} , while ϵ_0 is the permittivity of free space.

$$V_{Coulombic} = \sum_{i=1}^n \frac{1}{4\pi\epsilon_0} \left(\frac{q_i q_j}{d_{ij}^2} \right) \quad (1.1)$$

The generation of a valid electrostatic force field necessitates the use of a suitable computational model for calculating atomic charges. The MMFF94 method is a popular choice which assigns seed charges based on atom type and modifies these values depending on surrounding atomic charges and the bond type by which they are connected.¹⁶² Although it is possible to use more rigorous methods such as quantum mechanical calculations, the difference in the quality of the resulting CoMFA model is not statistically significant.¹⁶³

The Lennard-Jones potential¹⁶⁴ is used to describe steric interactions in accordance with equation 1.2, in which ϵ_i and σ_i are fitted parameters representing the minimum of the potential energy well and the distance at which the potential becomes zero, respectively; these parameters are chosen to reflect the nearby molecular atom i with which the steric probe atom j interacts. The distance between particles is again denoted d_{ij} .

$$V_{Lennard-Jones} = \sum_{i=1}^n 4\epsilon_i \left\{ \left(\frac{\sigma_i}{d_{ij}} \right)^{12} - \left(\frac{\sigma_i}{d_{ij}} \right)^6 \right\} \quad (1.2)$$

Both of these fields approach infinity as the distance d between the probe atom and an atomic nucleus within the molecule approaches zero. Thus, a cut-off value is incorporated into the model such that only those grid-points in the surrounding space, and not those nearby the atomic nucleus, are used to generate the model (Fig. 1.36).

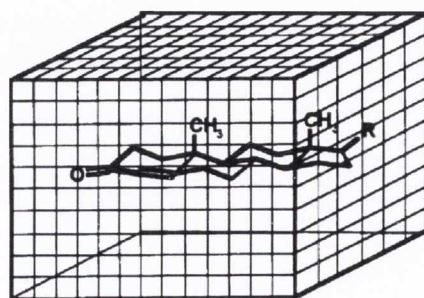


Fig. 1.36. An example of the grid used for a CoMFA analysis surrounding a steroid molecule.

The electrostatic and steric potential is evaluated at each point on the grid.¹⁶⁵

The fields thus calculated are then correlated with activity data using a statistical regression technique known as partial least squares (PLS).¹⁶⁶ The use of PLS is necessary because the steric/electrostatic potentials calculated at every grid-point represents a large, highly correlated dataset with many redundant variables and traditional multiple linear regression analysis is incapable of producing meaningful results with this type of data. PLS addresses this problem by analysing the dataset for highly-correlated variables in order to generate vectors termed latent variables. These latent variables are then cross-correlated to produce the final regression analysis (Fig. 1.37).

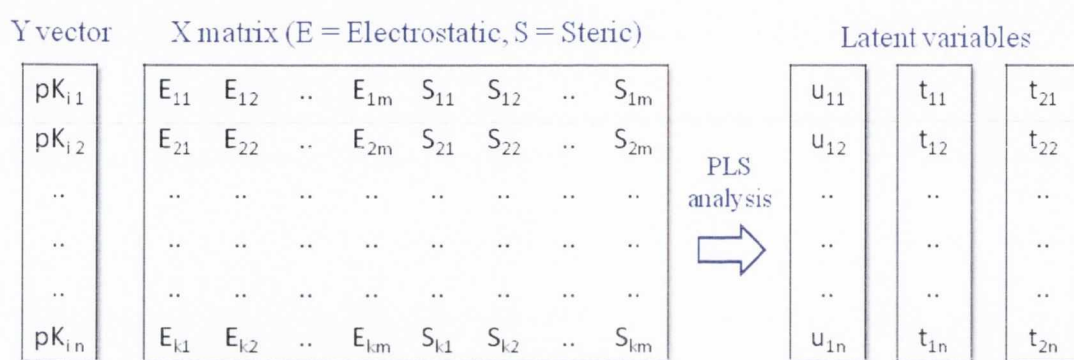


Fig. 1.37. Partial least squares regression addresses the problem of large datasets by assembling highly-correlated data into hypothetical vectors termed latent variables.¹⁶⁵

The quality of the resulting model is determined by ‘leave-one-out’ cross-validation, in which the regression formula is applied to the data set with the omission of a single compound. This process is repeated for each compound in the training set, and the deviation in the predicted values is used to generate a value for q^2 and $SE\vec{x}$, which are the cross-validated correlation coefficient (similar to Pearson coefficient R^2) and the standard error of prediction, respectively. The optimum model is determined by iteratively performing the cross-validation procedure with different numbers of latent variables until the either the highest q^2 or the lowest $SE\vec{x}$ values are obtained.

The CoMFA regression analysis can be visualised in 3D space to highlight regions in which favourable and unfavourable interactions with the receptor are statistically likely to occur; these regions are often referred to as CoMFA fields. This analysis may be also used as a pseudo-receptor to infer structure-activity relationships, to highlight possible pharmacophoric regions and to inform drug design.

While many studies have demonstrated the value of CoMFA analysis in the rational design of new drug-like compounds, few detailed examples of α_2 -AR CoMFA models are present within the literature. However, the closely related α_1 -AR has been studied extensively using the CoMFA technique,^{167,168} and recently Jowiak *et al.* successfully applied their CoMFA results to the rational design of a new series of β_2 -AR agonists.¹⁶⁹

To the best of our knowledge, the only α_2 -AR-related CoMFA data published to date corresponds to a series of studies by Grunewald *et al.*¹⁷⁰⁻¹⁷² In the search for a selective inhibitor of phenethanolamine N-methyltransferase (PNMT; responsible for the conversion of NA to AD), the authors began with a series of tetrahydroisoquinoline derivatives exhibiting high affinity for PNMT. However, these compounds were also known to bind to the α_2 -AR and the authors sought to design more selective ligands by constructing a CoMFA model for both the PNMT enzyme and the α_2 -AR. By comparing the two sets of CoMFA fields, Grunewald *et al.* successfully developed a series of selective inhibitors of PNMT (Fig. 1.38).¹⁷¹

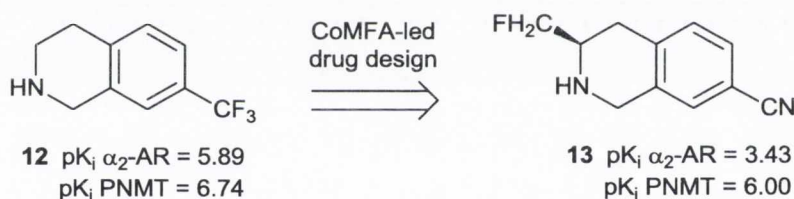


Fig. 1.38. Grunewald's development of selective inhibitors of the PNMT enzyme began with compounds similar to **12**. Using data from CoMFA studies, compound **13** was discovered.

Unfortunately, these studies are not readily transferable to our own research, as the authors were actively seeking to reduce affinity for the α_2 -AR using a series of ligands which are structurally disparate from our own. Moreover, the authors note their difficulties in developing a reliable CoMFA model for the α_2 -AR.¹⁷² Nonetheless, their eventual success and myriad reports of applied CoMFA analysis highlights the broad applicability of this technique to rational drug design.

Chapter 2 - Objectives

2.1 CoMFA and Rational Design

Recent pharmacological studies have established α_2 -AR affinity and activity data for a large library of guanidine and 2-iminoimidazolidine derivatives prepared within our research group (see Appendix A). However, it has proven difficult to establish which structural features are necessary to provide the desired pharmacological affinity and activity. In order to establish quantitative structure-activity relationships, a comparative molecular field analysis (CoMFA) study will be carried out using the α_2 -AR affinity values of those compounds previously prepared within our group. The development of a CoMFA model will highlight which structural features are necessary to provide strong affinity for the α_2 -AR, and which features might be detrimental to α_2 -AR affinity.

The question of pharmacological activity (agonism vs. antagonism) will be addressed by a comparison between α_2 -AR antagonists described in the literature and those discovered within our group. The structural similarities between our antagonists and those in the literature will allow us to extrapolate a hypothetical antagonist pharmacophore describing which structural features are necessary for antagonist activity at the α_2 -AR. Using our CoMFA results to determine which features lead to high α_2 -AR affinity, combined with pharmacophore studies to establish the features needed for antagonist activity; it will be possible to construct an informed molecular design for a new generation of high affinity α_2 -AR antagonist compounds. In addition to providing a rational design scheme for future compounds, these studies will also provide insights into the pharmacological behaviour of compounds already prepared within our group.

2.2 Chemical Synthesis

Following our studies in rational design, it will be possible to design synthetic targets which might act as novel α_2 -AR antagonists. The preparation of these compounds will utilise a combination of established procedures and new synthetic methodology in order to produce a new generation of rationally designed, high affinity α_2 -AR antagonists.

The Synthesis of N,N'-Disubstituted Guanidines

According to our rational design studies, *N,N'*-disubstituted guanidines have emerged as a promising synthetic target for the development of improved α_2 -AR antagonists. Although the literature includes several methods for the preparation of *N,N'*-disubstituted guanidines, many of these protocols necessitate lengthy synthetic procedures or are poorly suited to preparation of *N*-aryl-*N'*-alkyl and *N,N'*-bis(aryl) guanidines. In order to overcome the limitations of previous methods, a concise procedure for the synthesis of this class of compounds will be developed and applied to the preparation of a library of potential α_2 -AR antagonists.

The Synthesis of 4-Substituted-2-Iminoimidazolidines

A second class of compounds suggested by our rational design scheme are 4-substituted-2-iminoimidazolidines. In contrast with the synthesis of *N,N'*-disubstituted guanidines, there are fewer methods described in the literature for this class of compounds. Novel methods for the preparation of 4-substituted-2-iminoimidazolidines will be developed, including the investigation of asymmetric procedures for the 4-position, which comprises a chiral centre. These methods will facilitate the preparation of a focussed library of potential α_2 -AR antagonists of the 4-substituted-2-iminoimidazolidine type.

2.3 Pharmacology

The compounds prepared during these studies will be pharmacologically evaluated using competitive radioligand binding assays in order to establish their affinity for the α_2 -AR, while their activity as either agonists or antagonists will be determined using functional [35 S]GTP γ S binding assays. Both of these studies will be carried out in human prefrontal cortex tissue in order to closely mimic the target pharmacological environment.

Compounds with promising *in vitro* results will be subjected to further *in vivo* studies, beginning with microdialysis studies in rats which will allow us to determine the effect of these compounds upon intracellular neurotransmitter concentrations. Further *in vivo* evaluation may include behavioural assays such as the tail suspension test in order to further assess their antidepressant potential.

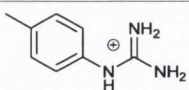
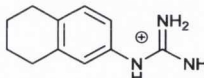
Chapter 3 - CoMFA and Rational Design

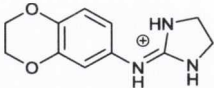
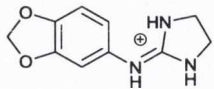
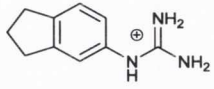
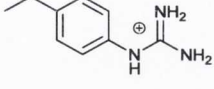
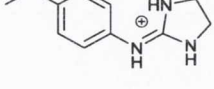
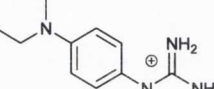
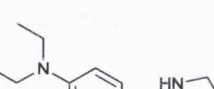
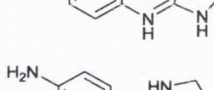
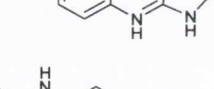
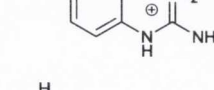
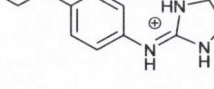
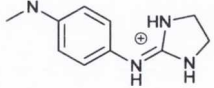
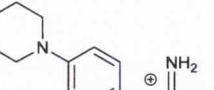
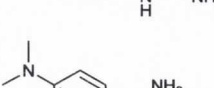
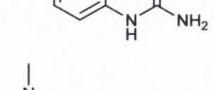
3.1 Data Selection and Alignment

In order to gain a better understanding of which structural features lead to favourable affinity for the α_2 -AR, we decided to carry out a comparative molecular field analysis (CoMFA) study using the compounds previously prepared within our research group. For the construction of a CoMFA model, the majority of the compounds under investigation are assigned to a training set from which the model is constructed. A small test set of representative compounds is not used to develop the model and is instead used to verify the predictive ability of the model by comparing their affinities as predicted by the model with experimental values.

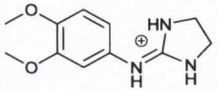
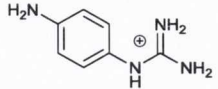
Previously, our group has published the preparation of more than 80 aryl-guanidine and aryl-2-iminoimidazolidine derivatives acting as ligands of the α_2 -AR (see Appendix A).¹⁵⁸⁻¹⁶⁰ From the initial pool of compounds described in these publications, all of the *bis*-aryl-guanidines and *bis*-aryl-2-iminoimidazolidines (for example, see compound **5** in Fig. 1.34, p38) were removed as their structures were deemed to be too heterogeneous for incorporation in the training set. Omission of these compounds afforded a library of 41 *mono*-amidine type compounds for the construction of a CoMFA analysis. For every compound in this series, affinity data for the α_2 -AR was acquired within the same laboratory¹⁷³ using identical procedures, affording a highly consistent set of experimental data. Values for pK_i range across three orders of magnitude and are well distributed within this range. Six molecules were selected as representative examples of variations in chemical structure and pK_i and assigned to a test set, including five molecules prepared within our group along with the clinically used α_2 -AR agonist clonidine, leaving a training set of 35 molecules (Table 3.1).

Table 3.1 Training set molecules chosen for study

| Compound | Structure | Experimental pK_i^a | Predicted pK_i^b |
|-----------|---|------------------------------|---------------------------|
| 14 |  | 6.53 | 6.23 |
| 6 |  | 7.11 | 7.21 |

| | | | |
|----|---|------|------|
| 15 |  | 7.85 | 8.18 |
| 7 |  | 7.33 | 7.30 |
| 16 |  | 6.51 | 6.82 |
| 17 |  | 6.41 | 6.42 |
| 18 |  | 6.68 | 6.78 |
| 19 |  | 6.34 | 6.27 |
| 20 |  | 7.09 | 7.08 |
| 21 |  | 6.92 | 7.03 |
| 8 |  | 6.58 | 6.51 |
| 22 |  | 6.75 | 6.73 |
| 23 |  | 7.27 | 7.25 |
| 24 |  | 5.52 | 5.77 |
| 11 |  | 7.06 | 6.70 |
| 9 |  | 7.42 | 7.60 |
| 25 |  | 6.39 | 6.67 |

| | | | |
|----|--|------|------|
| 26 | | 7.38 | 7.61 |
| 27 | | 6.95 | 6.87 |
| 28 | | 6.05 | 6.07 |
| 29 | | 6.58 | 6.64 |
| 30 | | 5.55 | 5.70 |
| 31 | | 6.85 | 6.89 |
| 32 | | 6.83 | 6.76 |
| 33 | | 6.56 | 6.57 |
| 34 | | 6.40 | 6.42 |
| 35 | | 6.56 | 6.81 |
| 36 | | 6.30 | 6.16 |
| 37 | | 6.62 | 6.54 |
| 38 | | 8.21 | 7.81 |
| 39 | | 8.26 | 7.57 |
| 40 | | 5.93 | 5.99 |
| 41 | | 5.84 | 5.84 |

| | | | |
|----|---|------|------|
| 42 |  | 6.66 | 6.45 |
| 43 |  | 5.58 | 5.66 |

^aDetermined using [³H] RX821002 competition assay in human prefrontal cortex.

^bPredicted by the region focussed CoMFA model described in this text.

The three-dimensional structures of all compounds were generated and optimised using the Tripos molecular mechanical force field¹⁷⁴ as implemented in the Sybyl 8.0 molecular modelling environment¹⁷⁵ with the Powell conjugate gradient method and a convergence criterion of 0.05 kcal mol⁻¹ Å. Atomic charges were generated using the MMFF94 method.¹⁶² The guanidine or 2-iminoimidazolidine moiety was always used in its protonated state, and the chloride counterion was omitted during these modelling procedures, as it is assumed to undergo solvation prior to drug-ligand binding.

The alignment procedure was carried out using a template-based approach. Compound **38** (see structure in Table 3.1) exhibits both a high affinity for the receptor and a rigid structure, and these two criteria are indicative of a close fit between the unbound conformation of the molecule and its configuration within the active site.¹⁷⁶ Thus, all other molecules were aligned using the minimised conformation of compound **38** as a template. This operation was performed via the Sybyl atom fit function using the carbon atoms at the 2, 4 and 6 positions of the aromatic ring and the three nitrogen atoms within the guanidine/2-iminoimidazolidine moiety. Following the initial alignment procedure, freely-rotatable torsional angles were manually adjusted to maximize the overlap of steric bulk and functional groups (Fig. 3.1).

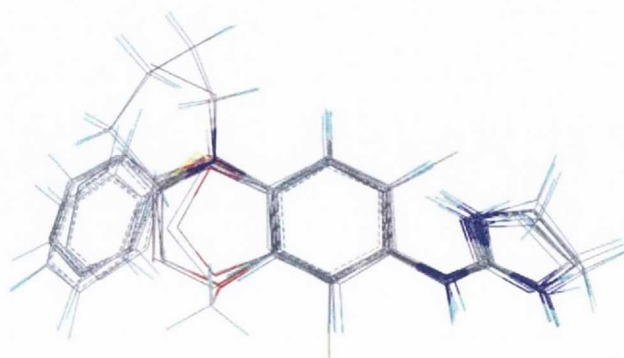


Fig. 3.1. The molecular alignment used for CoMFA analysis.

3.2 CoMFA Model: Results and Discussion

The electrostatic and steric CoMFA fields were calculated using a positively charged sp^3 carbon atom probe with a grid spacing of 2 Å. The best results were obtained using the parabolic electrostatic and indicator steric field types with energetic cut-off values of 10 kcal mol⁻¹ and 20 kcal mol⁻¹, respectively. These fields were correlated with experimental pK_i values using the SAMPLS method to determine the optimum number of latent variables employing leave-one-out cross-validation. The optimum number of variables was determined to be five, and a full PLS analysis was carried out with this number of components in order to generate an initial model with a cross-validated correlation coefficient $q^2 = 0.631$ and standard error of prediction $SE\vec{x} = 0.197$. Through the application of region focussing, the final CoMFA model was generated with $q^2 = 0.657$ and $SE\vec{x} = 0.192$. CoMFA contour maps were generated from this model using the standard deviation multiplied by the coefficient. Unless otherwise stated, all parameters were employed using their default values as implemented in the Sybyl 8.0 software suite running on a Linux workstation within the OpenSUSE 11.1 operating environment.¹⁷⁵

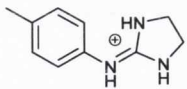
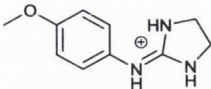
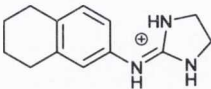
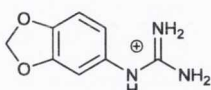
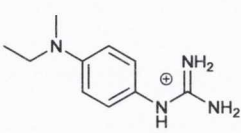
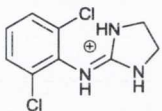
The final model exhibits a cross-validated correlation coefficient of $q^2 = 0.657$ with a Pearson correlation coefficient of $R^2 = 0.928$, indicating good internal agreement between predicted and experimental affinity data (Table 3.2).

Table 3.2 Key statistics of the final CoMFA model

| Statistical Features: | | Relative Contributions: | Norm. Coeff. | Fraction |
|------------------------|-------|-------------------------|--------------|----------|
| q^2 | 0.657 | Steric field | 3.335 | 0.778 |
| $SE\vec{x}$ | 0.192 | Electrostatic field | 0.950 | 0.222 |
| R^2 | 0.928 | | | |
| F-test value | 74.48 | | | |
| Probability of $R^2=0$ | 0.000 | | | |

Using this model, pK_i values for all molecules in our test set could be predicted within a single pK_i unit with the exception of compound **44**, which exhibits a deviation of 1.2 pK_i units (Table 3.3).

Table 3.3 Test set results using the final CoMFA model

| Compound | Structure | Experimental pK _i ^a | Predicted pK _i ^b |
|-----------|---|---|--|
| 44 |  | 7.82 | 6.59 |
| 45 |  | 7.77 | 7.08 |
| 10 |  | 7.33 | 7.57 |
| 46 |  | 6.40 | 6.93 |
| 47 |  | 7.12 | 6.82 |
| Clonidine |  | 7.68 | 7.07 |

^aDetermined using [³H] RX821002 competition assay in human prefrontal cortex.

^bPredicted by the region focussed CoMFA model described in this text.

The failure of this model to accurately predict the pK_i of *para*-methyl derivative **44** indicates that this ligand may interact with the receptor in a manner which is inconsistent with other molecules in the series. The low molecular weight of **44** in combination with its high receptor affinity implies an excellent efficiency of binding,¹⁷⁷ which may be worthy of further study. Indeed, minor structural changes in compounds of low molecular weight typically have a greater influence on affinity than in larger molecules,¹⁷⁸ and it follows that some authors have included molecular weight as an additional predictor in CoMFA studies.¹⁷⁹ However, in our experience this approach gave poor predictive results. The relatively high pK_i of **44** suggests that certain favourable interactions might only be available to smaller molecules; however, the literature suggests that smaller monoamine GPCR ligands are more likely to act as agonists, while larger molecules are more likely to function as antagonists.¹⁸⁰ Thus, a rational design scheme which opts for smaller ligands might also lead to a higher incidence of agonist activity, which is contrary to our intentions. The choice of which molecular features might lead to the desired antagonist activity is the subject of the following section.

Examining the composition of the CoMFA model, weighting of the steric *versus* the electrostatic components (78% steric; 22% electrostatic; Table 3.2) indicates that variations in affinity are controlled mainly by steric factors. It should be noted however that the dominant electrostatic element - the cationic guanidinium/2-iminoimidazolidinium moiety - exhibits little variation in this series. This factor may also contribute to the asymmetric weighting of the steric/electrostatic components of the model. Nonetheless, even with this small electrostatic component, the model exhibits good predictivity and it is likely that these CoMFA fields provide a good description of the steric environment within the binding site.

The steric and electrostatic CoMFA fields were visualised using contour plots in order to highlight which regions of space correspond to favourable and unfavourable interactions. Notably, a region beyond the cationic guanidinium/2-iminoimidazolidinium moiety is apparent in which steric bulk is strongly favoured (Fig. 3.2; *green region on right*). This result agrees with a first approximation made previously within our group that 2-iminoimidazolidine derivatives generally provide higher affinities for the α_2 -AR than their guanidine counterparts. A second sterically favoured region occurs near the *meta* position of the aromatic scaffold; molecule **39** bears a $-\text{CH}_2-$ substituent in this position and engenders the highest pK_i value in the series. Test set molecule **10** bears a similar substituent and also exhibits a relatively high pK_i value. In contrast, a region just beyond the *para* position is sterically disfavoured (Fig. 3.2; *yellow region*); molecules such as **24** which bear a ring or other forms of steric bulk in this position accordingly provide poor affinities.

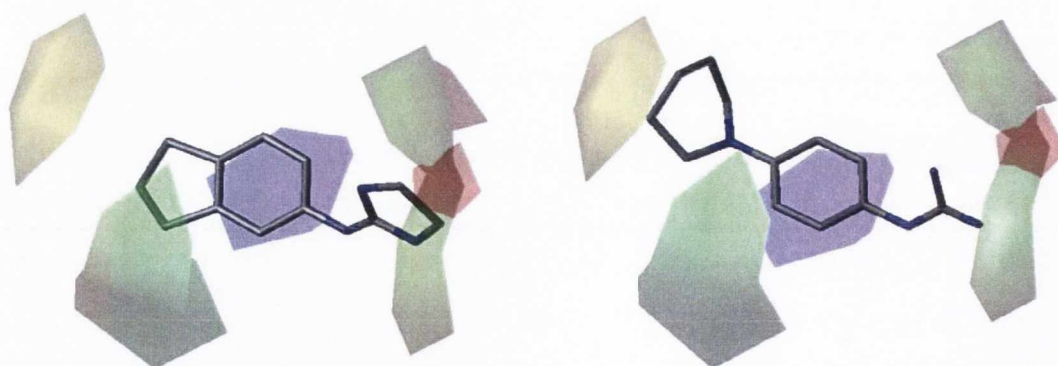


Fig. 3.2. CoMFA fields overlaid with (*left*) high affinity ligand **39** ($\text{pK}_i = 8.26$), and (*right*) low affinity ligand **24** ($\text{pK}_i = 5.52$). Green/yellow regions highlight sterically favoured and disfavoured interactions, respectively; while red/blue regions represent regions favouring electrostatically negative and positive charges, respectively.

In agreement with the smaller relative contribution they make to the model, the electrostatic contours appear to be less predictive. A region closely corresponding to the cationic moiety favours the presence of a negative charge (Fig. 3.2; *red region*), which at first seems counterintuitive. However, the only variation in this region stems from a choice of either a guanidinium or a 2-iminoimidazolidinium moiety, and it follows that the higher overall affinity of the 2-iminoimidazolidines – which are somewhat more electron rich – might result in such a feature in the CoMFA fields. A second region favouring a positive charge coincides with the phenyl group, close to the guanidine moiety (Fig. 3.2; *blue region*). This may reflect a preference for electron-withdrawing substituents in this position, as present in the two *ortho* chlorine atoms of clonidine (Table 3.3). The favourable contribution of *ortho* substituents to adrenoceptor affinity is well established in the literature, although generally the resulting compounds act as agonists rather than antagonists.¹⁸¹

3.3 Molecular Design

One striking feature of these CoMFA fields is the abundance of sterically favoured space surrounding these ligands. Accordingly, an examination of α_2 -AR antagonists in the literature suggests that the binding site provides enough room to accommodate even relatively large compounds such as yohimbine (Fig. 1.29; Fig. 3.3).¹⁸² There are also suggestions that an increase in molecular weight might also improve the occurrence of antagonistic rather than agonistic activity.¹⁸⁰ Therefore, the design of future ligands might benefit from the inclusion of hydrophobic R groups which expand into the sterically accessible regions highlighted in this CoMFA study.

The electrostatic CoMFA fields suggest that the introduction of an electron-rich moiety in the same region as this R group might also lead to good affinity for the α_2 -AR. Improvements to affinity should also arise from the presence of electron-withdrawing *ortho* substituents on the phenyl ring; however, this modification might also incur a higher incidence of agonist molecules.¹⁸¹ Moreover, the low relative contribution of the electrostatic field in our CoMFA model implies that these indications are less important than steric considerations.

An examination of classical α_2 -AR antagonists provides an important context for the application of these CoMFA results to drug design. The interaction of antagonists with the α_2 -AR was studied by Xhaard *et al.* using a homology modelling approach, in which a set of 12 structurally diverse antagonists were docked into α_2 -AR models constructed using the bovine

rhodopsin GPCR template.¹⁸³ Their results suggest that α_2 -AR antagonists may bind via a different set of interactions to those which have been established for agonists (Fig. 3.3; compare to Fig. 1.26).

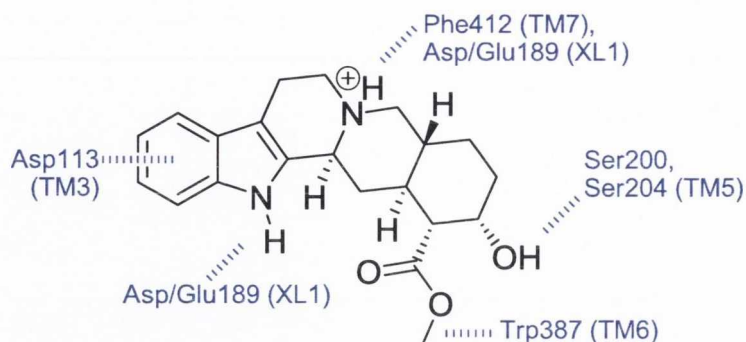


Fig. 3.3. Suggested binding interactions of α_2 -AR antagonists, illustrated using yohimbine.

In this motif, the ligand occupies the same binding site as agonist molecules, and many of the same amino acid residues are involved. However, the key interactions are highly dissimilar; the classical salt bridge involving Asp113 is replaced with a carboxylate- π interaction,¹⁸⁴ while the protonated amine interacts instead with Phe410 via cation- π interactions. In the α_{2A} subtype, this amine may also form a salt bridge with Asp189 on a nearby extracellular loop. Ser200 and Ser204 interact with hydrogen bonding functionalities, while Trp387 contributes to a possible methyl pocket. This model was the only one found to allow large antagonists such as yohimbine to occupy the binding site without incurring catastrophic steric clashes. It is also noteworthy that site-directed mutagenesis studies (see Section 1.4.1) provide no conflicting evidence with Xhaard's proposed binding mode.

Many features of this antagonist binding mode overlap with those of the classical agonist binding motif; this provides a possible explanation as to why many ligands previously prepared within our group exhibit opposite activities, in spite of structural similarities (see Fig. 1.35). Greater control over activity at the α_2 -AR might be incorporated into the design of future compounds through the combination of our CoMFA results with a consideration of possible antagonist binding interactions. The antagonist pharmacophore is readily outlined by considering the spatial relationships between key functionalities in the rigid antagonist yohimbine. By overlapping our previous molecules with yohimbine on the basis of shared pharmacophoric elements, and introducing the CoMFA contours to highlight which regions are amenable to modification; the antagonist pharmacophore can be included in the design of

future molecules while also fulfilling the suggestions of our CoMFA model. The outcome of this design scheme is detailed below, using the Tripos force field to estimate the 3D structures of molecules for which crystal structures are unavailable (Fig. 3.4).

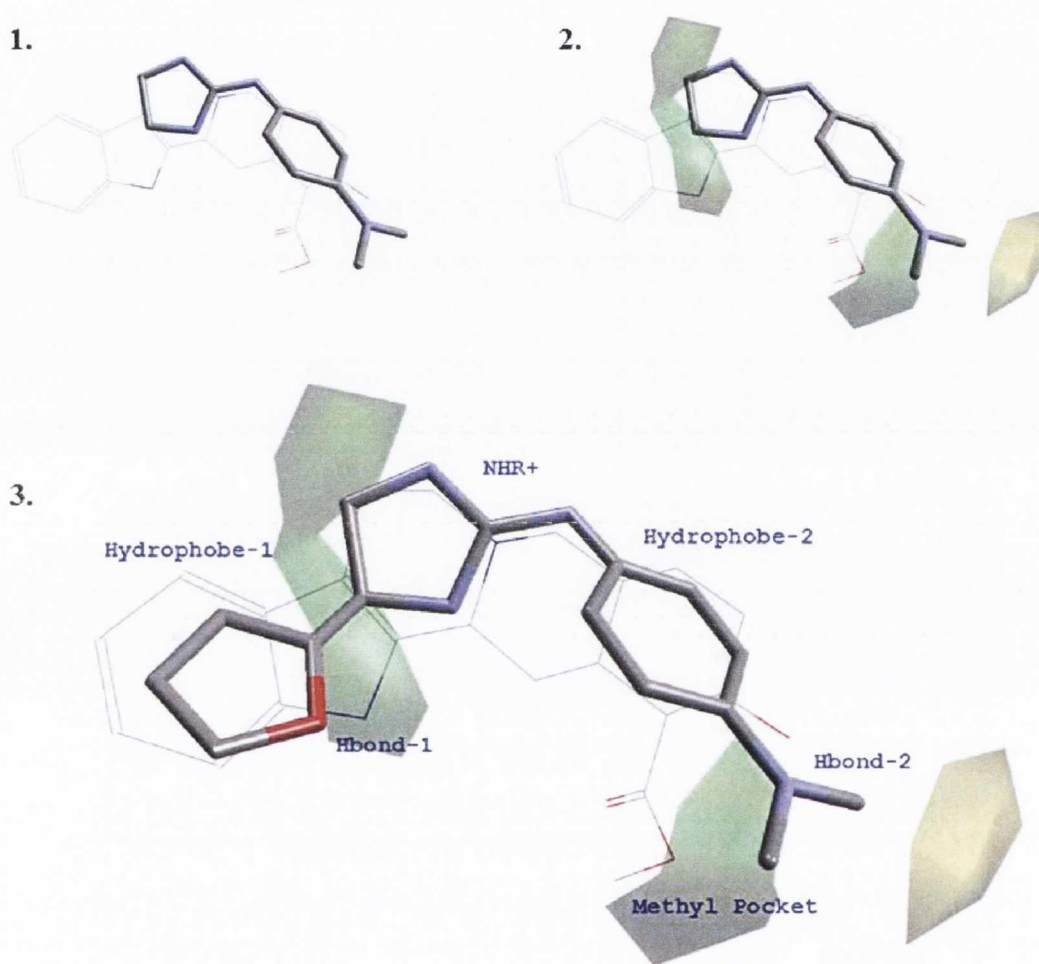


Fig. 3.4. Rational design scheme: (1) The structure of yohimbine¹⁸⁵ (*wireframe*) is aligned with α_2 -AR antagonist **9** (*cylinder*) using key pharmacophoric elements; (2) the same alignment overlaid with steric CoMFA fields (electrostatic fields omitted for clarity); and (3) the incorporation of the 2-furyl moiety shown is consistent with both our CoMFA results and the putative α_2 -AR antagonist pharmacophore, elements of which are labelled in blue.

Previous research within our group has extensively probed the effect of varying the substitution on the aromatic ring, with less attention paid to variations in the chemical space around the cationic moiety. This new design aims to explore the effect of extending the cationic moiety to incorporate various hydrophobic and/or hydrogen bonding functionalities

in order to satisfy the pharmacophore outlined above. To the best of our knowledge, few molecules of this general form have yet been prepared for investigation as potential α_2 -AR antagonists. In the absence of experimental information regarding the extension of aryl-guanidines and their analogues into this chemical space, the incorporation of functionalities beyond those suggested by our pharmacophore may also be of pharmacological interest.

This design scheme gives rise to two classes of compounds as natural extensions of our previous research: *N,N'*-disubstituted aryl-guanidinium and 4-substituted-2-aryl-iminoimidazolidinium derivatives (Fig. 3.5). The choice of aromatic substituents will be chiefly informed by our previous experience in this chemical space, and substituents which have given rise to high affinities and antagonistic activity in the past will also be incorporated into future molecules. Substituents on the cationic moiety (R_2 group, Fig. 3.5) will incorporate various hydrophobic and hydrogen bonding elements in an attempt to take advantage of putative antagonist binding interactions and in agreement with the large sterically favourable region in this position highlighted by our CoMFA fields.



Fig. 3.5. Proposed structures of potential α_2 -AR antagonists of the *N,N'*-disubstituted-aryl-guanidinium (*left*) and *N*-aryl-4-substituted-2-iminoimidazolidinium (*right*) types.

3.4 Context and Discussion

In spite of the strong predictive ability of the final CoMFA model, it is not possible to provide an accurate forecast for the affinity of the proposed molecular design. The CoMFA fields are constructed on the basis of the training set alone, and because the training set does not include any substituents beyond the cationic moiety (R_2 group = H only), the model has no basis on which to construct a quantitative prediction. Nonetheless, the abundance of sterically favoured space in this region of the CoMFA model is strongly indicative of a favourable outcome for the introduction of steric bulk in this position.

It is intriguing to note that few classical α_2 -AR ligands incorporate R groups which extend much further than the cationic moiety. Indeed, the endogenous ligand noradrenaline is distinguished from adrenaline (which has a higher affinity for the β -ARs) by the absence of a methyl group on the cationic nitrogen. Moreover, while many α_2 -AR antagonists incorporate an imidazolidine or imidazoline motif, almost all of their structures terminate at this moiety (see Section 1.4.2). This raises an important question of precedent, namely; are there any indications beyond the work of Xhaard *et al.* to suggest that the hypothetical pharmacophore has any basis in reality; and does the proposed molecular design seem unreasonable in the absence of this hypothetical pharmacophore and the predictions our CoMFA model? Certainly, these are issues which must be addressed prior to committing to the task of synthesis and pharmacological evaluation.

Fortunately, there are several examples of α_2 -AR antagonists which both fulfil the putative pharmacophore and embody extensions beyond a nitrogenous cation. One molecule exhibiting the putative pharmacophore is **48**, an α_2 -AR adrenoceptor antagonist developed by Abbott pharmaceuticals (Fig. 3.6).¹⁸⁶ More recently, Andrés *et al.* described the synthesis and evaluation of a series of benzopyranoisoxazoles acting as α_2 -AR antagonists and inhibitors of the SERT reuptake protein which also fulfil the suggested pharmacophore (Fig. 3.6; **49**).¹⁸⁷

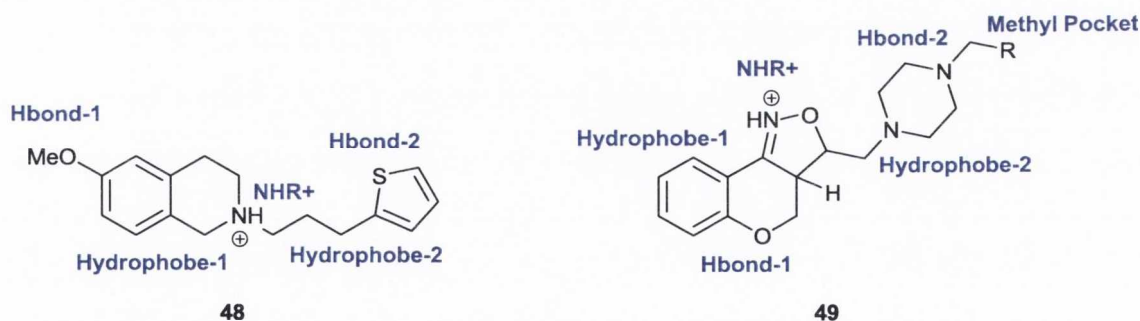


Fig. 3.6. Structures of two α_2 -AR antagonists fulfilling the general α_2 -AR pharmacophore.

Although both of these structures fulfil, to a first approximation, the general antagonist pharmacophore proposed by Xhaard *et al.* (compare to Fig. 3.3), neither of these examples incorporate a guanidine or 2-iminoimidazolidine moiety, and it remains crucial to consider what limitations might apply to the extension of this functional group. Positive indications are evident in the form of imiloxan, a potent and highly selective antagonist of the α_2 -AR, which

incorporates an *N*-ethyl group connected to a terminal imidazolidine moiety (Fig. 3.7).¹⁸⁸ In contrast, a study by Munk *et al.* determined that a terminal *N,N'*-dimethyl guanidine functionality could have a strongly deleterious effect on α_2 -AR receptor affinity (Fig. 3.7; 50).¹⁸⁹

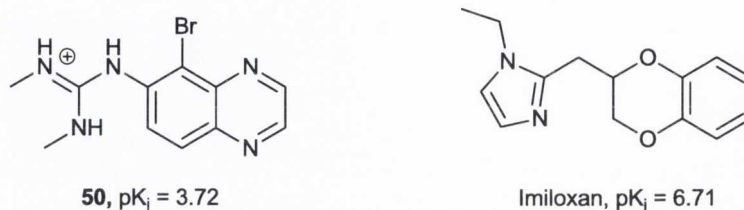


Fig. 3.7. Structures of two α_2 -AR antagonists; **50** has poor affinity for the α_2 -AR while imiloxan is a potent α_2 -AR antagonist with some selectivity for the α_{2B} -AR subtype.

These studies suggest that the nitrogenous cation is amenable to extension, but that limits must be placed on the degree of substitution. This is congruent with our intended molecular design; only a single substituent will be introduced in both the guanidine and the 2-iminoimidazolidine series of compounds.

Although the literature suggests that the introduction of a single well-placed R group should lead to retention of α_2 -AR affinity, the selection of which R groups should be explored is more subjective. The pharmacophore suggests that R groups should incorporate both hydrogen-bonding and hydrophobic interactions, however it is important from a structure-activity relationship standpoint to understand the connection between these two factors. Moreover, our model makes no distinction between simple hydrophobic and π -stacking interactions, and it is important to establish which type of contact is more favourable in this chemical space. As such, we have selected four R groups for initial evaluation to probe four possibilities; namely hydrophobic (n-propyl), π -stacking (phenyl), hydrophobic with hydrogen bonding (ethoxyl), and π -stacking with hydrogen bonding (furan-2-ylmethyl) interactions (Fig. 3.8). These R groups will be introduced to the *N,N'*-disubstituted guanidine series first, owing to the likelihood of a facile synthesis being available. Thereafter, the most promising R groups will be selected for incorporation into the more synthetically challenging 4-substituted-2-aryliminoimidazolidine series.

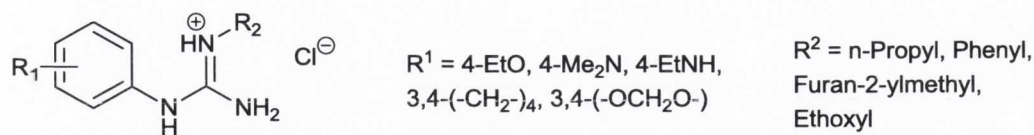


Fig. 3.8. Proposed structures of potential α_2 -AR antagonists of the *N,N'*-disubstituted arylguanidine type.

3.5 Conclusions

The application of CoMFA to the rational design of α_2 -AR antagonists

In order to facilitate the rational design of future α_2 -AR antagonists, we have constructed a CoMFA model based upon molecules prepared previously in our group. The model exhibits good predictivity and it has been possible to draw logical conclusions regarding which structural features are responsible for variations in affinity for the α_2 -AR. The design of future molecules will incorporate the information elucidated by this CoMFA model in order to capitalise on favourable steric and electrostatic interactions and omit features which are likely to diminish affinity for the α_2 -AR.

In an effort to ensure that future molecules also exhibit the desired antagonist activity, the CoMFA fields have been combined with the putative pharmacophoric elements as originally described by Xhaard *et al.*¹⁸³ The close similarity between this pharmacophore and the classical agonist binding mode concurs with the experimental observation that small structural changes can lead to an inversion of α_2 -AR activity. Other design features such as the omission of *ortho* substituents and the decision to increase the molecular volume have also been incorporated into our design scheme in order to increase the likelihood of generating antagonists.

Scope and limitations of our CoMFA methodology

It is important to distinguish between factors influencing affinity and activity; our CoMFA results provide quantitative information regarding affinity values, while our understanding of α_2 -AR activity remains much more subjective. Moreover, our CoMFA model incorporates both agonist and antagonist molecules and makes no distinction between the two, while at the

same time our activity schema suggests that agonists and antagonists exemplify two different binding modes and take up different alignments within the binding site. Given that our CoMFA model places the agonist and antagonist molecules into the same alignment regardless of activity, it is essential to clarify the nature of the 3D-QSAR technique in order to confirm that the CoMFA alignment does not need to reflect the bioactive alignment in order to provide accurate results.

The central dogma of QSAR is that changes in molecular structure can be correlated in a quantitative sense with changes in activity. In a CoMFA study, these structural changes are quantified by the evaluation of the electronic and steric fields surrounding each molecule. In reality, structural modifications impart changes both to these fields and to the flexibility of a molecule. Similarly, the interaction of a ligand with its receptor will impart changes to the conformation of each ligand. However, the CoMFA methodology holds each molecule in a constant alignment throughout the evaluation procedure. It is important to iterate this statement unambiguously: the CoMFA alignment exists to ensure that pharmacophoric elements are evaluated in the same chemical space, and not to place those elements into the hypothetical positions they might occupy while bound to the receptor.¹⁹⁰ It is worth noting that 3D-QSAR techniques which derive their alignments based heavily upon bioactive conformations provide poorer results than those based on shared pharmacophoric elements.¹⁹¹

This fact brings into question the importance of the initial template upon which molecules are aligned, and indeed recent developments in the field have sought to remove the need for alignment altogether. The topomer CoMFA technique (topCoMFA) was designed to be insensitive to molecular alignments while retaining many of the features of the classical CoMFA methodology.¹⁹⁰ Instead of manually aligning each molecule through the manipulation of rotatable bonds, these bonds are taken as dividing lines between the various pharmacophoric elements. In this manner, the fields surrounding each element can be evaluated and correlated with the biological activity with no need to consider the conformation (elements are treated as essentially unbound, free entities). Still other developments incorporate information about multiple conformations into their analyses. By evaluating several alignments and choosing the most statistically sound results, 4D-QSAR methods seek to address the problem of ligand alignment without the omission of conformational data. 5D-QSAR techniques go even further and also include information about the conformation of the receptor.¹⁹²

Even with the development of these new techniques, the original CoMFA methodology remains a powerful tool for molecular design and is far from obsolescent. In our study, a single rotatable bond is the dominant source of conformational complexity (namely, the C-N bond attaching the phenyl group to the guanidine/2-iminoimidazolidine moiety) and most of our molecules are linear, relatively rigid entities. As a result of the conformational simplicity of these molecules, it has been possible to extrapolate hypotheses regarding the nature of the binding site from our CoMFA fields, although in molecules of greater complexity this extrapolation becomes less valid.

Following the synthesis and evaluation of the proposed target molecules, further refinements to our CoMFA model will be possible as there will be a larger volume of data available to form a training set. Given that our proposed molecules universally incorporate additional rotatable bonds, the problem of alignment will be made more complex, and the use of next-generation 3D-QSAR techniques such as topCoMFA might be advantageous. Nonetheless, in the present analysis the original form of CoMFA has provided important indications regarding the steric environment of the binding site, and these features might actually be more difficult to observe and to interpret if topCoMFA were to be used instead.

The utility of rational design

During the course of this study, we were able to devise a new series of compounds which have been rationally designed to act as high affinity antagonists of the α_2 -AR. Although any theoretical model is capable of making incorrect predictions, there are strong indications in the statistical strength of our model that our molecules should fulfil their intended role. Comparisons with compounds described in the literature also suggest that our design rationale agrees with the structure of pre-existing antagonists.

It has also been possible to extrapolate a hypothesis regarding the phenomenon of small structural changes imparting an inversion of activity from agonist to antagonist. It is hoped that our rationally-designed molecules will act exclusively as antagonists, thereby supporting this hypothesis and providing a more accurate description of the structural requirements of aryl guanidine and aryl 2-iminoimidazolidine derived α_2 -AR antagonists.

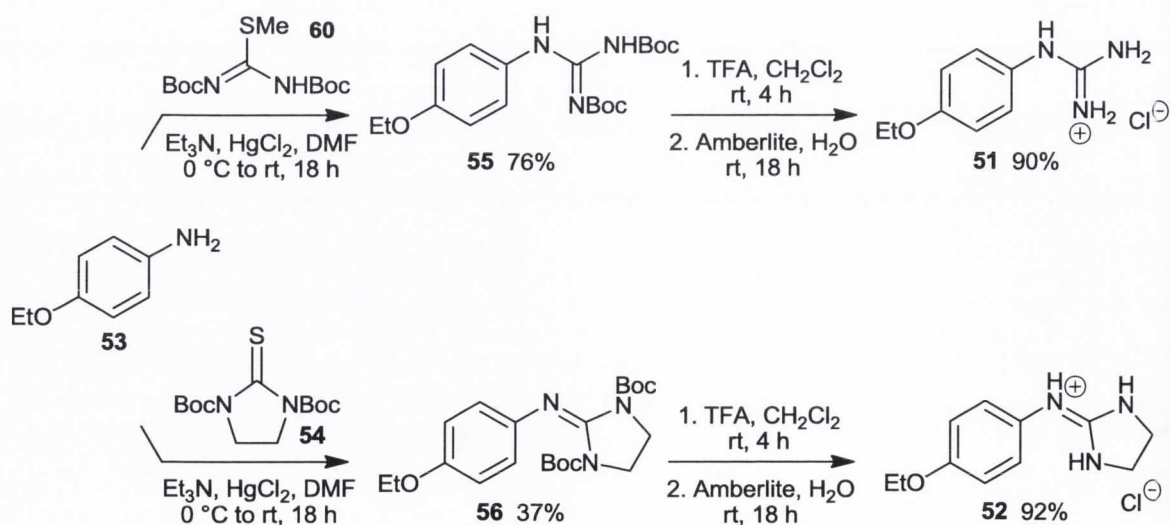
Chapter 4 - Chemical Synthesis

4.1 Modifications to Existing Lead Compounds

4.1.1 Analogues of *N*-(4-ethylaminophenyl)guanidine dihydrochloride

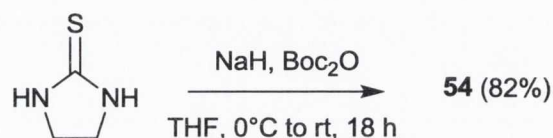
Our group has recently described the synthesis and evaluation of *N*-(4-ethylaminophenyl)-guanidine dihydrochloride **8** (Fig. 1.34)¹⁶⁰ as a potent antagonist of the α_2 -AR and as an *in vivo* antidepressant using tail suspension and force swimming tests in mice.¹⁹³ The promising activity of this compound led us to the preparation of the *O*-ethyl analogues **51** and **52** (Scheme 4.1). While compound **51** replaces the amine nitrogen of **8** with an oxygen atom generating an ether, compound **52** also replaces the guanidine group of **8** with a 2-iminoimidazolidine moiety, a design choice based on the high α_2 -AR affinities generally exhibited by ligands containing this group. The synthesis of **51** and **52** follows the methods of Kim and Qian,¹⁹⁴ and Dardonville *et al.*,¹⁹⁵ illustrating the use of mercury (II) chloride as an efficient reagent for amidylation using thiourea derivatives. The parent amine 4-ethoxyaniline **53** is treated with the appropriate *bis*-Boc protected (iso)thiourea in the presence of triethylamine and mercury (II) chloride. Deprotection with trifluoroacetic acid followed by ion exchange using Amberlite IRA-400 resin in its chloride form affords the hydrochloride salts.

Scheme 4.1 Preparation of compounds **51** and **52**



For the synthesis of **52** the appropriate amidylating agent was not available commercially, and therefore *N,N'*-bis-(*tert*-butoxycarbonyl)imidazolidine-2-thione **54** was prepared by treating imidazolidine-2-thione with NaH in the presence of di-*tert*-butyldicarbonate (Boc₂O) in dry tetrahydrofuran (Scheme 4.2). This is a general procedure for the Boc protection of imidazolidine-2-thiones and customarily proceeds in good yield; we return to this method in a following section detailing the preparation of 4-substituted 2-iminoimidazolidines.

Scheme 4.2 Synthesis of amidylating agent **54**



4.1.2 Conformational aspects of *bis*-Boc protected guanidine derivatives

By means of single crystal X-ray crystallography, it was possible to resolve the crystal structure of *bis*-Boc protected intermediate **55**, demonstrating co-planarity between the protected guanidine moiety and the core aromatic ring (Fig. 4.1). This stands in contrast with the final hydrochloride salts in which the guanidine group typically lies out-of-plane with the aromatic ring.¹⁹⁶

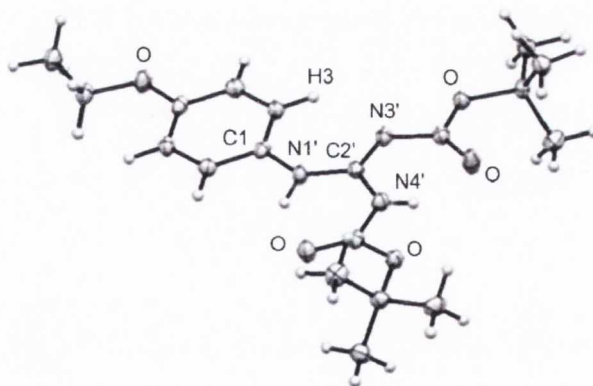


Fig. 4.1. X-ray crystal structure of *bis*-Boc protected intermediate **55**.

While protonated guanidines are characterised by the delocalisation of their positive charge throughout a π system involving a central sp^2 carbon atom and the adjoining triad of sp^2 nitrogen atoms, the imine double bond in neutral guanidine derivatives is formally localised. The most stable configuration of these compounds is dependent upon both the tautomeric state of the guanidine moiety, and upon the relative energies of the *E* and *Z* isomers with reference to the imine double bond. In the case of the crystal structure of **55**, the imine double bond is conjugated with one of the Boc groups and the formal *Z* isomer is observed.

The co-planarity of the *bis*-Boc protected guanidine moiety and the phenyl ring is concurrent with an array of intramolecular hydrogen bonding interactions (IMHBs) involving the Boc carbonyl oxygen atoms and NH protons. This hypothesis is supported by ^1H NMR data for **55**, in which the NH signals appear at 10.20 and 11.67 ppm; the large chemical shifts agree that these protons are involved in hydrogen bonding interactions. The Boc CH_3 protons also appear as two singlets both integrating for nine protons at 1.51 and 1.56 ppm; the occurrence of two separate peaks is concordant with either Boc group representing a different chemical environment owing to the rigid array of IMHBs (Fig. 4.2). The possibility of a third IMHB involving the lone pair of imine nitrogen $\text{N}3'$ and the adjacent *ortho* aryl proton $\text{H}3$ or $\text{H}3''$ is also indicated by the crystal structure; however the ^1H NMR data suggests that this IMHB is not maintained in solution. If this IMHB was present in solution phase, the four aromatic CH protons would be rendered chemically inequivalent and four aromatic CH signals would be seen. The observation of only two aromatic signals, which occur as two doublets ($J = 8.7$ Hz) at 7.47 and 6.87 ppm, indicates that free rotation occurs about the $\text{C}1\text{-N}1'$ axis, and that this IMHB is either transient or absent in the solution phase.

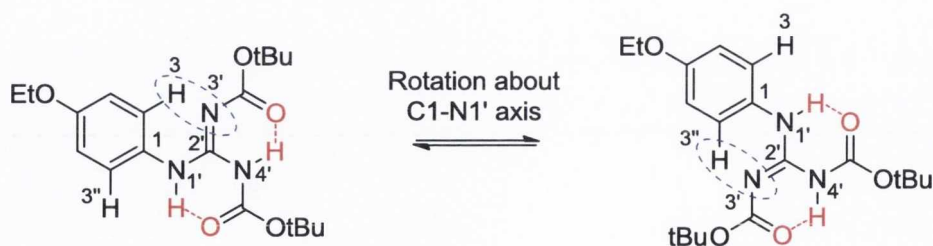


Fig. 4.2. Hydrogen bonding interactions in *bis*-Boc protected intermediate **55**. Hydrogen bonds observed by ^1H NMR are shown in red, while a possible transient hydrogen bond involving an aromatic CH proton and the nearby imine lone pair is circled in blue.¹⁹⁷

The same features occur in the ^1H NMR data of all of the *bis*-Boc protected guanidine derivatives prepared by our group in the past.¹⁵⁸⁻¹⁶⁰ The NH signals universally appear as two broad singlets around 9 - 12 ppm (indicating hydrogen bonding), and the Boc CH_3 signals always appear as two separate singlets integrating for nine protons each (distinct chemical environments). The conformational aspects of guanidine derivatives are an ongoing subject of research within our laboratory, and we will return to this subject in our discussion of *N,N'*-disubstituted guanidine derivatives and their *mono*-Boc protected analogues.

4.1.3 Reactivity of *bis*-Boc protected 2-iminoimidazolidine derivatives

During the chromatographic purification of *bis*-Boc protected 2-iminoimidazolidine derivative **56**, a small crop of crystalline material was observed in one of the fractions. In order to compare the crystal structure of guanidine derivative **55** with **56**, these crystals were isolated and analysed by single crystal X-ray crystallography. To our surprise, this analysis revealed the unexpected crystal structure **57** (Fig. 4.3).

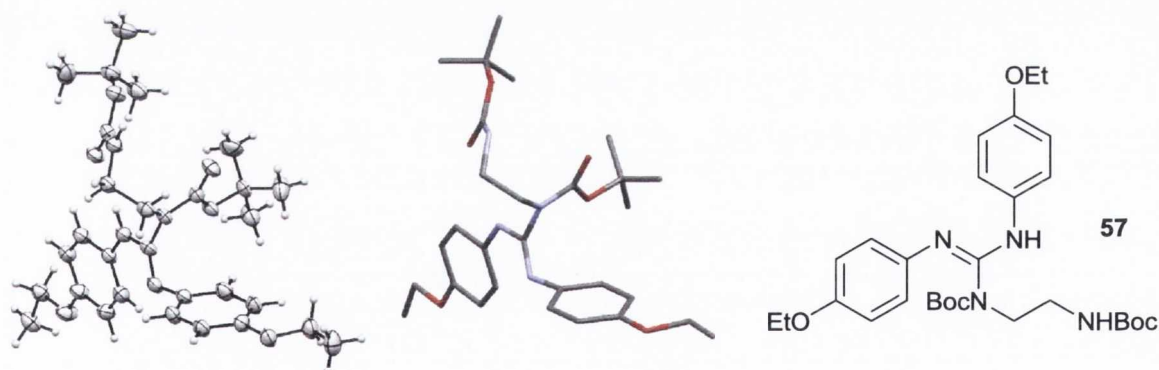


Fig. 4.3. X-ray crystal structure of **57** represented in ORTEP (*left*), and cylinder styles with hydrogen atoms omitted for clarity (*middle*). The chemical structure is also shown (*right*).

This *tetra*-substituted guanidine entity likely constitutes a side product of the amidylation reaction and offers a probable explanation for the low yield recorded in the preparation of **56**. The formation of **57** may occur *via* an addition-elimination mechanism involving nucleophilic attack by the unreacted amine starting material 4-ethoxyaniline upon the central carbon atom of the 2-iminoimidazolidine moiety of **56**.

The instability of *bis*-Boc protected 2-iminoimidazolidine derivatives is well known in our research group, and historically these derivatives have necessitated the use of aluminium oxide for chromatographic purification as they degrade using silica chromatography. This instability is likely to stem from two sources: (a) the increased basicity of the imine lone pair in *bis*-Boc protected 2-iminoimidazolidine derivatives compared with their guanidine analogues, and (b) the ring strain present in the 2-iminoimidazolidine compounds which is readily relieved by nucleophilic attack and ring opening.

In the case of *bis*-Boc guanidine derivative **55**, the tautomer observed by ^1H NMR and X-ray crystallography places the $\text{C}2'=\text{N}3'$ imine into conjugation with the carbonyl group, diminishing its basicity (see Fig. 4.2). In the case of **56**, the presence of the ethylene bridge negates this possibility and the imine is forced into conjugation with the aryl group, increasing its basicity and the likelihood of being protonated and undergoing nucleophilic attack (Fig. 4.4). Furthermore, the 2-iminoimidazolidine ring includes three sp^2 and two sp^3 hybridized atoms giving rise to significant ring strain; either the ethylene hydrogens must be forced into an eclipsed arrangement, or the sp^2 geometry of the adjacent nitrogens must be twisted out-of-plane. Given that nucleophilic attack results in the relief of this strain, the *bis*-Boc protected 2-iminoimidazolidine moiety is highly susceptible to ring opening in the presence of nucleophiles such as unreacted starting material, particularly in the presence of even weak acids such as silica gel.

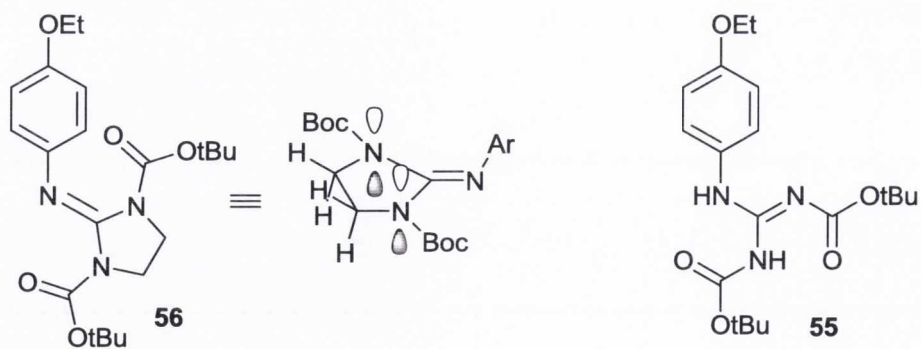


Fig. 4.4. The chemical structure of **56** compared with that of **55**.

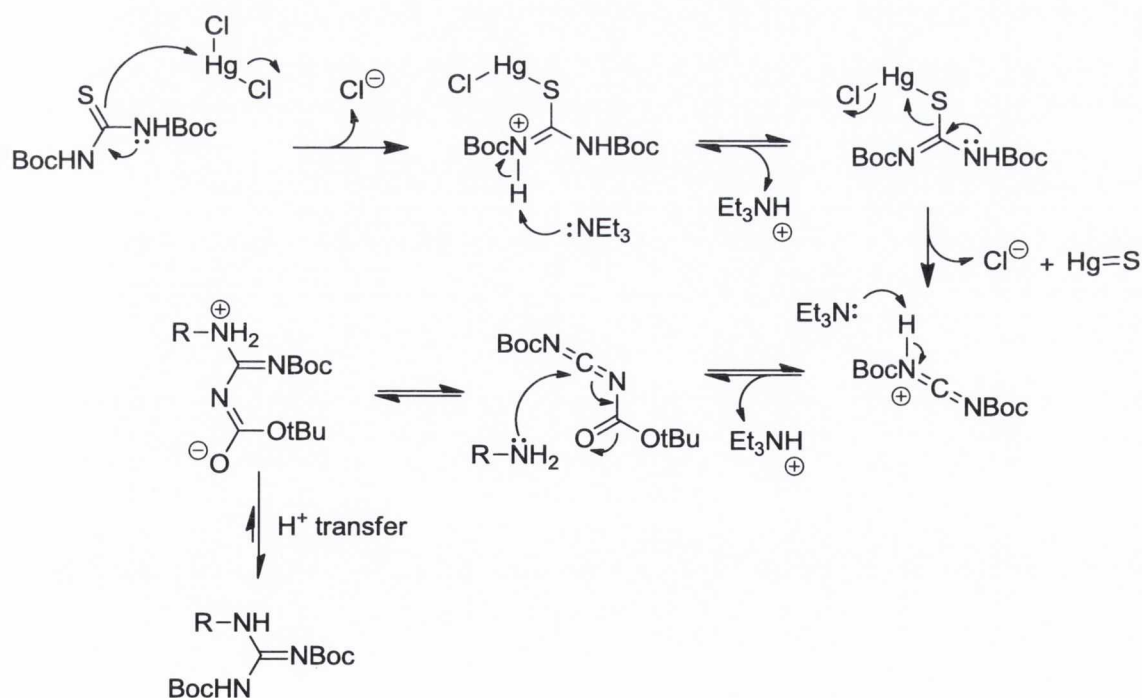
Although a crystal structure was not available for **56**, ^1H NMR data confirms that both Boc groups exist within an equivalent chemical environment, and only a single peak is observed for the Boc CH_3 groups integrating for eighteen protons at 1.36 ppm; this contrasts with the

two singlets each integrating for nine protons corresponding to the two different Boc groups observed in the case of **55**. A brief examination of ^1H NMR data published previously within our group confirms that this observation is also found in our other Boc protected 2-iminoimidazolidines; thus in their *bis*-Boc protected state the 2-iminoimidazolidine and guanidine classes of compounds are distinguished by different tautomeric forms giving rise to increased stability for guanidines *versus* their 2-iminoimidazoline analogues.

4.1.4 Mechanistic aspects of guanidylation using thiourea derivatives

In the original paper by Kim and Qian describing the guanidylation of amines using *bis*-Boc protected thiourea in the presence of mercury (II) chloride,¹⁹⁴ the authors suggest that the reaction proceeds through a carbodiimide intermediate formed by desulfurization of the substituted thiourea. The carbodiimide then undergoes nucleophilic attack by the amine to generate the product guanidine (Scheme 4.3).

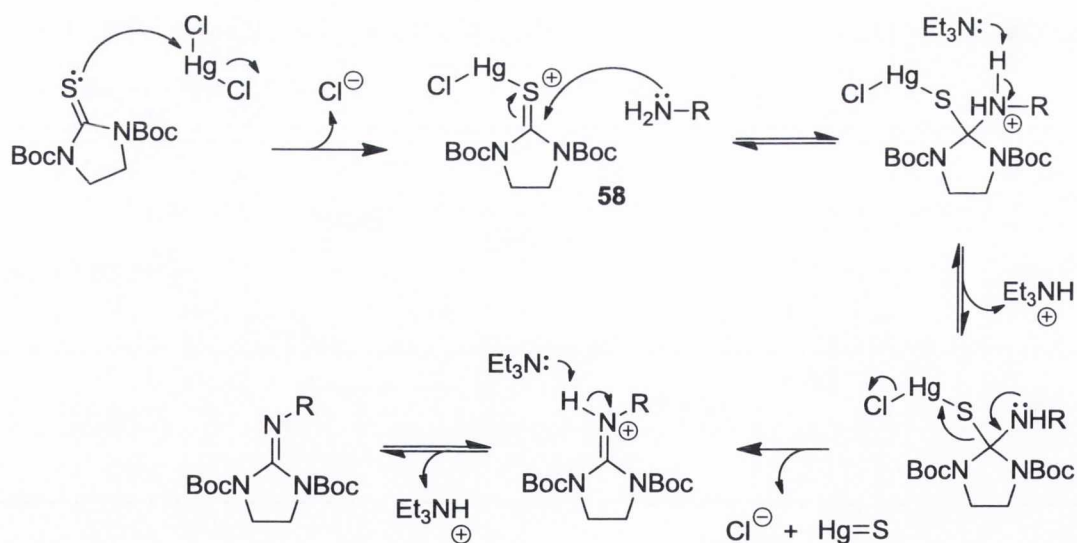
Scheme 4.3 Carbodiimide mechanism for mercury (II) chloride-promoted guanidylation of electron-withdrawing group (EWG) substituted thioureas in the presence of a mild base



The authors note that they were unable to isolate the *bis*-Boc carbodiimide intermediate; however, they observed spectroscopic data *in situ* which agrees with the presence of a mercury complex of *bis*-Boc carbodiimide. Unfortunately, the authors were unable to deduce the exact structure of this reactive intermediate.

Most papers using this methodology which discuss the reaction mechanism agree with the original hypothesis and posit a carbodiimide intermediate is likely to be involved. Other authors point out that an addition-elimination mechanism free from carbodiimide formation cannot be ruled out.¹⁹⁸ In the formation of 2-iminoimidazolidine derivative **56**, the requisite intermediate would incorporate a carbodiimide into a five membered ring; which is impossible given the degree of strain that a five membered ring incorporating a linear arrangement of three of its constituent atoms (the carbodiimide) would impose upon the ring. For the preparation of 2-iminoimidazolidines such as **56**, it is possible to invoke an addition-elimination mechanism to avoid this problem (Scheme 4.4).

Scheme 4.4 Addition-elimination mechanism for amidylation of electron-withdrawing group (EWG) bearing thioureas in the presence of mercury (II) chloride and a mild base



Notably, there are several papers which suggest similar addition-elimination mechanisms for related thioureas, providing reasonable precedent for this mechanism.^{198,199} There is also a wide body of research examining the complexation chemistry of the mercury (II) cation with sulphur which provides insight into the structure of reactive intermediate **58**. In a closely

related example, the addition of mercury (II) iodide to two equivalents of imidazolidine-2-thione allowed Butcher *et al.* to synthesise a complex exhibiting coordination between mercury and sulphur and to resolve the X-ray crystal structure of the resulting complex **59** $[\text{Hg}(\eta^1\text{-S-imidazolidine-2-thione-H}_2\text{)}\text{I}_2]$ (Fig. 4.5).²⁰⁰



Fig. 4.5. ORTEP style X-ray crystal structure of $[\text{Hg}(\eta^1\text{-S-imidazolidine-2-thione-H}_2\text{)}\text{I}_2]$ (*left*; CCDC deposition no. 658201), alongside its chemical structure (*right*).

While the preparation of the mercury (II) chloride analogue of **59** has also been reported,²⁰¹ a crystal structure has not yet been resolved. Importantly, neither of these complexes contains the electron-withdrawing *N*-substituents which are an essential component in the guanidylation reaction, and any analogy to reactive intermediate **58** must be drawn with this in mind. These complexes nonetheless verify that thiourea derivatives can coordinate to a mercury (II) cation to produce a relatively stable, cationic species which may be a key intermediate in the guanidylation reaction.

Both mechanisms represent plausible hypotheses for the formation of *bis*-Boc protected guanidine derivative **55**. In the case of the 2-iminoimidazolidine derivative **56**, geometrical requirements of the five-membered ring system may rule out the classical carbodiimide mechanism. However, Kim and Qian did observe spectroscopic evidence for the formation of a carbodiimide intermediate shortly after combining mercury (II) chloride with *bis*-Boc protected thiourea, and carbodiimides are well known to react readily with amines to produce guanidines.²⁰² Therefore, it is possible that the carbodiimide mechanism operates in the formation of guanidine derivatives, while the addition-elimination mechanism is reasonable for the formation of both guanidine and 2-iminoimidazolidine derivatives. While detailed mechanistic investigations are necessary to draw definite conclusions, it remains important to posit a reasonable hypothesis for the mechanistic aspects of these reactions prior to any attempt to expand upon the original methodology.

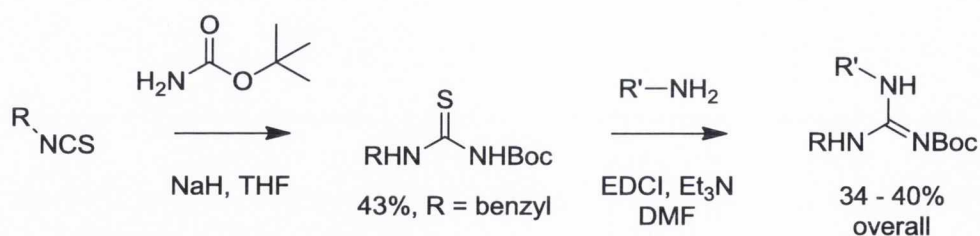
4.2 *N,N'*-Disubstituted Guanidines

4.2.1 Literature methods for preparing *N,N'*-disubstituted guanidines

In 1992, Poss and Iwanowicz described the reaction of aliphatic amines with Boc protected thiourea derivatives promoted by 1-ethyl-3-(3-dimethylaminopropyl)carbodiimide (EDCI),²⁰³ Their method was poorly suited to the synthesis of guanidines derived from weakly nucleophilic amines, and this deficiency was resolved by the use of mercury (II) chloride in the procedures developed shortly afterward by Kim and Qian in 1993.¹⁹⁴ The latter method provides higher yields and is compatible with weaker nucleophiles such as aromatic amines, and therefore the EDCI procedure is less popular throughout the current literature, in spite of the toxicity associated with the use of mercury (II) salts.²⁰⁴

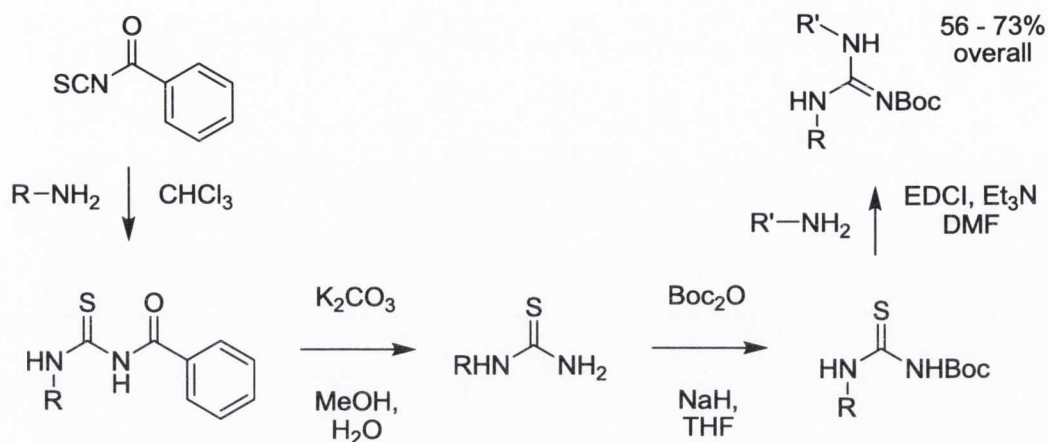
While Kim and Qian focused primarily on *mono*-substituted guanidine derivatives such as those discussed in the previous section, Poss and Iwanowicz also described two procedures for the synthesis of *N,N'*-disubstituted guanidines from *N*-Boc protected *N'*-substituted thiourea derivatives. In the first of these methods, *tert*-butyl carbamate is reacted with an alkyl or aryl isothiocyanate to furnish a Boc protected thiourea derivative, which is then subjected to guanidylation using their EDCI-promoted procedure (Scheme 4.5).

Scheme 4.5 The reaction of isocyanate derivatives with *tert*-butyl carbamate to produce *N*-Boc protected *N'*-substituted thioureas followed by guanidylation using EDCI



As the authors note, this procedure suffers from poor yields due to difficulties in the synthesis of the intermediate thiourea and necessitates the availability of the isothiocyanate precursor. To combat these problems, they developed a more general method involving reaction of benzoyl isothiocyanate with the appropriate amine, followed by basic deacylation and subsequent reacylation using Boc_2O in the presence of sodium hydride (Scheme 4.6).

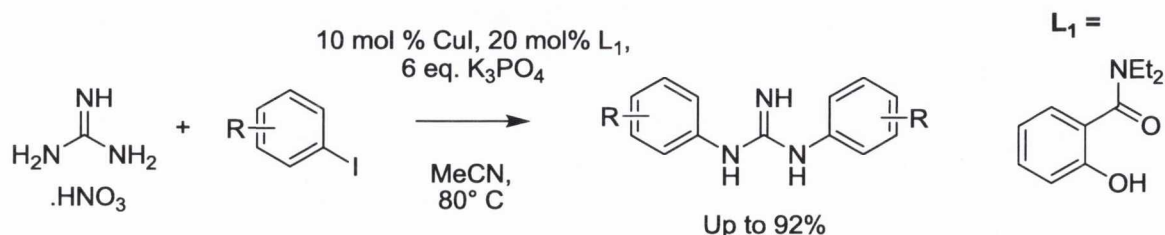
Scheme 4.6 The reaction of amines with benzoyl isothiocyanate followed by acyl group exchange to produce *N*-Boc protected *N'*-substituted thioureas for subsequent guanidylation



While this procedure represents a significant improvement over their original methodology in terms of both generality and overall yield, the scope remains limited to the preparation of alkyl guanidine derivatives. The number of stepwise transformations is also an impediment to the rapid generation of a library of *N,N'*-disubstituted guanidines; even with the omission of the final deprotection procedure, the synthetic route stands at four steps for the preparation of a single functional group.

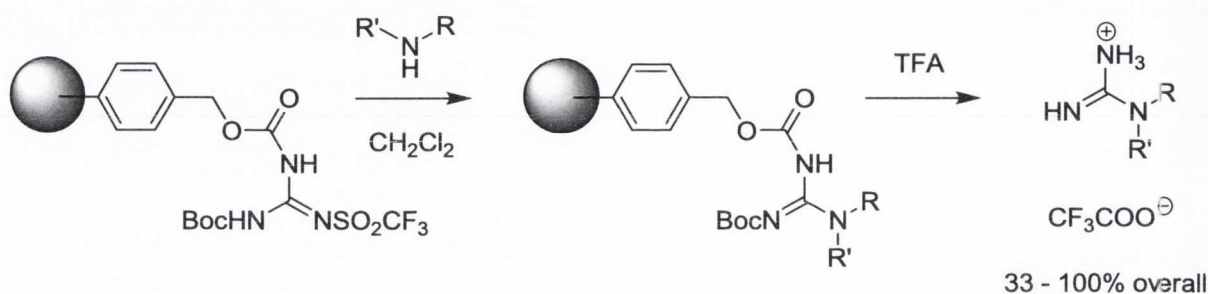
In order to overcome these limitations, we sought to develop our own concise procedure for the generation of *N*-aryl-*N'*-alkyl and *N*-aryl₁-*N'*-aryl₂ disubstituted guanidine derivatives, and began by examining methods which have been described in recent literature. A 2010 publication from Antilla *et al.* describes the copper-catalysed reaction of guanidine with aryl iodides to produce symmetrical *N,N'*-bis-aryl disubstituted guanidines in good yield (Scheme 4.7).²⁰⁵

Scheme 4.7 The copper catalysed reaction of aryl iodides with the free base of guanidine nitrate to produce *N,N'* bis-aryl disubstituted guanidines



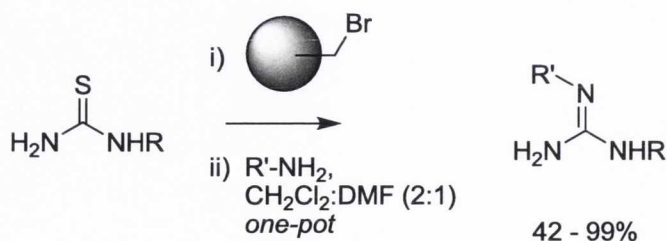
While this procedure is certainly concise, it remains limited to the synthesis of symmetrically substituted *bis*-aryl derivatives and has not been extended to *N*-alkyl substituted guanidines. Goodman and co-workers have reported a solid-phase strategy for the preparation of *N,N*-disubstituted guanidines which is also concise and high yielding (Scheme 4.8). Moreover, the use of a solid-phase guanidylating reagent makes this method amenable to combinatorial strategies, facilitating the rapid generation of a large library of compounds.²⁰⁶

Scheme 4.8 Goodman's solid-phase synthesis of *N,N*-disubstituted guanidine derivatives



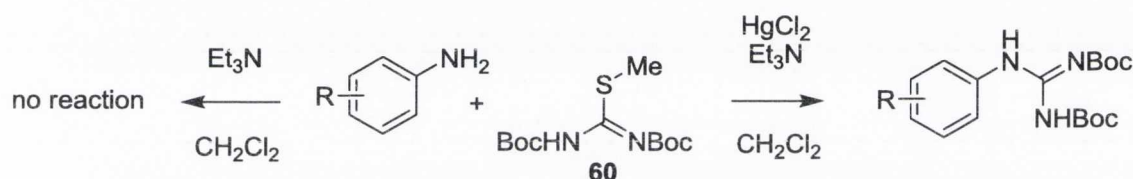
Sadly, the substitution pattern on the guanidine moiety is contrary to our target molecules and this method cannot be readily adapted to the synthesis of *N,N'*-disubstituted guanidine derivatives. Methods for the preparation of *N,N'*-disubstituted guanidines were developed by Wang and co-workers which utilise a solid-phase alkylating agent to activate an appropriately substituted thiourea toward nucleophilic attack; the immobilised *S*-alkyl isothiurea is then reacted with the requisite amine to produce the guanidine product in a two-step, one-pot 'catch-and release' protocol (Scheme 4.9).²⁰⁷

Scheme 4.9 Wang's 'catch-and-release' synthesis of *N,N'*-disubstituted guanidines



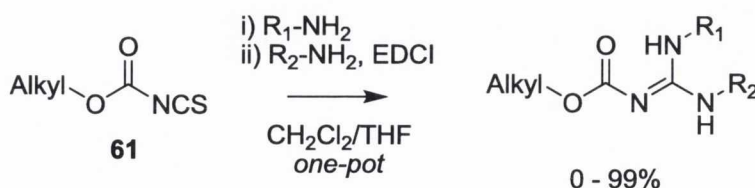
In this instance the substitution pattern is correct, however the authors fail to report anything other than alkyl substituted guanidine derivatives, suggesting that this strategy is unsuitable for the preparation of *N*-aryl guanidines. Indeed, the potent guanidylating reagent *N,N'*-bis(*tert*-butoxycarbonyl)-*S*-methylisothioarea **60** operates by a similar *S*-alkylation principal to Wang's methodology, and in our experience mercury (II) chloride is still required to promote guanidylation using this reagent in the presence of aromatic amines (Scheme 4.10). Furthermore, Wang's methodology is also dependent on the availability of the requisite thioureas, for which the authors provide no general preparative method.

Scheme 4.10 Guanidylation of aromatic amines using **60** with and without HgCl₂



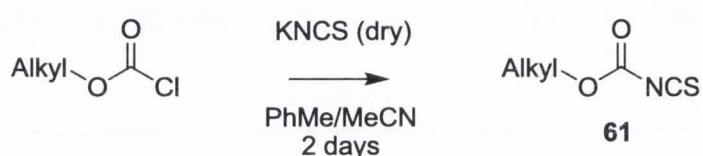
The method of Hamilton *et al.* is compatible with possibly the broadest range of substrates of any procedure published to date.²⁰⁸ The authors first prepare a carbamoyl isothiocyanate reagent **61** which is subjected to an appropriately substituted amine, followed by a second amine and EDCI in a one-pot procedure (Scheme 4.11). The authors report the successful preparation of several *N*-alkyl-*N'*-aryl and asymmetrical *N*-aryl₁-*N'*-aryl₂ disubstituted guanidines, incorporating a wide variety of electron-donating and electron-withdrawing substituents. Notably, the reaction failed to proceed when secondary amines or electron poor aromatic amines were utilised in the second step of the reaction.

Scheme 4.11 Hamilton's method for the preparation of *N,N'*-disubstituted guanidines



Although Hamilton's procedure is admirable in both scope and simplicity, several shortfalls remain which prompt the development of an improved methodology. Foremost among these concerns is key reagent **61**, the preparation of which necessitates a two-day reaction time, the special preparation of dry KNCS, and the use of expensive *S*-alkyl chlorothioformate precursors (Scheme 4.12).²⁰⁹

Scheme 4.12 Hamilton's method for the preparation of carbamoyl isothiocyanates **61**



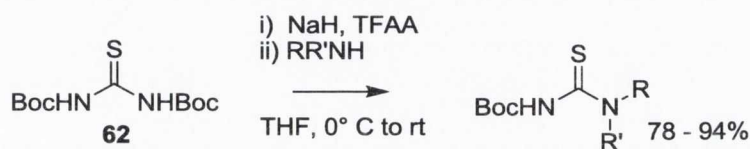
Secondly, in several instances the authors were forced to revert to a stepwise protocol, increasing the reaction length from two to three steps. In order to avoid the possibility of a failed reaction and wasted starting materials, the 'one-pot' protocol is therefore best carried out over three steps. It remains impressive, however, that Hamilton's method is among the few which allow for facile variation of which carbamate is incorporated into the product guanidine through selection of the appropriate carbamoyl isothiocyanate **61**. The authors note that base-sensitive carbamates such as fluorenylmethyloxycarbonyl (Fmoc) are incompatible with their reaction conditions, however this incompatibility is not limited to their procedure as the majority of guanidylation protocols employ basic conditions.

4.2.2 A concise synthesis of *N,N'*-disubstituted guanidines

To overcome the limitations of previous methodologies, we sought to develop a facile and robust procedure for the rapid generation of a structurally diverse library of *N,N'*-disubstituted guanidines.²¹⁰ The protocol should be amenable to the synthesis of asymmetrical *N*-alkyl-*N'*-aryl and *N*-aryl₁-*N'*-aryl₂ disubstituted guanidines, and be able to tolerate a wide range of functional groups. Moreover, the reaction conditions should be mild, expedient, and afford a productive yield. To facilitate the application to library synthesis, the reagents used should also be inexpensive and readily available.

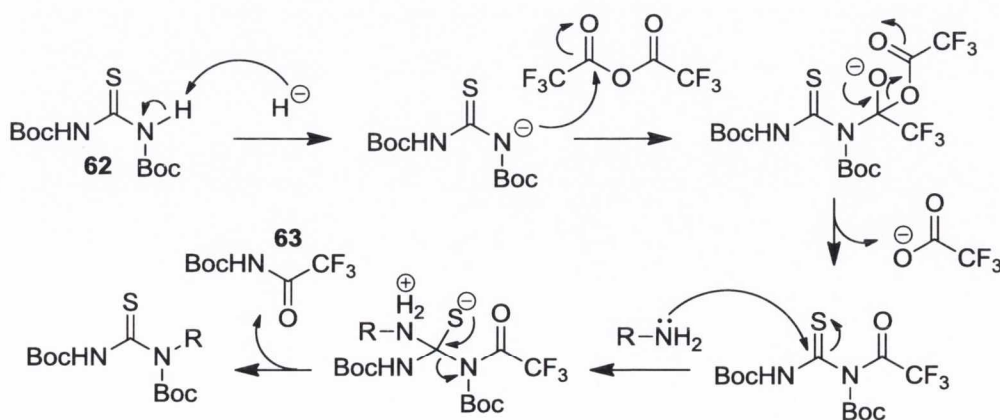
In a recent publication, Yin *et al.* have described the preparation of *N*-Boc-*N'*-substituted thioureas by treatment of *N,N'*-di-Boc-substituted thiourea **62** with sodium hydride and trifluoroacetic anhydride (TFAA) in the presence of an amine (Scheme 4.13).²¹¹ The reaction proceeds with both aryl and alkyl amines in good to excellent yield. Most importantly, the product thiourea derivatives are ideally functionalised for the synthesis of *N,N'*-disubstituted guanidines as suggested by methods previously developed by Poss²⁰³ and by Hamilton.²⁰⁸

Scheme 4.13 Yin's method for the synthesis of *N*-Boc-*N'*-substituted thioureas



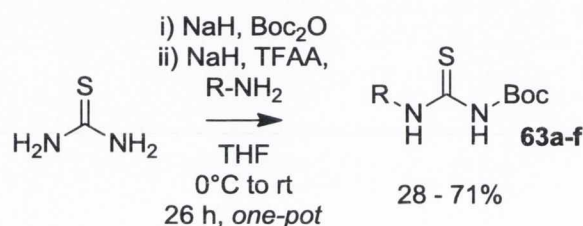
In a subsequent publication, Yin describes two possible mechanisms for this transformation.²¹² In the first of these, the anion formed by deprotonation of **62** is *N*-acylated to produce the *N*-Boc-*N*-trifluoroacetyl derivative, which undergoes nucleophilic attack by the amine during the second step. During our initial studies investigating this reaction, side product **63** was isolated, supporting this mechanism (Scheme 4.14). An alternative mechanism suggested by the authors involves acylation at the carbonyl oxygen to produce the *O*-trifluoroacetyl derivative; however, the latter mechanism is not supported by our studies. A further possibility involves displacement of the *N*-Boc-*N*-trifluoroacetyl group to generate an isothiocyanate intermediate prior to nucleophilic attack; nevertheless, the authors failed to comment on this third possibility.

Scheme 4.14 One possible mechanism for the formation of *N*-Boc-*N'*-substituted thioureas



With Yin's methodology at hand, we then turned our attention to *N,N'*-bis-Boc protected thiourea **62**, recognising that this expensive reagent²¹³ was available in a single step from inexpensive thiourea and Boc₂O in the presence of sodium hydride. The possibility of generating **62** *in situ* followed by the application of Yin's procedure would permit the preparation of the requisite *N*-Boc-*N'*-substituted thioureas from simple starting materials following a one-pot procedure (Scheme 4.15).

Scheme 4.15 One-pot procedure for the preparation of *N*-Boc-*N'*-substituted thioureas



In the event, the reaction conditions were optimised by varying reaction times and equivalents of each reagent, using *n*-propylamine as the amine component (Table 4.1). Sadly, the optimised procedure provided only small improvements in yield for amines other than *n*-propylamine, suggesting that while reaction conditions can be adjusted to improve the yield for different amines, the optimised procedure does not universally produce optimal yields.

Table 4.1 Optimisation of reaction conditions for the preparation of *N*-Boc-*N'*-substituted thioureas using *n*-propylamine as the amine component

| Step 1 | | | Step 2 | | | | Yield (%) |
|--------------|-----------------------------|--------------|--------------|---------------|----------------|--------------|-----------|
| NaH (equiv.) | Boc ₂ O (equiv.) | Time (hours) | NaH (equiv.) | TFAA (equiv.) | Amine (equiv.) | Time (hours) | |
| 3 | 2.4 | 18 | 1.2 | 1.1 | 1.1 | 18 | 37 |
| 4.5 | 2.4 | 18 | 1.2 | 1.1 | 1.1 | 18 | 36 |
| 6 | 2.4 | 18 | 1.2 | 1.1 | 1.1 | 18 | 43 |
| 6 | 1.9 | 18 | 1.2 | 1.2 | 1.1 | 18 | 29 |
| 6 | 2.3 | 18 | 0.9 | 1.2 | 1.1 | 18 | 12 |
| 6 | 2.2 | 6 | 1.2 | 1.1 | 1.1 | 18 | 55 |
| 4.5 | 2.2 | 8 | 1.7 | 1.5 | 1.5 | 18 | 71 |

The optimised procedure proved compatible with a range of aromatic and aliphatic amines (Table 4.2). Although it is difficult to decidedly state what effect the choice of R group has on yield, it appears that simple substrates with fewer functional groups perform significantly better in this reaction. The yields range from fair to good; however, our results compare poorly with those originally reported by Yin *et al.* Nonetheless, given that this protocol is a one-pot procedure, the fact that the first step of the reaction proceeds to only about 80% completion (see Scheme 4.2) significantly reduces the maximum possible yield. In spite of this disappointing result, our optimisation experience suggests that the conditions may be tuned to provide significantly improved yields where necessary.

Table 4.2 *N*-Boc-*N'*-substituted thioureas prepared as per Scheme 4.15

| Compound | R | Yield (%) |
|------------|---|-----------|
| 63a | -(CH ₂) ₂ -CH ₃ | 71 |
| 63b | -(CH ₂) ₂ -OH | 43 |
| 63c | -C ₆ H ₅ | 46 |
| 63d | -C ₆ H ₄ (<i>p</i> -NMe ₂) | 28 |
| 63e | -C ₆ H ₄ (<i>p</i> -OEt) | 49 |
| 63f | -CH ₂ -Fur-2-yl | 58 |

With the requisite thiourea derivatives in hand, we proceeded to prepare the *N,N'*-disubstituted guanidines described in our molecular design scheme (see Fig. 3.8). The mercury (II) chloride promoted procedure of Kim and Qian proceeded smoothly and afforded the desired products in generally good yields (Scheme 4.16; Table 4.3), with the exception of the 4-ethylaminophenyl derivatives (compounds **65d** - **68d**) which gave poorer yields, possibly as a result of the presence of two different amines within the substrate.

Scheme 4.16 Procedure for the preparation of Boc protected *N,N'*-disubstituted guanidines

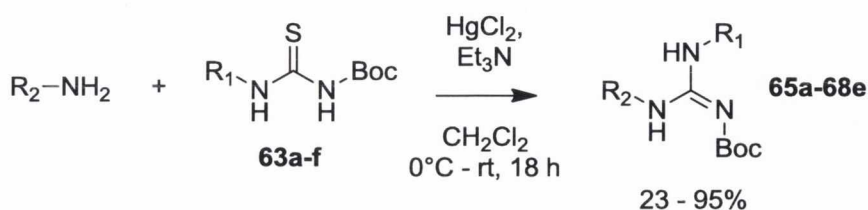
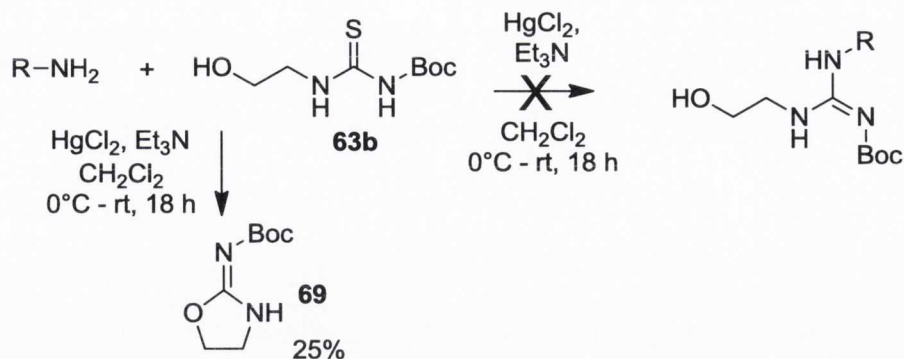


Table 4.3 Boc protected *N,N'*-di-substituted guanidines prepared as per Scheme 4.16

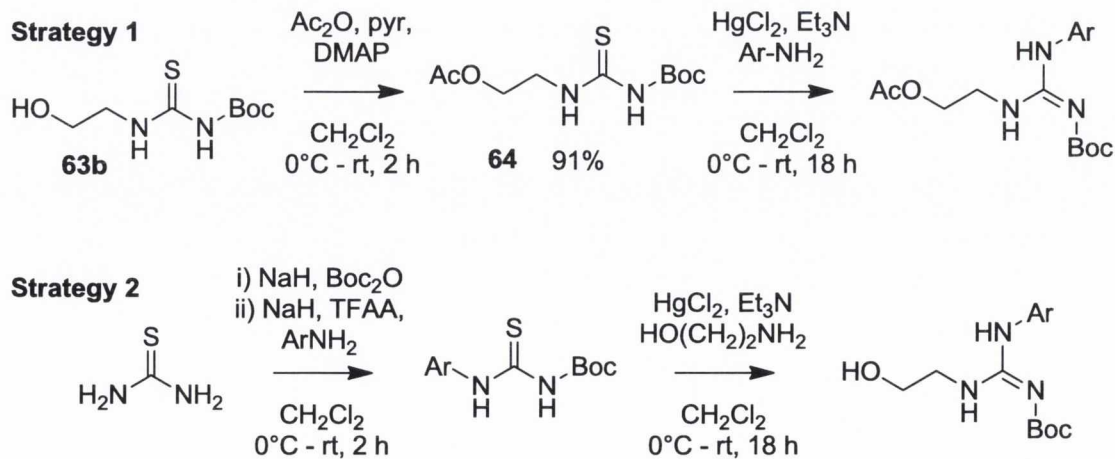
| Compound | Starting thiourea | R ₁ | R ₂ | Yield (%) |
|----------|-------------------|---|--|-----------|
| 65a | 63a | -(CH ₂) ₂ -CH ₃ | -C ₆ H ₄ (<i>p</i> -OEt) | 91 |
| 65b | 63d | -(CH ₂) ₂ -CH ₃ | -C ₆ H ₄ (<i>p</i> -NMe ₂) | 82 |
| 65c | 63a | -(CH ₂) ₂ -CH ₃ | -C ₆ H ₃ (-CH ₂ -) ₄ | 78 |
| 65d | 63a | -(CH ₂) ₂ -CH ₃ | -C ₆ H ₄ (<i>p</i> -NHEt) | 38 |
| 65e | 63a | -(CH ₂) ₂ -CH ₃ | -C ₆ H ₃ (-OCH ₂ O-) | 75 |
| 66a | 63e | -(CH ₂) ₂ -OH | -C ₆ H ₄ (<i>p</i> -OEt) | 49 |
| 66b | 63d | -(CH ₂) ₂ -OH | -C ₆ H ₄ (<i>p</i> -NMe ₂) | 67 |
| 66c | 64 | -(CH ₂) ₂ -OAc | -C ₆ H ₃ (-CH ₂ -) ₄ | 75 |
| 66d | 64 | -(CH ₂) ₂ -OAc | -C ₆ H ₄ (<i>p</i> -NHEt) | 23 |
| 66e | 64 | -(CH ₂) ₂ -OAc | -C ₆ H ₃ (-OCH ₂ O-) | 69 |
| 67a | 63c | -C ₆ H ₅ | -C ₆ H ₄ (<i>p</i> -OEt) | 53 |
| 67b | 63d | -C ₆ H ₅ | -C ₆ H ₄ (<i>p</i> -NMe ₂) | 88 |
| 67c | 63c | -C ₆ H ₅ | -C ₆ H ₃ (-CH ₂ -) ₄ | 84 |
| 67d | 63c | -C ₆ H ₅ | -C ₆ H ₄ (<i>p</i> -NHEt) | 55 |
| 67e | 63c | -C ₆ H ₅ | -C ₆ H ₃ (-OCH ₂ O-) | 84 |
| 68a | 63f | -CH ₂ -fur-2-yl | -C ₆ H ₄ (<i>p</i> -OEt) | 88 |
| 68b | 63d | -CH ₂ -fur-2-yl | -C ₆ H ₄ (<i>p</i> -NMe ₂) | 90 |
| 68c | 63f | -CH ₂ -fur-2-yl | -C ₆ H ₃ (-CH ₂ -) ₄ | 95 |
| 68d | 63f | -CH ₂ -fur-2-yl | -C ₆ H ₄ (<i>p</i> -NHEt) | 27 |
| 68e | 63f | -CH ₂ -fur-2-yl | -C ₆ H ₃ (-OCH ₂ O-) | 65 |

Notably, during the attempted guanidylation of *N*-Boc-*N'*-hydroxyethyl thiourea **63b** with *p*-ethoxyaniline, we found that this reaction failed to produce the intended guanidine derivative. Instead, the hydroxyethyl moiety of thiourea **63b** cyclised to produce (*E*)-oxazolidin-2-(*N*-*tert*-butoxycarbonyl)imine (**69**; Scheme 4.17). This intramolecular cyclisation is unsurprising given the proximity of the hydroxyl group to the electrophilic thiourea moiety, and we devised two possible strategies to circumvent this problem.

Scheme 4.17 The cyclisation of thiourea **63b** to produce 2-iminooxazolidine derivative **69**

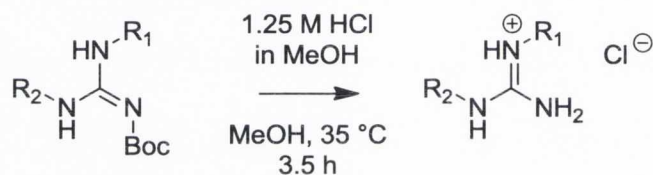
In the first approach, the corresponding *N*-Boc-*N'*-acetoxyethyl thiourea (**64**) was prepared from the hydroxyethyl derivative **63b** to avoid cyclisation (Scheme 4.18). It was reasoned that the acetyl group would be labile under the acidic conditions used for deprotection of the guanidine moiety, thereby producing the alcohol in the same reaction and economising the number of transformations. The acetylation proceeded smoothly and in high yield (91%) using acetic anhydride, pyridine and catalytic 4-dimethylaminopyridine (DMAP).

In an alternative approach, we considered the preparation of the asymmetric *N,N'*-substituted guanidine derivatives **65b**, **66b**, **67b**, **68b** and **66a** from the corresponding *N*-Boc-*N'*-arylthioureas **63d** and **63e** by reaction with the appropriate amine following the conditions shown in Scheme 4.16. Although both approaches proved successful, acetate **64** can be used as an intermediate for every one of the desired *N*-hydroxyethyl guanidine derivatives and therefore we selected the first approach throughout the remaining work.

Scheme 4.18 Two strategies used for the synthesis of *N*-aryl-*N'*-hydroxyethyl guanidines

In our previous publications,¹⁵⁸⁻¹⁶⁰ the *N,N'*-*bis*-Boc protected guanidine intermediates were generally deprotected by treatment with a 1:1 solution of trifluoroacetic acid in methylene chloride at room temperature overnight, obtaining the final hydrochloride salts by treatment with basic anion-exchange resin (Amberlite IRA-400) in its chloride form. Our previous experience with the deprotection of *N,N'*-*bis*-Boc protected guanidines using various solutions of hydrochloric acid often led to hydrolysis of the guanidine moiety. However, in the case of the present Boc protected asymmetric *N,N'*-disubstituted derivatives, deprotection using a 1.25 M solution of methanolic HCl typically proceeded readily and without hydrolysis, affording the desired guanidine hydrochloride salts in good to excellent yields (Table 4.4) and in less than 4 h at 35 °C (Scheme 4.19).

Scheme 4.19 Procedure for the deprotection of Boc protected *N,N'*-disubstituted guanidines



Notably, the Boc protected *N*-(furan-2-ylmethyl) guanidine derivatives **68a** - **68e** proved unstable under these conditions, and a black polymeric solid was formed in less than one hour. The sensitivity of furan derivatives to methanolic hydrogen chloride is well documented, with β -protonation giving rise to opening of the furan ring.²¹⁴ The benzylic position also lies directly adjacent to the guanidine functionality, further enhancing the potential for side reactions in these species.

Our original procedure using a 1:1 solution of trifluoroacetic acid in methylene chloride provided no improvement, and polymerisation occurred as before. After some experimentation, treatment with a 0.1% solution of trifluoroacetic acid in methylene chloride over 4.5 h proved successful, affording a yield of 51 – 57%. These procedures were later improved by treatment of a solution of the substrate in dry methylene chloride with 6 molar equivalents of dry HCl in dioxane, affording yields of 53 – 84% (Table 4.4).

Table 4.4 *N,N'*-disubstituted guanidine hydrochloride salts prepared as per Scheme 4.19

| Compound | Starting Material | R ₁ | R ₂ | Method* | Yield (%) |
|----------|-------------------|---|--|---------|-----------|
| 69a | 65a | -(CH ₂) ₂ -CH ₃ | -C ₆ H ₄ (<i>p</i> -OEt) | A | 83 |
| 69b | 65b | -(CH ₂) ₂ -CH ₃ | -C ₆ H ₄ (<i>p</i> -NMe ₂) | B | 65 |
| 69c | 65c | -(CH ₂) ₂ -CH ₃ | -C ₆ H ₃ (-CH ₂ -) ₄ | B | 73 |
| 69d | 65d | -(CH ₂) ₂ -CH ₃ | -C ₆ H ₄ (<i>p</i> -NH ₂) | B | 39 |
| 69e | 65e | -(CH ₂) ₂ -CH ₃ | -C ₆ H ₃ (-OCH ₂ O-) | B | 85 |
| 70a | 66a | -(CH ₂) ₂ -OH | -C ₆ H ₄ (<i>p</i> -OEt) | B | 94 |
| 70b | 66b | -(CH ₂) ₂ -OH | -C ₆ H ₄ (<i>p</i> -NMe ₂) | B | 80 |
| 70c | 66c | -(CH ₂) ₂ -OH | -C ₆ H ₃ (-CH ₂ -) ₄ | B | 87 |
| 70d | 66d | -(CH ₂) ₂ -OH | -C ₆ H ₄ (<i>p</i> -NH ₂) | B | 77 |
| 70e | 66e | -(CH ₂) ₂ -OH | -C ₆ H ₃ (-OCH ₂ O-) | B | 98 |
| 71a | 67a | -C ₆ H ₅ | -C ₆ H ₄ (<i>p</i> -OEt) | B | 87 |
| 71b | 67b | -C ₆ H ₅ | -C ₆ H ₄ (<i>p</i> -NMe ₂) | B | 70 |
| 71c | 67c | -C ₆ H ₅ | -C ₆ H ₃ (-CH ₂ -) ₄ | B | 88 |
| 71d | 67d | -C ₆ H ₅ | -C ₆ H ₄ (<i>p</i> -NH ₂) | B | 44 |
| 71e | 67e | -C ₆ H ₅ | -C ₆ H ₃ (-OCH ₂ O-) | B | 79 |
| 72a | 68a | -CH ₂ -Fur-2-yl | -C ₆ H ₄ (<i>p</i> -OEt) | C | 51 |
| 72b | 68b | -CH ₂ -Fur-2-yl | -C ₆ H ₄ (<i>p</i> -NMe ₂) | C | 57 |
| 72c | 68c | -CH ₂ -Fur-2-yl | -C ₆ H ₃ (-CH ₂ -) ₄ | D | 53 |
| 72d | 68d | -CH ₂ -Fur-2-yl | -C ₆ H ₄ (<i>p</i> -NH ₂) | D | 84 |
| 72e | 68e | -CH ₂ -Fur-2-yl | -C ₆ H ₃ (-OCH ₂ O-) | D | 65 |

**Method A*: 1:1 Trifluoroacetic acid/methylene chloride, rt, 2 h; then Amberlite/H₂O, rt, 24 h.

Method B: 1.25 M methanolic HCl, 35°C, 3.5 h.

Method C: 0.1 % v/v Trifluoroacetic acid/methylene chloride, rt, 2 h; then Amberlite/H₂O, rt, 24 h.

Method D: 6 M HCl/dioxane in methylene chloride, rt to 35°C, 4.5h.

Generally, the conditions used for deprotection benefit from some adjustment for different substrates. Acid-sensitive functional groups such as furan derivatives necessitate the use of stoichiometric quantities of acid, while simpler substrates can be deprotected with methanolic

HCl. In our experience, substrates bearing an electron-donating group at the 4 position of the aromatic ring (such as **66e**, **69a** and **71e**) were completely deprotected over a shorter reaction time (adjudged by TLC) than substrates with an electron-withdrawing moiety at this position (such as the 4-ethylamino derivatives **69d**, **70d**, **71d** and **72d**; the ethylamino group is generally protonated under the conditions of the reaction).

The difference in reactivity can be explained by the effect of this group upon the basicity of the Boc group, which must become protonated for deprotection to proceed. In substrates bearing an electron-donating substituent, the Boc group is made more basic through conjugate donation of electron density, while in substrates with an electron-withdrawing substituent, the Boc group becomes less basic and deprotection proceeds less readily. Thus, to a first approximation the reaction conditions can be selected on the basis of the electronic effects upon the Boc group. However, it is often more practical to initiate the reaction using mild conditions and to increase the acidity, reaction time and temperature according to reaction progress as monitored by TLC and MS.

In conclusion, we have developed a protocol which facilitates the synthesis of *N,N'*-disubstituted guanidine derivatives from two starting amines. In contrast with previous methodologies, our procedure utilises simple, inexpensive starting materials; can be carried out over a short timescale and with a minimum of steps, and is compatible with both aromatic and aliphatic amines. For troublesome substrates, the reaction conditions can be adjusted to improve the yield and substrate-compatibility of the procedure; however, the general procedure provides good yields for a broad range of substrates without further optimisation. Thus, our new route to *N,N'*-disubstituted guanidines is simple, affordable and shows the additional advantage of allowing the preparation of asymmetrically substituted *bis*-aryl guanidine derivatives, which have proven difficult to prepare in the past.^{205,215}

4.2.3 Conformational aspects of *N,N'*-disubstituted guanidines

As with their *N,N'*-*bis*-Boc protected analogues (Section 4.1.2), Boc protected *N,N'*-disubstituted guanidine derivatives also exhibit *E/Z* isomerism with reference to a localised imine double bond. In the case of *N*-alkyl-*N'*-aryl Boc protected guanidines, the most stable tautomer again places the C2'=N3' imine into conjugation with the Boc carbonyl group. Both the *E* and *Z* configurations about this imine double bond allow for a stabilising hydrogen

bond between a guanidine NH proton and the Boc carbonyl which is evocative of the hydrogen bonding already established for their *bis*-Boc protected analogues. However, in this case the *Z* isomer allows an IMHB to exist between the more acidic aryl NH proton and the Boc carbonyl, while the *E* isomer supports an IMHB involving the alkyl NH proton. As a result of the increased acidity of the anilinic NH proton (N1', Fig. 4.6), the *Z* isomer supports a more favourable IMHB and is likely to be lower in energy than the *E* isomer.

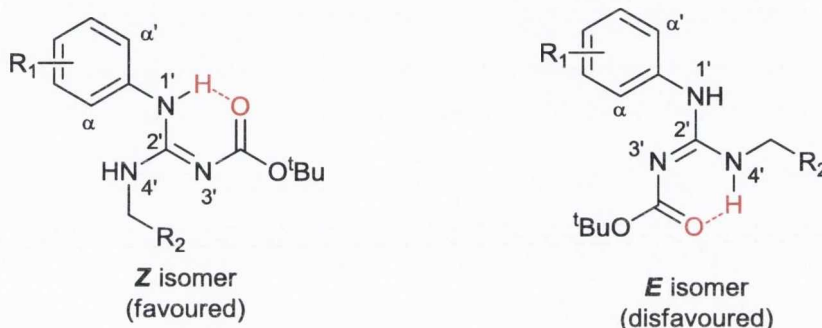


Fig. 4.6. *Left:* *Z* configuration of *N*-alkyl-*N'*-aryl Boc protected aryl guanidines. *Right:* *E* configuration of the same derivatives. Hydrogen bonding interactions are shown in red.

In agreement with this prediction, a single configuration predominates in the NMR spectra for *N*-alkyl-*N'*-aryl Boc protected guanidine derivatives. The existence of a single configuration exhibiting the expected arrangement of IMHBs finds experimental evidence in the ^1H NMR shifts recorded for the NH signals; the hydrogen-bonded NH signal (N1', Fig. 4.6) appears far downfield (10 - 11 ppm) from the second NH signal (N4', Fig. 4.6; 4 - 5 ppm; Fig. 4.7).

The prevalence of the *Z* isomer was also investigated using ROESY experiments in an attempt to confirm the presence of a through-space interaction between the non-hydrogen bonded NH proton (N4', Fig. 4.6) and the nearby CH protons on the aromatic substituent (C_α and $\text{C}_{\alpha'}$, Fig. 4.6). However, the amine NH signals proved unresponsive to the Nuclear Overhauser Effect in these experiments. As a result, definitive evidence in support of the *Z* configuration was not available through these experiments. Nonetheless, it is evident that a single isomer predominates in the ^1H NMR spectrum of these compounds, and energetic arguments strongly suggest that this is the *Z* isomer.

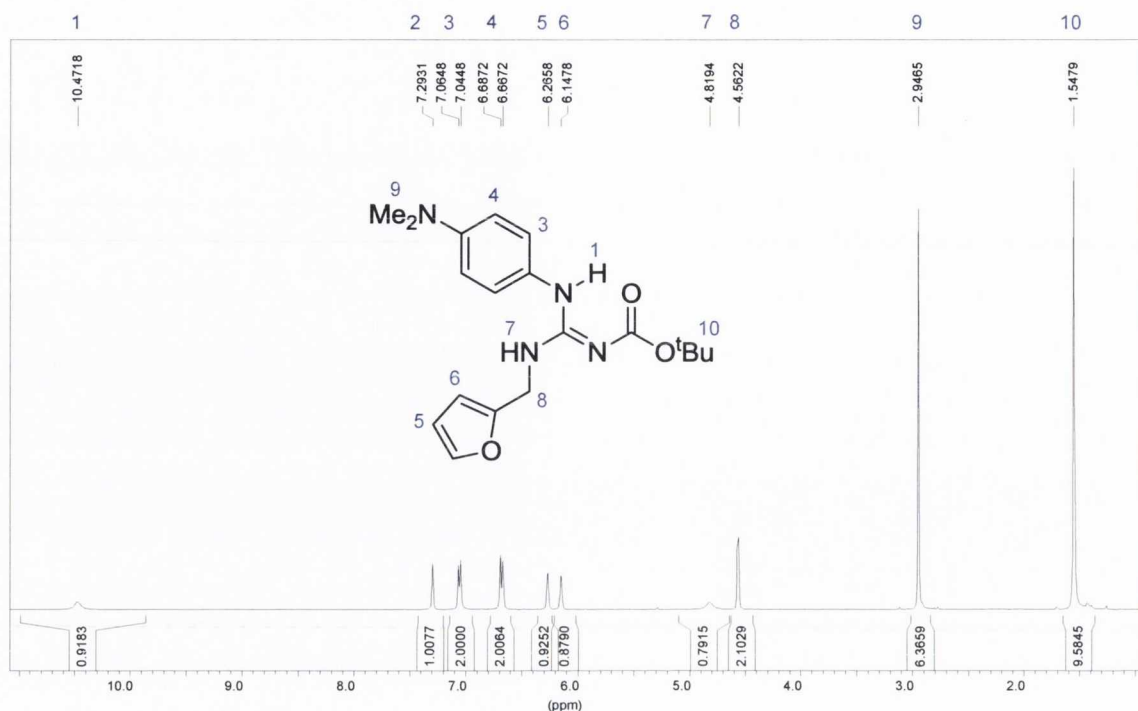


Fig. 4.7. The ¹H NMR spectrum of 1-[1-(*Tert*-butoxycarbonyl)-3-(fur-2-ylmethyl)guanidino]-4-(dimethylamino)benzene **68b** in CDCl₃ (400 MHz).

The closely related *N*-aryl₁-*N'*-aryl₂ Boc protected guanidine derivatives provide a special case with regard to the configurational preference described above. For these compounds, two nearly degenerate isomers can be drawn, with both structures incorporating the previously mentioned IMHB between the Boc carbonyl and a guanidine NH proton. Both isomers also incur steric hindrance between the remaining guanidine NH and the adjacent aromatic ring (Fig. 4.8). This configuration closely corresponds to the *Z* conformation suggested to predominate in *N*-alkyl-*N'*-aryl Boc protected guanidines (Fig. 4.6, *left*).

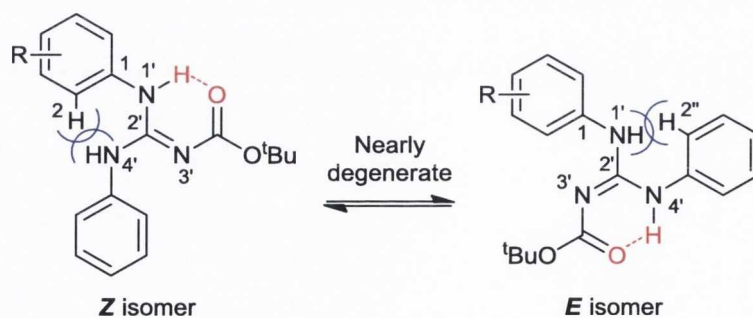


Fig. 4.8. The configuration of *bis*-aryl Boc protected guanidine derivatives. Stabilising hydrogen bonding interactions are shown in red, steric clashes are shown in blue.

The near-degeneracy of these two configurations implies that these compounds exist as a mixture of isomers. Owing to a severe broadening of the signals (even in the ^{13}C NMR spectrum), the actual *E:Z* ratio proved difficult to establish by NMR and it is possible that the two isomers rapidly interconvert in solution. In both isomers, steric crowding suggests that the co-planar arrangement of the guanidine and both aromatic rings which would allow conjugation between all three π systems (both phenyl rings and the Boc carbonyl) via the central guanidine moiety cannot be attained (Fig. 4.9). One of the rings must therefore adopt an out-of-plane conformation, and rotation of this ring about the C1-N1 bond becomes restricted by the nearby NH group of the guanidine (N1' and C2'', Fig. 4.8, *right*). The choice of which phenyl ring adopts the twisted geometry is energetically ambiguous; as a result it is likely that the molecule rapidly equilibrates between both possibilities.

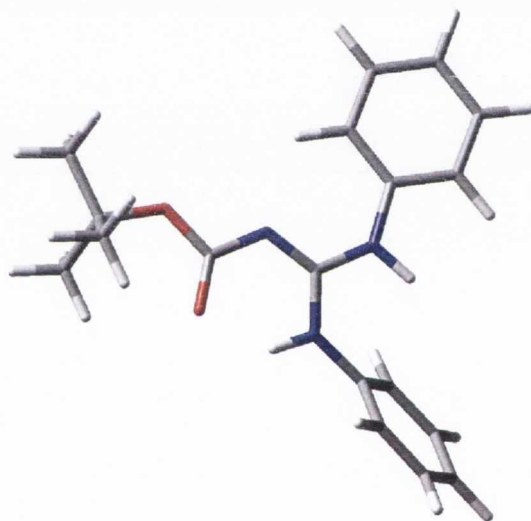


Fig. 4.9. DFT computational model (B3LYP) of 1-[1-(*tert*-butoxycarbonyl)-3-phenylguanidino]benzene²¹⁶ demonstrating the twisted geometry adopted by the phenyl rings.

In the ^1H NMR spectra of these species, restricted rotation of the phenyl rings results in a profoundly shorter relaxation time for the aromatic signals. Coupled with the potential for equilibration between the *E* and *Z* isomers, this phenomenon results in the aromatic protons appearing as a broad, amorphous multiplet spanning the aromatic region (Fig. 4.10). Aromatic signals in the ^{13}C spectra are also highly amorphous, and the definitive assignment of signals becomes impossible even when utilising 2D experiments such as HMBC and HSQC.

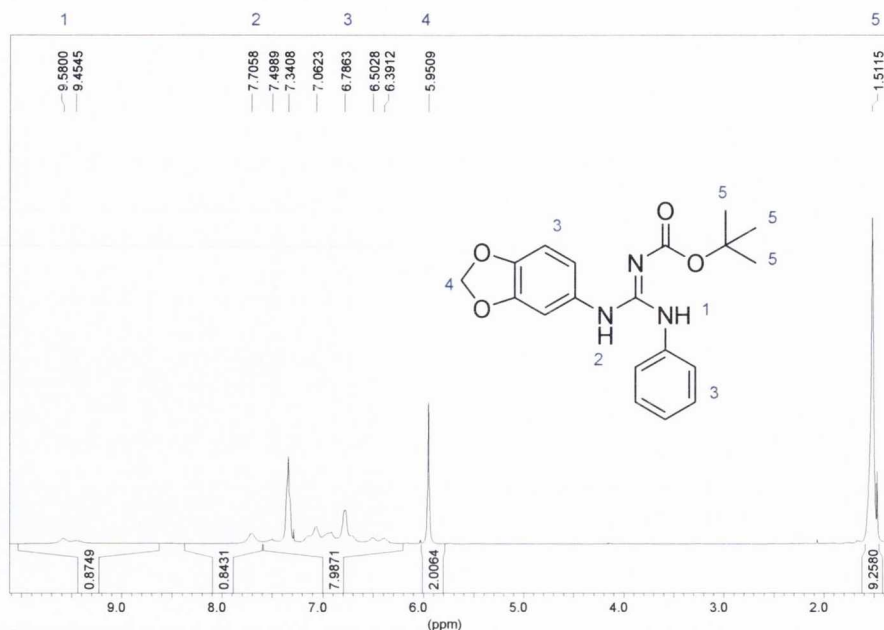


Fig. 4.10. The ¹H NMR spectrum of 1-[1-(*tert*-butoxycarbonyl)-3-phenylguanidino]-3,4-methylenedioxybenzene **67e** in CDCl₃ (400 MHz).

Deprotection of the Boc group alleviates the steric congestion experienced by the aromatic rings. The relaxation times return to ordinary levels and the aromatic NMR signals of the deprotected *bis*-aryl hydrochloride salts are correspondingly sharpened (Fig. 4.11).

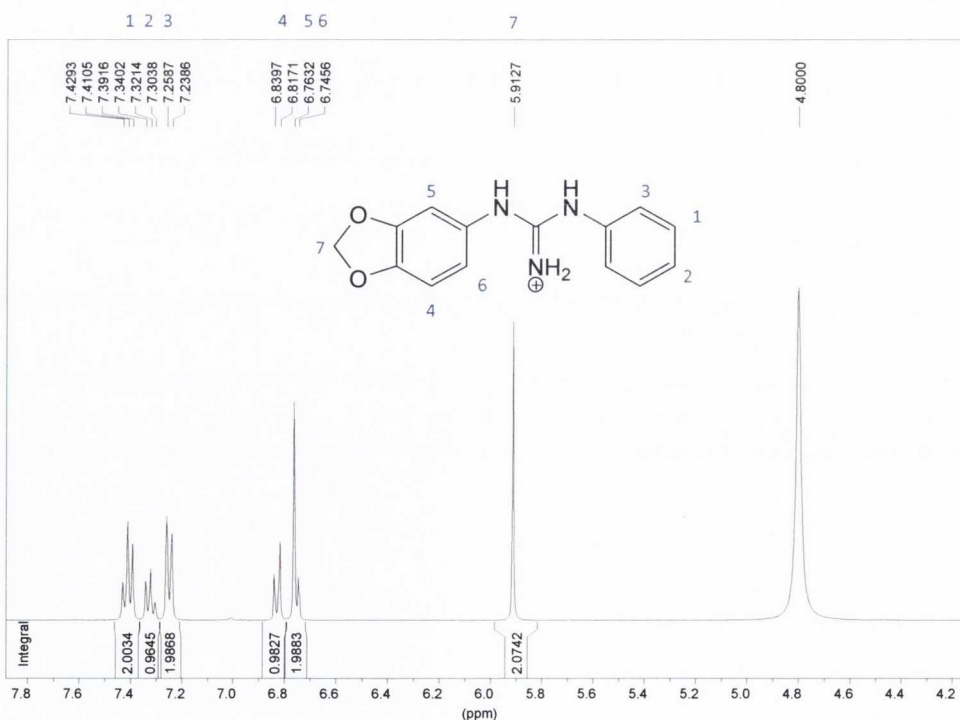


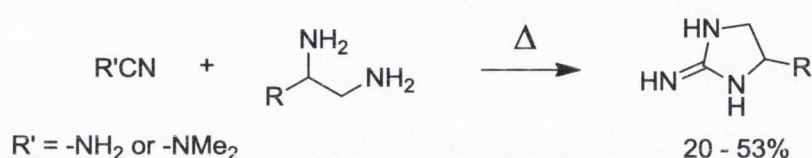
Fig. 4.11. ¹H NMR spectrum of *N*-(3,4-methylenedioxyphenyl)-*N'*-phenylguanidine hydrochloride **71e** in D₂O (400 MHz).

4.3 4-Substituted-2-Aryliminoimidazolidines

4.3.1 Literature methods for the preparation of 2-aryliminoimidazolidines

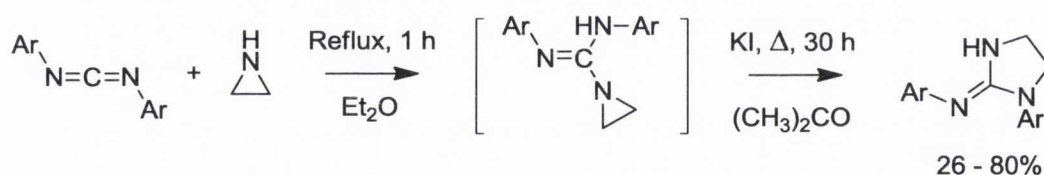
An early example of the synthesis of 2-iminoimidazolidines is described in a series of papers dating from the 1960s by Adcock and Lawson. According to their initial procedures, cyanamide or dimethylcyanamide is reacted with a 1,2-diamine to produce 2-iminoimidazolidine derivatives in relatively poor yields (Scheme 4.20).²¹⁷

Scheme 4.20 Lawson's method for preparing 2-iminoimidazolidines via 1,2 diamines



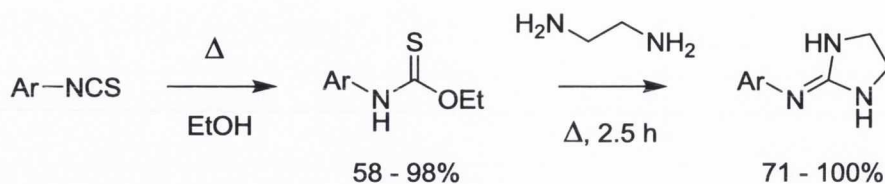
The authors later described the rearrangement of 1-(*N,N'*-diarylamidino)aziridines to generate the corresponding 2-aryliminoimidazolidine derivatives (Scheme 4.21)²¹⁸ in a reaction reminiscent of the vinyl cyclopropane rearrangement.²¹⁹ Although they suggest several methods for effecting this rearrangement, the use of potassium iodide provided the most direct route to the intended products.

Scheme 4.21 Lawson's method for preparing 2-aryliminoimidazolidines via the rearrangement of 1-(*N,N'*-bis-arylamidino)aziridines



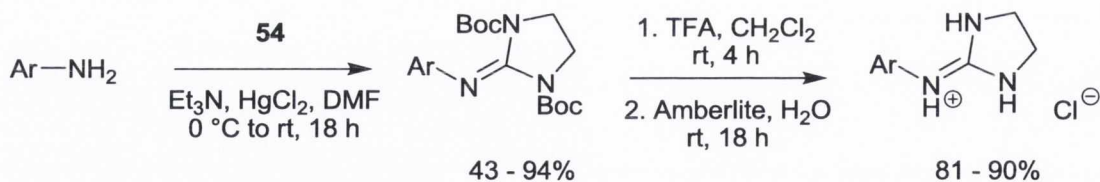
A milder and more general methodology was described in a 1980 publication by Reynaud in which aryl isothiocyanates are converted to their *O*-ethyl thiocarbamate derivatives by reflux in ethanol. The *O*-ethyl thiocarbamates are then reacted with ethylene diamine to produce the corresponding 2-aryliminoimidazolidine derivatives (Scheme 4.22).²¹⁸

Scheme 4.22 Reynaud's method for preparing 2-aryliminoimidazolidines via *O*-ethyl thiocarbamates prepared from isothiocyanates



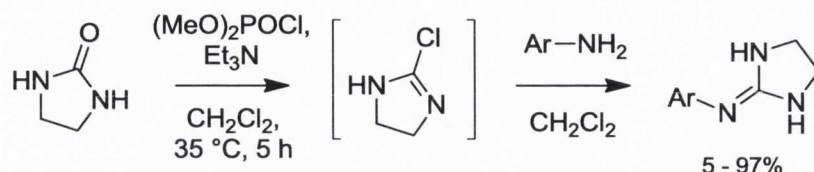
A protocol developed within our group for the synthesis of 2-aryliminoimidazolidine derivatives using *N,N'*-bis-(*tert*-butoxycarbonyl)imidazolidine-2-thione **54** was introduced at the beginning of this chapter (see Section 4.1.1).¹⁹⁵ The main advantages of this methodology are mild conditions, tolerance of a wide range of functional groups, and generally high yields. Most importantly, this procedure facilitates the preparation of 2-aryliminoimidazolidines from poorly reactive amines such as aniline derivatives, and affords the corresponding *bis*-Boc protected derivatives which can be readily deprotected using trifluoroacetic acid (Scheme 4.23).

Scheme 4.23 Rozas and Dardonville's method for the synthesis of 2-aryliminoimidazolidine derivatives from aniline analogues using mercury (II) chloride



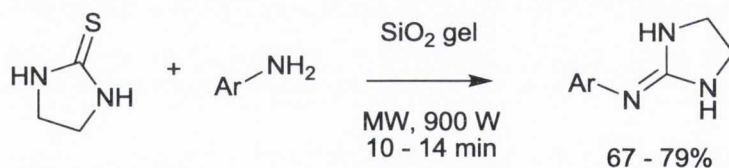
In contrast to earlier preparative procedures, many recent methods similarly employ aniline derivatives for the synthesis of 2-aryliminoimidazolidines, possibly owing to the broad range of anilines which are commercially available and the simplicity of handling these reagents. In 2005 Chern *et al.* described their synthesis using aniline derivatives with 2-chloro-2-imidazolidine (generated *in situ* from inexpensive imidazolidin-2-one) to afford good to excellent yields of the desired 2-aryliminoimidazolidines (Scheme 4.24).²²⁰

Scheme 4.24 Kan, Lin and Chern's method for the synthesis of 2-aryliminoimidazolidine derivatives from anilines using 2-chloro-2-imidazolidine



In 2007, Servi and Genc described the microwave-assisted preparation of 2-iminoimidazolidines from aniline derivatives in the presence of imidazolidine-2-thione and silica gel. Their procedure is among the most expedient described in the literature, with typical irradiation times of 10 - 14 min (900 W, 2450 MHz) and affords generally good yields. The authors only provide examples using electron-rich aniline derivatives; electron-poor and hence less nucleophilic anilines are absent from their reports (Scheme 4.25).²²¹

Scheme 4.25 Servi and Genc's method for the synthesis of 2-aryliminoimidazolidine derivatives via microwave irradiation of anilines in the presence of imidazolidine-2-thione

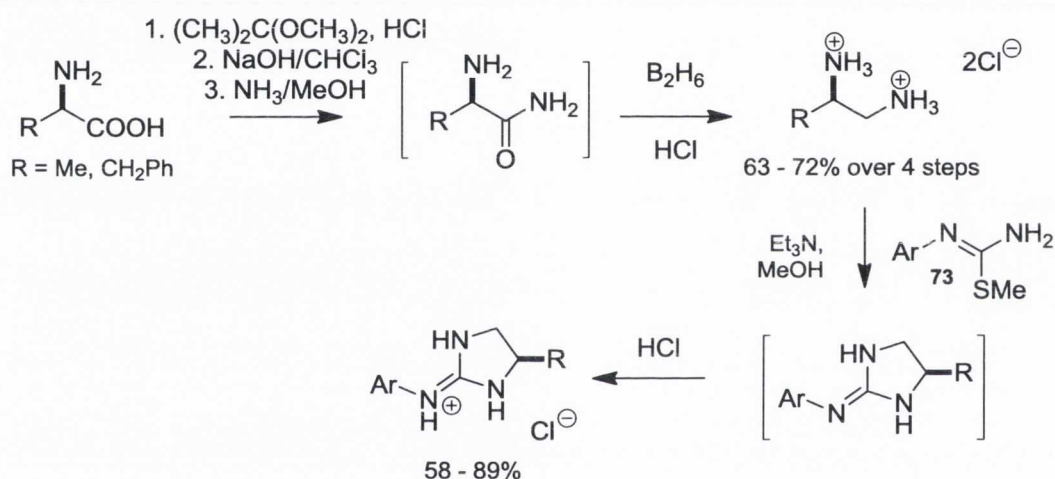


4.3.2 Literature reports of 4-substituted 2-aryliminoimidazolidines

An early example of the synthesis and α_2 -AR pharmacology of 4-substituted 2-aryliminoimidazolidines was reported in 1980 by Miller *et al.*²²² One striking observation made during these studies is the capacity of methyl substitution in the 4 position to induce a shift from agonism to antagonism at the α_2 -AR. These results provide an encouraging precedent for our molecular design scheme, which strongly suggests that the introduction of steric bulk at this position might induce such a shift (see Chapter 3, CoMFA and Rational Design).

Their synthetic procedures begin with optically active amino acids, which are converted to the corresponding 3-substituted 1,2-diaminopropanes with retention of stereochemistry. The 1,2-diaminopropanes are then reacted with *S*-methyl-*N*-aryl-isothiourea derivatives **73** to provide the desired 4-substituted 2-aryliminoimidazolidines (Scheme 4.26). In spite of the careful retention of chirality, the eutomeric ratio was close to unity for every compound tested and ranged from just 1.00 to 1.04, with the *S* enantiomer consistently producing stronger affinities, albeit only to a miniscule degree.

Scheme 4.26 Miller's synthesis of 4-substituted 2-aryliminoimidazolidines via 3-substituted 1,2-diaminopropanes derived from optically active amino acids



In 1987 and 1991, Leclerc and co-workers described the synthesis of 4-alkoxy derivatives as potential ocular antihypertensives for the treatment of glaucoma and related diseases.^{223,224}

By incorporating a side chain similar to that of known β -AR antagonists such as propranolol (Fig. 4.12), the authors hoped to incorporate some β -AR blocking character into their molecular design. The resulting derivatives exhibit selectivity for the α_2 -AR *versus* the α_1 -AR, alongside some affinity for the β -ARs. Sadly, the affinity of these derivatives was generally low, and activity (agonist *versus* antagonist) proved variable and difficult to interpret, with each compound exhibiting a different spectrum of activities at the various receptors. Once again, the authors note that the eutomeric ratio was close to unity for all three ARs under investigation.

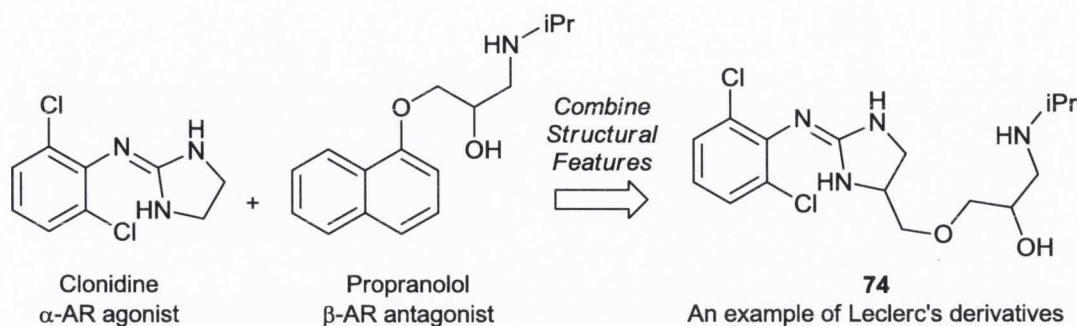
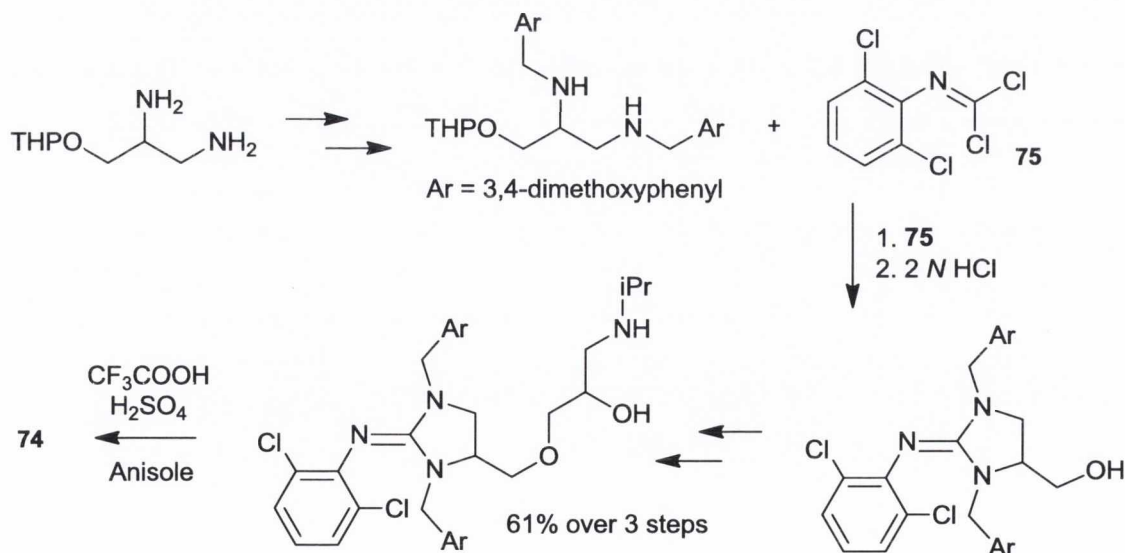


Fig. 4.12. Molecular design scheme of Leclerc and co-workers.

Leclerc's reports pay particular attention to difficulties encountered during the synthesis of these compounds. The *N*-acyl groups classically used to protect the 2-iminoimidazolidine functionality proved labile during their procedures, necessitating the development of a tailored protection strategy utilising the 3,4-dimethoxybenzyl group. Their synthesis begins in a similar vein to Miller *et al.*, employing a 1,2-diamine precursor which is combined with an aniline derivative to construct the central 1-aryl-2-iminoimidazolidine motif. Deprotection of the *N,N'*-bis-3,4-dimethoxybenzyl groups was effected using a mixture of trifluoroacetic and sulphuric acids in anisole (Scheme 4.27).

Scheme 4.27 Leclerc's synthesis of 4-substituted 2-aryliminoimidazolidines utilising their *N,N'*-bis-3,4-dimethoxybenzyl protecting group strategy



During a 1995 study examining analogues of the clinically used α_2 -AR agonist UK-14,304 (Brimonidine; Fig. 4.13), Jeon and co-workers prepared the 4-methyl analogue **76** and the *cis*-fused cyclohexyl analogue **77** and examined the affinity for each subtype of the α_2 -AR using cloned human ARs.²²⁵ While UK-14,304 is a potent agonist of all three subtypes, **76** is a competitive antagonist at the α_{2B} and α_{2C} subtypes, and **77** acts as an antagonist at all three subtypes. Their synthetic scheme follows a similar approach to that of Miller *et al.*, combining the requisite aryl isothiocyanate derivative with a 1,2 diamine precursor to form the central 2-iminoimidazolidine motif.

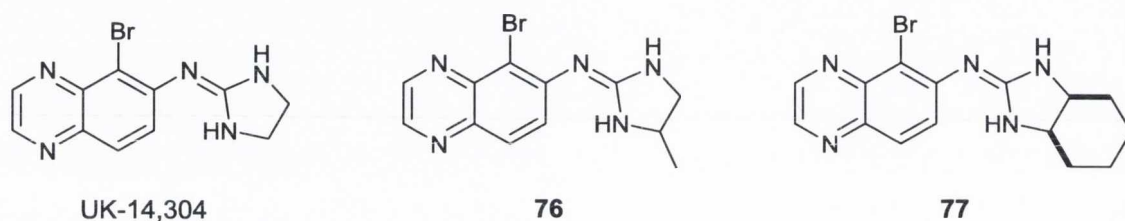


Fig. 4.13. Analogues of UK-14,304 examined by Jeon and co-workers.

A very recent example of the application of 4-substituted 2-aryliminoimidazolidines as α_2 -AR ligands can be found in a 2011 paper by Treder *et al.*²²⁶ The authors combine the structural features of the putative imidazoline binding site (IBS) neurotransmitter agmatine²²⁷ with the aryl-2-iminoimidazolidine motif to generate a series of novel α_2 -AR ligands derived from well-studied imidazoline-type ligands such as clonidine and idazoxan (Fig. 4.14). The preparative method of Treder *et al.* again follows Miller's approach using the appropriate 1,2 diamine with an *S*-alkyl-*N*-arylisothiourea derivative such as **73** (see Scheme 4.26).

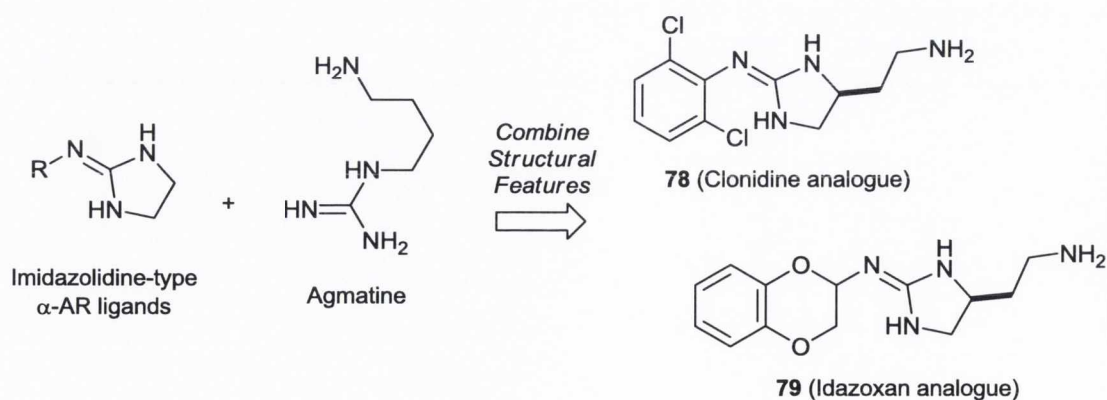


Fig. 4.14. Molecular design scheme of Treder and co-workers.

In contrast with the findings of Leclerc and those of Miller, the compounds prepared by Treder *et al.* exhibit a marked difference in affinity between the *R* and *S* isomers and the eutomeric ratio varies across four orders of magnitude (using IC₅₀ values). Notably, for 1-aryl derivatives such as **78** the *S* isomer gives consistently stronger affinities, in agreement with the findings of Miller *et al.* However, for benzodioxanes such as **79** and the related benzofurane analogues, the *R* isomer is consistently the eutomer. This suggests that the binding modes of these two classes of α_2 -AR ligands may be distinct, and that structural features responsible for strong affinity in 2-aryliminoimidazolidine derivatives are not immediately transferable to their benzodioxane counterparts.

4.3.3 Early strategies towards 4-substituted-2-aryliminoimidazolidines

Informed by observations in the literature and following our rational design scheme, it was anticipated that introduction of a substituent at the 4 position of 2-aryliminoimidazolidines might increase the likelihood of the resulting compounds acting as antagonists and improve their affinity for the α_2 -AR. Following our successful application of *N*-Boc-*N'*-substituted thioureas to the synthesis of *N,N'*-disubstituted guanidines, it was reasoned that a similar strategy might facilitate the preparation of their 2-iminoimidazolidine analogues. This approach builds on the methodology originally developed within our group for preparation of 2-iminoimidazolidines (see Scheme 4.23), and entails the retrosynthetic disconnection of 4-substituted 2-aryliminoimidazolidines to the parent aniline and an imidazolidine-2-thione derivative **80** bearing an electron withdrawing group conjugated with the central thiocarbonyl moiety (Fig. 4.15).

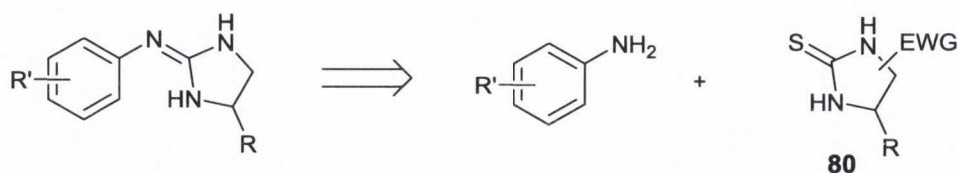


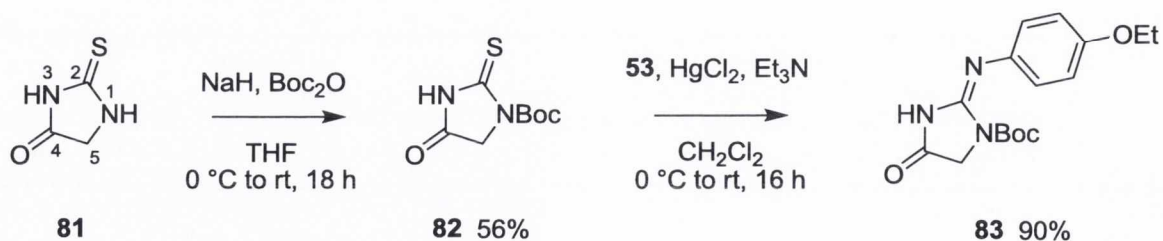
Fig. 4.15. Retrosynthetic approach to the synthesis of 4-substituted 2-aryliminoimidazolidine derivatives.

From a combinatorial standpoint, a strategy in which a large portion of the synthetic transformations are isolated to the preparation of the requisite activated imidazolidine-2-thione derivative **80** provides a distinct advantage in the synthesis of a large library of derivatives; this is particularly true if much of the molecular diversity comes from modifications to the aniline component, as is indeed the case with our own library of 4-substituted 2-aryliminoimidazolidines.

In our first approach to the general strategy outlined in Fig. 4.15, we considered the application of derivatives of 2-thiohydantoin **81** (Scheme 4.28) as the requisite imidazolidine-2-thione component **80**. Although **81** already contains an electron withdrawing carbonyl group, experiments using **81** in guanidylation reactions met with isolation problems, although the intended product was tentatively observed by ^1H NMR in the crude reaction mixture.

Given that a Boc substituent proved an efficient activating group in the synthesis of *N,N'*-disubstituted guanidines from *N*-Boc-*N'*-substituted thioureas, it was reasoned that the Boc protected derivative of 2-thiohydantoin **81** might provide an improved substrate for guanidylation. In order to investigate this possibility, 1-*tert*-butoxycarbonyl-2-thiohydantoin **82** was prepared from **81** using sodium hydride and excess Boc_2O (Scheme 4.28). Mercury (II) chloride promoted guanidylation using **82** with 4-ethoxyaniline **53** afforded the 2-iminoimidazolidine derivative **83** in excellent yield.

Scheme 4.28 The synthesis of 1-*tert*-butoxycarbonyl-2-thiohydantoin **82** en route to 1-*tert*-butoxycarbonyl-2-(4-ethoxyphenylimino)imidazolidin-4-one **83**.



During these procedures, **82** proved to be highly crystalline and it was possible to resolve an X-ray crystal structure to unambiguously determine the site of Boc protection (Fig. 4.16). The observed regioselectivity agrees with recent literature which posits that acylation of 2-thiohydantoin derivatives typically occurs at N1 rather than N3.²²⁸

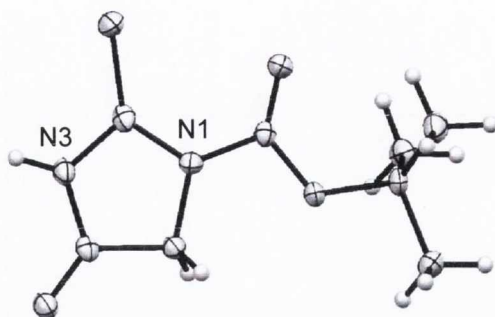
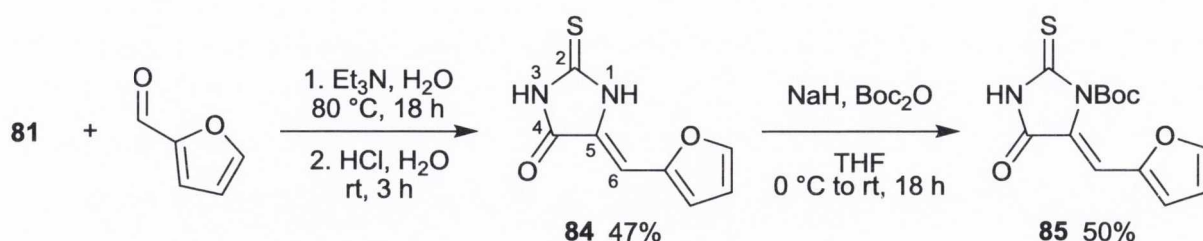


Fig. 4.16. X-ray crystal structure of **83** using the ORTEP representation.

Under the conditions used for the introduction of the Boc substituent (Scheme 4.28), it is possible that this group is first introduced at N3, but is highly labile at this position. Evidence for this suggestion comes from the fact that 2.2 equivalents of Boc_2O are necessary to provide a productive yield in this reaction, while using 1.1 equivalents of Boc_2O affords a yield of just 12%. It is therefore likely that protection takes place first at a site other than N1, but that this first Boc group is lost during the workup.

2-Thiohydantoin is readily functionalised at the 5 position using an aldol procedure originally outlined by Garst *et al.*²²⁹ For the synthesis of 5-substituted 2-thiohydantoin **84**, an aqueous solution of 2-thiohydantoin **81** was treated with 2-furfural in the presence of triethylamine, followed by dehydration using conc. HCl (Scheme 4.29). Purification afforded the aldol product **84** as a single geometrical isomer (assigned by NOE experiments). Boc protection using standard methods afforded **85** in 24% overall yield.

Scheme 4.29 Preparation and Boc protection of **84** via aldol reaction of **81** and 2-furfural.



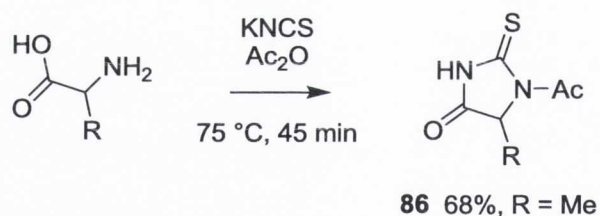
Initially we intended to prepare several 2-thiohydantoin derivatives for use in guanidylations reactions (see Scheme 4.28) followed by the complete reduction of the 4 carbonyl substituent and deprotection of the Boc group. However, this approach is poorly suited to the

introduction of an aromatic substituent at the 4 position of 2-iminoimidazolidines (C5 in 2-thiohydantoins; Scheme 4.29). The use of the aldol reaction necessitates the presence of an additional carbon in the structure (C6; Scheme 4.29) and is not readily amenable to the construction of a direct bond between an aromatic substituent and the 2-iminoimidazolidine core (Fig. 4.15; R = Ar). Given that our design scheme calls for the preparation of compounds of this type, the aldol reaction approach was abandoned at an early stage.

4.3.4 1-Acetyl-2-thiohydantoins in the synthesis of 2-iminoimidazolidines

An alternative approach to the synthesis of 5-substituted-2-thiohydantoins was first outlined by Nicolet and Johnson in 1911 and involves the treatment of an amino acid precursor with thiocyanate anion in acetic anhydride to produce the corresponding 1-acetyl-2-thiohydantoin (Scheme 4.30).²³⁰ Provided that the chirality of the parent amino acid can be maintained throughout our synthetic procedures, this protocol also presents the possibility of exploring optically active derivatives.

Scheme 4.30 Johnson and Nicolet's synthesis of 1-acetyl-2-thiohydantoin derivatives.



Our initial experiments employed L-alanine as the amino acid precursor (R = Me) to furnish the thiohydantoin derivative **86** in 68% yield. It became clear at this time that certain amino acids are not compatible with these conditions; for example serine fails to produce the expected 2-thiohydantoin derivative under these conditions.²³¹ Regardless, **86** proved to be compatible with our standard guanidylation procedures using a variety of anilines to afford the corresponding imidazolinones (Scheme 4.31; Table 4.5). Following guanidylation, the acetyl group proved to be highly labile and could be cleaved using methanolic HCl. Indeed, mass spectrometry experiments were unable to observe several of the acetylated intermediates **87** and instead the dominant MS peak exhibited an *m/z* ratio corresponding to the molecular mass minus the acetyl group.

Scheme 4.31 Application of **86** to the synthesis of 2-aryliminoimidazolidin-4-ones.

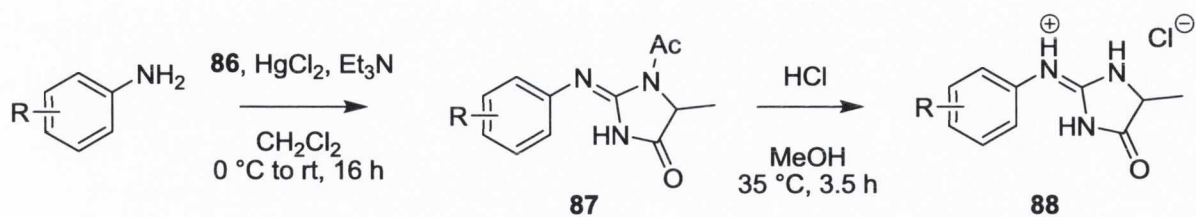


Table 4.5 2-Aryliminoimidazolidin-4-ones prepared as per Scheme 4.31

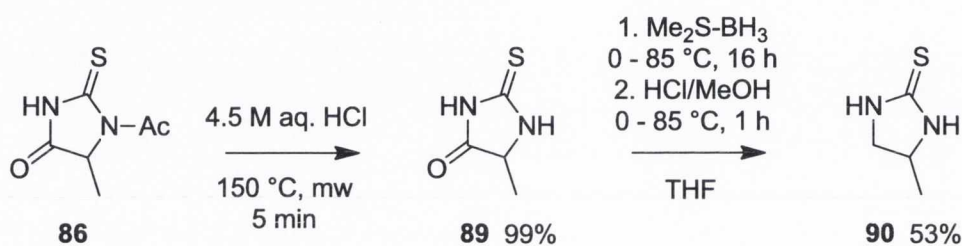
| Compound | N-Acetyl/HCl | R | Yield (%) |
|------------|------------------|---------------------------------------|----------------|
| 87a | <i>N</i> -Acetyl | 4-OEt | 71 |
| 87b | <i>N</i> -Acetyl | 3,4-(-CH ₂ -) ₄ | 60 |
| 87c | <i>N</i> -Acetyl | 4-NHEt | 16 |
| 87d | <i>N</i> -Acetyl | 3,4-(-OCH ₂ O-) | 33 |
| 88a | HCl | 4-OEt | 99 |
| 88b | HCl | 3,4-(-CH ₂ -) ₄ | 99 |
| 88c | HCl | 4-NHEt | 0 ^a |
| 88d | HCl | 3,4-(-OCH ₂ O-) | 74 |

^aTentatively observed by ¹H NMR and MS in the crude mixture, but could not be isolated.

In spite of some measure of success using this approach, difficulties in the synthesis of the *N*-ethyl derivative **88c** brought these investigations to a halt. Concerns were also raised regarding racemisation of the stereocentre, which is adjacent to a carbonyl group and might be enolised during these procedures leading to a loss of optical purity. The final step of this protocol was intended to be the reduction of the imidazolidinone carbonyl to afford the corresponding 2-iminoimidazolidine.²³² However, at this point it was decided to revise our synthetic approach to reduce this carbonyl group at an earlier stage in the procedure. It was hoped that such a strategy would be more likely to retain the chirality present in the parent amino acid, and to facilitate the synthesis of the desired *N*-ethyl derivative (the 2-iminoimidazolidine analogue of **88c**), the importance of which was outlined at the beginning of this chapter.

According to our revised procedure, the 1-acetyl-2-thiohydantoin derivative is synthesised as before and subsequently deacylated in quantitative yield using 4.5 M aqueous HCl under microwave irradiation (Scheme 4.32).²³³ The product 2-thiohydantoin **89** is then reduced to the corresponding imidazolidine-2-thione derivative **90** using borane dimethyl sulfide in tetrahydrofuran, followed by hydrolysis with methanolic HCl.

Scheme 4.32 Synthesis of 4-methylimidazolidine-2-thione **90**.



In practice, this reduction fails to proceed efficiently unless the dimethyl sulfide produced during the process is carefully distilled during the first few hours of the reaction.²³⁴ Indeed, initial experiments using a gentle positive pressure of argon (balloon) with a sealed apparatus resulted in a build-up of pressure which caused the seals of the reaction vessel to fail, allowing water from the outside environment to enter the vessel and hydrolysing the borane reducing agent, thereby halting the reaction. As a result, it is difficult to obtain a satisfactory yield without careful control of pressure within the reaction vessel, and in the event it is best to apply a small vacuum source during the first few hours of the procedure in order to capture the dimethyl sulfide produced using a suitable trap (in our experience, 10% aqueous hydrogen peroxide is appropriate for these purposes).

Standard Boc protection conditions using sodium hydride and Boc_2O were used to convert **90** to its *N,N'*-bis-Boc derivative **91**, which proved to be a reliable substrate for our standard guanidylation protocol using aniline derivatives in the presence of mercury (II) chloride and triethylamine (Scheme 4.33; Table 4.6). The *N,N'*-bis-Boc protected 2-iminoimidazolidine products **92** were readily deprotected using a 4 M solution of HCl in dry dioxane to afford the desired hydrochloride salts **93** in good to excellent yield.

Scheme 4.33 Application of **90** to synthesis of 4-methyl-2-aryliminoimidazolidines.

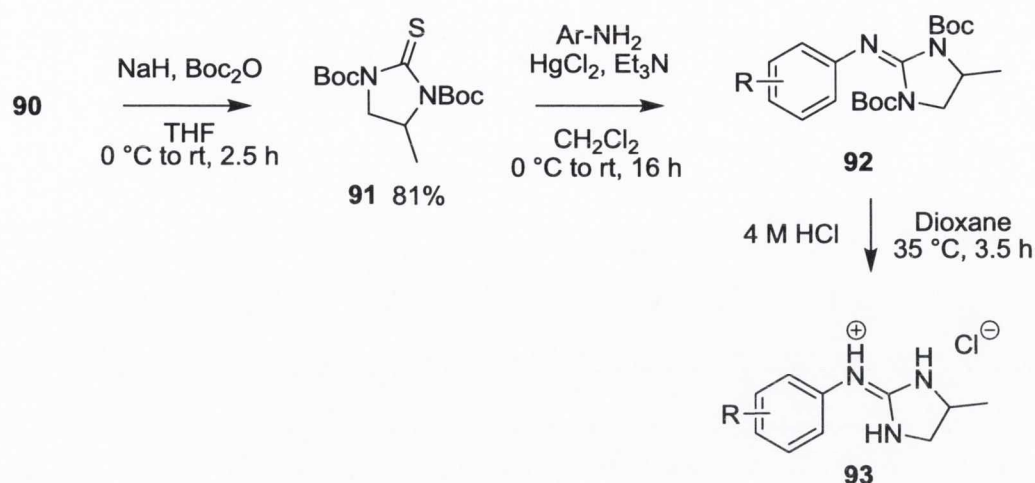


Table 4.6 4-Methyl-2-aryliminoimidazolidines prepared as per Scheme 4.33

| Compound | <i>N,N'</i> -bis-Boc/HCl | R | Yield (%) |
|------------|--------------------------|---------------------------------------|-----------|
| 92a | <i>N,N'</i> -bis-Boc | 4-OEt | 65 |
| 92b | <i>N,N'</i> -bis-Boc | 4-NMe ₂ | 78 |
| 92c | <i>N,N'</i> -bis-Boc | 3,4-(-CH ₂ -) ₄ | 88 |
| 92d | <i>N,N'</i> -bis-Boc | 4-NHEt | 65 |
| 92e | <i>N,N'</i> -bis-Boc | 3,4-(-OCH ₂ O-) | 69 |
| 93a | HCl | 4-OEt | 76 |
| 93b | HCl | 4-NMe ₂ | 71 |
| 93c | HCl | 3,4-(-CH ₂ -) ₄ | 73 |
| 93d | HCl | 4-NHEt | 90 |
| 93e | HCl | 3,4-(-OCH ₂ O-) | 78 |

This methodology demonstrates the applicability of 4-substituted imidazolidine-2-thiones to the synthesis of the desired 2-iminoimidazolidines. In contrast with the imidazolidin-4-one approach described in Scheme 4.31, products are readily isolated and the reaction provides consistently good yields. Unfortunately, as is discussed in the following section, the resulting products are also racemic, in spite of the use of an optically active amino acid.

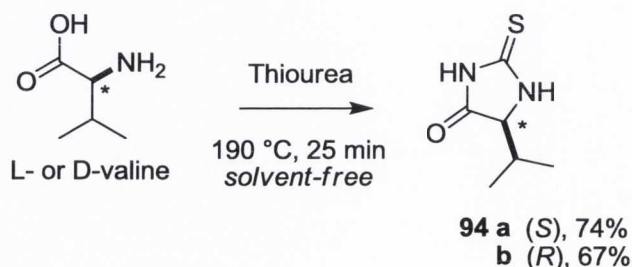
4.3.5 Determining the enantiomeric excess of 2-iminoimidazolidine precursors

Lanthanide shift reagents

In a 2006 paper, Wang *et al.* described the synthesis of optically active 4-substituted 2-thiohydantoins using a variation of Nicolet and Johnson's original methodology.²³⁵ The authors determined the optical purity of their products using a lanthanide shift reagent method. According to this approach, a ¹H NMR sample of the material under investigation is treated with a lanthanide shift reagent (LSR). Basic sites on the analyte molecule interact with the LSR through Lewis acid-base and outersphere interactions, and the paramagnetism of the LSR induces a change in the chemical shift of protons close to these basic sites. In the presence of a chiral LSR, the two enantiomers of the analyte give rise to two different diastereomeric complexes. If the ¹H NMR spectra of these two complexes are sufficiently different, it becomes possible to determine the enantiomeric excess of the analyte through integration of the ¹H NMR signals.

According to our procedures for the synthesis of 2-iminoimidazolidines (Schemes 4.32, 4.33), 5-methyl-2-thiohydantoin **89** comprises a common intermediate in the synthesis of 2-iminoimidazolidines **93a-e**. If the enantiomeric excess of **89** could be determined, it would prove that the chirality of the parent amino acid was retained through the early stages of our procedure. In their paper, Wang *et al.* determined the optical purity of (*S*)-5-isopropyl-2-thiohydantoin **94a**, an immediate analogue of **89**. In order to investigate the viability of their approach, **94a** and its enantiomer **94b** were prepared by the thermal fusion of thiourea with L- or D-valine, respectively; according to Wang's procedures (Scheme 4.34).

Scheme 4.34 Synthesis of 5-isopropyl-2-thiohydantoins **94a,b** following Wang's procedure.



A ^1H NMR spectrum (400 MHz) was acquired using 2 mg of **94a** dissolved in 0.6 ml of dry CD_3CN , showing two broad singlets at 9.31 and 7.93 ppm corresponding to the NH protons; a doublet at 4.04 ppm ($J = 3.9$ Hz) representing the CH proton at the chiral centre, a septet of doublets at 2.14 ppm ($J = 6.9, 3.9$ Hz) representing the CH proton in the isopropyl group, and two doublets at 1.00 and 0.88 ppm (both with $J = 6.9$ Hz) representing the isopropyl CH_3 signals (Fig. 4.17).

Initially, 0.5 equivalents of Europium(III)-tris[3-(trifluoromethylhydroxymethylene)-(+)-camphorate] [$\text{Eu}(\text{tfc})_3$] were added to this sample and a second ^1H NMR spectrum was acquired. Significantly, the CH signal at the chiral centre (marked * in Fig. 4.17) was shifted to 4.47 ppm; the other signals were also shifted downfield but to a lesser degree. All peaks exhibited line broadening, obfuscating the peak multiplicity. Upon the addition of a further 0.5 equivalents of $\text{Eu}(\text{tfc})_3$, the CH signal associated with the chiral centre was shifted further downfield to 4.84 ppm and again, all other signals were shifted downfield and broadened. An additional 0.5 equivalents of $\text{Eu}(\text{tfc})_3$ were added resulting in a further shift of the chiral CH signal to 5.06 ppm, but the solution was saturated and a precipitate was evident within the NMR tube. Thus, the experiment was halted after the addition of 1.5 equivalents of $\text{Eu}(\text{tfc})_3$.

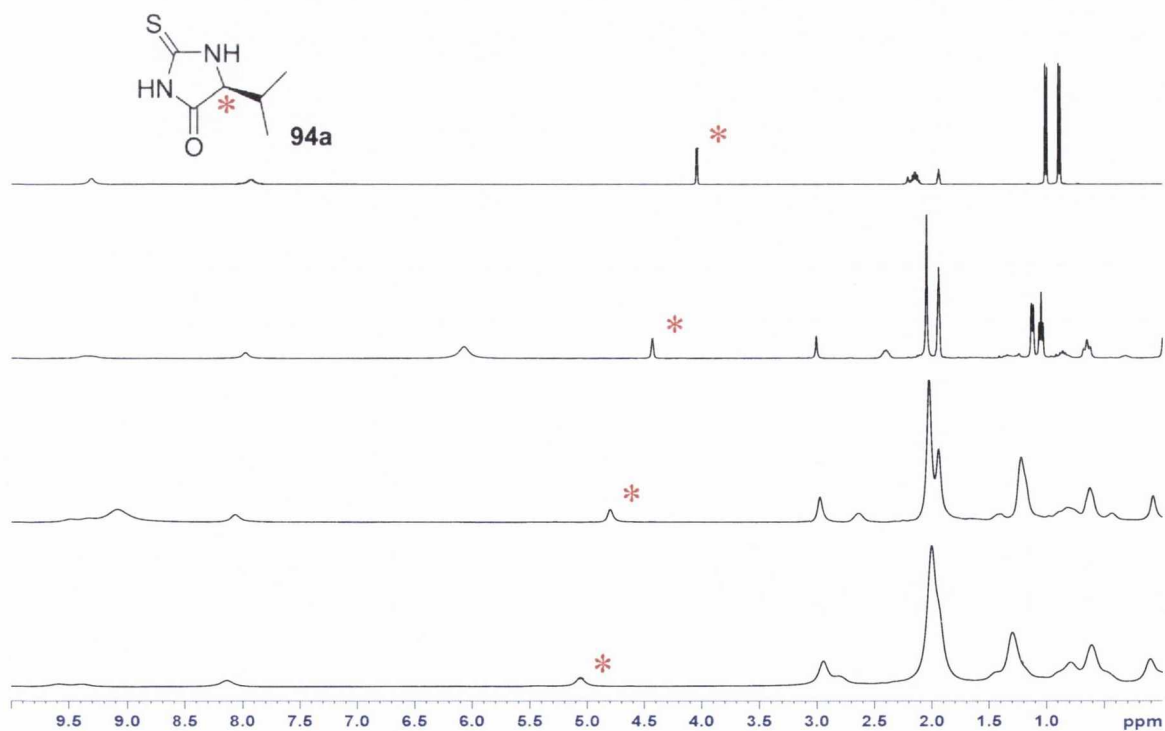


Fig. 4.17. ^1H NMR spectrum of **94a** in the presence of 0.0 (*top*), 0.5 (*top middle*), 1.0 (*bottom middle*) and 1.5 (*bottom*) equivalents of $\text{Eu}(\text{tfc})_3$ (400 MHz).

In a follow-on experiment, the *R*-isomer **94b** was prepared from D-Valine using an identical procedure. As expected, a ^1H NMR spectrum prepared using 2 mg of this material in 0.6 ml of CD_3CN exactly matched that of **94a**. $\text{Eu}(\text{tfc})_3$ was added in portions of 0.5 molar equivalents as before, and ^1H NMR spectra were acquired following each addition. Again, after 1.5 equivalents had been added a precipitate was evident within the NMR tube, and the experiment was halted (Fig. 4.18).

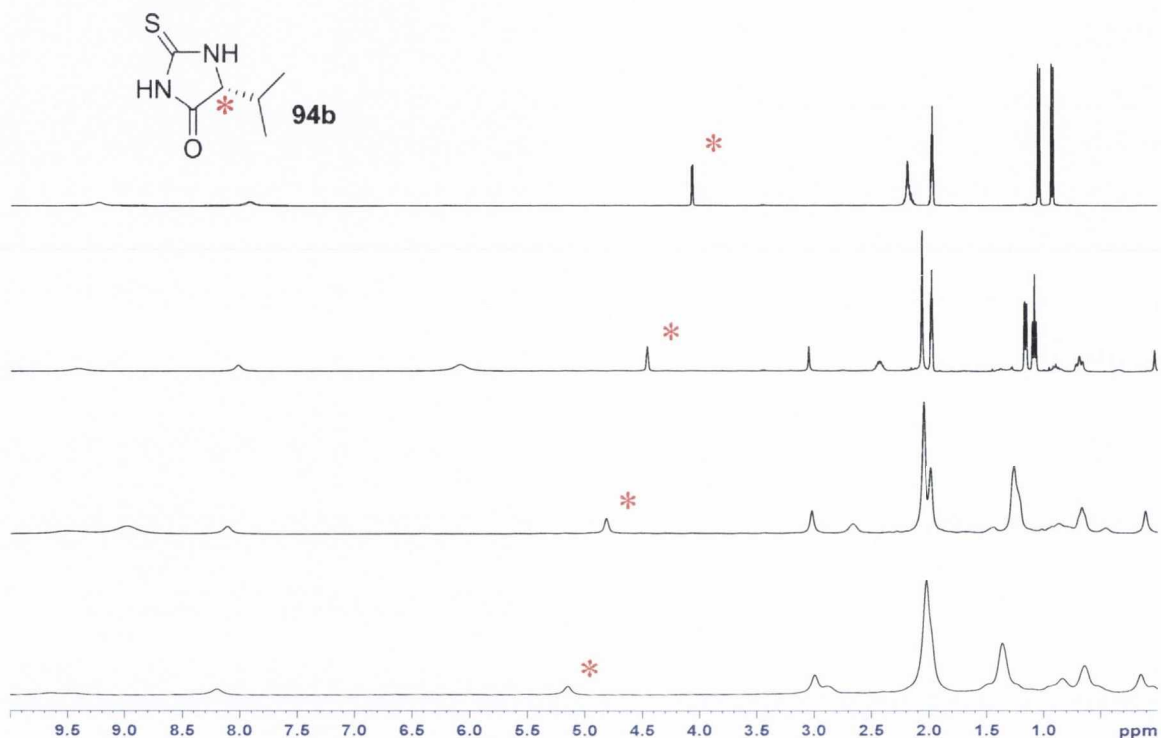


Fig. 4.18. ^1H NMR spectrum of **94b** in the presence of 0.0 (*top*), 0.5 (*top middle*), 1.0 (*bottom middle*) and 1.5 (*bottom*) equivalents of $\text{Eu}(\text{tfc})_3$ (400 MHz).

As can be seen from figures 4.16 and 4.17, the lanthanide induced shift (LIS) for the chiral CH signal (*) in the presence of 1.5 equivalents of $\text{Eu}(\text{tfc})_3$ is 1.02 ppm for the (*S*) enantiomer and 1.06 ppm for the (*R*) enantiomer, a difference which lies within experimental error. In order to determine the enantiomeric excess using a lanthanide shift reagent, the difference in induced shift should ideally exceed the width of the peak under investigation.²³⁶ Sadly, this requirement has not been fulfilled at any concentration of $\text{Eu}(\text{tfc})_3$, and therefore we conclude that, in our case, $\text{Eu}(\text{tfc})_3$ is poorly suited to the determination of enantiomeric excess of these thiohydantoin. Indeed, these ^1H NMR experiments do not rule out the possibility that

racemisation might occur during the preparation of these compounds or even through the introduction of the chiral shift reagent, which might promote enolisation via its Lewis acidity.

In their own studies, Wang *et al.* reported the application of Europium(III)-tris(1,1,1,2,2,3,3-heptafluoro-7,7-dimethyl-4,6-octanedionate) [Eu(fod)₃] to the determination of the optical purity of 2-thiohydantoin derivative **94a**. Although Eu(fod)₃ is an excellent shift reagent for the analysis of diastereomeric mixtures by NMR spectrometry, it is achiral and therefore not suited to the analysis of mixtures of enantiomers such as **94a** and **94b**.²³⁷ Our concerns regarding the validity of applying Eu(fod)₃ to the determination of enantiomeric excess were hardly assuaged by the failure of the chiral shift reagent Eu(tfc)₃ to distinguish between the two enantiomers by ¹H NMR. It was therefore decided to terminate our LSR studies for the determination of enantiomeric excess at this stage.

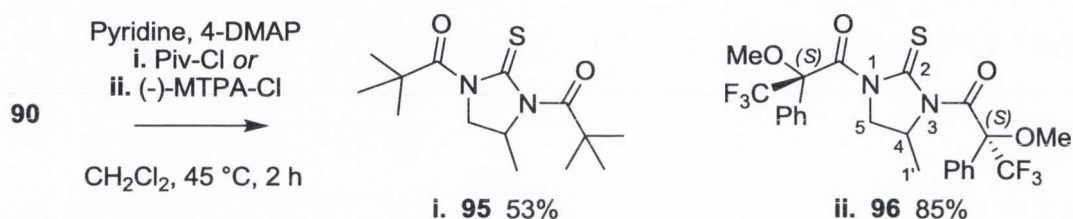
Chiral derivatizing agents

An alternative approach to the determination of optical purity is the application of chiral derivatizing agents (CDAs), in which the material under investigation is converted to a diastereomeric derivative through the introduction of a covalently-bonded appendage containing another, known chiral centre. The *R* and *S* isomers of the analyte are thereby converted into two physically distinct diastereomers, each of which is likely to have a different NMR spectrum. If the ¹H NMR spectra of the two diastereomers are sufficiently different, it becomes possible to determine the enantiomeric excess through integration of the ¹H NMR signals. It is critically important that the reaction conditions used to introduce the chiral appendage should be mild and selective enough to retain the chirality of the starting materials to ensure an accurate result.

It was decided to introduce the requisite chiral appendage using (*S*)- α -methoxy- α -trifluoromethylphenylacetyl chloride [Mosher's acid chloride; (-)MTPA-Cl], a well-studied chiral derivatizing agent.²³⁸ The 2-thiohydantoin precursor **89** was poorly suited to this purpose, as it was known that enolisation could occur under the mildly basic conditions necessary for this transformation, with concomitant loss of optical purity. It was therefore decided to react the central thiourea moiety of the reduction product 4-methylimidazolidine-2-thione **90**, another common intermediate in the synthesis of 2-iminoimidazolidines **93a-e**, with two equivalents of (-)MTPA-Cl to produce the *N,N'*-bis-(-)MTPA derivative **96**.

Prior to the event, mild conditions for this transformation were demonstrated by reacting pivaloyl chloride with **90** in the presence of pyridine and 4-(dimethylamino)pyridine (4-DMAP) to produce the dipivaloyl derivative **95**. The 53% yield recorded for the preparation of **95** was greatly improved in the reaction of **90** with (-)MTPA-Cl using the same conditions to afford an 85% yield of the desired *bis*-Mosher's acid derivative **96** (Scheme 4.35).

Scheme 4.35 Conversion of **90** to the corresponding 1,3-dipivaloyl derivative **95** and *N,N'*-*bis*-(-)MTPA derivative **96**.



It is important to note that this reaction introduces two (-)MTPA groups, although only one is necessary to produce a diastereomeric derivative. The presence of a second (-)MTPA group has the disadvantage of further complicating the resulting NMR spectra; however, the likelihood of observing a peak which differs greatly between the two diastereomers is actually somewhat increased, as there are more signals to choose from. It was hoped that the proximity of the (-)MTPA substituents to the chiral centre would produce a large difference in the NMR spectra for the two diastereomers, and might also assist in the assignment of the NMR spectra for the diastereomeric mixture by NOE and similar experiments.

Unfortunately, the ¹H NMR spectrum recorded for **96** confirms that the optical purity is almost completely lost during the synthesis of **90** from its parent amino acid L-alanine (Fig. 4.19). The chemical shift of the CH₃ protons at C1' (numbering as per Scheme 4.35) differs greatly between the (*S,S,R*) and (*S,S,S*) diastereomers, which appear as a pair of doublets at 0.43 and 0.71 ppm (both *J* = 6.5 Hz) respectively. It is possible to extrapolate an enantiomeric excess of approximately 5% using the integration of these signals, a figure which is close to experimental error. Although extensive NMR analysis allowed us to assign many of the peaks, it was not always possible to state whether a given signal corresponded to the (*S,S,R*) or (*S,S,S*) diastereomer, and the mixture proved to be inseparable by chromatography.

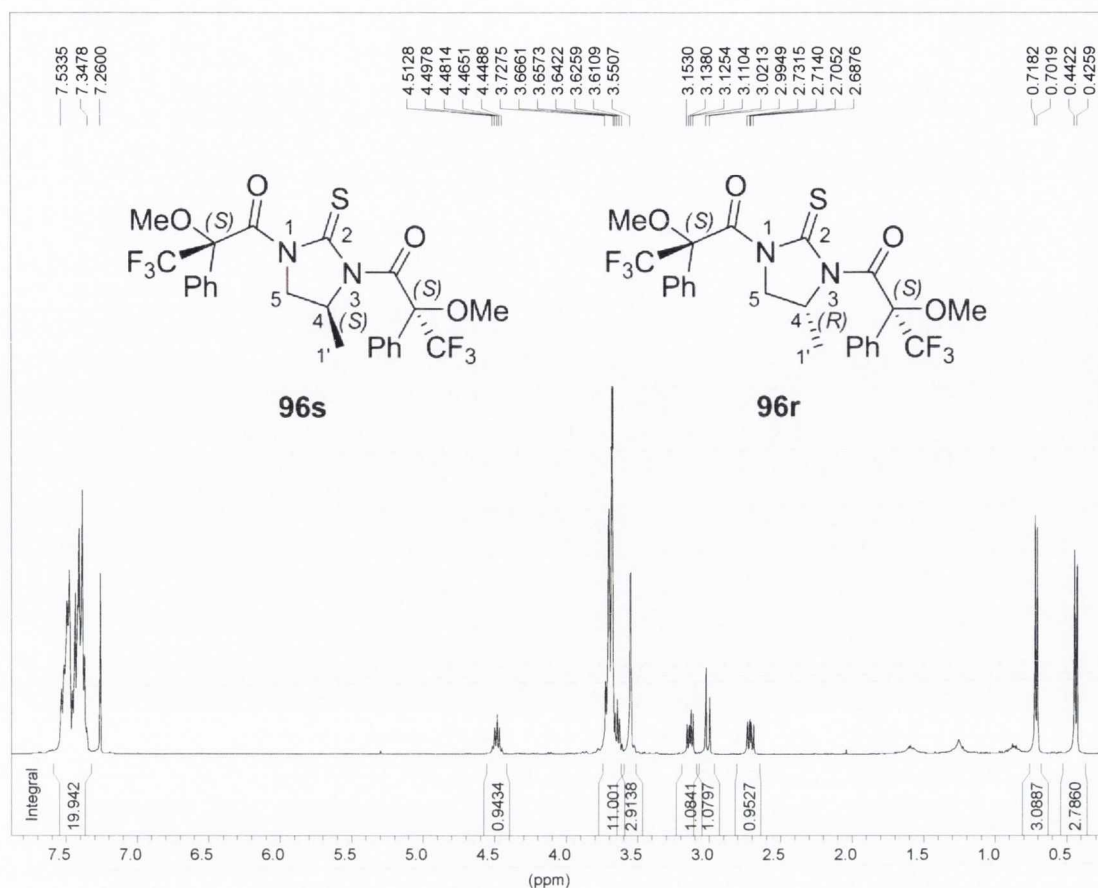


Fig. 4.19. The ^1H NMR spectrum of the diastereomeric mixture (*S,S,RS*) 1,3-di(1-methoxy-1-trifluoromethyl-1-phenylacetyl)-4-methylimidazolidine-2-thione **96** in CDCl_3 (600 MHz).

Further NMR spectra and signal assignments are provided in Appendix B.

In addition to the methyl group, the chemical shifts of the CH and CH_2 protons at C4 and C5, respectively, also differ greatly between the two diastereomers. The CH_2 signals for the (*S,S,S*) diastereomer **96s** appear at 3.01 and 3.13 ppm, with the signal at 3.01 exhibiting a characteristic *trans* J coupling of 10.6 ppm. The CH_2 signals for the (*S,S,R*) diastereomer **96r** appear at 2.71 and ~3.65 ppm, with the latter signal forming part of a large multiplet at 3.61 – 3.73 ppm. This multiplet represents three of the four methoxy CH_3 signals (9H total), the aforementioned CH_2 proton (1H), and the CH proton at the chiral centre (C4) of **96s** (1H). The fourth methoxy CH_3 signal appears at 3.55 ppm as a lone singlet (3H). Due to the close proximity of these signals, it was not possible to determine which methoxy signals correspond to which diastereomer. The remaining CH signal (C4 of **96r**) appears as an apparent quintet at 4.48 ppm, while the aromatic signals form a multiplet at 7.53 – 7.34 ppm.

The ^{13}C NMR spectrum is less suited to the quantitation of optical purity; however, the spectrum does help to confirm the presence of two distinct diastereomers. The highly shifted thiocarbonyl signals appear at 173.6 and 174.1 ppm, respectively. Long range C-H COSY experiments suggest that the peak at 173.6 corresponds to **96r**, while 174.1 corresponds to **96s**. Four carbonyl signals are observed at 166.6, 165.9, 165.8 and 164.8 ppm; correlation experiments suggest that the first two emanate from **96r** and the latter two from **96s**. Fifteen aryl signals are observed in the region 132.4 – 125.9 ppm. Although we would expect sixteen signals, it is likely that the signal at 128.4 ppm represents two coincident signals; however the crowded nature of the aromatic region rendered definite assignments here untenable. The four CF_3 signals are coincident and appear as a quartet due to C-F coupling ($J = 290.5$ Hz) at 122.9 ppm. The four quaternary carbon signals are also coincident, forming a quartet at 85.6 ppm ($J = 30.0$ Hz). All four methoxy CH_3 signals are observable at 56.3, 56.2, 55.9 and 55.6 ppm; exhibiting a small degree of C-F coupling ($J = 1.8$ Hz), but could not be readily assigned due to signal crowding. However, the CH and CH_2 protons (C4 and C5) could be assigned using CH COSY and DEPT-135 experiments. The CH signal of **96r** appears at 54.0 ppm; the adjoining CH_2 signal appears at 53.0 ppm. The order of these signals is inverted in **96s**, and the CH_2 signal appears first at 52.9 ppm followed by the CH signal at 52.6 ppm. Finally, the CH_3 signals of C1' appear at 17.7 ppm for **96s** and 17.3 ppm for **96r**.

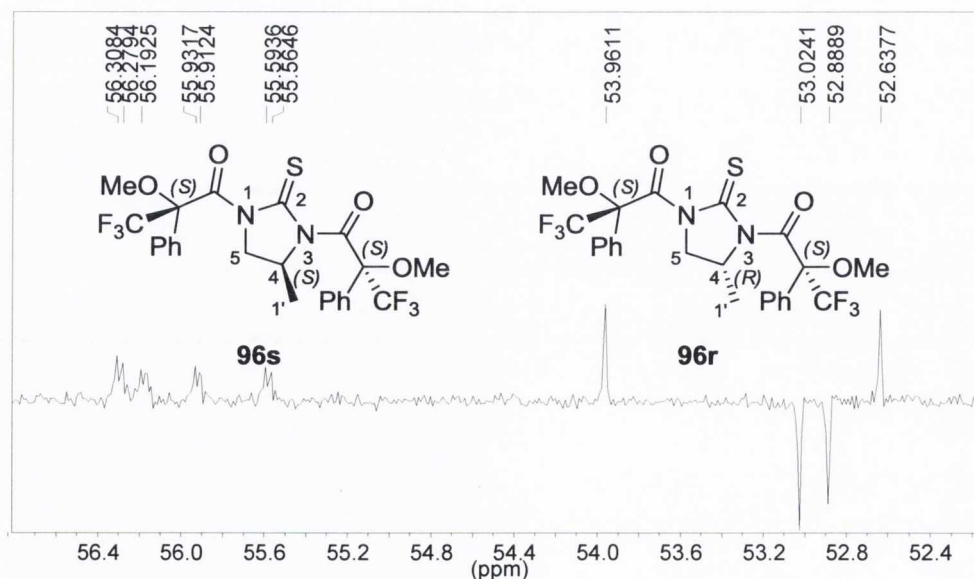


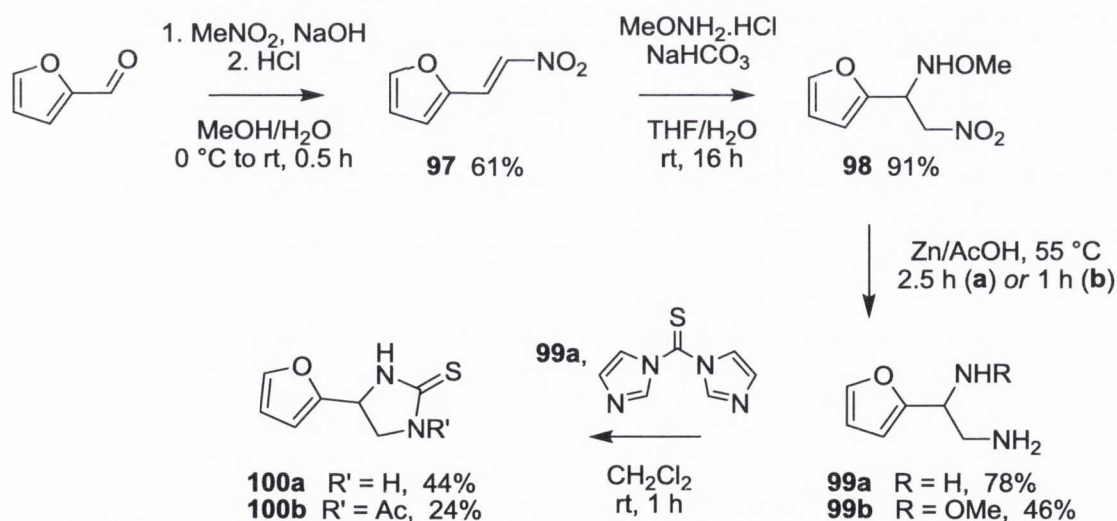
Fig. 4.20. Partial DEPT-135 spectrum of (*S,S,RS*) 1,3-di(1-methoxy-1-trifluoromethyl-1-phenylacetyl)-4-methylimidazolidine-2-thione **96** in CDCl_3 (150 MHz).

4.3.6 Method for the synthesis of 4-(2-furyl)-2-aryliminoimidazolidines

Our original design scheme suggested that the incorporation of a 2-furyl substituent at the 4 position of the imidazolidine ring might produce high affinity antagonists of the α_2 -AR (see Fig. 3.4). Although the synthetic procedures described earlier in this chapter should facilitate the preparation of these compounds from the 2-furyl derivative of the amino acid glycine, the expense of this reagent suggested that an alternative synthetic strategy would be preferable.²³⁹ Moreover, we also sought to explore other methods for the synthesis of enantiomerically enriched 4-substituted imidazolidine-2-thiones which might improve on the racemisation evident using our original amino acid-based methodology.

Fortunately, the requisite imidazolidine-2-thione derivative **100a** is described in a 2006 patent authored by Garst *et al.* (Scheme 4.36).²⁴⁰ Their procedure begins with the addition of the anion of nitromethane to 2-furfural to produce nitroalkene **97**, followed by the 1,4 addition of *O*-methyl hydroxylamine to produce **98**. Zinc reduction in acetic acid furnishes the 1,2 diamine **99a**, which is cyclised using 1,1-thiocarbonyldiimidazole to produce **100a**.

Scheme 4.36 The synthesis of 4-(2-furyl)-imidazolidine-2-thione **100a** according to the method of Garst *et al.*



In practise, this procedure took several attempts to reproduce, with the most significant difficulties encountered during the reduction of **98** to produce 1,2-diamine **99a**. In their original publication, the authors suggest a reaction time of 1 h; they also record a yield of just

40% for this challenging reaction. In our experience, terminating the reaction after 1 h at 55 °C produced only the partially-reduced product **99b**. Increasing the temperature to 100 °C failed to produce any isolable material, and decomposition was evident by the presence of a viscous black reaction mixture. Carefully monitoring the reaction using low resolution mass spectrometry suggested that optimum conversion to **99a** occurs after approximately 2.5 h at 55 °C; terminating the reaction at this time provided a satisfying 78% yield.

Difficulties were also encountered in the cyclisation of 1,2,-diamine **99a** to produce 4-(2-furyl)imidazolidine-2-thione **100a**. Initially, we attempted to convert the crude diacetate salt of **99a** to its freebase *in situ*, followed by the introduction of 1,1-thiocarbonyldiimidazole in an attempt to produce **100a**. However, this procedure afforded only a low yield of the *N*-acetyl derivative **100b** (Scheme 4.36). Isolating the freebase of **99a** prior to conducting the reaction circumvented this problem to afford **100a** in 44% yield.

The synthesis of the desired 4-(2-furyl)-2-aryliminoimidazolidines could be completed following the same approach as used for the 4-methyl-2-aryliminoimidazolidine compounds **93a-e** (see Scheme 4.33). In the event, **100a** was converted to its *N,N'*-bis Boc protected analogue **101** followed by guanidylated using our standard methods to produce the protected 2-iminoimidazolidines **102a-e**. Deprotection using 4 M HCl/dioxane afforded the hydrochloride salts **103a-e** in generally good yields (Scheme 4.37; Table 4.7).

Scheme 4.37 The application of **100a** to the synthesis of 4-(2-furyl)-2-aryliminoimidazolidines.

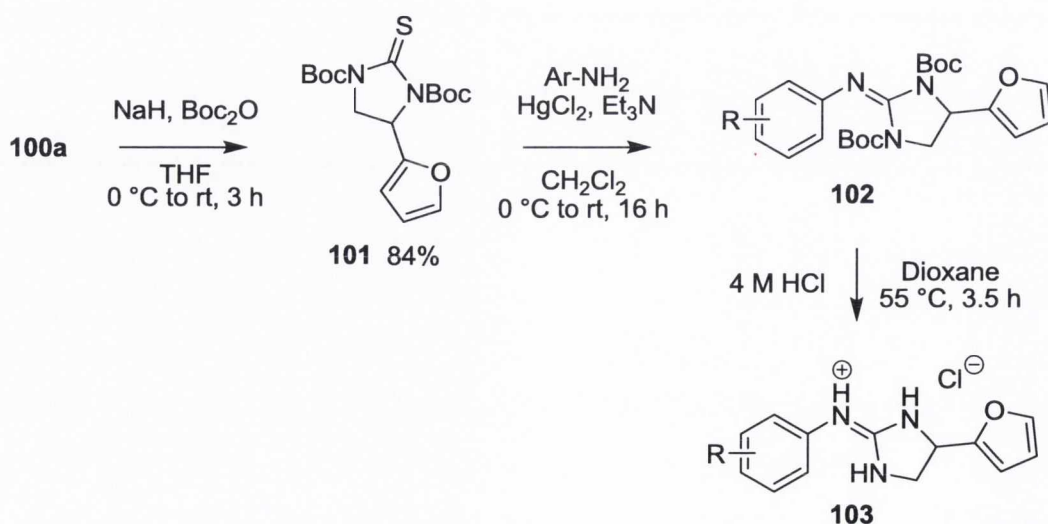


Table 4.7 4-(2-Furyl)-2-aryliminoimidazolidines prepared as per Scheme 4.37

| Compound | <i>N,N'</i> -bis-Boc/HCl | R | Yield (%) |
|-------------|--------------------------|---------------------------------------|-----------|
| 102a | <i>N,N'</i> -bis-Boc | 4-OEt | 62 |
| 102b | <i>N,N'</i> -bis-Boc | 4-NMe ₂ | 72 |
| 102c | <i>N,N'</i> -bis-Boc | 3,4-(-CH ₂ -) ₄ | 74 |
| 102d | <i>N,N'</i> -bis-Boc | 4-NHEt | 85 |
| 102e | <i>N,N'</i> -bis-Boc | 3,4-(-OCH ₂ O-) | 51 |
| 103a | HCl | 4-OEt | 70 |
| 103b | HCl | 4-NMe ₂ | 58 |
| 103c | HCl | 3,4-(-CH ₂ -) ₄ | 60 |
| 103d | HCl | 4-NHEt | 77 |
| 103e | HCl | 3,4-(-OCH ₂ O-) | 72 |

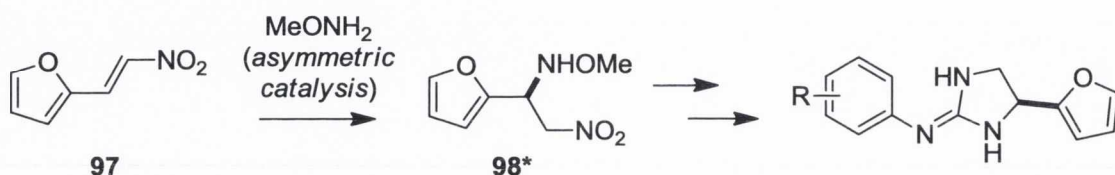
The success of this approach again demonstrates the broad applicability of 4-substituted imidazolidine-2-thiones to the synthesis of 2-iminoimidazolidinones, even in the presence of an acid-sensitive heterocycle such as furan. However, the method of Garst *et al.* provides access to the requisite imidazolidine-2-thiones (Scheme 4.36) over four steps while the amino acid-based methodology described in the preceding section requires only three steps (Schemes 4.30 and 4.32). Nonetheless, the application of Garst's methods to this synthetic approach significantly expands upon the number of imidazolidine-2-thiones available for incorporation into target molecules, as the starting material is an aldehyde rather than an amino acid as required in our original procedures.

4.3.7 Towards an asymmetric synthesis of 4-substituted 2-iminoimidazolidines

Although our original amino acid-based methodology may seem like a more intuitive approach to the synthesis of enantiomerically enriched imidazolidine-2-thiones, recent advances in asymmetric methodology suggest that Garst's procedures may also be adaptable to the synthesis of optically active products. Specifically, the 1,4 addition of *O*-methyl hydroxylamine to the nitroalkene **97** marks the stage at which the chiral centre is introduced; if this reaction could be carried out asymmetrically, then these procedures might be readily

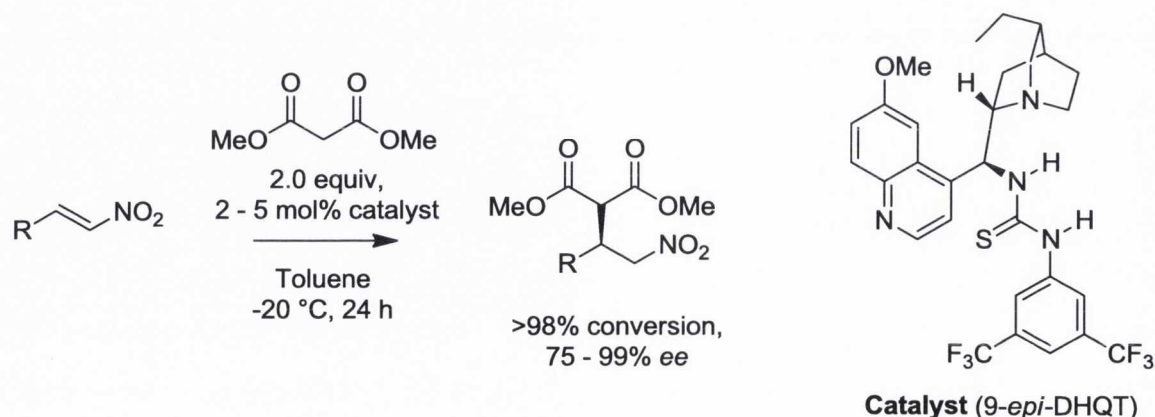
adapted to the synthesis of optically active 4-substituted 2-iminoimidazolidines (Scheme 4.38). It was reasoned that a chiral organocatalyst might promote the asymmetric conjugate addition of *O*-methyl hydroxylamine (or a suitable analogue) to nitroalkene **97**, and that the synthesis could be completed as previously described.

Scheme 4.38 Intended procedure for the asymmetric synthesis of 4-substituted 2-iminoimidazolidines.



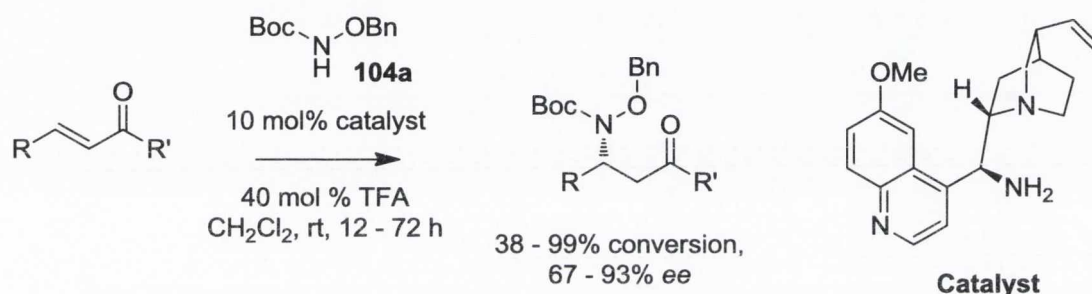
In 1981, Wynberg and Hiemstra published one of the first papers demonstrating the capacity of cinchona alkaloids to act as organocatalysts for the promotion of asymmetric conjugate addition reactions.²⁴¹ Twenty years later in 2002, Schreiner described the efficiency of electron-deficient thiourea derivatives as Lewis acid catalysts for the Diels Alder reaction.²⁴² In 2005, Connon and Soós independently discovered that the 9-epimer of cinchona alkaloid dihydroquinine could be combined with an electron-poor thiourea functionality to produce a highly efficient catalyst for asymmetric conjugate addition reactions (Scheme 4.39).^{243,244}

Scheme 4.39 Connon's cinchona-derived organocatalyst for the conjugate addition of malonates to nitroalkenes.



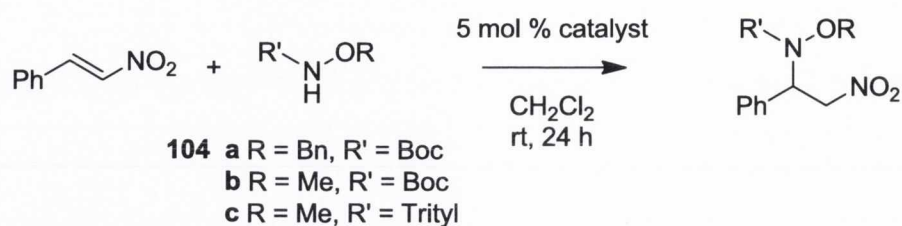
Connon's system is described as a bifunctional organocatalyst, in which the basic quinuclidine deprotonates the malonate to generate the nucleophile while the thiourea moiety simultaneously activates the nitroalkene through Lewis acidic interactions. In 2008, Deng described a similar cinchona-derived bifunctional organocatalyst for the addition of Boc protected *O*-benzyl hydroxylamine **104a** to α,β -unsaturated ketones (Scheme 4.40).²⁴⁵

Scheme 4.40 Deng's organocatalyst for the conjugate addition of Boc protected *O*-benzyl hydroxylamine to nitroalkenes.



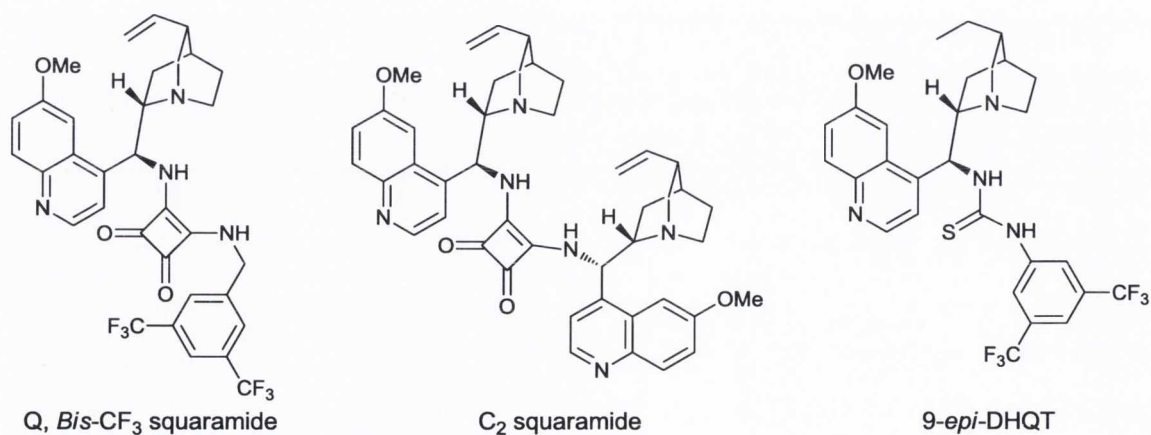
In Deng's methodology, the nucleophilicity of the hydroxylamine is mitigated through the use of a protecting group to dramatically decrease the rate of the uncatalysed reaction, thus allowing only the catalysed, asymmetric reaction to proceed at a productive rate. By combining Deng's approach with Connon's nitroalkene methodology (see Scheme 4.39), we sought to develop an organocatalytic system for the conjugate addition of hydroxylamine derivatives to nitroalkenes (Scheme 4.41).

As a preliminary screen for the necessary catalytic activity, we examined the three different catalysts using substrate **104a** under the conditions described in Scheme 4.41. These included Connon's original catalyst *9-epi*-DHQT and two closely-related analogues in which the thiourea functionality is replaced with a squaramide moiety of similar Lewis acidity (Fig. 4.21).²⁴⁶ Among these catalysts, *9-epi*-DHQT was determined to be the most promising candidate (Table 4.8), while the squaramide analogues demonstrated poorer enantioselectivity, and were omitted from further study. We proceeded to examine the activity of catalyst *9-epi*-DHQT using substrates **104b** and **104c** and an improvement in *ee* was observed when using **104b** as the hydroxylamine component; however, the considerable steric hindrance of substrate **104c** led to a complete loss of reactivity.

Scheme 4.41 Organocatalytic conjugate addition of hydroxylamines to nitrostyrene.**Table 4.8** Catalyst evaluation as per Scheme 4.41

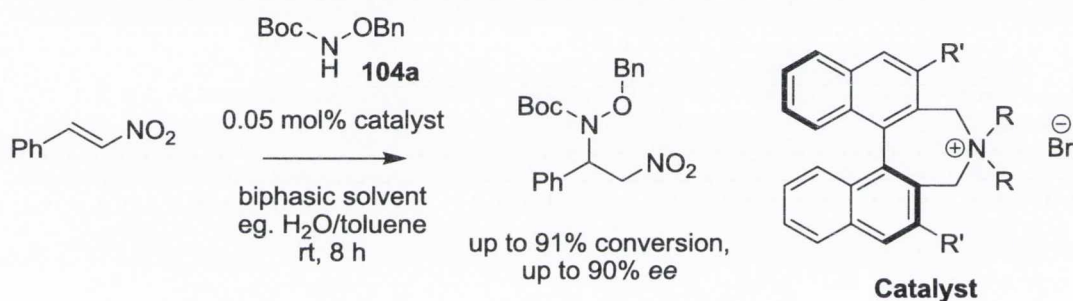
| Nucleophile | Catalyst | Conversion after 24 h (%) | ee (%) |
|-------------------------|-----------------------------------|---------------------------|--------|
| 104a^a | 9- <i>epi</i> -DHQT | 16 | 44 |
| 104a^a | C ₂ squaramide | 21 | 21 |
| 104a^a | Q, Bis CF ₃ squaramide | 25 | 28 |
| 104a^b | 9- <i>epi</i> -DHQT | 36 | 46 |
| 104b^b | 9- <i>epi</i> -DHQT | 23 | 56 |
| 104c^b | 9- <i>epi</i> -DHQT | 0 | - |

^aPerformed at 0.2 M conc. of nucleophile. ^bPerformed at 0.4 M conc. of nucleophile.

**Fig. 4.21.** Catalysts evaluated during this study.

Although several promising test reactions had been carried out, the study was terminated at this point for lack of time. Nonetheless, in 2011 a paper by Maruoka *et al.* described a phase-transfer catalyst system capable of performing the same reaction with excellent efficiency.²⁴⁷ Their catalyst system is active at concentrations as low as 0.05 mol % and produces yields of up to 91% (Scheme 4.42). Moreover, their procedure incorporates water as a solvent and therefore falls under the banner of “green” chemistry. The authors also describe the reduction of their products to produce the corresponding mono *N*-Boc protected 1,2-diamines with complete retention of *ee*.

Scheme 4.42 Maruoka’s phase-transfer catalyst for the conjugate addition of hydroxylamine derivatives to nitroalkenes.



It is likely that Maruoka’s methodology could be readily adapted to the asymmetric synthesis of 4-substituted 2-iminoimidazolidines following the same rationale as used during our organocatalytic investigations. Moreover, as discussed in Section 4.3.2, there are already several approaches to the synthesis of 4-substituted 2-iminoimidazolidines from 1,2-diamine precursors which afford optically active material. Although our own synthetic routes have produced universally racemic products, it is clear that there are many promising strategies which might be amenable to the asymmetric synthesis of 4-substituted 2-iminoimidazolidines.

Chapter 5 - Pharmacology

5.1 Introduction

In the past, the assessment of antidepressant potential in new compounds proved a difficult challenge, and indeed the effectiveness of early antidepressants was discovered serendipitously rather than through pharmacological assays (see Section 1.3.1). Towards the end of the 1950s, Costa *et al.* introduced the reserpine reversal test as an early pharmacological model of antidepressant effectiveness.²⁴⁸ According to this assay, a compound was judged to behave as an antidepressant if it could reverse the sedating effects of reserpine, a drug which was then thought to induce depression.

During the 1970s, several drugs were discovered which were clinically effective as antidepressants but failed to reverse the effects of reserpine, including the α_2 -AR antagonist type antidepressant mianserin.¹⁴² Inadequacies in the reserpine reversal test led to the emergence of new animal models in the late 1970s, in which the antidepressant effect could be determined by observing the behaviour of rodents in a water maze.²⁴⁹ All of the antidepressants tested in these experiments, along with several other treatments including electroconvulsive therapy, showed a reduction in the immobility time of rodents, which is indicative of increased pro-survival behaviour under the stressful environment of the water maze. These experiments marked the first example of the forced swim test, which remains a popular animal stress model of antidepressant potential today, albeit with some changes to the experimental protocol such as replacing the maze with a simple water tank.²⁵⁰ Other animal models examining the effect of potential antidepressants on animal immobility, such as the tail suspension test, have also been developed (see Section 1.4.3).

Although animal stress models provide an invaluable measure of the antidepressant potential of new compounds, these experiments are time-consuming and resource-intensive to conduct. As a result, behavioural assays are inappropriate for the initial evaluation of pharmacological activity. Among the compounds described in this text, only the most promising candidates will be subjected to animal behaviour experiments. The rapid evaluation of which compounds might show promise as antidepressant drugs necessitates an *in vitro* pharmacological approach.

As the pharmacological modes of action of antidepressants came to be established, researchers began to predict which compounds might exhibit antidepressant potential by examining their affinity for targets associated with the antidepressant effect. The SSRI family of antidepressants was famously designed on the basis of their affinity for the 5-HT reuptake protein SERT, demonstrating the successful application of this approach to the development of novel antidepressant drugs (see Section 1.3.2, *The Rise of the SSRIs*).

The compounds described in the present text are intended to exhibit their antidepressant effect by inhibition of the α_2 -AR family of receptors, and thus their affinity for the α_2 -AR provides an *in vitro* measurement of their pharmacological potential. It is also possible to utilise *in vitro* binding experiments to determine whether a given compound acts as an agonist or antagonist of the α_2 -AR, providing a further selection criterion as to which compounds exhibit the required functional activity. By performing these studies, only those compounds exhibiting both high affinity for the α_2 -AR and antagonist activity need to be selected for further pharmacological analysis.

The monoamine hypothesis provides another means of determining the antidepressant potential of new compounds. Generally, synaptic concentrations of monoaminergic neurotransmitters are lower in depressive patients than in the broader population; a factor which may contribute to symptoms such as sedation, reduced cognitive function, and anhedonia (see Section 1.2.3). Microdialysis experiments provide a direct, *in vivo* measurement of the effect of administering a compound upon neurotransmitter concentrations in live animals by monitoring the composition of extracellular fluids in the brain. If the administration of a compound results in increased concentrations of monoaminergic neurotransmitters, this demonstrates a promising indicator of antidepressant potential. Although a positive result using microdialysis experiments does not necessarily prove that a substance functions as an antidepressant, compounds which afford promising results in microdialysis experiments may be worthy of further study using a behavioural model of depression.

5.2 Pharmacological Methods

5.2.1 Determining receptor affinity: competitive radioligand binding assays

A competitive radioligand binding assay allows the determination of a ligand's affinity for a receptor by comparison with a radioisotopically labelled ligand for which the affinity is already known. The receptors are incubated with a constant concentration of radioligand, and then varying concentrations of a second ligand with unknown affinity are added. The degree to which the radioligand is displaced can be measured using a scintillation counter. A plot of radioligand binding as a percent of maximal *versus* the logarithm of ligand concentration can be used to determine the IC_{50} value, which is the concentration at which half of the total radioligand has been displaced and by implication the binding is 50% of maximal (Fig. 5.1).²⁵¹

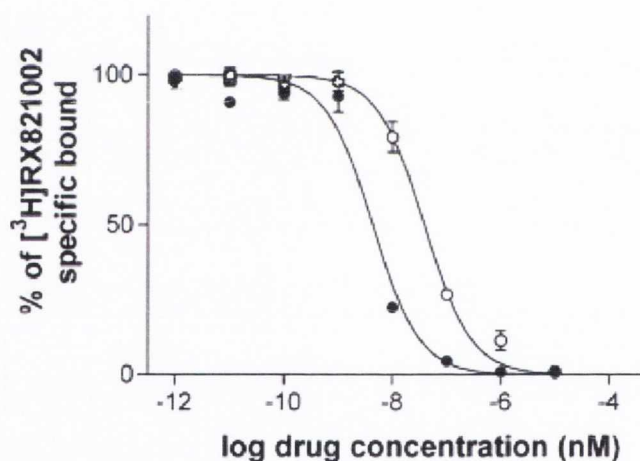


Fig. 5.1. Example of a competitive radioligand binding curve for compound **5**, an α_2 -AR discovered previously within our group (see also Section 1.4.3).¹⁵⁸

If the radioligand concentration $[L]$ and its affinity for the receptor K_d are known, the IC_{50} value can be transformed into the receptor affinity constant (K_i) using the Cheng-Prusoff equation (Equation 5.1).²⁵² The equilibrium constant K_i is defined as the concentration at which the ligand occupies half of the receptors; however unlike IC_{50} values, K_i is independent of the receptor concentration.

$$K_i = \frac{IC_{50}}{1 + \frac{[L]}{K_d}} \quad (5.1)$$

For practical purposes, pK_i (defined as the negative logarithm of K_i) is often used in place of K_i as it facilitates a more intuitive comparison between affinities. Several analytical techniques such as the CoMFA methodology (see Chapter 3) also necessitate the use of pK_i values in order to produce meaningful results. To maintain consistency with our previous publications, we have elected to use pK_i values as the principal measure of receptor affinity throughout this discussion.

5.2.2 Agonism versus antagonism: [^{35}S]GTP γ S binding functional assays

When a GPCR is activated, the α subunit of the associated G-protein becomes phosphorylated through the exchange of guanosine diphosphate (GDP) for guanosine triphosphate (GTP). The phosphorylated α subunit then dissociates from the G-protein and goes on to interact with various effector proteins to elicit physiological responses. After some time, the GTPase activity of the α subunit converts the bound GTP to GDP, which allows the G-protein to revert its heterotrimeric, inactive state (see Section 1.4.1, *Adrenoceptor Structure and Function*).

[^{35}S]GTP γ S is a radiolabelled analogue of GTP which replaces the terminal phosphate of endogenous GTP with a radiolabelled thiophosphate group (Fig. 5.2). As a result of this chemical modification, the α subunit is incapable of hydrolysing the γ -terminus and therefore cannot revert to the non-phosphorylated state in order to reform the inactive G-protein. The introduction of [^{35}S]GTP γ S into the GPCR's environment causes the α subunit to take up non-hydrolysable [^{35}S]GTP γ S in place of GTP, leading to an accumulation of radiolabelled, persistently active α subunits. By measuring the quantity of radiolabelled α subunits produced in the presence of a ligand, it is possible to determine the degree to which that ligand causes or prevents activation of a GPCR. The degree to which receptor activation occurs in turn determines whether a given ligand can be considered an agonist, an antagonist or an inverse agonist of that receptor.²⁵³

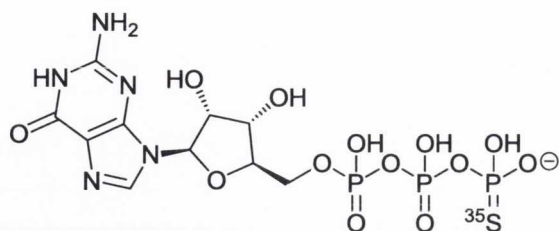


Fig. 5.2. Chemical structure of [^{35}S]GTP γ S ([^{35}S]guanosine 5'-O-[γ -thio]triphosphate).

Agonists generally provide an increase in the uptake of [^{35}S]GTP γ S, and a plot of ligand concentration versus bound [^{35}S]GTP γ S can be used to determine the EC_{50} value, *i.e.* the concentration at which the agonist effect is half of maximal. The same plot also provides a measure of EC_{max} , the concentration at which the maximum effect is observed.

The EC_{50} or IC_{50} value of a given ligand indicates its potency, *i.e.* the concentration required to generate half of the maximal response, while EC_{max} indicates the efficacy of the ligand, *i.e.* the maximum response which can be generated. EC_{max} and EC_{50} values may be compared between ligands as a relative measure of their pharmacological potential. A low EC_{50} value - typically 1 nM or below - implies that the ligand is a potent agonist, higher EC_{50} values imply that more ligand is necessary to provide the same effect and that the ligand is a weak agonist. Inverse agonists produce the opposite effect, causing the GPCR to become less active and producing a decrease in the quantity of bound [^{35}S]GTP γ S. For inverse agonists, EC_{50} and EC_{max} values can be calculated using the same procedure as used for agonists, but the effect will be in the reverse direction (Fig. 5.3).

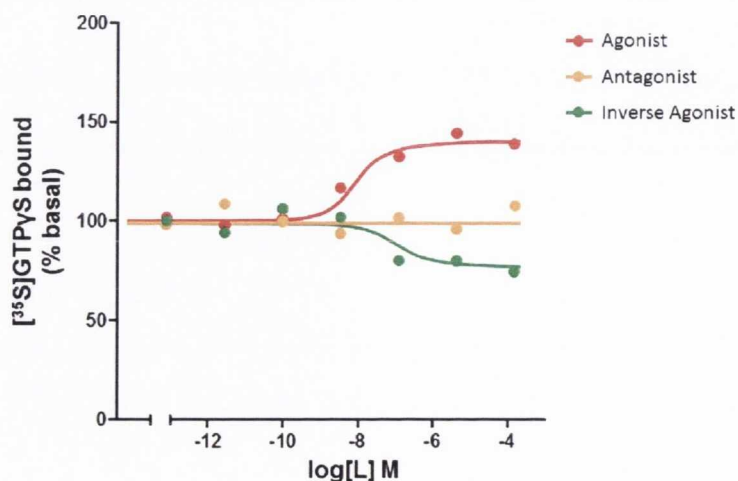


Fig. 5.3. Effect of agonist, antagonist and inverse agonist ligands on bound [^{35}S]GTP γ S.

In the absence of an agonist with which to compete, antagonists have no effect upon the quantity of bound [^{35}S]GTP γ S and hence their functional efficacy must be measured indirectly. The effect of ligand concentration upon the quantity of bound [^{35}S]GTP γ S is therefore measured in the presence of a constant concentration of a known agonist. A decrease in bound [^{35}S]GTP γ S suggests that the ligand is functioning as a competitive antagonist, with a larger decrease implying a more potent antagonist. The [^{35}S]GTP γ S assay can also provide data regarding the affinity of a given compound for the receptor, however the results are often 2 – 3 log units lower than those produced in radioligand binding assays owing to differences in experimental conditions.²⁵⁴ As a result, the [^{35}S]GTP γ S assay provides a much less sensitive tool for the study of affinity values compared with radioligand binding studies and in the present text only activity data will be taken from [^{35}S]GTP γ S assays, while receptor affinities are taken from competitive binding assays.

5.2.3 Confirming activity *in vivo*: microdialysis experiments

Microdialysis is a technique which allows for the continuous sampling of extracellular fluid in a live animal. A small probe is inserted into the site of investigation, and an aqueous solution which closely matches the endogenous fluid in ionic strength and composition is perfused at a very low rate. The probe is designed to mimic a natural capillary, which allows the technique to be compatible with almost any tissue in the body. In the brain, artificial cerebrospinal fluid (CSF) is used as the perfusate and is delivered via a catheter within the probe. A semi-permeable membrane at the end of the probe allows intracellular fluid to diffuse into a second catheter which collects fluid returning from the site of investigation (the dialysate); this allows microdialysis to sample the tissue with no net loss of fluid (Fig. 5.4). The returning fluid is analysed using such techniques as HPLC to provide a quantitative analysis of the site under investigation. The low flow rate and semi-permeability of the membrane prevents the leeching of cells or large proteins into the probe, resulting in minimal damage to the surrounding tissue.

One application of microdialysis which has been particularly successful is the monitoring of changes in neurotransmitter concentrations in response to chemical stimuli.²⁵⁵ The effects of a potentially neuroactive compound can be determined either by local administration or by systemic administration, in which case it is also possible to provide an early indication of whether a given compound can cross the blood-brain barrier (BBB). As a result of this

advantage and its minimally-invasive nature, microdialysis has found extensive applications in the investigation of central nervous system agents.²⁵⁶

In previous studies, our group has demonstrated the capability of several aryl guanidine and aryl 2-iminoimidazolidine type α_2 -AR antagonists to increase extracellular concentrations of noradrenaline (NA) in the rat brain (Fig. 5.4). These compounds were shown to increase levels of NA using both local and intraperitoneal administration, suggesting that these compounds are capable of crossing the BBB. In the present study, those compounds exhibiting high affinities using radioligand binding assays and antagonist activity using [³⁵S]GTP γ S functional assays will also be studied using the microdialysis technique.

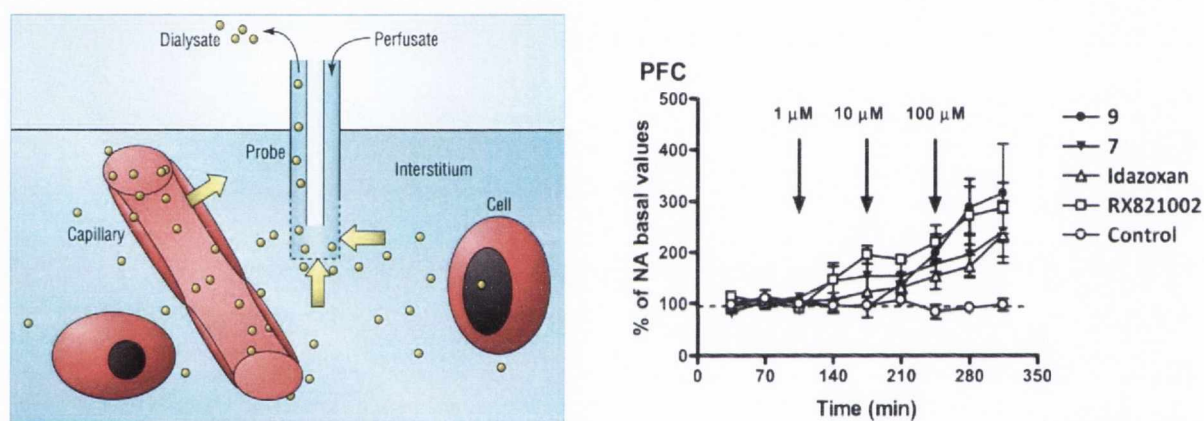
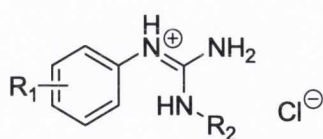


Fig. 5.4. Microdialysis probe showing the sampling of extracellular material (*left*), and the effect of compounds **9** and **7** on extracellular NA using the microdialysis method (*right*).¹⁵⁸

5.3 Results and Discussion

5.3.1 Affinity of the *N,N'*-disubstituted guanidine hydrochloride salts

The affinity towards the α_2 -AR was determined in human pre-frontal cortex tissue using a competitive binding assay with the α_2 -AR selective radioligand [³H]RX821002 (2-methoxyidazoxan; Fig. 1.31), which was used at a constant concentration of 2 nM. Affinity data, calculated as pK_i values, for the *N,N'*-disubstituted hydrochloride salts are presented in Table 5.1; the pK_i of RX821002 and of the corresponding monosubstituted guanidines are also included for comparison.

Table 5.1 Affinity values (pK_i) obtained for guanidine derivatives

| Compound | R ₁ | R ₂ | pK _i |
|-------------------------|---------------------------------------|---|-----------------|
| RX821002 | - | - | 8.72 |
| 69a | 4-OEt | -(CH ₂) ₂ -CH ₃ | 5.37 |
| 69b | 4-NMe ₂ | -(CH ₂) ₂ -CH ₃ | 5.95 |
| 69c | 3,4-(-CH ₂ -) ₄ | -(CH ₂) ₂ -CH ₃ | 6.17 |
| 69d | 4-NHEt | -(CH ₂) ₂ -CH ₃ | 5.08 |
| 69e | 3,4(-OCH ₂ O-) | -(CH ₂) ₂ -CH ₃ | 4.82 |
| 70a | 4-OEt | -(CH ₂) ₂ -OH | 4.72 |
| 70b | 4-NMe ₂ | -(CH ₂) ₂ -OH | 5.73 |
| 70c | 3,4-(-CH ₂ -) ₄ | -(CH ₂) ₂ -OH | 5.76 |
| 70d | 4-NHEt | -(CH ₂) ₂ -OH | 4.73 |
| 70e | 3,4(-OCH ₂ O-) | -(CH ₂) ₂ -OH | 4.93 |
| 71a | 4-OEt | -C ₆ H ₅ | 5.65 |
| 71b | 4-NMe ₂ | -C ₆ H ₅ | 6.41 |
| 71c | 3,4-(-CH ₂ -) ₄ | -C ₆ H ₅ | 6.58 |
| 71d | 4-NHEt | -C ₆ H ₅ | 5.31 |
| 71e | 3,4(-OCH ₂ O-) | -C ₆ H ₅ | 5.36 |
| 72a | 4-OEt | -CH ₂ -(fur-2-yl) | 5.83 |
| 72b | 4-NMe ₂ | -CH ₂ -(fur-2-yl) | 6.67 |
| 72c | 3,4-(-CH ₂ -) ₄ | -CH ₂ -(fur-2-yl) | 6.29 |
| 72d | 4-NHEt | -CH ₂ -(fur-2-yl) | 5.97 |
| 72e | 3,4(-OCH ₂ O-) | -CH ₂ -(fur-2-yl) | 5.82 |
| 51 | 4-OEt | -H | 6.85 |
| 105b^a | 4-NMe ₂ | -H | 7.06 |
| 105c^b | 3,4-(-CH ₂ -) ₄ | -H | 7.11 |
| 105d^c | 4-NHEt | -H | 6.58 |
| 105e^a | 3,4(-OCH ₂ O-) | -H | 6.40 |

^aReference 158, ^breference 159, ^creference 160.

Perhaps the most striking result in these experiments is the reduced affinity of the *N,N'*-disubstituted guanidine derivatives when compared with their *mono*-substituted analogues with $R_2 = H$. This effect is most pronounced in the case of compound **70a** ($pK_i = 4.72$), in which the introduction of an *N*-ethoxy R_2 substituent reduces affinity for the α_2 -AR by more than two log units compared with its *mono*-substituted analogue **51** ($pK_i = 6.85$). Compound **72b** bearing a furan-2-ylmethyl R_2 group incurs the least loss of potency ($pK_i = 6.67$) and its affinity compares favourably with that of the monosubstituted analogue **105b** ($pK_i = 7.06$).

The effect of the aryl R_1 substituent upon affinity in the *N,N'*-disubstituted guanidines is similar to that observed in *mono*-substituted guanidines, loosely following the order: 3,4-tetrahydronaphthyl > 4-dimethylamino > 3,4-methylenedioxy > 4-ethylamino > 4-ethoxy. The fact that this order is maintained both in the presence and absence of an R_2 substituent suggests that the aryl R_1 group is likely to occupy the same position when bound to the receptor in both disubstituted and *mono*-substituted guanidines. However, several exceptions to this ranking order exist, and it remains possible that the presence of an R_2 substituent may modulate the position of the R_1 group within the binding site.

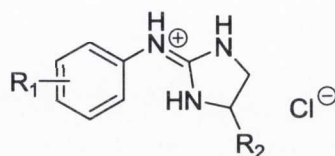
The presence of an R_2 substituent generally results in a decrease in binding affinity; this effect is most prominent in compounds with the aromatic substituent $R_1 = 4$ -ethoxy. The most favourable affinities are associated with the phenyl and furan-2-ylmethyl R_2 substituents, while the *n*-propyl and ethoxy substituents generally provide poorer affinities. It is possible that the lower affinities endowed by the latter two substituents is a result of their flexibility, as both groups introduce several additional degrees of rotational freedom which increases the entropic cost of binding. However, the furan-2-ylmethyl substituent also introduces two degrees of rotation and yet it produces higher affinities; it is possible that in this case the entropic penalty is offset by enthalpically favourable interactions. The phenyl and furan-2-ylmethyl substituents are also substantially larger than the *n*-propyl and ethoxy groups; this may reflect a preference for bulky substituents in this position as highlighted by the large, sterically favoured region corresponding to this space in our CoMFA model (see Fig. 3.4).

5.3.2 Affinity of the 4-substituted-2-iminoimidazolidine hydrochloride salts

Table 5.2 presents affinity data (pK_i values) for 4-substituted-2-iminoimidazolidine derivatives towards the α_2 -AR, determined using the same methodology as for *N,N'*-

disubstituted guanidines. The pK_i of RX821002 and that of the corresponding unsubstituted 2-iminoimidazolidines are included as a reference.

Table 5.2 Affinity values (pK_i) obtained for 2-iminoimidazolidine derivatives



| Compound | R ₁ | R ₂ | pK_i |
|-------------------|---------------------------------------|------------------|--------|
| RX821002 | - | - | 8.72 |
| 93a | 4-OEt | -CH ₃ | 4.85 |
| 93b | 4-NMe ₂ | -CH ₃ | 5.48 |
| 93c | 3,4-(-CH ₂ -) ₄ | -CH ₃ | 6.00 |
| 93d | 4-NHEt | -CH ₃ | 4.91 |
| 93e | 3,4(-OCH ₂ O-) | -CH ₃ | 5.63 |
| 103a | 4-OEt | -(fur-2-yl) | 5.58 |
| 103b | 4-NMe ₂ | -(fur-2-yl) | 5.88 |
| 103c | 3,4-(-CH ₂ -) ₄ | -(fur-2-yl) | 6.16 |
| 103d | 4-NHEt | -(fur-2-yl) | 5.66 |
| 103e | 3,4(-OCH ₂ O-) | -(fur-2-yl) | 5.77 |
| 52 | 4-OEt | -H | 7.10 |
| 105b ^a | 4-NMe ₂ | -H | 7.42 |
| 105c ^b | 3,4-(-CH ₂ -) ₄ | -H | 7.33 |
| 105d ^c | 4-NHEt | -H | 6.75 |
| 105e ^a | 3,4(-OCH ₂ O-) | -H | 7.33 |

^aReference 158, ^breference 159, ^creference 160.

These results reflect a general observation already seen with *N,N'*-disubstituted guanidines; the introduction of an R₂ substituent leads to reduced affinity for the α_2 -AR. Compound **93a** ($pK_i = 4.85$) incurs the most significant loss of affinity, with a difference of more than two log units compared with its demethylated analogue **52** ($pK_i = 7.10$). In comparison with the

N,N'-disubstituted guanidine series, the 2-iminoimidazolidines on average incur a greater loss in affinity with the introduction of an R_2 group. This effect sharply contrasts with previous observations in our research group, which suggested that 2-iminoimidazolidines provide higher affinities than their corresponding guanidine analogues. With the introduction of an R_2 substituent this observation is apparently reversed; for example, the 4-(furan-2-yl)-2-iminoimidazolidine derivatives **103a-e** provide consistently lower affinities than their *N'*-furan-2-ylmethyl guanidine counterparts **72a-e**. This result also contradicts the predictions of our CoMFA model, which suggests that bulkier substituents should provide higher affinities, a prediction which was upheld in the case of *N,N'*-disubstituted guanidines where the phenyl and furan-2-ylmethyl groups provided the highest affinities. This observation is further complicated by the fact that 2-iminoimidazolidines include fewer rotatable bonds and should intuitively provide lower binding entropies. The improved affinity of the guanidine species suggests that their rotational freedom allows the furan moiety to undergo favourable interactions which are inaccessible under the restricted geometry of 2-iminoimidazolidines.

The 4-methyl-2-iminoimidazolidine derivatives **93a-e** provide much poorer affinities, and the introduction of a single methyl group reduces affinity by an average of 1.8 pK_i units. This observation agrees with earlier reports by Miller *et al.*, who found that a larger substituent at this position (R_2 = benzyl) gave larger affinities than a methyl substituent alone.²²²

The effect of the aryl R_1 substituent loosely follows the same order as observed in the guanidine derivatives, namely: 3,4-tetrahydronaphthyl > 4-dimethylamino > 3,4-methylenedioxy > 4-ethylamino > 4-ethoxy. As with the guanidine series, the 4-ethoxy series incurs the greatest loss in affinity with the introduction of an R_2 group. This suggests that both the *N,N'*-disubstituted guanidines and 2-iminoimidazolidines place the R_1 group in the same region of space within the binding site, as the effect of R_1 is nearly identical in both of these series of compounds.

5.3.3 [³⁵S]GTPγS binding functional assays

The ten compounds with the highest level of affinity for the α₂-AR (**51**, **52**, **72b**, **71c**, **71b**, **72c**, **69c**, **103c**, **93c**, **72d**) were subjected to [³⁵S]GTPγS binding experiments to determine their effect upon the receptor as either agonists or antagonists (Fig. 5.5). A small

selection of six representative compounds with lower affinities was also studied in these experiments (**69a**, **70e**, **72a**, **69b**, **70b**, **72e**) for comparative purposes.

Among these compounds, **52** was the only compound seen to stimulate binding of [³⁵S]GTPγS, suggesting that it acts as a partial agonist of the α₂-AR. Compound **52** is the only member of the 4-unsubstituted-2-iminoimidazolidine series included in these experiments, which suggests that all of the 4-substituted-2-iminoimidazolidines and *N,N'*-disubstituted guanidines tested in these experiments do not activate the α₂-AR; *i.e.* these compounds do not act as α₂-AR agonists and instead function as antagonists and/or inverse agonists.

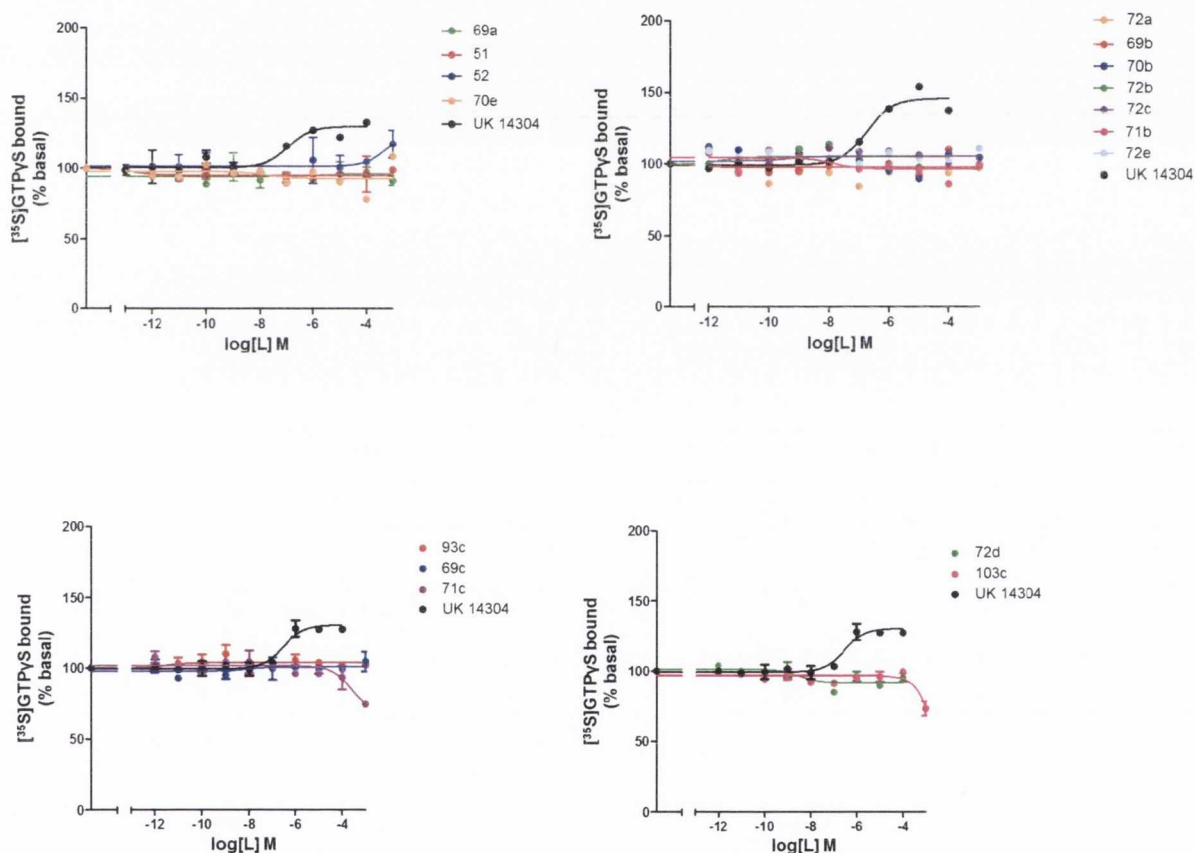


Fig. 5.5. Dose-response curves for [³⁵S]GTPγS binding *versus* ligand concentration.

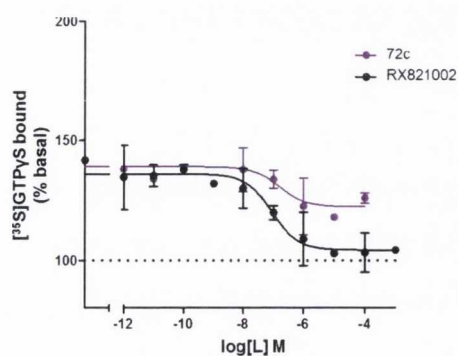
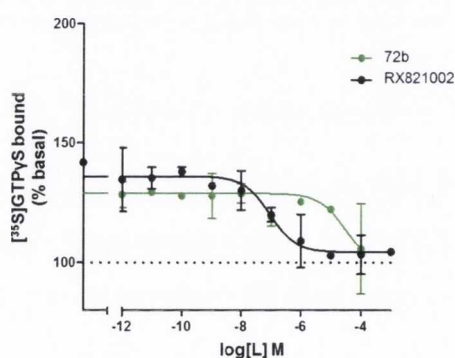
As shown in Fig. 5.5, compounds **71b**, **71c**, **72d** and **103c** induce a decrease in [³⁵S]GTPγS binding, indicating that they act as inverse agonists of the α₂-AR. It is interesting to note that all of these compounds include an aromatic R₂ substituent; with R₂ = phenyl in the case of **71b** and **71c**, and R₂ = -CH₂-fur-2-yl for **72d** and R₂ = fur-2-yl for **103c**. Nonetheless, it would

be inaccurate to state that an aromatic R_2 group ensures that a compound will act as an inverse agonist, as neither **72a** nor **72c** ($R_2 = -CH_2\text{-fur-2-yl}$) function as inverse agonists.

Compounds that do not stimulate $[^{35}\text{S}]\text{GTP}\gamma\text{S}$ binding in this assay may be subjected to $[^{35}\text{S}]\text{GTP}\gamma\text{S}$ binding experiments in the presence of the $\alpha_2\text{-AR}$ selective agonist UK 14304 at a constant concentration of 10 μM in order to confirm their activity as antagonists. In these experiments, UK 14304 stimulates the uptake of $[^{35}\text{S}]\text{GTP}\gamma\text{S}$ and the ligand is then introduced at varying concentrations. The degree to which the ligand can mitigate agonist-promoted $[^{35}\text{S}]\text{GTP}\gamma\text{S}$ binding determines its effectiveness as a competitive antagonist. At the time of writing, these experiments have been carried out for N,N' -disubstituted guanidines **72b** and **72c**, neither of which acted as an agonist or inverse agonist; and for **71b** which induced a decrease in $[^{35}\text{S}]\text{GTP}\gamma\text{S}$ binding (Table 5.3; Fig. 5.6).²⁵⁷ All three compounds exhibit a reduction in $[^{35}\text{S}]\text{GTP}\gamma\text{S}$ binding, confirming that the first two can be considered as antagonists while **71b** can be confirmed as an inverse agonist of the $\alpha_2\text{-AR}$.

Table 5.3 IC_{50} values for N,N' -disubstituted guanidines determined using $[^{35}\text{S}]\text{GTP}\gamma\text{S}$ binding inhibition experiments in the presence of UK 14304 (10 μM)

| Compound | R_1 | R_2 | IC_{50} (nM) \pm SEM |
|-----------------|---------------------------------------|--------------------------------|---------------------------------|
| RX821002 | - | - | 89.29 \pm 4.2 |
| 72b | 4-NMe ₂ | -CH ₂ -(Fur-2-yl) | 29840 \pm 7946.3 |
| 72c | 3,4-(-CH ₂ -) ₄ | -CH ₂ -(Fur-2-yl) | 158.6 \pm 15.3 |
| 71b | 4-NMe ₂ | -C ₆ H ₅ | 554.5 \pm 15.8 |



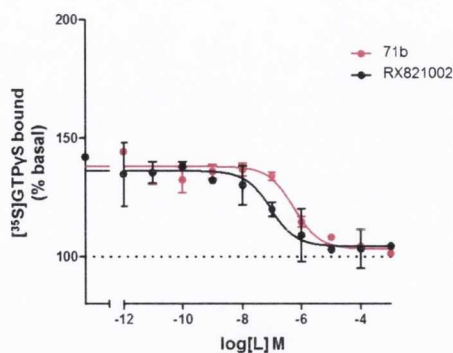


Fig. 5.6. Dose-response curves for [³⁵S]GTPγS binding *versus* ligand concentration in the presence of the α₂-AR selective agonist UK 14304 (10 μM).

Among these three compounds, **72b** presents a significantly poorer IC₅₀ value and is unlikely to comprise a useful lead compound in the development of α₂-AR antagonists. However, compounds **71b** and **72c** both present IC₅₀ values which compare favourably with the potent α₂-AR antagonist RX821002. Of these two compounds **71b** presents both a higher pK_i value (6.41 vs. 6.29 for **72c**) and a greater reduction in agonist-induced [³⁵S]GTPγS binding (see Fig. 5.4); however, the IC₅₀ value of **72c** is more than three times lower than that of **71b**. Clearly, either compound could be selected on differing criteria as a lead compound for the further development of α₂-AR antagonists.

5.4 Conclusions

In our previous studies examining *mono*-substituted guanidine and 4-unsubstituted 2-iminoimidazolidine derivatives,¹⁵⁸⁻¹⁶⁰ it was often difficult to determine the structure-activity relationships which govern functional activity at the α₂-AR. Relatively few of these unsubstituted compounds were seen to act as antagonists, and a significant portion of these compounds acted as potent agonists of the α₂-AR. It is clear from competitive binding assay experiments that the extension of the guanidine or 2-iminoimidazolidine functional group to incorporate an R₂ substituent leads to reduced affinity for the α₂-AR; however [³⁵S]GTPγS binding functional assays also suggest that this modification leads to consistent antagonist or inverse agonist activity at the α₂-AR.

From a molecular design standpoint, this observation gives rise to an interesting dilemma. The *mono*-substituted compounds exhibit consistently higher affinities but many of these compounds function as agonists, while the disubstituted derivatives give poorer affinities yet are more likely to function as antagonists. Several disubstituted compounds bearing a large R_2 group were even observed to function as inverse agonists, an activity which was never observed among the *mono*-substituted derivatives. To a first approximation, the R_2 substituent appears to determine the functional activity at the α_2 -AR, with smaller substituents giving rise to a greater likelihood of receptor activation. This continuum is exemplified by compounds **106**, **9** and **71b**, in which the increase in substituent size produces a greater degree of receptor deactivation (Fig. 5.7).¹⁵⁸

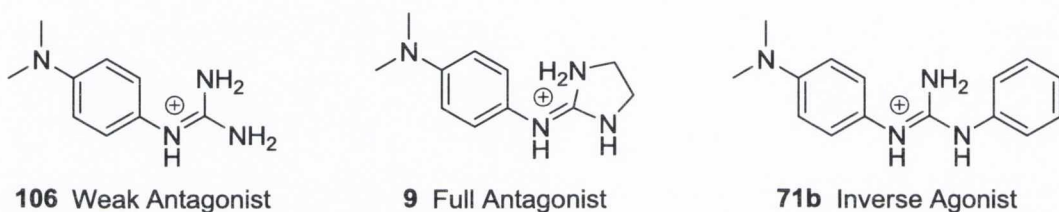


Fig. 5.7. Effect of substituent size on functional activity at the α_2 -AR, exemplified using 4-dimethylamino compounds **106**, **9** and **71b**.

It would be inaccurate to state that the relationship between functional activity and substituent size is absolute, as there are several instances in which the 2-iminoimidazolidine compound functions as an agonist while its guanidine analogue acts as an antagonist, such as compounds **51** and **52** (Tables 4.1 and 4.2, Fig. 5.5); our previous studies include many further counterexamples. Nonetheless, it is tempting to suggest that the functional activity within this series of compounds might be controllable by the incorporation of a suitable R_2 group.

Moreover, while the incorporation of an R_2 group has thus far led to reduced affinity for the α_2 -AR, there are indications that certain R_2 groups might produce improved affinities. This is exemplified by the 4-methyl-2-iminoimidazolidine derivatives **93a-e**, which produce consistently poorer affinities compared with their bulkier 4-(2-furyl)-2-iminoimidazolidine counterparts **103a-e**. This suggests that the relationship between substituent size and receptor

affinity is far from linear; and in some instances the incorporation of an R₂ group can produce a receptor affinity which compares favourably with the unsubstituted analogue.

At the time of writing, several of the [³⁵S]GTPγS binding experiments remain to be completed and microdialysis experiments will be needed to confirm their activity *in vivo*. Moreover, further behavioural assays such as the tail suspension test and the forced swim test will also be carried out to assess whether this new series of compounds can provide an antidepressant effect in an animal model. As these experiments progress, it will become possible to draw further conclusions regarding structure-activity relationships. Nonetheless, even at this early stage it is clear that the incorporation of an R₂ substituent provides access to α₂-AR antagonists with greater consistency than their unsubstituted counterparts, and that *N,N'*-disubstituted guanidines and 4-substituted-2-iminoimidazolidines provide promising candidates for the development of future antidepressants.

Chapter 6 - Future Work

According to the results of the [³⁵S]GTPγS binding assay, every one of the new *N,N'*-disubstituted guanidine and 4-substituted 2-iminoimidazolidine compounds described in this text do not stimulate binding of [³⁵S]GTPγS. This strongly indicates that all of these compounds act as either antagonists or inverse agonists of the α₂-AR. However, at the present time only three of the 32 new compounds reported in this thesis have been examined using the [³⁵S]GTPγS assay in the presence of the α₂-AR selective agonist UK-14304. This second assay is necessary to confirm the activity of these compounds as antagonists and inverse agonists, and the resulting pharmacological data will solidify whether these two new series of compounds act exclusively to inhibit the activity of the α₂-AR.

Following the completion of these studies, compounds exhibiting the most favourable combination of affinity and activity will be subjected to *in vivo* microdialysis experiments in order to determine their ability to increase extracellular concentrations of NA, and to investigate whether these compounds can successfully cross the blood-brain barrier (BBB). It is tempting to speculate that the increased lipophilicity introduced by the new R substituent may lead to improved bioavailability and an increased capacity to cross the BBB. However, the increased molecular weight may actually diminish their blood-brain barrier permeability, and the actual performance of these compounds *in vivo* remains to be seen.

These experiments will be followed by animal stress behavioural assays such as the forced swim test²⁵⁰ and the tail suspension test (TST)¹⁶¹ in order to confirm the ability of these compounds to exhibit an antidepressant-like effect *in vivo*. At the time of writing, promising behavioural results are forthcoming for several of the compounds prepared previously in our group.¹⁹³ It remains to be seen whether the positive performance of these older, closely-related compounds is transferable to the new compounds described in this text.

Another issue that warrants consideration is the generally reduced affinity of the new, substituted compounds in comparison with their unsubstituted analogues. The affinity of these compounds might be improved through the development of a new CoMFA model incorporating the full set of compounds, both new and old, in order to highlight which regions of chemical space might benefit from the incorporation or removal of steric and electronic features.

In contrast with the CoMFA model described earlier in this text, the proposed CoMFA model would include a detailed description of the chemical space beyond the guanidine or 2-iminoimidazolidine moiety and should therefore be able to provide much more accurate predictions of which chemical groups in this region might give rise to improved affinity for the α_2 -AR. The development of a new CoMFA model may, however, prove more difficult than the previous model as a result of the increased number of freely rotatable torsional angles in these new compounds. It might be worthwhile to examine extended approaches designed to simplify torsional considerations, such as the topomer CoMFA approach described in Chapter 2, in order to mitigate these difficulties.

One final consideration is the design of next-generation α_2 -AR antagonists. Although a new CoMFA model or similar QSAR approach would be necessary to draw quantitative predictions, it is interesting to speculate as to which chemical modifications might lead to improved affinity for the α_2 -AR, while simultaneously maintaining the increased probability of acting exclusively as antagonists. It is evident from a comparison of the furan-bearing guanidine compounds **72a-e** with their cyclised, 2-iminoimidazolidine counterparts **103a-e** that restricting the spatial location of furan moiety to its location in 2-iminoimidazolidine compounds **103a-e** leads to a reduction in affinity. It might therefore be interesting to restrict the location of this chemical group to a position adjacent to the guanidine moiety, rather than at its terminus, generating a new class of 1-aryl-2-iminoimidazolidine derivatives (Fig. 6.1).

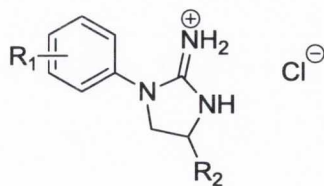


Fig. 6.1. General form of potential 1-aryl-2-iminoimidazolidine antagonists of the α_2 -AR.

At the time of writing, an expedient synthetic approach to the preparation of this class of compounds is already under investigation. It will be interesting to determine whether the restriction of the substituent to this chemical space will lead to improved affinity while maintaining the desired antagonistic activity.

A second approach to restricting the substituent to the desired spatial location is conformational control, as described in a recent publication emanating from our group.¹⁹⁷ Use of an aromatic heterocycle in place of the phenyl moiety allows the guanidine group to be conformationally restricted via hydrogen bonding interactions between the guanidine protons and the heterocyclic lone pair (Fig. 6.2). Although this research is still at an early stage, these types of compounds are already showing promising antagonistic pharmacological activity.

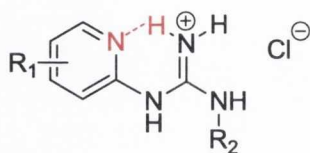


Fig. 6.2. Pyridin-2-yl guanidines as potential antagonists of the α_2 -AR with IMHB interactions leading to conformational control shown in red.

Pharmacological results described in the present text, combined with parallel studies examining the effectiveness of aromatic heterocyclic guanidines and other conformationally-restricted analogues, will provide a wealth of information regarding which chemical features lead to the most desirable pharmacological attributes. Even compounds exhibiting poor affinities or undesired agonist activity profiles can provide useful information for the design of future compounds. Thus, whatever the outcome of present and future investigations, it is certain that a combined approach of rational design and synthesis will continue to lead to potent α_2 -AR antagonists as potential antidepressants.

Chapter 7 - Experimental

7.1 General Procedures: Pharmacology

Preparation of Membranes

Neural membranes (P2 fractions) were prepared from the prefrontal cortex of human brain tissue obtained at autopsy in the Instituto Vasco de Medicina Legal, Bilbao, Spain. Postmortem human brain samples of each subject (~1 g) were homogenized using a Teflon-glass grinder (10 up-and-down strokes at 1500 rpm) in 30 volumes of homogenization buffer (1 mM MgCl₂ and 5 mM Tris-HCl, pH 7.4) supplemented with 0.25 M sucrose. The crude homogenate was centrifuged for 5 min at 1000 × g (4 °C), and the supernatant was centrifuged again for 10 min at 40 000 × g (4 °C). The resultant pellet was washed twice in 20 volumes of homogenization buffer and recentrifuged in similar conditions. Aliquots of 1 mg protein were stored at -70 °C until assay. Protein content was measured according to the Bradford method using BSA as standard and was similar in the different brain samples.

[³H]RX821002 Binding Assays

Specific [³H]RX821002 binding was measured in 0.55 ml aliquots (50 mM Tris-HCl, pH 7.5) of the neural membranes, which were incubated with [³H]RX821002 (1 nM) for 30 min at 25 °C in the absence or presence of the competing compounds (10⁻¹² M to 10⁻³ M, 10 concentrations). Specific binding was determined and plotted as a function of the compound concentration. Incubations were terminated by diluting the samples with 5 ml of ice-cold Tris incubation buffer (4 °C). Membrane-bound [³H]RX821002 was separated by vacuum filtration through Whatman GF/C glass fiber filters. The filters were then rinsed twice with 5 ml of incubation buffer and transferred to minivials containing 3 ml of OptiPhase “HiSafe” II cocktail and counted for radioactivity by liquid scintillation spectrometry.

Analysis of Binding Data

Analysis of competition experiments to obtain the inhibition constant (K_i) were performed by nonlinear regression using the GraphPad Prism program. All experiments were analysed assuming a one-site model of radioligand binding. K_i values were normalized to pK_i values.

[³⁵S]GTP γ S Binding Assays

The incubation buffer for measuring [³⁵S]GTP γ S binding to brain membranes contained, in a total volume of 500 μ l, 1 mM EGTA, 3 mM MgCl₂, 100 mM NaCl, 50 mM GDP, 50 mM Tris-HCl at pH 7.4, and 0.5 nM [³⁵S]GTP γ S. Protein aliquots were thawed and resuspended in the same buffer. The incubation was started by addition of the membrane suspension (40 μ g of membrane proteins) to the previous mixture and was performed at 30 °C for 120 min with shaking. To evaluate the influence of the compounds on [³⁵S]GTP γ S binding, eight concentrations (10⁻¹⁰ to 10⁻³ M) of the compounds were added to the assay. Incubations were terminated by adding 3 ml of ice-cold resuspension buffer followed by rapid filtration through Whatman GF/C filters presoaked in the same buffer. The filters were rinsed twice with 3 ml of ice-cold resuspension buffer, transferred to vials containing 5 ml of OptiPhase HiSafe II cocktail (Wallac, U.K.), and the radioactivity trapped was determined by liquid scintillation spectrometry (Packard 2200CA). The [³⁵S]GTP γ S bound was about 7 - 14% of the total [³⁵S]GTP γ S added. Nonspecific binding of the radioligand was defined as the remaining [³⁵S]GTP γ S binding in the presence of 10 μ M unlabeled GTP γ S.

In Vivo Microdialysis Assays

Experiments were carried out in male Sprague-Dawley rats weighing between 250 and 300 g. At the beginning of the experiments, animals were anaesthetized with chloral hydrate (400 mg/kg i.p.) and a microdialysis probe was implanted by stereotaxic surgery into prefrontal cortex (PFC) brain area. The coordinates selected for the PFC were as follows: AP (anterior to bregma), +2.8 mm; L (lateral from the mid-sagittal suture), +1 mm; DV (ventral from the dura surface), -5 mm. After 24 h, for animal recovery, perfusion fluid (artificial cerebrospinal fluid) is pumped through the probe at a flow rate of 1 μ l/min. In the semipermeable membrane (on the critical side of the probe) which is placed on the selected area, molecules flow into and out the cannulae by diffusion. Therefore, the microdialysis technique allows local administration of substrates dissolved in the perfusion fluids.

Compounds to be tested were dissolved in artificial cerebrospinal fluid (148 mM NaCl, 2.7 mM KCl, 1.2 mM CaCl₂, and 0.85 mM MgCl₂; pH 7.4), and were perfused by reverse microdialysis in increasing concentrations of 1, 10, and 100 μ M. Each concentration was administered for two sampling periods of 35 min each. Systemic administration of the compounds was made intraperitoneally, dissolved in saline. After collection, samples were

analysed by HPLC with electrochemical detection to monitor NA extracellular concentrations as a measure of antidepressant activity. The mean values of the first three samples before drug administration were considered as 100% basal value. All measures of extracellular NA concentrations are expressed as a percentage of the baseline value \pm s.e. mean. One-way analysis of variance (ANOVA) for control group or two-way ANOVA between control and each treated group was assessed by statistical analysis. At the end of the experiments, animals were euthanized and the brains were dissected to check the correct implantation of the probe.

Drug Compounds

[³H]RX821002 (specific activity 59 Ci/mmol) was obtained from Amersham International, U.K. [³⁵S]GTP γ S (1250 Ci/mmol) was purchased from DuPont NEN (Brussels, Belgium). Idazoxan HCl was synthesized by Dr. F. Geijo at S.A. Lasa Laboratories, Barcelona, Spain. Clonidine HCl, GDP, GTP, GTP γ S, RX821002 HCl, and UK14304 were purchased from Sigma (St. Louis, U.S.A.). All other chemicals were of the highest purity commercially available.

7.2 General Procedures: Chemical Synthesis

Materials and Methods

All commercial chemicals were obtained from Sigma-Aldrich or Fluka and were used without further purification. Deuterated solvents for NMR use were purchased from Apollo. Dry solvents were prepared using standard procedures, according to Vogel, with distillation prior to use. Chromatographic columns were run using a Biotage SP4 flash purification system with Biotage SNAP silica cartridges. Solvents for synthesis purposes were used at GPR grade. Analytical TLC was performed using Merck Kieselgel 60 F254 silica gel plates or Polygram Alox N/UV254 aluminium oxide plates. Visualisation was by UV light (254 nm). NMR spectra were recorded in a Bruker DPX-400 Avance spectrometer, operating at 400.13 MHz and 600.1 MHz for ¹H-NMR; 100.6 MHz and 150.9 MHz for ¹³C-NMR. Shifts are referenced to the internal solvent signals. NMR data were processed using Bruker Win-NMR 5.0 and Bruker TOPSPIN software. HRMS spectra were measured on a Micromass LCT electrospray TOF instrument with a WATERS 2690 autosampler with methanol as

carrier solvent; LRMS spectra were measured using an API 2000 electrospray instrument from Applied Biosystems. Melting points were determined using a Stuart Scientific Melting Point SMP1 apparatus and are uncorrected. Infrared spectra were recorded on a Perkin Elmer Spectrum One FT-IR Spectrometer equipped with a Universal ATR sampling accessory.

Purity by HPLC/CSP-HPLC

HLPC purity analysis was carried out using a Varian ProStar system equipped with a Varian Prostar 335 diode array detector and a manual injector (20 μ l). UV detection was performed at 245 nm and peak purity was confirmed using a purity channel. The stationary phase consisted of an ACE 5 C18-AR column (150 x 4.6 mm), and the mobile phase used the following gradient system, eluting at 1.0 ml/min: aqueous formate buffer (30 mM, pH 3.0) for 10 minutes, linear ramp to 85% methanol buffered with the same system over 25 minutes, hold at 85% buffered methanol for 10 minutes.

For analysis of enantiomeric excess, CSP-HPLC utilised a Chiralcel OD-H column (4.6 mm x 25 cm) as the stationary phase with hexane/IPA (9:1) as the mobile phase with a flow rate of 1.0 ml/min. UV detection was performed at 220 nm.

Method A: *General method for the preparation of N-Boc protected guanidines and N-Boc protected 2-iminoimidazolidines*

To a stirred solution of the starting amine (2.5 ml) at 0 °C were added 1.0 equivalents of the appropriate Boc protected thiourea derivative, 3.5 equivalents of triethylamine (726 μ l, 5.25 mmol) and 1.2 equivalents of mercury (II) chloride (489 mg, 1.80 mmol). The 0 °C temperature was maintained for 30 min before allowing the reaction to come to room temperature. After 16 h stirring, EtOAc (50 ml) was added prior to filtering the reaction through a pad of Celite[®]. The filter cake was rinsed twice with EtOAc (2 x 25 ml) and the organic phase washed first with water (50 ml) and then with brine (50 ml), followed by drying over anhydrous MgSO₄ and removal of solvents under vacuum. The resulting residue was purified by silica gel chromatography using gradient elution (hexane:EtOAc), followed by recrystallisation (where necessary) using a minimal quantity of ether to dissolve the residue, followed by dropwise addition of hexane until precipitation. Recrystallisation was

allowed to progress at 0 °C overnight and after 18 h the product was collected by filtration. In cases where recrystallization was not necessary (material was pure by TLC), solvents were evaporated *in vacuo* following chromatography to afford the pure product.

Method B: *General method for the synthesis of N-Boc protected N'-substituted thioureas, starting from N,N'-bis-(tert-butoxycarbonyl)thiourea*

N,N'-bis-(tert-butoxycarbonyl)thiourea (1000mg, 3.64 mmol) was dissolved in dry tetrahydrofuran (40 ml) under argon at 0 °C, to which was added 1.2 equivalents of sodium hydride as a 60% suspension in mineral oil (194 mg, 4.36 mmol). After 1 h stirring, 1.2 equivalents of trifluoroacetic anhydride were added (928 mg, 4.40 mmol) and the reaction was stirred for 1 h more. At this point 1.1 equivalents of the appropriate amine (4.00 mmol) were added and the reaction was allowed to come to room temperature, followed by stirring for a further 18 h. Dropwise H₂O (25 ml) was next added to quench the reaction, followed by extraction with EtOAc (3 x 30 ml). The combined organic phase was dried using anhydrous MgSO₄, followed by removal of solvents under vacuum. Purification proceeded by silica gel chromatography using gradient elution (hexane:EtOAc) followed by removal of solvents under vacuum to afford the product.

Method C: *General one-pot method for the synthesis of N-Boc protected N'-substituted thioureas, starting from thiourea*

Thiourea (500mg, 6.58 mmol) was dissolved in dry tetrahydrofuran (120 ml) under argon at 0 °C, to which was added 4.5 equivalents of sodium hydride as a 60% suspension in mineral oil (1184 mg, 29.61 mmol). The reaction was stirred at room temperature for 45 min to complete formation of the anion and cooled again to 0° C prior to the addition of 2.2 equivalents of di-*tert*-butyl dicarbonate (3.155 g, 14.47 mmol). After stirring at room temperature for 8 h, the reaction was again cooled to 0 °C and a second portion of 60% sodium hydride was added (442 mg, 11.05 mmol). This was followed 1 h later by the addition of 1.54 equivalents of trifluoroacetic anhydride (1.41 ml, 10.13 mmol), and the reaction was stirred for 1 h more. The appropriate amine (1.54 equivalents, 10.13 mmol) was then added and the reaction was

allowed to come to room temperature, followed by stirring for 18 h. The reaction was cooled again to 0 °C and dropwise H₂O (20 ml) was added to quench the reaction, followed by extraction with EtOAc (3 x 20 ml). The combined organic phase was washed with 80% brine (30 ml) and dried using anhydrous MgSO₄, followed by removal of solvents under vacuum. Purification proceeded by silica gel chromatography using gradient elution (hexane:EtOAc), followed by removal of solvents under vacuum to afford the product.

Method D: *General method for the deprotection of N-Boc protected guanidines using trifluoroacetic acid*

The Boc protected guanidine (0.73 mmol) was treated with solution of 50% trifluoroacetic acid in methylene chloride (10 ml). After 3 h stirring at room temperature, methylene chloride and trifluoroacetic acid were removed by evaporation, and the residue was dissolved in H₂O (10 ml). To this solution, 1000 mg Amberlite resin in its Cl⁻ form was added, and the reaction was allowed to proceed overnight. After 16 h the Amberlite was removed by filtration, and the filtrate was washed twice with methylene chloride (2 x 15 ml). The aqueous phase was evaporated to yield the crude hydrochloride salt. The product was purified by reverse phase chromatography (C-8 silica, typical elution gradient: 100% H₂O to 85:15 H₂O:acetonitrile). Solvents were removed *in vacuo* to afford the product.

Method E: *General method for the deprotection of N-Boc protected guanidines using hydrochloric acid*

The Boc protected guanidine (0.39 mmol) was dissolved in 1.25 M methanolic HCl and stirred under argon until the reaction was adjudged complete (Note: If the reaction fails to proceed to completion after 3 h by TLC, an additional 0.5 ml conc. HCl may be added to the mixture). At the reaction endpoint, evaporation of solvents and HCl was followed by reverse phase chromatography (C-8 silica, typical elution gradient: 100% H₂O to 85:15 H₂O:acetonitrile). The purified fractions were evaporated to dryness to yield the product.

Method F: *General method for the Boc protection of imidazolidine-2-thione derivatives*

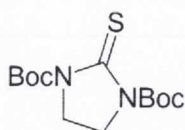
To a cooled solution of the imidazolidine-2-thione derivative (1.77 mmol) in dry tetrahydrofuran (20 ml) under argon, NaH as a 60% suspension in mineral oil (318 mg, 7.95 mmol) was added. After 5 min, the ice-bath was removed and the reaction was stirred for 10 min at room temperature. The reaction mixture was again cooled to 0 °C and di-*tert*-butyldicarbonate (848 mg, 3.89 mmol) was added neat. After 30 min, the ice-bath was removed and the reaction mixture was stirred for a further 3 h at room temperature (reaction progress adjudged by TLC). The reaction was quenched by the dropwise addition of saturated NaHCO₃ solution (5 ml) and extracted three times with EtOAc (3 x 40 ml). The organic phase was washed with brine (25 ml), dried over MgSO₄, filtered, and concentrated under vacuum. The product was purified by flash chromatography (eluting with hexane:EtOAc) and crystallised slowly (1 to 5 days) when dry.

Method G: *General method for the deprotection of N,N'-bis-Boc protected 2-iminoimidazolidines using hydrochloric acid*

The *bis*-Boc protected 2-iminoimidazolidine (0.26 mmol) was dissolved in methylene chloride (0.8 ml) under argon, to which 4 M HCl in dioxane (0.765 ml, 3.06 mmol) were added. The mixture was stirred at 55 °C until the reaction was adjudged complete (typically 3 h, adjudged by TLC and MS analysis). At the reaction endpoint, solvents and HCl were evaporated, followed by either of two chromatographic methods. Method 1 comprised of normal phase silica gel chromatography using a solvent system consisting of methylene chloride and 80:20:3 CHCl₃:MeOH:NH₄OH (CMA), respectively (typical elution gradient: 100% methylene chloride to 1:1 methylene chloride:CMA). The purified fractions were evaporated to dryness, and the residue was dissolved in 1.25 M methanolic HCl (2.5 ml). Evaporation of solvents and HCl gas afforded the product. Method 2 comprised of reverse phase chromatography using C-8 silica, typical elution gradient: 100% H₂O to 85:15 H₂O:acetonitrile, respectively. The purified fractions were evaporated to dryness to afford the product.

7.3 Synthesis and Characterisation

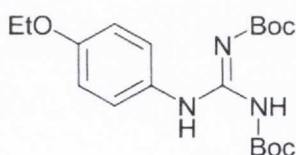
1,3-Di(*tert*-butoxycarbonyl)imidazolidine-2-thione (54)



Following Method F, to a cooled solution of imidazolidine-2-thione (500 mg, 4.92 mmol) in tetrahydrofuran (40 ml) was added NaH as a 60% suspension in mineral oil (882 mg, 22.1 mmol). After 15 min, di-*tert*-butyldicarbonate was added neat (2.35 g, 10.78 mmol). After 16 h, usual work up followed by recrystallisation from hexane afforded the title compound as lustrous yellow needles (1.24 g, 84%). Mp: 115 °C (literature: 117 - 119 °C).¹⁹⁵

¹H NMR (400 MHz, CDCl₃): δ3.90 (s, 4H, CH₂), 1.47 (s, 18H, Boc).

1-[2,3-Di(*tert*-butoxycarbonyl)guanidino]-4-ethoxybenzene (55)



Following Method A, HgCl₂ (1485 mg, 11 mmol) was added over a solution of *N,N'*-bis(*tert*-butoxycarbonyl)-*S*-methylisothiourea **60** (1060 mg, 3.7 mmol), 4-ethoxyaniline (473 μl, 3.7 mmol), and triethylamine (3.03 mL, 21.9 mmol) in methylene chloride (5 ml) at 0 °C. The mixture was stirred for 1 h at 0 °C and a further 14 h at room temperature. Usual work up followed by silica gel chromatography, eluting with hexane:EtOAc, afforded the title compound as a white solid (1016 mg, 76%). Mp: 118 – 120 °C.

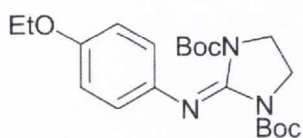
¹H NMR (400 MHz, CDCl₃): δ11.67 (br s, 1H, NH), 10.20 (br s, 1H, NH), 7.47 (d, J = 8.7 Hz, 2H, CH Ar.), 6.87 (d, J = 8.7 Hz, 2H, CH Ar.), 4.03 (q, J = 7.1 Hz, 2H, CH₂CH₃), 1.56 (s, 9H, Boc), 1.51 (s, 9H, Boc), 1.42 (t, J = 7.1 Hz, 3H, CH₂CH₃).

¹³C NMR (100 MHz, CDCl₃): δ163.2 (C=N), 155.7 (C=O), 153.2 (C=O), 152.9 (Cq Ar.), 129.2 (Cq Ar.), 123.4 (CH Ar.), 114.2 (CH Ar.), 83.1 (Cq Boc), 79.0 (Cq Boc), 63.1 (CH₂CH₃), 27.8 (CH₃ Boc), 27.6 (CH₃ Boc), 14.4 (CH₂CH₃).

IR (neat, cm⁻¹): ν_{max} 3280 (NH), 3165 (NH), 2933, 1716, 1630 (C=O), 1605 (C=N), 1573, 1511 (Aryl), 1390, 1345, 1227, 1155, 1117, 1057.

HRMS (m/z ES): Found: 380.2181 ($M^+ + H$, $C_{19}H_{29}N_3O_5Na$ Requires: 380.2185).

1-[1,3-Di(*tert*-butoxycarbonyl)-2-iminoimidazolidinyl]-4-ethoxybenzene (56)



Following Method A, $HgCl_2$ (745 mg, 2.7 mmol) was added over a solution of **54** (646 mg, 1.83 mmol), 4-ethoxyaniline (237 μ l, 1.83 mmol) and triethylamine (885 μ L, 6.4 mmol) in methylene chloride (3 ml) at 0 °C. The resulting mixture was stirred for 1 h at 0° C and a further 18 h at room temperature. Usual work up followed by neutral alumina chromatography, eluting with hexane:EtOAc, afforded the title compound as a white solid (271 mg, 37%). Mp: 123 – 125 °C.

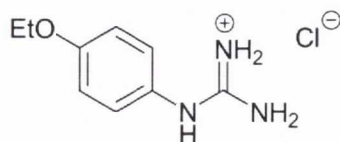
1H NMR (400 MHz, $CDCl_3$): δ 6.98 (d, $J = 8.1$ Hz, 2H, CH Ar.), 6.80 (d, $J = 8.1$ Hz, 2H, CH Ar.), 4.00 (q, $J = 7.0$ Hz, 2H, \underline{CH}_2CH_3), 3.84 (s, 4H, CH_2CH_2), 1.40 (t, $J = 7.0$ Hz, 3H, CH_2CH_3), 1.36 (s, 18H, Boc).

^{13}C NMR (100 MHz, $CDCl_3$): δ 154.3 (C=N), 149.1 (C=O), 141.1 (Cq Ar.), 138.2 (Cq Ar.), 122.1 (CH Ar.), 114.3 (CH Ar.), 82.1 (Cq Boc), 63.3 (\underline{CH}_2CH_3), 42.7 (CH_2CH_2), 27.4 (CH_3 Boc), 14.4 ($CH_2\underline{CH}_3$).

IR (neat, cm^{-1}): ν_{max} 2981, 2918, 1754, 1723, 1690 (C=O), 1572 (C=N), 1505, 1476 (Aryl), 1367, 1292, 1232, 1175, 1114, 976.

HRMS (m/z ES): Found: 406.2342 ($M^+ + H$, $C_{21}H_{32}N_3O_5$ Requires: 406.2337).

N-(4-Ethoxyphenyl)guanidine hydrochloride (51)



Following Method D, **55** (235mg, 0.62 mmol) was treated with a solution of 50% trifluoroacetic acid in methylene chloride (5 ml). After 3 h, solvents were evaporated and the residue was dissolved in H_2O (6 ml) to which was added

1000 mg Amberlite resin in its Cl⁻ form. After 16 hours the Amberlite was removed by filtration; usual workup afforded the title compound without further purification as hygroscopic, off-white solid (120 mg, 90%). Mp: 138 - 140 °C.

¹H NMR (400 MHz, D₂O): δ 7.16 (d, J = 7.5 Hz, 2H, CH Ar.), 6.94 (d, J = 7.5 Hz, 2H, CH Ar.), 4.02 (q, J = 6.5 Hz, 2H, CH₂CH₃), 1.27 (t, J = 6.5 Hz, 3H, CH₂CH₃).

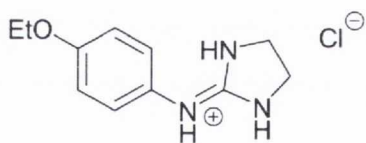
¹³C NMR (100 MHz, D₂O): δ 157.7 (C=N), 156.7 (Cq Ar.), 128.1 (Cq Ar.), 126.9 (CH Ar.), 115.8 (CH Ar.), 64.6 (CH₂CH₃), 13.9 (CH₂CH₃).

IR (neat, cm⁻¹): ν_{max} 3126 (NH), 2978 (CH), 1663 (C=N), 1619, 1582 (C=N), 1510 (Aryl), 1238, 1114 (C-O), 1041.

HRMS (*m/z* ES): Found: 180.1131 (M⁺ + H. C₉H₁₄N₃O Requires: 180.1137).

Purity by HPLC: 97.8% (*t*_R 21.96 min).

N-(4-Ethoxyphenyl)-2-iminoimidazolidine hydrochloride (52)



Following Method D, **56** (200 mg, 0.49 mmol) was treated with a solution of 50% trifluoroacetic acid in methylene chloride (5 ml). After 3 h, solvents were evaporated and the residue was dissolved in H₂O (6 ml) to which was added

1000 mg Amberlite resin in its Cl⁻ form. After 16 hours the Amberlite was removed by filtration; usual workup afforded the title compound without further purification as a hygroscopic, off-white solid (110 mg, 92%). Mp: 142 - 144 °C.

¹H NMR (400 MHz, D₂O): δ 7.10 (d, J = 8.7 Hz, 2H, CH Ar.), 6.89 (d, J = 8.7 Hz, 2H, CH Ar.), 3.99 (q, J = 7.0 Hz, 2H, CH₂CH₃), 3.60 (s, 4H, CH₂CH₂), 1.26 (t, J = 7.0 Hz, 3H, CH₂CH₃).

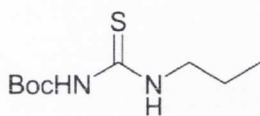
¹³C NMR (100 MHz, D₂O): δ 159.1 (C=N), 157.3 (Cq Ar.), 127.9 (Cq Ar.), 126.6 (CH Ar.), 115.6 (CH Ar.), 64.5 (CH₂CH₃), 42.7 (CH₂CH₂), 13.8 (CH₂CH₃).

IR (neat, cm^{-1}): ν_{max} 3134 (NH), 2975 (CH), 2878, 1646, 1621 (C=N), 1512 (Aryl), 1488, 1394, 1293, 1238, 1174, 1116 (C-O), 1083, 1045.

HRMS (m/z ES): Found: 206.1294 ($M^+ + H$, $\text{C}_{11}\text{H}_{16}\text{N}_3\text{O}$ Requires: 206.1293).

Purity by HPLC: 98.7% (t_R 23.09 min).

N-Tert-butoxycarbonyl-N'-propylthiourea (63a)



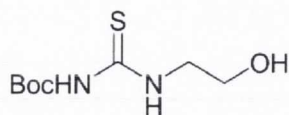
Following Method C, a solution of thiourea (500 mg, 6.58 mmol) in tetrahydrofuran (120 ml) was treated with NaH (1184 mg, 29.60 mmol), followed by di-*tert*-butyl dicarbonate (3155 mg, 14.47 mmol). After 8 h, a second portion of NaH (442 mg, 11.05 mmol) was added followed 1 h later by the addition of trifluoroacetic anhydride (1.41 ml, 10.13 mmol). 45 min later this was followed by the addition of 1-propylamine (830 μl , 10.13 mmol). After 18 h, workup and purification afforded the product as a low-melting, white, crystalline solid (1019 mg, 71%). Mp: 58 - 60 $^{\circ}\text{C}$.

^1H NMR (400 MHz, CDCl_3): δ 9.74 (br s, 1H, NH), 7.97 (br s, 1H, NH), 3.63 (m, 2H, $\text{CH}_2\text{CH}_2\text{CH}_3$), 1.71 (app q, $J = 7.3$ Hz, 2H, $\text{CH}_2\text{CH}_2\text{CH}_3$), 1.52 (s, 9H, Boc), 1.01 (t, $J = 7.3$ Hz, 3H, $\text{CH}_2\text{CH}_2\text{CH}_3$).

^{13}C NMR (100 MHz, DMSO): δ 179.4 (C=S), 151.8 (C=O), 83.4 (Cq Boc), 47.1 ($\text{CH}_2\text{CH}_2\text{CH}_3$), 27.8 (CH_3 Boc), 21.5 ($\text{CH}_2\text{CH}_2\text{CH}_3$), 11.3 ($\text{CH}_2\text{CH}_2\text{CH}_3$).

IR (neat, cm^{-1}): ν_{max} 3245, 3175 (NH), 2961, 2934, 2875, 1720 (C=O), 1523 (C=N), 1243, 1206, 1142 (C=S), 1073, 1008.

HRMS (m/z ES): Found: 219.1167 ($M^+ + H$, $\text{C}_9\text{H}_{19}\text{N}_2\text{O}_2\text{S}$ Requires: 219.1167).

N-Tert-butoxycarbonyl-N'-(2-hydroxyethyl)thiourea (63b)

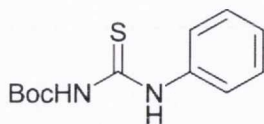
Following Method C, a solution of thiourea (1750 mg, 23.03 mmol) in tetrahydrofuran (450 ml) was treated with NaH (4.60 g, 115.1 mmol), followed by di-*tert*-butyl dicarbonate (10.79 g, 49.51 mmol). After 8 h, a second portion of NaH (1289 mg, 32.24 mmol) was added followed 1 h later by the addition of trifluoroacetic anhydride (3.52 ml, 25.33 mmol). 45 min later this was followed by the addition of 2-aminoethanol (1.53 ml, 25.33 mmol). After 18 h, workup and purification followed by recrystallisation from hexane afforded the product as a white powder (2.16 g, 43%). Mp: 100 - 102 °C.

¹H NMR (400 MHz, CDCl₃): δ10.02 (br s, 1H, NH), 8.28 (br s, 1H, NH), 3.88 (m, 4H, 2CH₂), 2.47 (br s, 1H, OH), 1.49 (s, 9H, Boc).

¹³C NMR (100 MHz, CDCl₃): δ179.9 (C=S), 151.4 (C=O), 83.3 (Cq Boc), 60.4 (CH₂OH), 47.0 (NHCH₂), 27.5 (CH₃ Boc).

IR (neat, cm⁻¹): ν_{max} 3217 (NH), 2981, 2937, 2881, 1709 (C=O), 1559, 1526 (C=N), 1449, 1388, 1373, 1364, 1327, 1251, 1148 (C=S), 1045, 1004.

HRMS (*m/z* ES): Found: 243.0781 (M⁺ + Na. C₈H₁₆N₂O₃SNa Requires: 243.0779).

N-Tert-butoxycarbonyl-N'-phenylthiourea (63c)

Following Method C, a solution of thiourea (1750 mg, 23.03 mmol) in tetrahydrofuran (450 ml) was treated with NaH (4.14 g, 103.6 mmol), followed by di-*tert*-butyl dicarbonate (11.04 g, 50.66 mmol). After 12 h, a second portion of NaH (1105 mg, 27.63 mmol) was added followed 1 h later by the addition of trifluoroacetic anhydride (3.52 ml, 25.33 mmol). 45 min later this was followed by the addition of aniline (2.31 ml, 25.33 mmol). After 4 h, workup and purification followed by recrystallisation from boiling hexane afforded the product as white needles (2650 mg, 46%). Mp: 106 °C.

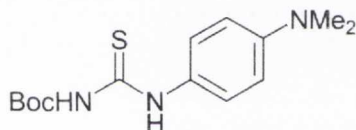
¹H NMR (400 MHz, CDCl₃): δ11.55 (br s, 1H, NH), 8.24 (br s, 1H, NH), 7.66 (d, J = 7.7 Hz, 2H, CH Ar.), 7.42 (t, J = 7.7 Hz, 2H, CH Ar.), 7.28 (t, J = 7.7 Hz, 1H CH Ar.), 1.55 (s, 9H, Boc).

¹³C NMR (100 MHz, CDCl₃): δ177.9 (C=S), 151.5 (C=O), 137.3 (Cq Ar.), 128.4 (CH Ar.), 126.25 (CH Ar.), 123.9 (CH Ar.), 83.8 (Cq Boc), 27.59 (CH₃ Boc).

IR (neat, cm⁻¹): ν_{max} 3172 (NH), 3006, 2984, 1709 (C=O), 1591, 1528 (C=N), 1477, 1451, 1391, 1366, 1321, 1252, 1196, 1143, 1075, 1048, 1016, 1004.

HRMS (*m/z* ES): Found: 275.0828 (M⁺ + Na. C₁₂H₁₆N₂O₂SNa Requires: 275.0830).

N-Tert-butoxycarbonyl-N'-(4-dimethylaminophenyl)thiourea (63d)



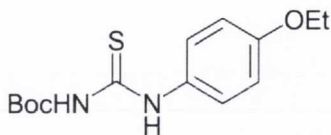
Following Method C, a solution of thiourea (1000 mg, 13.16 mmol) in tetrahydrofuran (260 ml) was treated with NaH (2.37 g, 59.2 mmol), followed by di-*tert*-butyl dicarbonate (6.31 g, 28.95 mmol). After 5 h, a second portion of NaH (632 mg, 15.79 mmol) was added followed 1 h later by the addition of trifluoroacetic anhydride (2.01 ml, 14.47 mmol). 45 min later this was followed by the addition of 4-(dimethylamino)aniline (1.97 ml, 14.47 mmol). After 18 h, workup and purification followed by recrystallisation from hexane afforded the product as pale yellow crystals (1.10 g, 28%). Mp: 136 - 138 °C.

¹H NMR (400 MHz, CDCl₃): δ11.25 (br s, 1H, NH), 8.01 (br s, 1H, NH), 7.41 (d, J = 8.6 Hz, 2H, CH Ar.), 6.73 (d, J = 8.6 Hz, 2H, CH Ar.), 2.98 (s, 6H, N(CH₃)₂), 1.55 (s, 9H, Boc).

¹³C NMR (100 MHz, CDCl₃): δ177.9 (C=S), 151.4 (C=O), 148.8 (Cq Ar.), 126.4 (Cq Ar.), 125.3 (CH Ar.), 111.7 (CH Ar.), 83.5 (Cq Boc), 40.1 (N(CH₃)₂), 27.6 (CH₃ Boc).

IR (neat, cm⁻¹): ν_{max} 3174 (NH), 2985 (CH), 1702, 1612, (C=O), 1578 (C=N), 1520 (Aryl), 1444, 1252, 1143 (C-O), 1143, 1014.

HRMS (*m/z* ES): Found: 296.1422 (M⁺ + H. C₁₄H₂₂N₃O₂S Requires: 296.1433).

N-Tert-butoxycarbonyl-N'-(4-ethoxyphenyl)thiourea (63e)

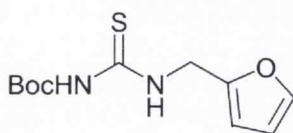
Following Method C, a solution of thiourea (875 mg, 17.27 mmol) in tetrahydrofuran (225 ml) was treated with NaH (3.11 g, 77.7 mmol), followed by di-*tert*-butyl dicarbonate (7.91 g, 36.27 mmol). After 20 h, a second portion of NaH (553 mg, 13.82 mmol) was added followed 1 h later by the addition of trifluoroacetic anhydride (1.84 ml, 13.24 mmol). 45 min later this was followed by the addition of 4-ethoxyaniline (1.64 ml, 12.66 mmol). After 18 h, workup and purification followed by recrystallisation from hexane afforded the product as a white powder (1.66 g, 49%). Mp: 142 - 144 °C.

¹H NMR (400 MHz, CDCl₃): δ 11.34 (br s, 1H, NH), 8.14 (br s, 1H, NH), 7.48 (d, J = 9.7 Hz, 2H, CH Ar.), 6.91 (d, J = 9.7 Hz, 2H, CH Ar.), 4.04 (q, J = 6.9 Hz, 2H, CH₂CH₃), 1.54 (s, 9H, Boc), 1.43 (t, J = 6.9 Hz, 3H, CH₂CH₃).

¹³C NMR (100 MHz, CDCl₃): δ 178.2 (C=S), 157.1 (C=O), 151.5 (Cq Ar.), 130.0 (Cq Ar.), 125.6 (CH Ar.), 114.0 (CH Ar.), 83.6 (Cq Boc), 63.2 (CH₂CH₃), 27.6 (CH₃ Boc), 14.4 (CH₂CH₃).

IR (neat, cm⁻¹): ν_{max} 3187 (NH), 2985 (CH), 2932 (Aryl), 1720, 1618 (C=O), 1509, 1372, 1250, 1232, 1180 (C-O), 1136 (C=S), 1045 (C-O).

HRMS (*m/z* ES): Found: 197.1272 (M⁺ + H. C₁₄H₂₁N₂O₃S Requires: 197.1273).

N-Tert-butoxycarbonyl-N'-(furan-2-ylmethyl)thiourea (63f)

Following Method B, a solution of *N,N'*-bis-(*tert*-butoxycarbonyl)thiourea (1000 mg, 3.64 mmol) in dry tetrahydrofuran (40 ml) was treated with NaH (194 mg, 4.36 mmol) and trifluoroacetic anhydride (614 μl, 4.40 mmol), to which was added 2-furfurylamine (370 μl, 4.00 mmol). After 18 h, workup and purification afforded the product as a white, crystalline solid (572 mg, 58%). Mp: 100 °C.

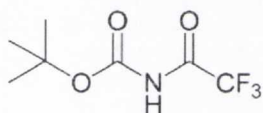
¹H NMR (400 MHz, DMSO): δ10.82 (br s, 1H, NH), 10.13 (t, J = 5.4 Hz, 1H, NH), 7.63 (dd, J = 2.9, 0.8 Hz, 1H, CH-O Fur.), 6.43 (t, J = 2.9 Hz, 1H, CH Fur.), 6.37 (dd, J = 2.9, 0.8 Hz, 1H, CH Fur.), 4.79 (d, J = 5.4 Hz, 2H, CH₂), 1.44 (s, 9H, Boc).

¹³C NMR (100 MHz, DMSO): δ180.4 (C=S), 153.1 (Cq Fur.), 150.7 (C=O), 143.1 (CH-O Fur.), 111.0 (CH Fur.), 108.6 (CH Fur.), 82.7 (Cq Boc), 41.6 (CH₂), 28.1, (CH₃ Boc).

IR (neat, cm⁻¹): ν_{max} 3279, 3251, 3174 (NH), 2983 (Aryl), 1711 (C=O), 1642, 1535 (C=N), 1443 (Aryl), 1368, 1321, 1252, 1132 (C=S), 1011.

HRMS (*m/z* ES): Found: 279.0793 (M⁺ + Na. C₁₁H₁₆N₂O₃SNa Requires: 279.0779).

***Tert*-butyl (2,2,2-trifluoroacetyl)carbamate (63)**



Isolated by column chromatography during the purification of **63f**.

The off-white solid was further purified by recrystallisation from 10:1 hexane:EtOAc to afford a white solid, which decomposed

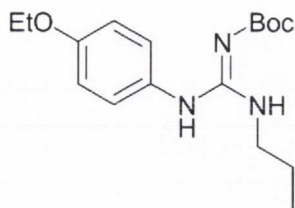
within a week after isolation (66 mg, 8%). Mp: 118 - 120 °C (literature: 114 °C).²⁵⁸

¹H NMR (400 MHz, CDCl₃): δ7.90 (br s, 1H, NH), 1.57 (s, 9H, Boc).

¹³C NMR (100 MHz, CDCl₃): δ154.0 (q, J = 40 Hz, C=O CF₃), 147.3 (s, C=O Boc), 113.5 (q, J = 288 Hz, CF₃), 84.6 (s, Cq Boc), 27.3 (s, CH₃ Boc).

IR (neat, cm⁻¹): ν_{max} 3276 (NH), 3210, 3049, 2985, 1776, 1719, 1530, 1374, 1340, 1251, 212, 1163, 1110, 943, 837.

HRMS (*m/z* ES): Found: 236.0507 (M⁺ + Na. C₇H₁₀F₃NO₃Na Requires: 236.0510).

1-[1-(*Tert*-butoxycarbonyl)-3-propylguanidino]-4-ethoxybenzene (**65a**)

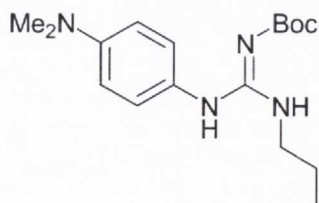
Following Method A, HgCl_2 (486 mg, 1.79 mmol) was added over a solution of **63a** (300 mg, 1.38 mmol), 4-ethoxyaniline (191 μl , 1.51 mmol) and triethylamine (838 μl , 6.06 mmol) in dry dimethylformamide (1.1 ml) at 0 °C. The reaction was stirred for 1 h at 0° C and a further 16 h at room temperature. Usual work up followed by silica gel chromatography, eluting with hexane:EtOAc, afforded the title compound as an amber-coloured oil (401 mg, 91%).

$^1\text{H NMR}$ (400 MHz, CDCl_3): δ 10.47 (br s, 1H, NH), 7.07 (d, $J = 5.8$ Hz, 2H, CH Ar.), 6.85 (d, $J = 5.8$ Hz, 2H, CH Ar.), 4.48 (br s, 1H, NH), 3.96 (q, $J = 6.9$ Hz, 2H, CH_2CH_3), 3.26 (m, 2H, $\text{CH}_2\text{CH}_2\text{CH}_3$), 1.48 (s, 9H, Boc), 1.42 (m, 2H, $\text{CH}_2\text{CH}_2\text{CH}_3$), 1.37 (t, $J = 6.9$ Hz, 3H, CH_2CH_3), 0.81 (m, 3H, $\text{CH}_2\text{CH}_2\text{CH}_3$).

$^{13}\text{C NMR}$ (100 MHz, CDCl_3): δ 164.4 (C=N), 159.3 (C=O), 157.8 (Cq Ar.), 128.4 (Cq Ar.), 127.8 (CH Ar.), 115.5 (CH Ar.), 78.3 (Cq Boc), 63.6 (CH_2CH_3), 42.7 ($\text{CH}_2\text{CH}_2\text{CH}_3$), 28.6 (CH₃ Boc), 22.7 ($\text{CH}_2\text{CH}_2\text{CH}_3$), 14.7 (CH_2CH_3), 11.2 ($\text{CH}_2\text{CH}_2\text{CH}_3$).

IR (neat, cm^{-1}): ν_{max} 3144 (NH), 2974 (CH), 2931 (Aryl), 2876, 1736, 1627 (C=O), 1592 (C=N), 1509 (Aryl), 1478, 1335, 1234, 1168 (C-O), 1129, 1115 (C-O), 1047.

HRMS (m/z ES): Found: 322.2132 ($\text{M}^+ + \text{H}$, $\text{C}_{17}\text{H}_{28}\text{N}_3\text{O}_3$ Requires: 322.2131).

1-[1-(*Tert*-butoxycarbonyl)-3-propylguanidino]-4-(dimethylamino)benzene (**65b**)

Following Method A, HgCl_2 (248 mg, 0.92 mmol) was added over a solution of **63d** (225 mg, 0.76 mmol), 1-propylamine (63 μl , 0.76 mmol) and triethylamine (372 μl , 2.67 mmol) in methylene chloride (1.5 ml) at 0 °C. The resulting mixture was stirred for 1 h at 0° C and a further 14 h at room

temperature. Usual work up followed by silica gel chromatography, eluting with hexane:EtOAc, afforded the title compound as a white solid (200 mg, 82%). Mp: 122 - 124 °C.

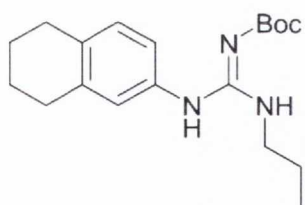
¹H NMR (400 MHz, CDCl₃): δ10.39 (br s, 1H, NH), 7.08 (d, J = 8.5 Hz, 2H, CH Ar.), 6.72 (d, J = 8.5 Hz, 2H, CH Ar.), 4.50 (br s, 1H, NH), 3.32 (m, 2H, CH₂CH₂CH₃), 2.99 (s, 6H, N(CH₃)₂), 1.56 (s, 9H, Boc), 1.45 (m, 2H, CH₂CH₂CH₃), 0.86 (m, 3H, CH₂CH₂CH₃).

¹³C NMR (100 MHz, CDCl₃): δ163.9 (C=N), 159.3 (C=O), 149.0 (Cq Ar.), 127.2 (CH Ar.), 123.7 (Cq Ar.), 112.6 (CH Ar.), 77.6 (Cq Boc), 42.2 (CH₂CH₂CH₃), 40.0 (N(CH₃)₂), 28.0 (CH₃ Boc), 22.3 (CH₂CH₂CH₃), 10.7 (CH₂CH₂CH₃).

IR (neat, cm⁻¹): ν_{max} 3427, 3211 (NH), 2964 (CH), 2930 (Aryl), 1720, 1625 (C=O), 1590 (C=N), 1519 (Aryl), 1478, 1336, 1239, 1168 (C-O), 1128, 1054.

HRMS (*m/z* ES): Found: 321.2297 (M⁺ + H. C₁₇H₂₉N₄O₂ Requires: 321.2291).

2-[1-(*Tert*-butoxycarbonyl)-3-propylguanidino]-5,6,7,8-tetrahydronaphthalene (65c)



Following Method A, HgCl₂ (299 mg, 1.10 mmol) was added over a solution of **63a** (200 mg, 0.92 mmol), 2-amino-5,6,7,8-tetrahydronaphthalene (135 mg, 0.92 mmol) and triethylamine (397 μl, 2.85 mmol) in methylene chloride (1.5 ml) at 0 °C. The reaction was stirred for 1 h at 0° C and a further 16 h at room temperature. Usual work up followed by silica gel chromatography, eluting with hexane:EtOAc, afforded the title compound as a clear gum (236 mg, 78%).

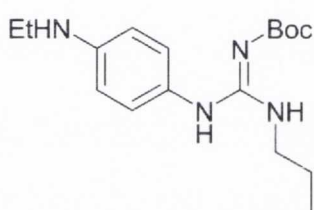
¹H NMR (400 MHz, CDCl₃): δ10.59 (br s, 1H, NH), 7.07 (d, J = 7.6 Hz, 1H, CH Ar.), 6.90 (d, J = 7.6 Hz, 1H, CH Ar.), 6.89 (s, 1H, CH Ar.), 4.69 (br s, 1H, NH), 3.31 (q, J = 6.0 Hz, 2H, CH₂CH₂CH₃), 2.73 (m, 4H, 2CH₂), 1.79 (m, 4H, 2CH₂), 1.53 (s, 9H, Boc), 1.48 (m, 2H, CH₂CH₂CH₃), 0.86 (t, J = 7.0 Hz, 3H, CH₂CH₂CH₃).

^{13}C NMR (100 MHz, CDCl_3): δ 163.9 (C=N), 158.4 (C=O), 138.5 (Cq Ar.), 135.4 (Cq Ar.), 133.0 (Cq Ar.), 130.0 (CH Ar.), 125.8 (CH Ar.), 122.4 (CH Ar.), 77.9 (Cq Boc), 42.3 ($\text{CH}_2\text{CH}_2\text{CH}_3$), 28.9 (Cq CH_2CH_2), 28.5 (Cq CH_2CH_2), 28.0 (CH_3 Boc), 22.5 (Cq CH_2CH_2), 22.4 ($\text{CH}_2\text{CH}_2\text{CH}_3$), 22.3 (Cq CH_2CH_2), 10.8 ($\text{CH}_2\text{CH}_2\text{CH}_3$).

IR (neat, cm^{-1}): ν_{max} 2963 (CH), 2929, 1724, 1591 (C=N), 1555, 1502 1455, 1336, 1246, 1153 (C-O), 1130, 1055.

HRMS (m/z ES): Found: 332.2340 ($\text{M}^+ + \text{H}$. $\text{C}_{19}\text{H}_{30}\text{N}_3\text{O}_2$ Requires: 332.2338).

1-[1-(*Tert*-butoxycarbonyl)-3-propylguanidino]-4-ethylaminobenzene (**65d**)



Following Method A, HgCl_2 (335 mg, 1.24 mmol) was added over a solution of **63a** (224 mg, 1.03 mmol), **105** (133 μl , 1.03 mmol) and triethylamine (445 μl , 3.19 mmol) in methylene chloride (1.5 ml) at 0 °C. The resulting mixture was stirred for 1 h at 0° C and a further 14 h at room temperature. Usual work up followed by silica gel chromatography, eluting with hexane:EtOAc, afforded the title compound as dark yellow solid (140 mg, 38%). Mp: 106 - 108 °C.

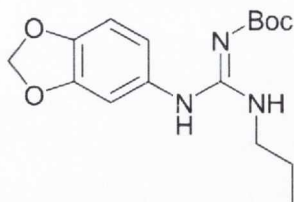
^1H NMR (400 MHz, CDCl_3): δ 10.35 (br s, 1H, NH), 6.97 (d, $J = 8.0$ Hz, 2H, CH Ar.), 6.57 (d, $J = 8.0$ Hz, 2H, CH Ar.), 4.47 (br s, 1H, NH), 3.78 (br s, 1H, NH), 3.27 (m, 2H, $\text{CH}_2\text{CH}_2\text{CH}_3$), 3.12 (q, $J = 7.0$ Hz, 2H, CH_2CH_3), 1.51 (s, 9H, Boc), 1.41 (m, 2H, $\text{CH}_2\text{CH}_2\text{CH}_3$), 1.27 (t, $J = 7.0$ Hz, 3H, CH_2CH_3), 0.81 (t, $J = 7.0$ Hz, 3H, $\text{CH}_2\text{CH}_2\text{CH}_3$).

^{13}C NMR (100 MHz, CDCl_3): δ 163.9 (C=N), 159.3 (C=O), 147.2 (Cq Ar.), 127.6 (CH Ar.), 124.3 (Cq Ar.), 112.8 (CH Ar.), 77.7 (Cq Boc), 42.2 ($\text{CH}_2\text{CH}_2\text{CH}_3$), 37.9 (CH_2CH_3), 28.0 (CH_3 Boc), 22.3 ($\text{CH}_2\text{CH}_2\text{CH}_3$), 14.3 (CH_2CH_3), 10.7 ($\text{CH}_2\text{CH}_2\text{CH}_3$).

IR (neat, cm^{-1}): ν_{max} 3403 (NH), 3435 (NH), 3328 (NH), 2971 (CH), 2931 (Aryl), 2873, 1628 (C=O), 1592 (C=N), 1522 (Aryl), 1362, 1328, 1262, 1171 (C-O), 1154, 1131, 1055.

HRMS (*m/z* ES): Found: 321.2298 ($M^+ + H$, $C_{17}H_{29}N_4O_2$ Requires: 321.2291).

1-[1-(*Tert*-butoxycarbonyl)-3-propylguanidino]-3,4-methylenedioxybenzene (65e)



Following Method A, $HgCl_2$ (356 mg, 1.31 mmol) was added over a solution of **63a** (239 mg, 1.09 mmol), 3,4-methylenedioxyaniline (150 mg, 1.09 mmol) and triethylamine (473 μ l, 3.39 mmol) in methylene chloride (1.5 ml) at 0 °C.

The resulting mixture was stirred for 1 h at 0° C and a further 14 h at room temperature. Usual work up followed by silica gel chromatography, eluting with hexane:EtOAc, afforded the title compound as a pale yellow solid (262 mg, 75%). Mp: 104 - 106 °C.

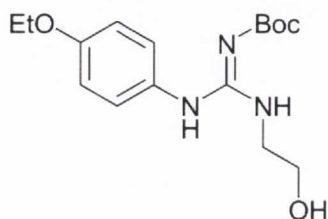
1H NMR (400 MHz, $CDCl_3$): δ 10.49 (br s, 1H, NH), 6.77 - 6.26 (m, 3H, 3CH Ar.), 5.97 (s, 2H, OCH₂O), 4.56 (br s, 1H, NH), 3.27 (q, $J = 5.5$ Hz, 2H, CH₂CH₂CH₃), 1.53 (m, 2H, CH₂CH₂CH₃), 1.49 (s, 9H, Boc), 0.81 (m, 3H, CH₂CH₂CH₃).

^{13}C NMR (100 MHz, $CDCl_3$): δ 163.9 (C=N), 158.7 (C=O), 148.1 (Cq-O Ar.), 146.1 (Cq-O Ar.), 129.4 (Cq Ar.), 119.3 (CH Ar.), 108.3 (CH Ar.), 107.2 (CH Ar.), 101.3 (OCH₂O), 77.9 (Cq Boc), 42.3 (CH₂CH₂CH₃), 28.0 (CH₃ Boc), 22.2 (CH₂CH₂CH₃), 10.8 (CH₂CH₂CH₃).

IR (neat, cm^{-1}): ν_{max} 3372 (NH), 2967 (CH), 2932, 2978, 1725, 1590 (C=N), 1554, 1450 (Aryl), 1330, 1239, 1170 (C-O), 1135 (C-O), 1056, 1034.

HRMS (*m/z* ES): Found: 322.1771 ($M^+ + H$, $C_{16}H_{24}N_3O_4$ Requires: 322.1767).

1-[1-(*Tert*-butoxycarbonyl)-3-(2-hydroxyethyl)guanidino]-4-ethoxybenzene (66a)



Following Method A, $HgCl_2$ (596 mg, 2.20 mmol) was added over a solution of **63e** (500 mg, 1.69 mmol), 2-aminoethanol (92 μ l, 1.69 mmol) and triethylamine (730 μ l, 5.24 mmol) in methylene chloride (3.5 ml) at 0 °C. The reaction was stirred for

1 h at 0° C, then 16 h at rt. Usual work up followed by silica gel chromatography, eluting with hexane:EtOAc, afforded the product as an off-white solid (262 mg, 49%). Mp: 155 °C.

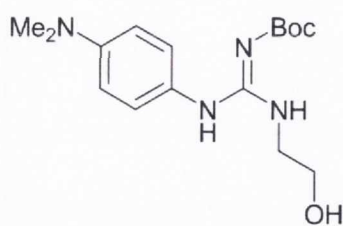
¹H NMR (400 MHz, CDCl₃): δ10.53 (br s, 1H, NH), 7.14 (d, J = 8.2 Hz, 2H, CH Ar.), 6.91 (d, J = 8.2 Hz, 2H, CH Ar.), 5.61 (br s, 1H, OH), 5.01 (br s, 1H, NH), 4.03 (q, J = 7.0 Hz, 2H, CH₂CH₃), 3.71 (br s, 2H, CH₂OH), 3.48 (br s, 2H, NHCH₂), 1.51 (s, 9H, Boc), 1.44 (t, J = 7.0 Hz, 3H, CH₂CH₃).

¹³C NMR (100 MHz, CDCl₃): δ163.3 (C=N), 160.2 (C=O), 158.0 (Cq Ar.), 127.8 (CH Ar.), 127.6 (Cq Ar.), 115.5 (CH Ar.), 78.6 (Cq Boc), 63.6 (CH₂CH₃), 60.2 (CH₂OH), 44.6 (NHCH₂), 28.2 (CH₃ Boc), 14.6 (CH₂CH₃).

IR (neat, cm⁻¹): ν_{max} 3304 (OH), 2974 (CH), 2936 (Aryl CH), 2874, 1637 (C=O), 1587 (Aryl), 1511, 1391, 1303, 1246, 1225, 1163 (C-O), 1140 (C-O), 1098, 1067, 1046.

HRMS (*m/z* ES): Found: 324.1917 (M⁺ + H. C₁₆H₂₆N₃O₄ Requires: 324.1923).

1-[1-(*Tert*-butoxycarbonyl)-3-(2-hydroxyethyl)guanidino]-4-(dimethylamino)benzene (66b)



Following Method A, HgCl₂ (248 mg, 0.92 mmol) was added over a solution of **63d** (225 mg, 0.76 mmol), 2-aminoethanol (46 μl, 0.76 mmol) and triethylamine (372 μl, 2.67 mmol) in methylene chloride (1.5 ml) at 0 °C. The resulting mixture was stirred for 1 h at 0° C and a further 14 h at room temperature.

Usual work up followed by silica gel chromatography, eluting with hexane:EtOAc, afforded the title compound as a white solid (166 mg, 67%). Mp: 150 °C.

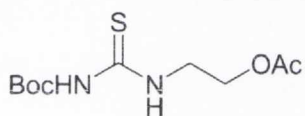
¹H NMR (400 MHz, CDCl₃): δ10.36 (br s, 1H, NH), 7.05 (d, J = 7.5 Hz, 2H, CH Ar.), 6.69 (d, J = 7.5 Hz, 2H, CH Ar.), 5.81 (br s, 1H, OH), 5.05 (br s, 1H, NH), 3.65 (t, J = 3.5 Hz, 2H, CH₂OH), 3.41 (t, 2H, J = 3.5 Hz, NHCH₂), 2.96 (s, 6H, N(CH₃)₂), 1.49 (s, 9H, Boc).

^{13}C NMR (100 MHz, CDCl_3): δ 163.0 (C=N), 160.1 (C=O), 149.2 (Cq Ar.), 127.3 (CH Ar.), 123.3 (Cq Ar.), 112.7 (CH Ar.), 78.1 (Cq Boc), 63.4 (CH_2OH), 44.2 (NHCH_2), 40.1 ($\text{N}(\text{CH}_3)_2$), 27.9 (CH_3 Boc).

IR (neat, cm^{-1}): ν_{max} 3327, 2967 (CH), 2863, 1637 (C=O), 1586 (Aryl), 1521, 1344, 1241, 1163 (C-O), 1140, 1094, 1065, 1048, 1031.

HRMS (m/z ES): Found: 323.2074 ($\text{M}^+ + \text{H}$, $\text{C}_{16}\text{N}_{27}\text{N}_4\text{O}_3$ Requires: 323.2083).

2-(3-(*Tert*-butoxycarbonyl)thioureido)ethyl acetate (**64**)



Over a stirred solution of **63b** (600 mg, 2.73 mmol) in methylene chloride (3 ml) at 0 °C were added pyridine (658 μl , 8.18 mmol), acetic anhydride (386 μl , 4.09 mmol) and 4-(dimethylamino)pyridine (17 mg, 0.14 mmol), sequentially. The mixture was stirred at rt for 3 h. Saturated sodium bicarbonate solution (15 ml) was added to quench the reaction (effervescence observed) and the mixture was stirred vigorously for 30 min. The reaction was extracted using two volumes of Et_2O (2 x 15 ml) and the combined organic layer was washed with H_2O (15 ml), then 0.5 M HCl (15 ml), and finally brine (15 ml). The organic layer was made basic with a few drops of triethylamine, dried over MgSO_4 , and filtered. Evaporation of solvents under reduced pressure yielded the product as a white crystalline solid (650 mg, 91%). Mp: 96 °C.

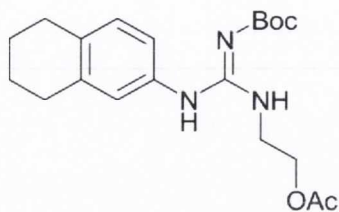
^1H NMR (400 MHz, CDCl_3): δ 9.93 (br s, 1H, NH), 7.94 (br s, 1H, NH), 4.32 (t, $J = 5.5$ Hz, 2H, OCH_2), 3.97 (q, 2H, $J = 5.5$ Hz, NHCH_2), 2.15 (s, 3H, Ac), 1.52 (s, 9H, Boc).

^{13}C NMR (100 MHz, CDCl_3): δ 179.8 (C=S), 170.4 (C=O Ac), 151.3 (C=O Boc), 83.5 (Cq Boc), 61.6 (CH_2O), 43.9 (NHCH_2), 27.5 (CH_3 Boc), 20.4 (CH_3 Ac).

IR (neat, cm^{-1}): ν_{max} 3259 (NH), 3179 (NH), 2988 (CH), 2957, 1738, 1718, 1558, 1526, 1391, 1365, 1329, 1240, 1195, 1133 (C-O), 1050, 1039.

HRMS (m/z ES): Found: 285.0876 ($\text{M}^+ + \text{Na}$, $\text{C}_{10}\text{H}_{18}\text{N}_2\text{O}_4\text{SNa}$ Requires: 285.0885).

2-[1-(*Tert*-butoxycarbonyl)-3-(5,6,7,8-tetrahydronaphthalen-2-yl)guanidino]ethyl acetate (66c)



Following Method A, HgCl₂ (310 mg, 1.15 mmol) was added over a solution of **64** (250 mg, 0.95 mmol), 2-amino-5,6,7,8-tetrahydronaphthalene (140 mg, 0.95 mmol) and triethylamine (412 μl, 2.96 mmol) in methylene chloride (2.0 ml) at 0 °C. The reaction was stirred for 1 h at 0° C and a further 16 h at room temperature. Usual work up followed by silica gel chromatography, eluting with hexane:EtOAc, afforded the title compound as a viscous yellow oil (268 mg, 75%).

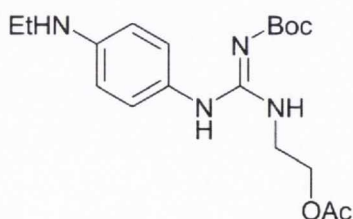
¹H NMR (400 MHz, CDCl₃): δ10.66 (br s, 1H, NH), 7.09 (d, J = 7.5 Hz, 1H, CH Ar.), 6.93 (d, J = 7.5 Hz, 1H, CH Ar.), 6.92 (s, 1H, CH Ar.), 5.05 (br s, 1H, NH), 4.16 (t, J = 5.0 Hz, 2H, CH₂O), 3.66 (q, 2H, J = 5.0 Hz, NHCH₂), 2.76 (m, 4H, 2CH₂), 2.02 (s, 3H, Ac), 1.81 (m, 4H, 2CH₂), 1.55 (s, 9H, Boc).

¹³C NMR (100 MHz, CDCl₃): δ170.4 (C=O Ac), 163.8 (C=N), 158.3 (C=O Boc), 138.5 (Cq Ar.), 135.7 (Cq Ar.), 132.7 (Cq Ar.), 130.0 (CH Ar.), 125.8 (CH Ar.), 122.4 (CH Ar.), 78.1 (Cq Boc), 62.9 (CH₂O), 39.5 (NHCH₂), 28.9 (CqCH₂CH₂), 28.5 (CqCH₂CH₂), 28.0 (CH₃ Boc), 22.6 (CqCH₂CH₂), 22.4 (CqCH₂CH₂), 20.4 (CH₃ Ac).

IR (neat, cm⁻¹): ν_{max} 3374 (NH), 2930 (CH), 1739, 1592 (C=N), 1551, 1502, 1451, 1337, 1227, 1156 (C-O), 1042.

HRMS (*m/z* ES): Found: 376.2220 (M⁺ + H. C₂₀H₃₀N₃O₄ Requires: 376.2236).

2-[1-(*Tert*-butoxycarbonyl)-3-(4-ethylaminophenyl)guanidino]ethyl acetate (66d)



Following Method A, HgCl₂ (335 mg, 1.24 mmol) was added over a solution of **64** (270 mg, 1.03 mmol), **105** (133 μl, 1.03 mmol) and triethylamine (445 μl, 3.19 mmol) in methylene chloride (1.5 ml) at 0 °C. The resulting mixture

was stirred for 1 h at 0° C and a further 14 h at room temperature. Usual work up followed by silica gel chromatography, eluting with hexane:EtOAc, afforded the title compound as a brown solid (87 mg, 23%). Mp: 86 - 88 °C.

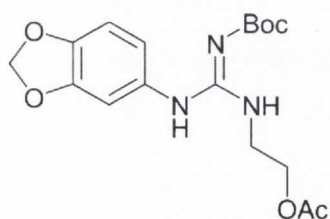
¹H NMR (400 MHz, CDCl₃): δ10.40 (br s, 1H, NH), 6.99 (d, J = 8.6 Hz, 2H, CH Ar.), 6.59 (d, J = 8.6 Hz, 2H, CH Ar.), 4.83 (br s, 1H, NH), 4.10 (t, J = 5.3 Hz, 2H, OCH₂CH₂), 3.74 (br s, 1H, NH), 3.61 (m, 2H, OCH₂CH₂), 3.15 (q, J = 7.0 Hz, 2H, CH₂CH₃), 1.98 (s, 3H, Ac), 1.53 (s, 9H, Boc), 1.27 (t, J = 7.0 Hz, 3H, CH₂CH₃).

¹³C NMR (100 MHz, CDCl₃): δ170.4 (C=O Ac), 163.8 (C=N), 159.2 (C=O Boc), 147.3 (Cq Ar.), 127.6 (CH Ar.), 124.1 (Cq Ar.), 112.8 (CH Ar.), 77.9 (Cq Boc), 63.0 (OCH₂CH₂), 39.4 (OCH₂CH₂), 38.0 (CH₂CH₃), 28.0 (CH₃ Boc), 20.3 (CH₃ Ac), 14.3 (CH₂CH₃).

IR (neat, cm⁻¹): ν_{max} 3334 (NH), 2975 (CH), 2932, 1721, 1635, 1583 (C=N), 1584, 1523, 1364, 1336, 1246, 1172 (C-O), 1151 (C-O), 1126, 1045, 1023.

HRMS (*m/z* ES): Found: 365.2196 (M⁺ + H. C₁₈H₂₉N₄O₄ Requires: 365.2189).

2-[1-(*Tert*-butoxycarbonyl)-3-(3,4-methylenedioxyphenyl)guanidino]ethyl acetate (66e)



Following Method A, HgCl₂ (310 mg, 1.15 mmol) was added over a solution of **64** (350 mg, 0.95 mmol), 3,4-methylenedioxyaniline (131 mg, 0.95 mmol) and triethylamine (412 μl, 2.96 mmol) in methylene chloride (2.0 ml) at 0 °C. The resulting mixture was stirred for 1 h at 0° C and a further

14 h at room temperature. Usual work up followed by silica gel chromatography, eluting with hexane:EtOAc, afforded the product. Recrystallisation from diethyl ether:hexane yielded the title compound as a white, crystalline solid (240 mg, 69%). Mp: 108 °C.

¹H NMR (400 MHz, CDCl₃): δ10.58 (br s, 1H, NH), 6.81 – 6.25 (m, 3H, 3CH Ar.), 6.03 (s, 2H, OCH₂O), 4.95 (br s, 1H, NH), 4.16 (m, 2H, OCH₂CH₂), 3.64 (q, J = 5.0 Hz, 2H, OCH₂CH₂), 2.03 (s, 3H, Ac), 1.53 (s, 9H, Boc).

^{13}C NMR (100 MHz, CDCl_3): δ 170.6 (C=O Ac), 163.8 (C=N), 158.6 (C=O Boc), 148.1 (Cq-O Ar.), 146.3 (Cq-O Ar.), 129.1 (Cq Ar.), 119.3 (CH Ar.), 108.3 (CH Ar.), 107.2 (CH Ar.), 101.3 (OCH₂O), 78.2 (Cq Boc), 62.8 (OCH₂CH₂), 39.7 (OCH₂CH₂), 28.0 (CH₃ Boc), 20.4 (CH₃ Ac).

IR (neat, cm^{-1}): ν_{max} 3386 (NH), 2988 (CH), 2963, 2904, 1720, 1592 (C=N), 1560, 1503, 1489, 1450, 1411, 1354, 1252, 1170 (C-O), 1146 (C-O), 1118, 1036.

HRMS (m/z ES): Found: 366.1657 ($\text{M}^+ + \text{H}$. $\text{C}_{17}\text{H}_{24}\text{N}_3\text{O}_6$ Requires: 366.1665).

1-[1-(*Tert*-butoxycarbonyl)-3-phenylguanidino]-4-ethoxybenzene (**67a**)



Following Method A, HgCl_2 (257 mg, 0.95 mmol) was added over a solution of **63c** (259 mg, 0.73 mmol), 4-ethoxyaniline (94 μl , 0.73 mmol) and triethylamine (315 μl , 2.26 mmol) in methylene chloride (1.5 ml) at 0 °C. The resulting mixture was stirred for 1 h at 0° C and a further 16 h at room temperature.

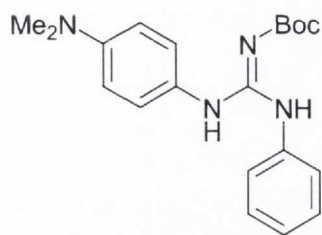
Usual work up followed by silica gel chromatography, eluting with hexane:EtOAc, afforded the title compound as an amorphous white solid (138 mg, 53%). Mp: 126 - 127 °C.

^1H NMR (400 MHz, CDCl_3): δ 9.48 (br m, 1H, NH), 7.66 (br m, 1H, NH), 6.89 – 7.34 (m, 9H, CH Ar.), 4.03 (q, $J = 6.5$ Hz, 2H, CH₂CH₃), 1.53 (m, 9H, Boc), 1.42 (t, $J = 6.5$ Hz, 3H, CH₂CH₃).

^{13}C NMR (100 MHz, CDCl_3): δ 163.9 (C=N), 156.5 (C=O), 154.4 (Cq Ar.), 152.5 (Cq Ar.), 140.0 (Cq Ar.), 128.8 - 114.9 (signals in this range could not be assigned as they were broad and highly amorphous), 82.6 (Cq Boc), 63.2 (CH₂CH₃), 27.7 (CH₃ Boc), 14.5 (CH₂CH₃).

IR (neat, cm^{-1}): ν_{max} 3412 (NH), 3301 (NH), 2980 (CH), 2927 (Aryl), 1715, 1658, (C=O), 1588 (C=N), 1553, 1510 (Aryl), 1461, 1236, 1146 (C-O), 1117 (C-O), 1091, 1049, 977.

HRMS (m/z ES): Found: 356.1976 ($\text{M}^+ + \text{H}$. $\text{C}_{20}\text{H}_{26}\text{N}_3\text{O}_3$ Requires: 356.1974).

1-[1-(*Tert*-butoxycarbonyl)-3-phenylguanidino]-4-(dimethylamino)benzene (67b)

Following Method A, HgCl₂ (276 mg, 1.02 mmol) was added over a solution of **63d** (250 mg, 0.85 mmol), aniline (77 μl, 0.85 mmol) and triethylamine (413 μl, 2.97 mmol) in methylene chloride (1.5 ml) at 0 °C. The resulting mixture was stirred for 1 h at 0° C and a further 14 h at room temperature. Usual work up

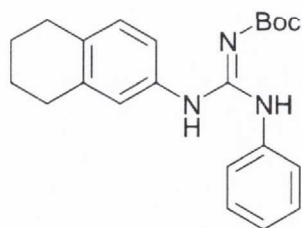
followed by silica gel chromatography, eluting with hexane:EtOAc, afforded the title compound as a clear, viscous oil (265 mg, 88%).

¹H NMR (400 MHz, CDCl₃): δ9.56 (br m, 1H, NH), 7.72 (br m, 1H, NH), 6.70 – 7.35 (m, 9H, CH Ar.), 2.97 (s, 6H, N(CH₃)₂), 1.54 (s, 9H, Boc).

¹³C NMR (100 MHz, CDCl₃): δ164.5 (C=N), 157.4 (C=O), 137.5 - 113.2 (Signals in this range could not be assigned as they were broad and highly amorphous), 82.9 (Cq Boc), 40.6 (N(CH₃)₂), 28.4 (CH₃ Boc).

IR (neat, cm⁻¹): ν_{max} 3412 (NH), 3300 (NH), 2981 (CH), 2927 (Aryl), 1715, 1658, (C=O), 1589 (C=N), 1553, 1510 (Aryl), 1461, 1368, 1236, 1208, 1146 (C-O), 1117 (C-O), 1091, 1049.

HRMS (*m/z* ES): Found: 355.2151 (M⁺ + H. C₂₀H₂₇N₄O₂ Requires: 355.2134).

2-[1-(*Tert*-butoxycarbonyl)-3-phenylguanidino]-5,6,7,8-tetrahydronaphthalene (67c)

Following Method A, HgCl₂ (299 mg, 1.10 mmol) was added over a solution of **63c** (231 mg, 0.92 mmol), 2-amino-5,6,7,8-tetrahydronaphthalene (135 mg, 0.92 mmol) and triethylamine (397 μl, 2.85 mmol) in methylene chloride (1.5 ml) at 0 °C.

The resulting mixture was stirred for 1 h at 0° C and a further 14 h at room temperature. Usual work up followed by silica gel chromatography, eluting with hexane:EtOAc, afforded the title compound as a clear gum (280 mg, 84%).

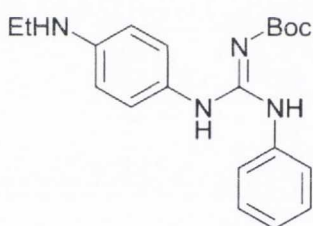
$^1\text{H NMR}$ (400 MHz, CDCl_3): δ 9.65 (br m, 1H, NH), 7.79 (br m, 1H, NH), 6.50 – 7.50 (m, 8H, CH Ar.), 2.81 (m, 4H, 2CH_2), 1.87 (m, 4H, 2CH_2), 1.54 (br m, 9H, Boc).

$^{13}\text{C NMR}$ (100 MHz, CDCl_3): δ 163.9 (C=N), 156.2 (C=O), 152.7 (Cq Ar.), 146.8 (Cq Ar.), 143.7 - 117.6 (signals in this range could not be assigned as they were broad and highly amorphous), 82.6 (Cq Boc), 29.2 (Cq $\underline{\text{C}}\text{H}_2\text{CH}_2$), 28.5 (CH_3 Boc), 27.7 (Cq $\underline{\text{C}}\text{H}_2\text{CH}_2$), 23.1 (Cq CH_2CH_2), 22.9 (Cq CH_2CH_2).

IR (neat, cm^{-1}): ν_{max} 3408 (NH), 3302 (NH), 2978 (CH), 1719, 1662, (C=O), 1590 (C=N), 1555, 1492 (Aryl), 1462, 1368, 1235, 1147 (C-O), 1088.

HRMS (m/z ES): Found: 370.2124 ($\text{M}^+ + \text{H}$. $\text{C}_{21}\text{H}_{28}\text{N}_3\text{O}_3$ Requires: 370.2131).

1-[1-(*Tert*-butoxycarbonyl)-3-phenylguanidino]-4-ethylaminobenzene (67d)



Following Method A, HgCl_2 (335 mg, 1.24 mmol) was added over a solution of **63c** (259 mg, 1.03 mmol), **105** (133 μl , 1.03 mmol) and triethylamine (445 μl , 3.19 mmol) in methylene chloride (1.5 ml) at 0 °C. The resulting mixture was stirred for 1 h at 0° C and a further 14 h at room temperature. Usual work up followed by silica gel chromatography, eluting with hexane:EtOAc, afforded the title compound as a viscous yellow oil (210 mg, 55%).

$^1\text{H NMR}$ (400 MHz, CDCl_3): δ 9.62 (br m, 1H, NH), 7.63 – 6.60 (m, 11H, 9CH Ar. + 2NH), 3.90 (q, $J = 7.5$ Hz, 2H, $\underline{\text{C}}\text{H}_2\text{CH}_3$), 1.52 (br s, 9H, Boc), 1.25 (t, $J = 7.5$ Hz, 3H, $\text{CH}_2\underline{\text{C}}\text{H}_3$).

$^{13}\text{C NMR}$ (100 MHz, CDCl_3): δ 163.4 (C=N), 160.3 (C=O), 152.5 (Cq Ar.), 146.2 (Cq Ar.), 139.4 (Cq Ar.), 129.2 - 112.8 (Signals in this range could not be assigned as they were broad and highly amorphous), 83.0 (Cq Boc), 46.2 ($\underline{\text{C}}\text{H}_2\text{CH}_3$), 27.9 (CH_3 Boc), 13.0 ($\text{CH}_2\underline{\text{C}}\text{H}_3$).

IR (neat, cm^{-1}): ν_{max} 3403 (NH), 2977 (CH), 2932, 1721, 1629, (C=O), 1589 (C=N), 1554, 1509 (Aryl), 1463, 1448, 1366, 1236, 1148 (C-O), 1052, 1031, 976.

HRMS (m/z ES): Found: 353.1977 ($M^- - H$, $C_{20}H_{25}N_4O_2$ Requires: 353.1978).

1-[1-(*Tert*-butoxycarbonyl)-3-phenylguanidino]-3,4-methylenedioxybenzene (67e)



Following Method A, $HgCl_2$ (356 mg, 1.31 mmol) was added over a solution of **63c** (276 mg, 1.09 mmol), 3,4-methylenedioxyaniline (150 mg, 1.09 mmol) and triethylamine (473 μ l, 3.39 mmol) in methylene chloride (1.5 ml) at 0 °C. The resulting mixture was stirred for 1 h at 0° C and a further 14 h at room temperature. Usual work up followed by silica gel chromatography, eluting with hexane:EtOAc, afforded the title compound as a clear gum (324 mg, 84%).

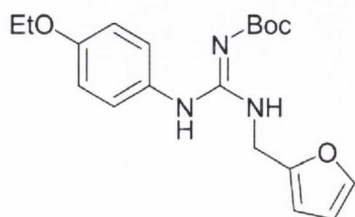
1H NMR (400 MHz, $CDCl_3$): δ 9.52 (br m, 1H, NH), 7.71 (br m, 1H, NH), 6.39 – 7.49 (m, 8H, CH Ar.), 5.95 (s, 2H, CH_2), 1.51 (s, 9H, Boc).

^{13}C NMR (100 MHz, $CDCl_3$): δ 163.8 (C=N), 156.4 (C=O), 152.5 (Cq-O Ar.), 147.9 (Cq-O Ar.), 142.9 (Cq Ar.), 140.1 (Cq Ar.), 136.5 - 103.8 (Signals in this range could not be assigned as they were broad and highly amorphous), 100.6 (CH_2), 82.8 (Cq Boc), 27.7 (CH_3 Boc).

IR (neat, cm^{-1}): ν_{max} 3409 (NH), 3333 (NH), 2971 (CH), 1722, 1661, (C=O), 1594 (C=N), 1562, 1481 (Aryl), 1456, 1367, 1231, 1148 (C-O), 1078, 1036.

HRMS (m/z ES): Found: 356.1619 ($M^+ + H$, $C_{19}H_{22}N_3O_4$ Requires: 356.1610).

1-[1-(*Tert*-butoxycarbonyl)-3-(furan-2-ylmethyl)guanidino]-4-ethoxybenzene (68a)



Following Method A, $HgCl_2$ (1.3 equivalents, 643 mg, 2.37 mmol) was added over a solution of **63f** (466 mg, 1.82 mmol), 4-ethoxyaniline (236 μ l, 1.82 mmol) and triethylamine (787 μ l, 5.65 mmol) in methylene chloride (3 ml) at 0 °C. The resulting mixture was stirred for 1 h at 0° C and a further 14 h

at room temperature. Usual work up followed by silica gel chromatography, eluting with hexane:EtOAc, afforded the title compound as a viscous yellow oil (254 mg, 88%).

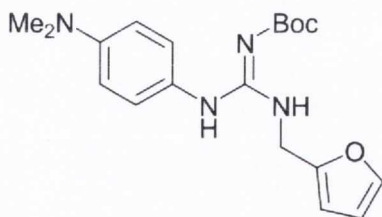
¹H NMR (400 MHz, CDCl₃): δ10.57 (br s, 1H, NH), 7.29 (app s, 1H, CH-O Fur.), 7.08 (d, J = 9.0 Hz, 2H, CH Ar.), 6.86 (d, J = 9.0 Hz, 2H, CH Ar.), 6.26 (app s, 1H, CH Fur.), 6.16 (app s, 1H, CH Fur.), 4.81 (br s, 1H, NH), 4.55 (d, J = 3.5 Hz, 2H, CH₂NH), 3.99 (q, J = 7.0 Hz, 2H, CH₂CH₃), 1.52 (s, 9H, Boc), 1.39 (t, J = 7.0 Hz, 3H, CH₂CH₃).

¹³C NMR (100 MHz, CDCl₃): δ164.2 (C=N), 158.9 (C=O), 157.9 (Cq Fur.), 151.2 (Cq Ar.), 142.1 (CH-O Fur.), 128.1 (Cq Ar.), 127.7 (CH Ar.), 115.5 (CH Ar.), 110.3 (CH Fur.), 107.3 (CH Fur.), 78.4 (Cq Boc), 63.6 (CH₂CH₃), 38.2 (CH₂NH), 28.4 (CH₃ Boc), 14.7 (CH₂CH₃).

IR (neat, cm⁻¹): ν_{max} 3363 (NH), 3165 (NH), 2977 (CH), 2930 (Aryl), 1724, 1624, (C=O), 1591 (C=N), 1548, 1509 (Aryl), 1342, 1234, 1167 (C-O), 1115 (C-O), 1066, 1045, 1009.

HRMS (*m/z* ES): Found: 360.1926 (M⁺ + H. C₁₉H₂₆N₃O₄ Requires: 360.1923).

1-[1-(*Tert*-butoxycarbonyl)-3-(furan-2-ylmethyl)guanidino]-4-(dimethylamino)benzene (68b)



Following Method A, HgCl₂ (276 mg, 1.02 mmol) was added over a solution of **63d** (250 mg, 0.85 mmol), 2-furfurylamine (75 μl, 0.85 mmol) and triethylamine (413 μl, 2.97 mmol) in methylene chloride (1.5 ml) at 0 °C. The resulting mixture was stirred for 1 h at 0° C and a further

14 h at room temperature. Usual work up followed by silica gel chromatography, eluting with hexane:EtOAc, afforded the title compound as a viscous yellow oil (272 mg, 90%).

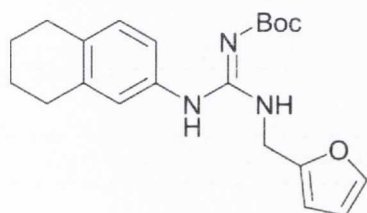
¹H NMR (400 MHz, CDCl₃): δ10.45 (br s, 1H, NH), 7.26 (app s, 1H, CH-O Fur.), 7.02 (d, J = 8.5 Hz, 2H, CH Ar.), 6.64 (d, J = 8.5 Hz, 2H, CH Ar.), 6.23 (app s, 1H, CH Fur.), 6.12 (app s, 1H, CH Fur.), 4.83 (br s, 1H, NH), 4.54 (d, J = 3.5 Hz, 2H, CH₂), 2.91 (s, 6H, N(CH₃)₂), 1.52 (s, 9H, Boc).

^{13}C NMR (100 MHz, CDCl_3): δ 163.8 (C=N), 158.8 (C=O), 150.9 (Cq Fur.), 149.1 (Cq Ar.), 141.6 (CH-O Fur.), 127.1 (CH Ar.), 123.4 (Cq Ar.), 112.6 (CH Ar.), 109.8 (CH Fur.), 106.7 (CH Fur.), 77.8 (Cq Boc), 40.0 ($\text{N}(\text{CH}_3)_2$), 37.8 (CH_2), 28.0 (CH_3 Boc).

IR (neat, cm^{-1}): ν_{max} 3428 (NH), 3146 (NH), 2975 (CH), 2929 (Aryl), 1721, 1626, (C=O), 1589 (C=N), 1520 (Aryl), 1340, 1240, 1167 (C-O), 1148, 1116 (C-O), 1064, 1008.

HRMS (m/z ES): Found: 359.2092 ($\text{M}^+ + \text{H}$, $\text{C}_{19}\text{H}_{27}\text{N}_4\text{O}_3$ Requires: 359.2083).

2-[1-(*Tert*-butoxycarbonyl)-3-(furan-2-ylmethyl)guanidino]-5,6,7,8-tetrahydronaphthalene (68c)



Following Method A, HgCl_2 (299 mg, 1.10 mmol) was added over a solution of **63f** (235 mg, 0.92 mmol), 2-amino-5,6,7,8-tetrahydronaphthalene (135 mg, 0.92 mmol) and triethylamine (397 μl , 2.85 mmol) in methylene chloride (1.5 ml) at 0 °C. The resulting mixture was stirred

for 1 h at 0° C and a further 14 h at room temperature. Usual work up followed by silica gel chromatography, eluting with hexane:EtOAc, afforded the title compound as a viscous yellow oil (335 mg, 95%).

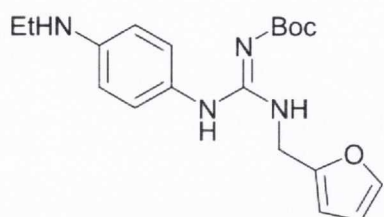
^1H NMR (400 MHz, CDCl_3): δ 10.67 (br s, 1H, NH), 7.31 (app s, 1H, CH-O Fur.), 7.06 (d, $J = 8.8$ Hz, 1H, CH Ar.), 6.92 (d, $J = 8.8$ Hz, 1H, CH Ar.), 6.90 (s, 1H, CH Ar.), 6.30 (app s, 1H, CH Fur.), 6.19 (app s, 1H, CH Fur.), 5.02 (br s, 1H, NH), 4.59 (d, $J = 4.7$ Hz, 2H, NHCH_2), 2.74 (m, 4H, 2 CH_2), 1.80 (m, 4H, 2 CH_2), 1.56 (s, 9H, Boc).

^{13}C NMR (100 MHz, CDCl_3): δ 164.3 (C=N), 158.5 (C=O), 151.3 (Cq Fur.), 142.2 (CH-O Fur.), 139.0 (Cq Ar.), 136.1 (Cq Ar.), 133.2 (Cq Ar.), 130.5 (CH Ar.), 126.2 (CH Ar.), 122.7 (CH Ar.), 110.4 (CH Fur.), 107.3 (CH Fur.), 78.5 (Cq Boc), 38.4 (NHCH_2), 29.3 (Cq CH_2CH_2), 28.9 (Cq CH_2CH_2), 28.5 (CH_3 Boc), 23.0 (Cq CH_2CH_2), 22.8 (Cq CH_2CH_2).

IR (neat, cm^{-1}): ν_{max} 2929 (CH), 1724, 1630, (C=O), 1591 (C=N), 1546, 1501 (Aryl), 1342, 1248, 1124 (C-O), 1085, 1066, 1009.

HRMS (m/z ES): Found: 366.2179 ($M^+ + H$, $C_{22}H_{28}N_3O_2$ Requires: 366.2182).

1-[1-(*Tert*-butoxycarbonyl)-3-(furan-2-ylmethyl)guanidino]-4-ethylaminobenzene (68d)



Following Method A, $HgCl_2$ (335 mg, 1.24 mmol) was added over a solution of **63f** (264 mg, 1.03 mmol), **105** (133 μ l, 1.03 mmol) and triethylamine (445 μ l, 3.19 mmol) in methylene chloride (1.5 ml) at 0 °C. The resulting mixture was stirred for 1 h at 0° C and a further 14 h at room temperature. Usual work up followed by silica gel chromatography, eluting with hexane:EtOAc, afforded the title compound as a viscous yellow oil (100 mg, 27%).

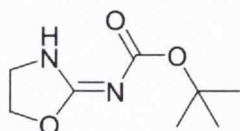
1H NMR (400 MHz, $CDCl_3$): δ 10.47 (br s, 1H, NH), 7.32 (app s, 1H, CH-O Fur.), 7.00 (d, $J = 7.6$ Hz, 2H, CH Ar.), 6.58 (d, $J = 7.6$ Hz, 2H, CH Ar.), 6.29 (app s, 1H, CH Fur.), 6.17 (app s, 1H, CH Fur.), 4.78 (br s, 1H, NH), 4.57 (d, $J = 3.5$ Hz, 2H, $CqCH_2$), 3.72 (br s, 1H, NH), 3.15 (q, $J = 7.0$ Hz, 2H, CH_2CH_3), 1.55 (s, 9H, Boc), 1.27 (t, $J = 7.0$ Hz, 3H, CH_2CH_3).

^{13}C NMR (100 MHz, $CDCl_3$): δ 163.7 (C=N), 158.8 (C=O), 150.8 (Cq Fur.), 147.2 (Cq Ar.), 141.7 (CH-O Fur.), 127.4 (CH Ar.), 123.9 (Cq Ar.), 112.9 (CH Ar.), 109.9 (CH Fur.), 106.8 (CH Fur.), 78.0 (Cq Boc), 38.0 (CH_2CH_3), 37.9 ($CqCH_2$), 28.0 (CH_3 Boc), 14.3 (CH_2CH_3).

IR (neat, cm^{-1}): ν_{max} 3427 (NH), 3362 (NH), 3252 (NH), 2973 (CH), 2930 (Aryl), 1721, 1589 (C=N), 1519 (Aryl), 1340, 1321, 1252, 1168 (C-O), 1121 (C-O), 1147, 1086, 1009.

HRMS (m/z ES): Found: 359.2082 ($M^+ + H$, $C_{19}H_{27}N_4O_3$ Requires: 359.2083).

(*E*)-Oxazolidin-2-(*N-tert*-butoxycarbonyl)imine (69)



Following Method A, $HgCl_2$ (257 mg, 0.95 mmol) was added over a solution of **63b** (259 mg, 0.73 mmol), 4-ethoxyaniline (94 μ l, 0.73 mmol) and triethylamine (315 μ l, 2.26 mmol) in methylene chloride

(1.5 ml) at 0 °C. The resulting mixture was stirred for 1 h at 0° C and a further 20 h at room temperature. Usual work up followed by silica gel chromatography, eluting with hexane:EtOAc, did not afford the intended guanidine product but instead afforded the title compound as a white solid (50 mg, 25%). Mp: 100 - 102 °C.

¹H NMR (400 MHz, CDCl₃): δ8.42 (br s, 1H, NH), 4.50 (t, J = 8.0 Hz, 2H, CH₂O), 3.83 (t, J = 8.0 Hz, 2H, CH₂NH), 1.51 (s, 9H, Boc).

¹³C NMR (100 MHz, CDCl₃): δ167.0 (C=N), 163.0 (C=O), 78.8 (Cq Boc), 64.9 (CH₂O), 42.1 (CH₂NH), 27.6 (CH₃ Boc).

IR (neat, cm⁻¹): ν_{max} 3380 (NH), 2979 (CH), 2931, 1651 (C=O), 1512 (C=N), 1440, 1362, 1316, 1237, 1162 (C-O), 1072, 1050, 1038, 969.

HRMS (*m/z* ES): Found: 187.1085 (M⁺ + H. C₈H₁₄N₂O₃ Requires: 187.1083).

N-(4-Ethoxyphenyl)-*N'*-propylguanidine hydrochloride (**69a**)



Following Method D, **65a** (108 mg, 0.42 mmol) was treated with a solution of 50% trifluoroacetic acid in methylene chloride (2 ml). After 2 h, solvents were evaporated and the residue was dissolved in H₂O (5 ml) to which was added 500

mg Amberlite resin in its Cl⁻ form. After 16 hours the Amberlite was removed by filtration; usual workup was followed by purification by reverse phase chromatography (C-8 silica using gradient elution from 100% H₂O to 85:15 H₂O:acetonitrile). Removal of solvents afforded the title compound as yellow hygroscopic gum (90 mg, 83%). Mp: 104 - 106 °C.

¹H NMR (400 MHz, D₂O): δ7.22 (d, J = 8.5 Hz, 2H, CH Ar.), 7.02 (d, J = 8.5 Hz, 2H, CH Ar.), 4.10 (q, J = 7.0 Hz, 2H, CH₂CH₃), 3.18 (t, J = 7.0 Hz, 2H, CH₂CH₂CH₃), 1.59 (m, 2H, CH₂CH₂CH₃), 1.36 (t, 3H, J = 7.0 Hz, CH₂CH₃), 0.91 (t, 3H, J = 7.6 Hz, CH₂CH₂CH₃).

^{13}C NMR (100 MHz, D_2O): δ 157.1 (Cq Ar.), 155.0 (C=N), 127.6 (CH Ar.), 126.5 (Cq Ar.), 115.3 (CH Ar.), 64.1 ($\underline{\text{C}}\text{H}_2\text{CH}_3$), 42.6 ($\underline{\text{C}}\text{H}_2\text{CH}_2\text{CH}_3$), 21.0 ($\text{CH}_2\underline{\text{C}}\text{H}_2\text{CH}_3$), 13.4 ($\text{CH}_2\underline{\text{C}}\text{H}_3$), 9.9 ($\text{CH}_2\text{CH}_2\underline{\text{C}}\text{H}_3$).

IR (neat, cm^{-1}): ν_{max} 3125 (NH), 2964 (CH), 2874, 2367, 1616, 1509, 1474, 1393, 1234, 1172 (C-O), 1112 (C-O), 1047.

HRMS (m/z ES): Found: 222.1608 (M^+ . $\text{C}_{12}\text{H}_{20}\text{N}_3\text{O}$ Requires: 222.1606).

Purity by HPLC: 97.9% (t_{R} 25.19 min).

N-[4-(Dimethylamino)phenyl]-*N'*-propylguanidine hydrochloride (**69b**)



Following Method E, **65b** (125 mg, 0.39 mmol) was treated with a 1.25 M solution of methanolic HCl (3.5 ml). After 2 h, solvents were evaporated and the residue was purified by reverse phase chromatography (C-8 silica using gradient elution from 100% H_2O to 85:15 H_2O :acetonitrile). Removal of solvents afforded the title compound as a clear hygroscopic gum (65 mg, 65%). Mp: 50 - 55 $^{\circ}\text{C}$.

^1H NMR (400 MHz, D_2O): δ 7.68 (d, $J = 8.6$ Hz, 2H, CH Ar.), 7.47 (d, $J = 8.6$ Hz, 2H, CH Ar.), 3.29 (s, 6H, $\text{N}(\text{CH}_3)_2$), 3.23 (t, $J = 6.6$ Hz, 2H, $\underline{\text{C}}\text{H}_2\text{CH}_2\text{CH}_3$), 1.61 (m, 2H, $\text{CH}_2\underline{\text{C}}\text{H}_2\text{CH}_3$), 0.92 (t, $J = 7.5$ Hz, 3H, $\text{CH}_2\text{CH}_2\underline{\text{C}}\text{H}_3$).

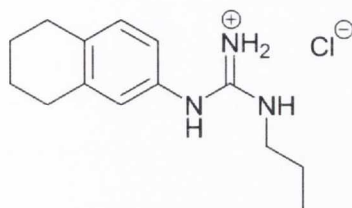
^{13}C NMR (100 MHz, D_2O): δ 154.4 (C=N), 136.7 (Cq Ar.), 136.2 (Cq Ar.), 126.3 (CH Ar.), 121.7 (CH Ar.), 46.0 ($\text{N}(\text{CH}_3)_2$), 42.9 ($\underline{\text{C}}\text{H}_2\text{CH}_2\text{CH}_3$), 20.9 ($\text{CH}_2\underline{\text{C}}\text{H}_2\text{CH}_3$), 10.0 ($\text{CH}_2\text{CH}_2\underline{\text{C}}\text{H}_3$).

IR (neat, cm^{-1}): ν_{max} 3149 (NH), 2465, 2449, 1624, 1591, 1515, 1463, 1260, 1183, 1134, 1017, 995.

HRMS (m/z ES): Found: 221.1772 (M^+ . $\text{C}_{12}\text{H}_{21}\text{N}_4$ Requires: 221.1766).

Purity by HPLC: 99.4% (t_R 21.52 min).

***N*-(5,6,7,8-Tetrahydronaphth-2-yl)-*N*'-propylguanidine hydrochloride (69c)**



Following Method E, **65c** (230 mg, 0.70 mmol) was treated with a 1.25 M solution of methanolic HCl (10 ml). After 2 h, conc. HCl was added (0.4 ml) and the reaction continued for 2 h more. At this point the reaction was adjudged complete (TLC), solvents were evaporated, and the residue

was purified by reverse phase chromatography (C-8 silica using 100% H₂O mobile phase). Removal of solvents afforded the title compound as a yellow hygroscopic gum (135 mg, 73%).

¹H NMR (400 MHz, D₂O): δ7.08 (d, *J* = 8.0 Hz, 1H, CH Ar.), 6.89 (d, *J* = 8.0 Hz, 1H, CH Ar.), 6.88 (s, 1H, CH Ar.), 3.16 (t, *J* = 7.0 Hz, 2H, CH₂CH₂CH₃), 2.65 (m, 4H, 2CH₂), 1.67 (m, 4H, 2CH₂), 1.56 (m, 2H, CH₂CH₂CH₃), 0.90 (t, *J* = 7.0 Hz, 3H, CH₂CH₂CH₃).

¹³C NMR (100 MHz, D₂O): δ154.6 (C=N), 138.6 (Cq Ar.), 136.6 (Cq Ar.), 130.8 (Cq Ar.), 129.9 (CH Ar.), 125.5 (CH Ar.), 122.2 (CH Ar.), 42.6 (CH₂CH₂CH₃), 28.3 (CqCH₂CH₂), 28.0 (CqCH₂CH₂), 22.0 (CqCH₂CH₂), 21.9 (CqCH₂CH₂), 21.0 (CH₂CH₂CH₃), 9.9 (CH₂CH₂CH₃).

IR (neat, cm⁻¹): ν_{max} 3147 (NH), 2930 (CH), 1630, 1602, 1501, 1458, 1436, 1354, 1249, 1135.

HRMS (*m/z* ES): Found: 232.1814 (M⁺. C₁₄H₂₂N₃ Requires: 232.1814).

Purity by HPLC: 95.1% (t_R 29.19 min).

***N*-(4-Ethylaminophenyl)-*N'*-propylguanidine hydrochloride (69d)**

A solution of **65d** (140 mg, 0.44 mmol) in methanol (3.7 ml) was treated with 60 equivalents of conc. HCl (2.17 ml, 26.25 mmol). After 2 h stirring at 45 °C, the reaction was adjudged complete (TLC, MS), solvents were evaporated, and the residue was purified by reverse phase chromatography (C-8 silica using 100% H₂O mobile phase). Removal of solvents afforded the title compound as a yellow hygroscopic gum (50 mg, 39%).

¹H NMR (400 MHz, D₂O): δ7.48 (d, J = 8.6 Hz, 2H, CH Ar.), 7.40 (d, J = 8.6 Hz, 2H, CH Ar.), 3.42 (q, J = 7.6 Hz, 2H, CH₂CH₃), 3.18 (t, J = 6.5 Hz, 2H, CH₂CH₂CH₃), 1.56 (m, 2H, CH₂CH₂CH₃), 1.25 (t, 3H, J = 7.6 Hz, CH₂CH₃), 0.86 (t, J = 7.5 Hz, CH₂CH₂CH₃).

¹³C NMR (100 MHz, D₂O): δ154.5 (C=N), 135.8 (Cq Ar.), 132.4 (Cq Ar.), 126.3 (CH Ar.), 123.8 (CH Ar.), 46.9 (CH₂CH₃), 42.8 (CH₂CH₂CH₃), 20.9 (CH₂CH₂CH₃), 9.9 (CH₂CH₂CH₃), 9.7 (CH₂CH₃).

IR (neat, cm⁻¹): ν_{max} 3162 (NH), 2966 (CH), 2359, 1621, 1590, 1514, 1455, 1142 (C-O), 1106 (C-O), 1020.

HRMS (*m/z* ES): Found: 221.1763 (M⁺. C₁₂H₂₁N₄ Requires: 221.1766).

Purity by HPLC: 96.8% (*t*_R 19.51 min).

***N*-(3,4-Methylenedioxyphenyl)-*N'*-propylguanidine hydrochloride (69e)**

Following Method E, **65e** (250 mg, 0.78 mmol) was treated with a 1.25 M solution of methanolic HCl (10 ml). After 4 h stirring at rt, 0.5 ml conc. HCl was added and stirring continued for a further 1 h. At this point, the reaction was adjudged complete (TLC), solvents were evaporated, and the

residue was purified by reverse phase chromatography (C-8 silica using 100% H₂O mobile phase). Removal of solvents afforded the title compound as an off-white hygroscopic solid (145 mg, 85%). Mp: 176 – 178 °C.

¹H NMR (400 MHz, D₂O): δ6.80 (d, J = 9.0 Hz, 1H, CH Ar.), 6.67 (m, 2H, 2CH Ar.), 5.91 (s, 1H, OCH₂O), 3.11 (t, J = 7.0 Hz, 2H, CH₂CH₂CH₃), 1.51 (m, 2H, CH₂CH₂CH₃), 0.85 (t, J = 7.0 Hz, 3H, CH₂CH₂CH₃).

¹³C NMR (100 MHz, D₂O): δ154.9 (C=N), 147.5 (Cq Ar.), 146.3 (Cq Ar.), 127.1 (Cq Ar.), 119.8 (CH Ar.), 108.4 (CH Ar.), 107.1 (CH Ar.) 101.5 (OCH₂O), 42.6 (CH₂CH₂CH₃), 21.0 (CH₂CH₂CH₃), 9.9 (CH₂CH₂CH₃).

IR (neat, cm⁻¹): ν_{max} 3136 (NH), 2966 (CH), 1638 (C=N), 1622, 1598, 1501, 1486, 1244, 1200 (C-O), 1124 (C-O), 1032.

HRMS (*m/z* ES): Found: 222.1239 (M⁺. C₁₁H₁₆N₃O₂ Requires: 222.1243).

Purity by HPLC: 97.1% (*t*_R 22.53 min).

N-(4-Ethoxyphenyl)-*N'*-(2-hydroxyethyl)guanidine hydrochloride (70a)



Following Method E, **66a** (60 mg, 0.19 mmol) was treated with a 1.25 M solution of methanolic HCl (5 ml). After 2.5 h, solvents were evaporated and the residue was purified by reverse phase chromatography (C-8 silica using gradient elution from 100% H₂O to 85:15 H₂O:acetonitrile). Removal

of solvents afforded the title compound as a brown, very hygroscopic gum (45 mg, 94%). Mp: 42 - 46 °C.

¹H NMR (400 MHz, D₂O): δ7.20 (d, J = 8.5 Hz, 2H, CH Ar.), 6.99 (d, J = 8.5 Hz, 2H, CH Ar.), 4.05 (q, J = 7.0 Hz, 2H, CH₂CH₃), 3.69 (t, J = 5.0 Hz, 2H, CH₂OH), 3.36 (t, J = 5.0 Hz, 2H, NHCH₂), 1.33 (t, J = 7.0 Hz, 3H, CH₂CH₃).

^{13}C NMR (100 MHz, D_2O): δ 157.1 (Cq Ar.), 155.6 (C=N), 127.5 (CH Ar.), 126.4 (Cq Ar.), 115.2 (CH Ar.), 64.0 ($\underline{\text{C}}\text{H}_2\text{CH}_3$), 59.3 ($\underline{\text{C}}\text{H}_2\text{OH}$), 43.1 ($\text{NH}\underline{\text{C}}\text{H}_2$), 13.3 ($\text{CH}_2\underline{\text{C}}\text{H}_3$).

IR (neat, cm^{-1}): ν_{max} 3158 (NH), 2979 (CH), 2368, 1617, 1514, 1476, 1394, 1237, 1171 (C-O), 1114 (C-O), 1042.

HRMS (m/z ES): Found: 224.1403 (M^+ . $\text{C}_{11}\text{H}_{18}\text{N}_3\text{O}_2$ Requires: 224.1399).

Purity by HPLC: 96.8% (t_{R} 21.97 min).

***N*-[4-(Dimethylamino)phenyl]-*N'*-(2-hydroxyethyl)guanidine hydrochloride (70b)**



Following Method E, **66b** (100 mg, 0.31 mmol) was treated with a 1.25 M solution of methanolic HCl (3.5 ml). After 2 h, solvents were evaporated and the residue was purified by reverse phase chromatography (C-8 silica using a 100% H_2O mobile phase). Removal of solvents afforded the title compound as an off-white hygroscopic gum (65 mg, 80%). Mp: 54 - 62 $^{\circ}\text{C}$.

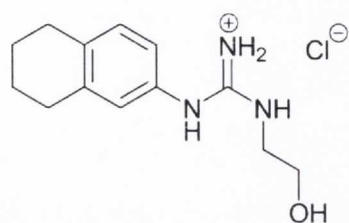
^1H NMR (400 MHz, D_2O): δ 7.68 (d, $J = 9.0$ Hz, 2H, CH Ar.), 7.49 (d, $J = 9.0$ Hz, 2H, CH Ar.), 3.74 (t, $J = 5.0$ Hz, 2H, $\underline{\text{C}}\text{H}_2\text{OH}$), 3.44 (t, $J = 5.0$ Hz, 2H, $\text{NH}\underline{\text{C}}\text{H}_2$), 3.29 (s, 6H, $\text{N}(\text{CH}_3)_2$).

^{13}C NMR (100 MHz, D_2O): δ 155.1 (C=N), 139.8 (Cq Ar.), 136.1 (Cq Ar.), 126.3 (CH Ar.), 121.7 (CH Ar.), 59.4 ($\underline{\text{C}}\text{H}_2\text{OH}$), 45.9 ($\text{N}(\text{CH}_3)_2$), 43.4 ($\text{NH}\underline{\text{C}}\text{H}_2$).

IR (neat, cm^{-1}): ν_{max} 3164 (NH), 2578, 2453, 1662, 1628, 1592, 1516, 1469, 1410, 1260, 1184, 1135, 1063.

HRMS (m/z ES): Found: 223.1550 (M^+ . $\text{C}_{11}\text{H}_{19}\text{N}_4\text{O}$ Requires: 223.1559).

Purity by HPLC: 99.3% (t_{R} 15.76 min).

***N*-(5,6,7,8-Tetrahydronaphth-2-yl)-*N'*-(2-hydroxyethyl)guanidine hydrochloride (70c)**

Following Method E, **66c** (230 mg, 0.61 mmol) was treated with a 1.25 M solution of methanolic HCl (10 ml). After 4 h stirring at 60 °C, the reaction was allowed to cool to rt and stirred for a further 18 h. The reaction continued to appear incomplete by MS analysis, therefore 0.4 ml conc. HCl was

added and stirring continued for 4 h. At this point, the reaction was adjudged complete (TLC), solvents were evaporated, and the residue was purified by reverse phase chromatography (C-8 silica using 100% H₂O mobile phase). Removal of solvents afforded the title compound as a yellow hygroscopic solid (144 mg, 87%). Mp: 64 – 70 °C.

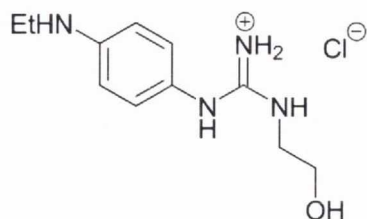
¹H NMR (400 MHz, D₂O): δ7.04 (d, *J* = 7.5 Hz, 1H, CH Ar.), 6.88 (d, *J* = 7.5 Hz, 1H, CH Ar.), 6.87 (s, 1H, CH Ar.), 3.68 (t, *J* = 5.0 Hz, 2H, CH₂OH), 3.36 (t, *J* = 5.0 Hz, 2H, NHCH₂), 2.60 (m, 4H, 2CH₂), 1.63 (m, 4H, 2CH₂).

¹³C NMR (100 MHz, D₂O): δ155.0 (C=N), 138.3 (Cq Ar.), 135.9 (Cq Ar.), 130.8 (Cq Ar.), 129.8 (CH Ar.), 125.0 (CH Ar.), 121.8 (CH Ar.), 59.4 (CH₂OH), 43.2 (NHCH₂), 28.3 (CqCH₂CH₂), 28.0 (CqCH₂CH₂), 22.1 (CqCH₂CH₂), 22.0 (CqCH₂CH₂).

IR (neat, cm⁻¹): ν_{max} 3265 (OH), 3154 (NH), 2928 (CH), 1628, 1601, 1501, 1435, 1352, 1249, 1136, 1062 (C-O).

HRMS (*m/z* ES): Found: 234.1609 (M⁺. C₁₃H₂₀N₃O Requires: 234.1606).

Purity by HPLC: 95.9% (*t*_R 26.85 min).

***N*-(4-Ethylaminophenyl)-*N'*-(2-hydroxyethyl)guanidine hydrochloride (70d)**

A solution of **66d** (87 mg, 0.24 mmol) in methanol (1.8 ml) was treated with 35 equivalents of conc. HCl (0.70 ml, 8.40 mmol). After 3 h stirring at 60 °C, the reaction was adjudged complete (TLC, MS), solvents were evaporated,

and the residue was purified by reverse phase chromatography (C-8 silica using 100% H₂O mobile phase). Removal of solvents afforded the title compound as an off-white solid (49 mg, 77%). Mp: 172 - 178 °C.

¹H NMR (400 MHz, D₂O): δ 7.49 (d, J = 8.5 Hz, 2H, CH Ar.), 7.42 (d, J = 8.5 Hz, 2H, CH Ar.), 3.70 (t, J = 4.5 Hz, 2H, CH₂OH), 3.42 (m, 4H, 2CH₂), 1.26 (t, 3H, J = 7.0 Hz, CH₂CH₃).

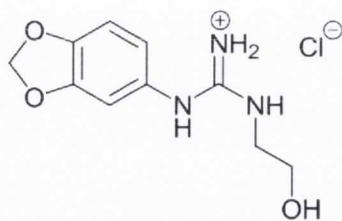
¹³C NMR (100 MHz, D₂O): δ 155.1 (C=N), 135.7 (Cq Ar.), 132.4 (Cq Ar.), 126.3 (CH Ar.), 123.9 (CH Ar.), 59.3 (CH₂OH), 46.9 (CH₂CH₃), 43.4 (NHCH₂), 9.7 (CH₂CH₃).

IR (neat, cm⁻¹): ν_{max} 3266 (OH), 3161 (NH), 2943 (CH), 2662, 2479, 1660, 1626, 1591, 1513, 1443, 1350, 1252, 1058, 1019.

HRMS (*m/z* ES): Found: 223.1557 (M⁺. C₁₁H₁₉N₄O Requires: 223.1559).

Purity by HPLC: 98.5% (*t_R* 7.60 min).

N-(3,4-Methylenedioxyphenyl)-*N'*-(2-hydroxyethyl)guanidine hydrochloride (70e)



Following Method E, **66e** (162 mg, 0.44 mmol) was treated with a 1.25 M solution of methanolic HCl (10 ml). After 3 h stirring at rt, the reaction was heated to 60 °C for a further 0.5 h; at this point the reaction was adjudged complete (TLC). Solvents were evaporated and the residue was purified by reverse phase chromatography (C-8 silica using 100% H₂O mobile phase). Removal of solvents afforded the title compound as a yellow hygroscopic gum (113 mg, 98%).

¹H NMR (400 MHz, D₂O): δ 6.85 (d, J = 7.5 Hz, 1H, CH Ar.), 6.74 (m, 2H, CH Ar.), 5.96 (s, 1H, OCH₂O), 3.70 (t, J = 5.0 Hz, 2H, CH₂OH), 3.37 (t, J = 5.0 Hz, 2H, NHCH₂).

^{13}C NMR (100 MHz, D_2O): δ 155.6 (C=N), 147.5 (Cq Ar.), 146.4 (Cq Ar.), 127.1 (Cq Ar.), 119.8 (CH Ar.), 108.4 (CH Ar.), 107.1 (CH Ar.) 101.5 (OCH₂O), 59.4 (CH₂OH), 43.2 (NHCH₂).

IR (neat, cm^{-1}): ν_{max} 3163, 1602 (C=N), 1501, 1486, 1352, 1245, 1203 (C-O), 1062, 1032.

HRMS (m/z ES): Found: 224.1030 (M^+ . $\text{C}_{10}\text{H}_{14}\text{N}_3\text{O}_3$ Requires: 224.1035).

Purity by HPLC: 96.0% (t_{R} 18.23 min).

N-(4-Ethoxyphenyl)-*N'*-phenylguanidine hydrochloride (71a)



Following Method E, **67a** (138 mg, 0.39 mmol) was treated with a 1.25 M solution of methanolic HCl (5 ml). After 2 h, solvents were evaporated and the residue was purified by reverse phase chromatography (C-8 silica using gradient elution from 100% H_2O to 85:15 H_2O :acetonitrile). Removal

of solvents afforded the title compound as an off-white hygroscopic gum (98 mg, 87%). Mp: 48 - 55 °C.

^1H NMR (400 MHz, D_2O): δ 7.49 (t, J = 8.0 Hz, 2H, CH Ar.), 7.41 (t, J = 8.0 Hz, 1H, CH Ar.), 7.35 (d, J = 8.0 Hz, 2H, CH Ar.), 7.30 (d, J = 9.0 Hz, 2H, CH Ar.), 7.04 (d, J = 9.0 Hz, 2H, CH Ar.), 4.11 (q, J = 7.0 Hz, 2H, CH₂CH₃), 1.37 (t, J = 7.0 Hz, 3H, CH₂CH₃).

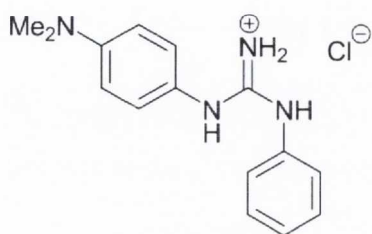
^{13}C NMR (100 MHz, D_2O): δ 157.3 (Cq Ar.), 154.7 (C=N), 133.5 (Cq Ar.), 129.5 (CH Ar.), 127.6 (Cq Ar.), 127.5 (CH Ar.), 126.2 (CH Ar.), 125.4 (CH Ar.), 115.3 (CH Ar.), 64.0 (CH₂CH₃), 13.4 (CH₂CH₃).

IR (neat, cm^{-1}): ν_{max} 3059 (NH), 2978 (CH), 2929 (CH), 2282, 1738, 1616, 1575 (C=N), 1509 (Aryl), 1498, 1476, 1448, 1393, 1301, 1222, 1172, 1114 (C-O), 1087, 1042.

HRMS (m/z ES): Found: 256.1439 (M^+ . $\text{C}_{15}\text{H}_{18}\text{N}_3\text{O}$ Requires: 256.1450).

Purity by HPLC: 98.8% (t_R 25.95 min).

***N*-[4-(Dimethylamino)phenyl]-*N'*-phenylguanidine hydrochloride (71b)**



Following Method E, **67b** (122 mg, 0.35 mmol) was treated with a 1.25 M solution of methanolic HCl (5 ml). After 2 h, solvents were evaporated and the residue was purified by reverse phase chromatography (C-8 silica using gradient elution from 100% H₂O to 85:15 H₂O:acetonitrile). Removal of solvents afforded the title compound as an off-white hygroscopic gum (69 mg, 70%). Mp: 112 - 130 °C.

¹H NMR (400 MHz, D₂O): δ7.68 (d, *J* = 8.7 Hz, 2H, CH Ar.), 7.53 (d, *J* = 8.7 Hz, 2H, CH Ar.), 7.47 (t, *J* = 7.0 Hz, 2H, CH Ar.), 7.37 (t, *J* = 7.0 Hz, 1H, CH Ar.), 7.33 (d, *J* = 7.0 Hz, 2H, CH Ar.), 3.28 (s, 6H, N(CH₃)₂).

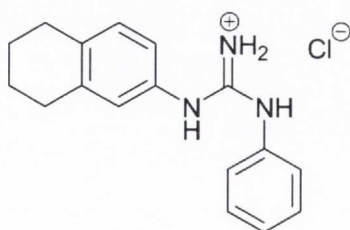
¹³C NMR (100 MHz, D₂O): δ154.1 (C=N), 140.0 (Cq Ar.), 135.9 (Cq Ar.), 133.4 (Cq Ar.), 129.5 (CH Ar.), 127.6 (CH Ar.), 126.5 (CH Ar.), 125.1 (CH Ar.), 121.7 (CH Ar.), 45.9 (N(CH₃)₂).

IR (neat, cm⁻¹): ν_{\max} 3017 (NH), 2429, 1624, 1575, 1514, 1494, 1232, 1183, 1132, 1019.

HRMS (*m/z* ES): Found: 255.1609 (M⁺. C₁₅H₁₉N₄ Requires: 255.1610).

Purity by HPLC: 99.1% (t_R 24.07 min).

***N*-(5,6,7,8-Tetrahydronaphth-2-yl)-*N'*-phenylguanidine hydrochloride (71c)**



Following Method E, **67c** (280 mg, 0.77 mmol) was treated with a 1.25 M solution of methanolic HCl (15 ml). After 8 h, solvents were evaporated and the residue was purified by reverse phase chromatography (C-8 silica using 100% H₂O

mobile phase). Removal of solvents afforded the title compound as a yellow hygroscopic gum. Recrystallisation from warm H₂O provided the purified product as a beige solid (203 mg, 88%). Mp: 154 - 156 °C.

¹H NMR (400 MHz, D₂O): δ7.40 (t, J = 7.5 Hz, 2H, CH Ar.), 7.35 (t, J = 7.5 Hz, 1H, CH Ar.), 7.25 (d, J = 7.5 Hz, 2H, CH Ar.), 7.10 (d, J = 8.0 Hz, 1H, CH Ar.), 6.96 (d, J = 8.0 Hz, 1H, CH Ar.), 6.95 (s, 1H, CH Ar.), 2.65 (br s, 4H, 2CH₂), 1.67 (br s, 4H, 2CH₂).

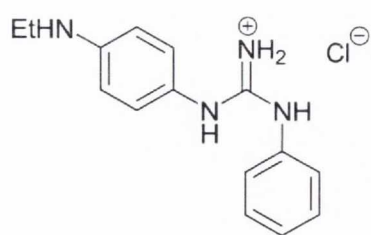
¹³C NMR (100 MHz, D₂O): δ154.3 (C=N), 138.7 (Cq Ar.), 136.9 (Cq Ar.), 133.5 (Cq Ar.), 130.6 (Cq Ar.), 130.0 (CH Ar.), 129.5 (CH Ar.), 127.5 (CH Ar.), 125.5 (CH Ar.), 125.2 (CH Ar.), 122.2 (CH Ar.), 28.3 (CqCH₂CH₂), 28.0 (CqCH₂CH₂), 22.0 (CqCH₂CH₂), 21.9 (CqCH₂CH₂).

IR (neat, cm⁻¹): ν_{max} 3170 (NH), 2928 (CH), 1654, 1629, 1593, 1574, 1496, 1371, 1229, 1163.

HRMS (*m/z* ES): Found: 266.1651 (M⁺. C₁₇H₂₀N₃ Requires: 266.1657).

Purity by HPLC: 97.3% (*t*_R 29.43 min).

N-(4-Ethylaminophenyl)-*N'*-phenylguanidine hydrochloride (71d)



Following Method E, **67d** (210 mg, 0.59 mmol) was treated with a 1.25 M solution of methanolic HCl (7.7 ml). After 4 h stirring at rt, 0.3 ml conc. HCl was added and stirring continued for a further 1 h. At this point, the reaction was complete (TLC), solvents were evaporated, and the residue was

purified by reverse phase chromatography (C-8 silica using 100% H₂O mobile phase). Removal of solvents afforded the title compound as a clear hygroscopic gum (75 mg, 44%).

¹H NMR (400 MHz, D₂O): δ7.49 – 7.30 (m, 9H, 9CH Ar.), 3.43 (q, 2H, J = 7.0 Hz, CH₂CH₃), 1.26 (t, 3H, J = 7.0 Hz, CH₂CH₃).

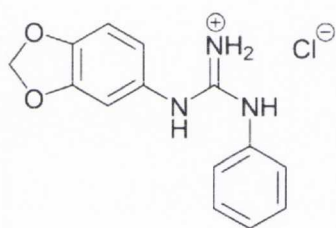
^{13}C NMR (100 MHz, D_2O): δ 154.3 (C=N), 135.5 (Cq Ar.), 133.5 (Cq Ar.), 132.7 (Cq Ar.), 129.5 (CH Ar.), 127.6 (CH Ar.), 126.5 (CH Ar.), 125.2 (CH Ar.), 123.8 (CH Ar.), 46.9 (CH_2CH_3), 9.7 (CH_2CH_3).

IR (neat, cm^{-1}): ν_{max} 2942 (CH), 2651, 2473, 1655, 1624, 1577, 1513, 1496, 1233, 1104, 1021.

HRMS (m/z ES): Found: 255.1597 (M^+ . $\text{C}_{15}\text{H}_{19}\text{N}_4$ Requires: 255.1610).

Purity by HPLC: 97.7% (t_{R} 22.56 min).

N-(3,4-Methylenedioxyphenyl)-*N'*-phenylguanidine hydrochloride (71e)



Following Method E, **67e** (320 mg, 0.90 mmol) was treated with a 1.25 M solution of methanolic HCl (10 ml). After 4 h stirring at rt, 0.4 ml conc. HCl was added and stirring continued for a further 1 h. At this point, the reaction was adjudged complete (TLC), solvents were evaporated, and the residue was purified by reverse phase chromatography (C-8 silica using 100% H_2O mobile phase). Removal of solvents afforded the title compound as an off-white hygroscopic solid (208 mg, 79%). Mp: 96 - 102 °C.

^1H NMR (400 MHz, D_2O): δ 7.42 (t, $J = 7.5$ Hz, 2H, CH Ar.), 7.36 (t, $J = 7.5$ Hz, 1H, CH phenyl), 7.30 (d, $J = 7.5$ Hz, 2H, CH Ar.), 6.82 (d, $J = 9.0$ Hz, 1H, CH Ar.), 6.76 (s, 1H, CH Ar.), 6.75 (d, $J = 9.0$ Hz, 2H, CH Ar.), 5.91 (s, 1H, OCH_2O).

^{13}C NMR (100 MHz, D_2O): δ 154.7 (C=N), 147.5 (Cq Ar.), 146.6 (Cq Ar.), 133.4 (Cq Ar.), 129.5 (CH Ar.), 127.6 (CH Ar.), 126.8 (Cq Ar.), 125.5 (CH Ar.), 119.9 (CH Ar.), 108.4 (CH Ar.), 107.1 (CH Ar.) 101.5 (OCH_2O).

IR (neat, cm^{-1}): ν_{max} 3129 (NH), 3105 (NH), 2975 (CH), 1619 (C=N), 1580, 1486, 1449, 1244, 1195 (C-O), 1138, 1104, 1032 (C-O), 925.

HRMS (m/z ES): Found: 256.1082 (M^+ . $C_{14}H_{14}N_3O_2$ Requires: 256.1086).

Purity by HPLC: 99.9% (t_R 23.99 min).

***N*-(4-Ethoxyphenyl)-*N'*-(furan-2-ylmethyl)guanidine hydrochloride (72a)**



Following Method D, **68a** (260 mg, 0.73 mmol) was treated with a solution of 0.1% trifluoroacetic acid in methylene chloride (10 ml). After 2 h, solvents were evaporated and the residue was dissolved in H_2O (10 ml) to which was added 1000 mg Amberlite resin in its Cl^- form. After 16 hours the

Amberlite was removed by filtration; usual workup was followed by purification by reverse phase chromatography (C-8 silica using gradient elution from 100% H_2O to 85:15 H_2O :acetonitrile). Removal of solvents afforded the title compound as pale yellow hygroscopic gum (110 mg, 51%). Mp: 52 - 60 °C.

1H NMR (400 MHz, D_2O): δ 7.48 (app s, 1H, CH-O Fur.), 7.12 (d, $J = 8.6$ Hz, 2H, CH Ar.), 6.94 (d, $J = 8.6$ Hz, 2H, CH Ar.), 6.40 (app s, 2H, 2CH Fur.), 4.44 (s, 2H, $NHCH_2$), 4.02 (q, $J = 7.0$ Hz, 2H, CH_2CH_3), 1.31 (t, $J = 7.0$ Hz, 3H, CH_2CH_3).

^{13}C NMR (100 MHz, D_2O): δ 157.2 (Cq Ar.), 155.1 (C=N), 148.7 (Cq Fur.), 142.8 (CH-O, Fur.), 127.5 (CH Ar.), 126.2 (Cq Ar.), 115.3 (CH Ar.), 110.2 (CH Fur.), 107.8 (CH Fur.), 64.0 (CH_2CH_3), 37.6 ($NHCH_2$), 13.4 (CH_2CH_3).

IR (neat, cm^{-1}): ν_{max} 3126 (NH), 2979 (CH), 2343, 1619, 1509, 1476, 1394, 1238, 1172 (C-O), 1114 (C-O), 1042.

HRMS (m/z ES): Found: 260.1393 (M^+ . $C_{14}H_{18}N_3O_2$ Requires: 260.1399).

Purity by HPLC: 95.1% (t_R 25.96 min).

***N*-[4-(Dimethylamino)phenyl]-*N'*-(furan-2-ylmethyl)guanidine hydrochloride (72b)**

Following Method D, **68b** (260 mg, 0.72 mmol) was treated with 0.2% trifluoroacetic acid in methylene chloride (10 ml). After 2 h, solvents were evaporated and the residue was dissolved in 10 ml H₂O, to which was added 1.0 g Amberlite resin in its Cl⁻ form. After 16 h the Amberlite was removed by filtration; usual workup was followed by purification by reverse phase chromatography (C-8 silica, gradient elution from 100% H₂O to 85:15 H₂O:acetonitrile). Removal of solvents afforded the title compound as an orange hygroscopic gum (122 mg, 57%). Mp: 96 - 104 °C.

¹H NMR (400 MHz, D₂O): δ7.66 (d, J = 9.0 Hz, 2H, CH Ar.), 7.46 (app s, 1H, CH-O Fur.), 7.44 (d, J = 9.0 Hz, 2H, CH Ar.), 6.41 (app s, 2H, 2CH Fur.), 4.49 (s, 2H, CH₂), 3.28 (s, 6H, N(CH₃)₂).

¹³C NMR (100 MHz, D₂O): δ154.6 (C=N), 148.4 (C_q Fur.), 142.9 (CH-O Fur.), 139.9 (C_q Ar.), 136.0 (C_q Ar.), 126.4 (CH Ar.), 121.8 (CH Ar.), 110.2 (CH Fur.), 108.0 (CH Fur.), 45.9 (N(CH₃)₂), 37.9 (CH₂).

IR (neat, cm⁻¹): ν_{max} 3114 (NH), 2322, 1620, 1584, 1515, 1465, 1374, 1258, 1195, 1133, 1072, 1016.

HRMS (*m/z* ES): Found: 259.1554 (M⁺. C₁₄H₁₉N₄O Requires: 259.1559).

Purity by HPLC: 95.7% (*t*_R 23.55 min).

***N*-(5,6,7,8-Tetrahydronaphth-2-yl)-*N'*-(furan-2-ylmethyl)guanidine hydrochloride (72c)**

To a solution of **68c** (155 mg, 0.42 mmol) in methylene chloride (3.5 ml) was added a 4 M solution of HCl in dioxane (630 μl, 2.52 mmol). After 4 h stirring at 30 °C, solvents were evaporated and the residue was purified by reverse phase chromatography (C-8 silica using a 100%

H₂O mobile phase). Removal of solvents *in vacuo* at a temperature not exceeding 35 °C afforded the title compound as a clear hygroscopic gum (68 mg, 53%). Mp: 72 – 78 °C.

¹H NMR (400 MHz, D₂O): δ7.48 (m, 1H, CH-O Fur.), 7.13 (d, J = 9.0 Hz, 1H, CH Ar.), 6.92 (m, 2H, 2CH Ar.), 6.41 (dd, J = 3.5, 2.0 Hz, 1H, CH Fur.), 6.38 (d, J = 3.5 Hz, 1H, CH Fur.), 4.44 (s, 2H, NHCH₂), 2.68 (m, 4H, 2CH₂), 1.70 (m, 4H, 2CH₂).

¹³C NMR (100 MHz, D₂O): δ154.9 (C=N), 148.7 (Cq Fur.), 142.8 (CH-O, Fur.), 138.8 (Cq Ar.), 137.0 (Cq Ar.), 130.6 (Cq Ar.), 130.0 (CH Ar.), 125.8 (CH Ar.), 122.5 (CH Ar.), 110.1 (CH Fur.), 107.7 (CH Fur.), 37.6 (NHCH₂), 28.2 (CqCH₂CH₂), 27.9 (CqCH₂CH₂), 22.0 (CqCH₂CH₂), 21.8 (CqCH₂CH₂).

IR (neat, cm⁻¹): ν_{max} 3143 (NH), 2929 (CH), 2858, 1631, 1600, 1501, 1436, 1346, 1247, 1148, 1074, 1014.

HRMS (*m/z* ES): Found: 270.1608 (M⁺. C₁₆H₂₀N₃O Requires: 270.1606).

Purity by HPLC: 95.2% (*t*_R 29.12 min).

***N*-(4-Ethylaminophenyl)-*N'*-(furan-2-ylmethyl)guanidine hydrochloride (72d)**



To a solution of **68d** (90 mg, 0.25 mmol) in a 1:1 mixture of isopropyl alcohol and methylene chloride (630 μl) was added a 4 M solution of HCl in dioxane (377 μl, 1.51 mmol). After 3.5 h stirring at 35 °C, solvents were evaporated and the residue was purified by reverse phase

chromatography (C-8 silica using a 100% H₂O mobile phase). Removal of solvents *in vacuo* at a temperature not exceeding 35 °C afforded the title compound as a yellow hygroscopic gum (70 mg, 84%).

¹H NMR (400 MHz, D₂O): δ7.49 (d, J = 8.5 Hz, 2H, CH Ar.), 7.48 (app s, 1H, CH-O Fur.), 7.40 (d, J = 8.5 Hz, 2H, CH Ar.), 6.29 (app d, J = 3.0 Hz, 2H, 2CH Fur.), 4.47 (s, 2H, NHCH₂), 3.43 (q, J = 7.5 Hz, 2H, CH₂CH₃), 1.27 (t, J = 7.5 Hz, 3H, CH₂CH₃).

^{13}C NMR (100 MHz, D_2O): δ 154.6 (C=N), 148.5 (Cq-O Fur.), 142.9 (CH-O Fur.), 135.6 (Cq Ar.), 132.6 (Cq Ar.), 126.4 (CH Ar.), 123.9 (CH Ar.), 110.1 (CH Fur.), 107.9 (CH Fur.), 46.9 (CH_2CH_3), 37.8 (NHCH $_2$), 9.7 (CH_2CH_3).

IR (neat, cm^{-1}): ν_{max} 3146 (NH), 2943 (CH), 2477, 1656, 1625, 1590, 1513, 1444, 1148 (C-O), 1105 (C-O), 1018.

HRMS (m/z ES): Found: 259.1548 (M^+ . $\text{C}_{14}\text{H}_{19}\text{N}_4\text{O}$ Requires: 259.1599).

Purity by HPLC: 95.7% (t_{R} 22.12 min).

***N*-(3,4-Methylenedioxyphenyl)-*N'*-(furan-2-ylmethyl)guanidine hydrochloride (72e)**



To a solution of **68e** (165 mg, 0.46 mmol) in methylene chloride (4.0 ml) was added a 4 M solution of HCl in dioxane (689 μl , 2.76 mmol). After 4.5 h stirring at rt, solvents were evaporated and the residue was purified by reverse phase chromatography (C-8 silica using a 100% H_2O

mobile phase). Removal of solvents *in vacuo* at a temperature not exceeding 35 $^\circ\text{C}$ afforded the title compound as a yellow hygroscopic solid (88 mg, 65%). Mp: 78 – 82 $^\circ\text{C}$.

^1H NMR (400 MHz, D_2O): δ 7.46 (app s, 1H, CH-O Fur.), 6.84 (d, $J = 8.0$ Hz, 1H, CH Ar.), 6.73 (s, 1H, CH Ar.), 6.71 (d, $J = 8.0$ Hz, 1H, CH Ar.), 6.39 (s, 1H, CH Fur.), 6.37 (s, 1H, CH Fur.), 5.96 (s, 2H, OCH_2O), 4.42 (s, 2H, NHCH $_2$).

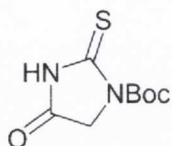
^{13}C NMR (100 MHz, D_2O): δ 155.2 (C=N), 148.7 (Cq Fur.), 147.5 (Cq Ar.), 146.5 (Cq Ar.), 142.8 (CH-O, Fur.), 126.9 (Cq Ar.), 120.0 (CH Ar.), 110.1 (CH Fur.), 108.4 (CH Ar.), 107.7 (CH Fur.), 107.2 (CH Ar.), 101.4 (OCH_2O), 37.6 (NHCH $_2$).

IR (neat, cm^{-1}): ν_{max} 3121, 1596 (C=N), 1501, 1486, 1446, 1346, 1246, 1204 (C-O), 1032, 923.

HRMS (m/z ES): Found: 260.1032 (M^+ . $\text{C}_{13}\text{H}_{14}\text{N}_3\text{O}_3$ Requires: 260.1035).

Purity by HPLC: 97.0% (t_R 23.79 min).

1-*Tert*-butoxycarbonyl-2-thiohydantoin (**82**)



Following Method F, to a cooled solution of 2-thiohydantoin **81** (580 mg, 5.00 mmol) in tetrahydrofuran (25 ml) was added NaH as a 60% suspension in mineral oil (920 mg, 22.50 mmol). After 15 min, di-*tert*-butyldicarbonate was added neat (2400 mg, 11.00 mmol). After 18 h, usual work up followed by chromatography over silica, eluting with hexane:EtOAc, afforded the title compound as an off-white powder (610 mg, 56%). Mp: 148 °C.

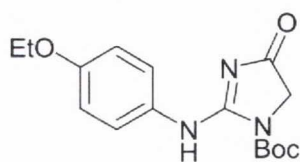
$^1\text{H NMR}$ (400 MHz, CDCl_3): δ 9.28 (s, 1H, NH), 7.29 (s, 2H, CH_2), 1.58 (s, 9H, Boc).

$^{13}\text{C NMR}$ (100 MHz, CDCl_3): δ 178.2 (C=S), 168.1 (NHC=O), 147.9 (C=O Boc), 85.1 (Cq Boc), 52.3 (CH_2), 27.5 (CH_3 Boc).

IR (neat, cm^{-1}): ν_{max} 3160 (NH), 2983, 2923 (CH), 1741 (C=O), 1690 (C=O), 1453, 1344, 1323, 1217, 1144 (C=S), 1059.

HRMS (m/z ES): Found: 239.0466 ($\text{M}^+ + \text{Na}$. $\text{C}_8\text{H}_{12}\text{N}_2\text{O}_3\text{SNa}$ Requires: 239.0463).

2-[(4-Ethoxyphenyl)amino]-1-(*tert*-butoxycarbonyl)imidazolin-4-one (**83**)



Following Method A, HgCl_2 (174 mg, 0.64 mmol) was added over a solution of **82** (95 mg, 0.44 mmol), triethylamine (190 μl , 1.36 mmol), and 4-ethoxyaniline (57 μl , 0.44 mmol) in methylene chloride (2 ml) at 0 °C. The resulting mixture was stirred for 1 h at 0 °C and a further 18 h at room temperature. Usual work up followed by silica gel chromatography, eluting with hexane:EtOAc, afforded the title compound as an off-white solid (125 mg, 90%). Mp: 275 °C (decomp.).

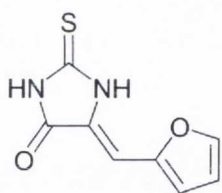
$^1\text{H NMR}$ (400 MHz, CDCl_3): δ 10.24 (br s, 1H, NH), 7.57 (d, $J = 8.5$ Hz, 2H, CH Ar.), 6.90 (d, $J = 8.5$ Hz, 2H, CH Ar.), 4.16 (s, 2H, CH_2), 4.04 (q, $J = 6.5$ Hz, 2H, CH_2CH_3), 1.61 (s, 9H, Boc), 1.44 (t, $J = 6.5$ Hz, 3H, CH_2CH_3).

$^{13}\text{C NMR}$ (100 MHz, CDCl_3): δ 181.6 ($\text{CH}_2\text{C}=\text{O}$), 164.5 (C=N), 156.3 (C=O Boc), 150.8 (Cq Ar.), 128.6 (Cq Ar.), 122.4 (CH Ar.), 114.4 (CH Ar.), 85.1 (Cq Boc), 63.3 (CH_2CH_3), 50.0 (C=O CH_2), 27.6 (CH_3 Boc), 14.3 (CH_2CH_3).

IR (neat, cm^{-1}): ν_{max} 3168 (NH), 2984, 2969 (CH), 2940 (Aryl), 2873, 1740, 1698 (C=O), 1610 (C=O), 1549 (C=N), 1578, 1549, 1509 (Aryl), 1480, 1357, 1278, 1229, 1188, 1155 (C-O), 1134, 1113 (C-O), 1047, 922.

HRMS (m/z ES): Found: 380.2181 ($\text{M}^+ + \text{H}$. $\text{C}_{19}\text{H}_{29}\text{N}_3\text{O}_5\text{Na}$ Requires: 380.2185).

(5Z)-5-(2-Furylmethylene)-2-thioxo-4-imidazolidinone (**84**)



An RBF charged with 2-thiohydantoin **81** (500 mg, 4.30 mmol), distilled H_2O (2.5 ml), and triethylamine (1180 μl , 8.60 mmol) was stirred for 30 min prior to addition of furfural (360 μl ; 4.30 mmol). Reflux at 80 $^\circ\text{C}$ over a period of 18 h was followed by cooling to rt prior to the addition of excess conc. HCl (2 ml, 24.20 mmol). The reaction was stirred for 3 h more, quenched with dropwise sat. NaHCO_3 solution, and diluted with EtOAc (150 ml). The organic phase was washed once with water (150 ml), twice with brine (2 x 150 ml), and then dried using anhydrous MgSO_4 , followed by removal of solvents under vacuum. Purification was carried out by silica gel chromatography using gradient elution (hexane:EtOAc) followed by removal of solvents under vacuum to afford the product as a brown solid (392 mg, 47%), revealed as the *Z* isomer by NMR (NOE experiments). Mp: 270 $^\circ\text{C}$ (Lit. 265 $^\circ\text{C}$).²⁵⁹

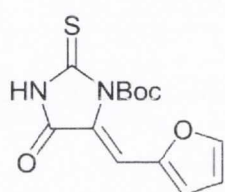
$^1\text{H NMR}$ (400 Hz, DMSO): δ 12.33 (br s, 1H, NH), 12.80 (br s, 1H, NH), 7.83 (d, $J = 2.0$ Hz, 1H, CH-O Fur.), 7.12 (d, $J = 3.4$ Hz, 1H, CH Fur.), 6.65 (dd, $J = 3.4, 2.0$ Hz, 1H, CH Fur.), 6.38 (s, 1H, CH alkene).

^{13}C NMR (100 Hz, DMSO): δ 178.5 (C=S), 165.8 (C=O), 149.3 (Cq Fur.), 146.3 (Cq alkene), 125.9 (CH-O Fur.), 116.0 (CH Fur.), 113.6 (CH Fur.), 99.5 (CH alkene).

IR (neat, cm^{-1}): ν_{max} 3126 (NH), 3099 (NH), 2825 (Aryl), 1717, 1646 (C=O), 1563, 1466, 1358, 1250, 1176 (C=S), 1099.

HRMS (m/z ES): Found: 194.0144 (M^+ . $\text{C}_8\text{H}_6\text{N}_2\text{O}_2\text{S}$ Requires: 190.0150).

(5Z)-5-(2-Furylmethylene)-1-tert-butoxycarbonyl-2-thioxo-4-imidazolidinone (85)



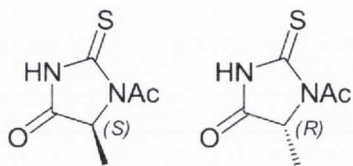
Following Method F, to a cooled solution of **84** (120 mg, 0.62 mmol) in tetrahydrofuran (10 ml) was added NaH as a 60% suspension in mineral oil (112 mg, 2.79 mmol). After 15 min, di-*tert*-butyldicarbonate was added neat (296 mg, 1.36 mmol). After 18 h, usual work up followed by chromatography over silica, eluting with hexane:EtOAc, afforded the title compound as a yellow powder (90 mg, 50%). Mp: 138 - 139 °C.

^1H NMR (400 Hz, DMSO): δ 12.42 (br s, 1H, NH), 7.93 (d, $J = 1.3$ Hz, 1H, CH-O Fur.), 7.22 (d, $J = 3.3$ Hz, 1H, CH Fur.), 6.72 (dd, $J = 3.3, 1.3$ Hz, 1H, CH Fur.), 6.61 (s, 1H, CH alkene), 1.56 (s, 9H, Boc).

^{13}C NMR (100 Hz, DMSO): δ 173.3 (C=S), 161.4 (C=O Boc), 149.3 (NHC=O), 147.1 (CH-O Fur.), 146.7 (Cq Fur.), 123.3 (Cq alkene), 117.7 (CH Fur.), 113.9 (CH Fur.), 102.1 (CH alkene), 86.9 (Cq Boc), 27.7 (CH_3 Boc).

IR (neat, cm^{-1}): ν_{max} 3249, 3125, 3115, 3067 (NH), 2983 (CH), 2929 (Aryl), 1781, 1770, 1754, 1727 (C=O), 1654 (C=N), 1563 (Aryl), 1487, 1448, 1340, 1245, 1149 (C=S), 1125 (C-O), 1015.

HRMS (m/z ES): Found: 317.0565 ($\text{M}^+ + \text{Na}$. $\text{C}_{13}\text{H}_{14}\text{N}_2\text{O}_4\text{SNa}$ Requires: 317.0572).

(*S/R*)-1-Acetyl-5-methyl-2-thioxohydantoin (86 and 86b)

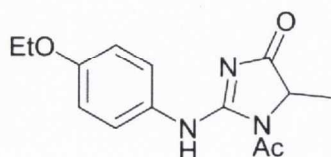
For the preparation of the *S* enantiomer **86**, L-alanine (1.50 g, 16.85 mmol) and potassium thiocyanate (2.72 g, 16.85 mmol) were ground together using a mortar and pestle. The mixed solid was transferred to a round-bottom flask and acetic anhydride (7.96 ml, 84.27 mmol) was added, and the mixture was heated at 75 °C for 45 min. The reaction was terminated by addition of 7 ml cold water (while the vessel was still warm), and the reaction was stored in a freezer overnight. In the morning, the whitish solid precipitate was filtered, washed with water, and air-dried to afford **86** as a white solid (1.64 g, 68%). Mp: 166-168 °C (literature: 165-166 °C).²³⁰ The *R* enantiomer **86b** was prepared from D-alanine using an identical procedure. Spectral and characterisation data matched that of the *S* enantiomer to within experimental limits. Although the enantiomeric excess was not measured in these experiments, a value of 66% has been suggested in the literature.²⁶⁰

¹H NMR (400 MHz, DMSO): δ 12.65 (br s, 1H, NH), 4.64 (q, J = 6.5 Hz, 1H, CHCH₃), 2.70 (s, 3H, Ac), 1.41 (d, J = 6.5 Hz, 3H, CHCH₃).

¹³C NMR (100 MHz, DMSO): δ 182.3 (C=S), 173.9 (C=O), 169.8 (C=O Ac), 58.8 (CHCH₃), 27.4 (CH₃ Ac), 15.9 (CHCH₃).

IR (neat, cm⁻¹): ν_{max} 3394, 3095, 2946, 1743, 1705, 1440, 1331, 1216, 1193, 1095, 1051, 1038, 981, 924.

HRMS (*m/z* ES): Found: 172.0306 (M⁺. C₆H₈N₂O₂S Requires: 172.0306).

1-Acetyl-2-[(4-ethoxyphenyl)amino]-5-methylimidazolinon-4-one (87a)

Following Method A, HgCl₂ (240 mg, 0.88 mmol) was added over a solution of **86** (138 mg, 0.80 mmol), triethylamine (350 μl, 2.49 mmol), and 4-ethoxyaniline (104 μl, 0.80 mmol) in methylene chloride (2 ml) at 0 °C. The resulting mixture was stirred for 1 h at 0 °C and a further 18 h at room temperature. Usual work up followed by

chromatography over alumina, eluting with hexane:EtOAc, afforded the title compound as an off-white solid (156 mg, 71%). Mp: 158 - 160 °C.

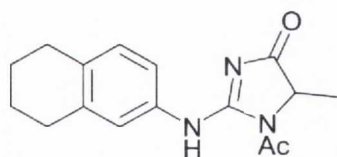
¹H NMR (400 MHz, CDCl₃): δ 11.03 (br s, 1H, NH), 7.52 (d, J = 9.3 Hz, 2H, CH Ar.), 6.84 (d, J = 9.3 Hz, 2H, CH Ar.), 4.25 (q, J = 7.0, 1H, CHCH₃), 3.99 (q, J = 6.9 Hz, 2H, CH₂CH₃), 2.36 (s, 3H, Ac), 1.61 (d, J = 7.0 Hz, 3H, CHCH₃), 1.38 (t, J = 6.9 Hz, 3H, CH₂CH₃).

¹³C NMR (100 MHz, CDCl₃): δ 185.1 (CHC=O), 171.7 (C=O Ac), 164.6 (C=N), 156.9 (Cq Ar.), 128.9 (Cq Ar.), 123.1 (CH Ar.), 114.8 (CH Ar.), 63.7 (CH₂CH₃), 57.6 (CHCH₃), 24.3 (CH₃ Ac), 18.3 (CHCH₃), 14.8 (CH₂CH₃).

IR (neat, cm⁻¹): ν_{max} 3111 (NH), 2992, 2938 (Aryl), 1732, 1669 (C=O), 1611 (C=O), 1575 (C=N), 1542, 1509 (Aryl), 1480, 1371, 1340, 1271, 1244, 1213, 1176 (C-O), 1116 (C-O), 1045, 993.

HRMS (*m/z* ES): Found: 276.1362 (M⁺ + H. C₁₄H₁₈N₃O₃ Requires: 276.1348).

1-Acetyl-5-methyl-2-(5,6,7,8-tetrahydronaphth-2-yl)amino-4-imidazolinone (87b)



Following Method A, HgCl₂ (488 mg, 1.80 mmol) was added over a solution of **86** (281 mg, 1.63 mmol), triethylamine (707 μl, 5.06 mmol), and 2-amino-5,6,7,8-tetrahydronaphthalene (240 mg, 1.63 mmol) in methylene

chloride (3 ml) at 0 °C. The resulting mixture was stirred for 1 h at 0° C and a further 18 h at room temperature. Usual work up followed by chromatography over alumina, eluting with hexane:EtOAc, afforded the title compound as an off-white residue, which was recrystallized from isopropyl alcohol and ether to provide a white solid (280 mg, 60%). Mp: 149 °C.

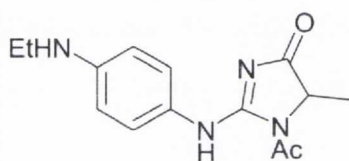
¹H NMR (400 MHz, DMSO): δ 11.01 (br s, 1H, NH), 7.35 (m, 2H, CH Ar.), 7.06 (d, J = 8.0 Hz, 1H, CH Ar.), 4.46 (q, J = 7.0, 1H, CHCH₃), 2.70 (m, 4H, 2CH₂), 2.35 (s, 3H, Ac), 1.72 (m, 4H, 2CH₂), 1.46 (d, J = 7.0 Hz, 3H, CHCH₃).

^{13}C NMR (100 MHz, DMSO): δ 185.5 (CHC=O), 172.5 (C=O Ac), 164.6 (C=N), 137.2 (Cq Ar.), 133.9 (Cq Ar.), 133.8 (Cq Ar.), 129.4 (CH Ar.), 121.7 (CH Ar.), 119.0 (CH Ar.), 57.1 (CHCH₃), 28.9 (CH₂), 28.3 (CH₂), 24.2 (CH₃ Ac), 22.7 (CH₂), 22.6 (CH₂), 17.6 (CHCH₃).

IR (neat, cm⁻¹): ν_{max} 3181 (NH), 2924 (Aryl), 1727, 1664 (C=O), 1596 (C=N), 1536, 1500 (Aryl), 1376, 1335, 1227, 1244, 1210, 1154, 997.

HRMS (*m/z* ES): Found: 244.1443 ([M - C₂HO]⁺. C₁₄H₁₈N₃O Requires: 244.1450).

1-Acetyl-2-(4-ethylaminophenyl)amino-5-methyl-4-imidazolinone (87c)



Following Method A, HgCl₂ (1535 mg, 5.66 mmol) was added over a solution of **86** (885 mg, 5.15 mmol), triethylamine (2230 μ l, 15.96 mmol), and **105** (1060 μ l, 5.15 mmol) in methylene chloride (15 ml) at 0 °C. The resulting mixture was stirred for 1 h at 0° C and a further 18 h at room temperature. Usual work up followed by chromatography over alumina, eluting with hexane:EtOAc, afforded the title compound as a pink solid (226 mg, 16%). Mp: 195 °C.

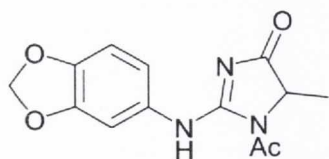
^1H NMR (400 MHz, CDCl₃): (400 MHz, DMSO): δ 10.81 (br s, 1H, NH), 7.30 (d, J = 9.0 Hz, 2H, CH Ar.), 6.54 (d, J = 9.0 Hz, 2H, CH Ar.), 5.61 (br t, J = 6.0 Hz, 1H, NH_{Et}), 4.43 (q, J = 7.0 Hz, 1H, CHCH₃), 3.01 (quintet, J = 6.0 Hz, 2H, CH₂CH₃), 2.32 (s, 3H, Ac), 1.44 (d, J = 7.0 Hz, 3H, CHCH₃), 1.15 (q, J = 6.0 Hz, 3H, CH₂CH₃).

^{13}C NMR (100 MHz, DMSO): δ 185.3 (CHC=O), 172.3 (C=O Ac), 164.3 (C=N), 146.9 (Cq Ar.), 125.0 (Cq Ar.), 123.2 (CH Ar.), 111.7 (CH Ar.), 57.3 (CHCH₃), 37.4 (CH₂CH₃), 24.1 (CH₃ Ac), 17.7 (CHCH₃), 14.3 (CH₂CH₃).

IR (neat, cm⁻¹): ν_{max} 3309 (NH), 3142 (NH), 2975 (Aryl), 2984, 1734, 1662 (C=O), 1604 (C=N), 1576, 1517, 1480 (Aryl), 1372, 1290, 1207, 1183, 1152.

HRMS (*m/z* ES): Found: 233.1403 ([M - C₂HO]⁺. C₁₂H₁₇N₄O Requires: 233.1402).

1-Acetyl-2-(benzo[d][1,3]dioxol-5-amino)-5-methyl-4-imidazolinone (87d)



Following Method A, HgCl₂ (501 mg, 1.85 mmol) was added over a solution of **86** (289 mg, 1.68 mmol), triethylamine (727 μl, 5.20 mmol), and 3,4-methylenedioxyaniline (230 mg, 1.68 mmol) in methylene chloride (3 ml) at 0 °C. The resulting mixture was stirred for 1 h at 0° C and a further 18 h at room temperature. Usual work up followed by chromatography over alumina, eluting with hexane:EtOAc, afforded the title compound as a brown solid (155 mg, 33%). Mp: 275 °C.

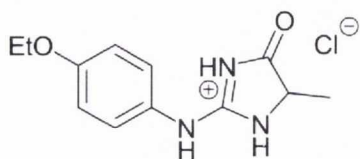
¹H NMR (400 MHz, DMSO): δ10.95 (br s, 1H, NH), 7.37 (s, 1H, CH Ar.), 7.05 (d, J = 8.0 Hz, 1H, CH Ar.), 6.93 (d, J = 8.0 Hz, 1H, CH Ar.), 6.05 (s, 2H, OCH₂O), 4.47 (q, J = 7.0 Hz, 1H, CHCH₃), 2.34 (s, 3H, Ac), 1.46 (d, J = 7.0 Hz, CHCH₃).

¹³C NMR (100 MHz, DMSO): δ185.3 (CHC=O), 172.3 (C=O Ac), 164.8 (C=N), 147.3 (Cq Ar.), 144.7 (Cq Ar.), 130.7 (Cq Ar.), 115.3 (CH Ar.), 108.0 (CH Ar.), 103.9 (CH Ar.), 57.3 (CHCH₃), 24.2 (CH₃ Ac), 17.6 (CHCH₃).

IR (neat, cm⁻¹): ν_{max} 2906 (Aryl), 1736, 1668 (C=O), 1581 (C=N), 1541, 1486 (Aryl), 1375, 1337, 1287, 1207, 1032, 996, 925.

HRMS (*m/z* ES): Found: 234.0869 ([M - C₂HO]⁺. C₁₁H₁₂N₃O₃ Requires: 234.0879).

1-Acetyl-2-[(4-ethoxyphenyl)amino]-5-methylimidazolinon-4-one hydrochloride (88a)



To a solution of **87a** (28 mg, 0.10 mmol) in methanol (0.3 ml) was added a 4 M solution of HCl in dioxane (150 μl, 0.60 mmol). After 3.5 h stirring at 35 °C, solvents were evaporated and the residue was purified by reverse phase chromatography (C-8 silica using a 100% H₂O mobile phase). Removal of solvents afforded the title compound as a white solid (27 mg, 99%). Mp: 246 – 248 °C.

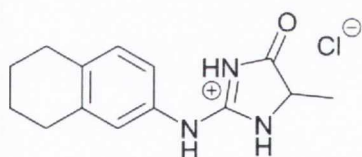
¹H NMR (400 MHz, D₂O): δ7.30 (d, J = 7.5 Hz, 2H, CH Ar.), 7.06 (d, J = 7.5 Hz, 2H, CH Ar.), 4.39 (q, J = 6.5 Hz, 1H, CHCH₃), 4.11 (q, J = 7.0 Hz, 2H, CH₂CH₃), 1.41 (d, J = 6.5 Hz, 3H, CHCH₃), 1.36 (t, J = 7.0 Hz, 3H, CH₂CH₃).

¹³C NMR (100 MHz, D₂O): δ177.1 (C=N), 157.9 (CHC=O), 155.8 (Cq Ar.), 126.7 (CH Ar.), 124.9 (Cq Ar.), 115.4 (CH Ar.), 64.1 (CH₂CH₃), 55.1 (CHCH₃), 14.7 (CHCH₃), 13.3 (CH₂CH₃).

IR (neat, cm⁻¹): ν_{max} 3105 (NH), 2987 (Aryl), 1772, 1686 (C=O), 1601, 1585 (C=N), 1512, 1442, 1390, 1238, 1177 (C-O), 1040.

HRMS (*m/z* ES): Found: 234.1239 (M⁺. C₁₂H₁₆N₃O₂ Requires: 234.1243).

1-Acetyl-5-methyl-2-(5,6,7,8-tetrahydronaphth-2-yl)amino-4-imidazolinone hydrochloride (88b)



To a solution of **87b** (100 mg, 0.35 mmol) in methanol (1.5 ml) was added a 4 M solution of HCl in dioxane (528 μl, 2.11 mmol). After 2.5 h stirring at 35 °C, solvents were evaporated and the residue was purified by reverse phase chromatography (C-8 silica using a 100% H₂O mobile phase). Removal of solvents afforded the title compound as a white solid (98 mg, 99%). Mp: 254 – 256 °C.

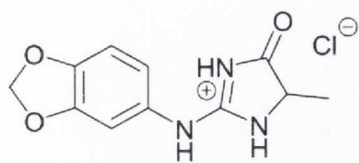
¹H NMR (400 MHz, D₂O): δ7.21 (d, J = 7.5 Hz, 1H, CH Ar.), 7.04 – 7.09 (m, 2H, CH₂), 4.39 (q, J = 7.0 Hz, 1H, CHCH₃), 2.75 (m, 4H, 2CH₂), 1.74 (m, 4H, 2CH₂), 1.42 (d, J = 7.0 Hz, CHCH₃).

¹³C NMR (100 MHz, D₂O): δ177.0 (C=N), 155.3 (CHC=O), 139.1 (Cq Ar.), 138.1 (Cq Ar.), 130.1 (CH Ar.), 129.2 (Cq Ar.), 124.9 (CH Ar.), 121.5 (CH Ar.), 55.1 (CHCH₃), 28.2 (CqCH₂CH₂), 28.0 (CqCH₂CH₂), 21.9 (CqCH₂CH₂), 21.8 (CqCH₂CH₂), 14.7 (CHCH₃).

IR (neat, cm⁻¹): ν_{max} 2935 (Aryl), 1773, 1677 (C=O), 1608 (C=N), 1576, 1441 (Aryl), 1271, 1230, 1185, 1047.

HRMS (m/z ES): Found: 244.1440 (M^+ . $C_{14}H_{18}N_3O$ Requires: 244.1450).

1-Acetyl-2-(benzo[*d*][1,3]dioxol-5-amino)-5-methyl-4-imidazolinone hydrochloride (88d)



To a solution of **87d** (75 mg, 0.27 mmol) in methanol (1.0 ml) was added a 4 M solution of HCl in dioxane (409 μ l, 1.64 mmol). After 3.5 h stirring at 35 °C, solvents were evaporated and the residue was purified by reverse phase chromatography (C-8 silica using a 100% H_2O mobile phase). Removal of solvents afforded the title compound as a white solid (54 mg, 74%). Mp: 80 °C.

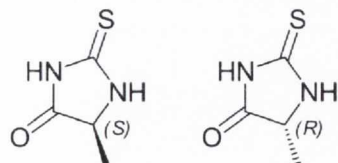
1H NMR (400 MHz, D_2O): δ 6.81 – 6.87 (m, 3H, CH Ar.), 5.95 (s, 2H, OCH_2O), 4.33 (q, $J = 6.7$ Hz, 1H, $CHCH_3$), 1.34 (d, $J = 6.7$ Hz, 3H, $CHCH_3$).

^{13}C NMR (100 MHz, D_2O): δ 176.6 (C=N), 155.5 ($CHC=O$), 147.7 (Cq Ar.), 147.2 (Cq Ar.), 125.4 (Cq Ar.), 119.1 (CH Ar.), 108.5 (CH Ar.), 106.2 (CH Ar.), 101.7 (OCH_2O), 55.1 ($CHCH_3$), 14.7 ($CHCH_3$).

IR (neat, cm^{-1}): ν_{max} 2903 (Aryl), 1775, 1668 (C=O), 1587 (C=N), 1501, 1488 (Aryl), 1450, 1246, 1185, 1031.

HRMS (m/z ES): Found: 234.0883 (M^+ . $C_{11}H_{12}N_3O_3$ Requires: 234.0879).

(*S* and *R*)-5-Methyl-2-thiohydantoin (89 and 89b, respectively)



For the preparation of the *S* enantiomer **89**, the starting *N*-acetyl thiohydantoin **86** (750 mg, 4.36 mmol) was suspended in a 4.5 M solution of hydrochloric acid (14.5 ml, 65.41 mmol) and heated in a microwave at 150 °C for 5 min. The reaction was allowed to cool to rt and extracted 4 times with EtOAc (4 x 10 ml). The combined organic phase was dried over $MgSO_4$, filtered, and evaporated to dryness *in vacuo* (using cyclohexane to assist in the azeotropic removal of the acetic acid side-product) to afford the

product as a white solid (560 mg, 99%). Mp: 165 °C (literature: 164 – 165 °C).²⁶¹ The *R* enantiomer **89b** was prepared from **86b** using an identical procedure (544 mg, 96%). Spectral and characterisation data matched that of the *S* enantiomer within experimental limits. The enantiomeric excess was not measured in these experiments.

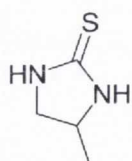
¹H NMR (400 MHz, DMSO): δ 11.64 (s, 1H, NH), 10.02 (s, 1H, NH), 4.22 (q, J = 7.0 Hz, 1H, CHCH₃), 1.23 (d, J = 7.0 Hz, CHCH₃).

¹³C NMR (100 MHz, DMSO): δ 182.0 (C=S), 177.3 (C=O), 56.3 (CHCH₃), 16.1 (CHCH₃).

IR (neat, cm⁻¹): ν_{max} 3154 (NH), 3100 (NH), 2899, 1739, 1541, 1405, 1386, 1301, 1176, 1090, 1036, 924, 781.

HRMS (*m/z* ES): Found: 129.0128 (M⁻ - H). C₄H₅N₂OS Requires: 129.0123).

(*S/R*)-4-Methylimidazolidine-2-thione (**90**)



To a solution of **89** (415 mg, 3.19 mmol) in tetrahydrofuran (27.5 ml) under argon at 0 °C was added 10.0 M borane dimethyl sulfide complex (4.47 ml, 44.69 mmol). The mixture was warmed to 85 °C and a vacuum was applied to the top of the condenser; outgoing gas was bubbled through 10% aqueous H₂O₂. After 1 h, the system was repressurised using argon, and the reaction was allowed to proceed for 16 h at 85 °C. The reaction was cooled to rt and quenched by dropwise addition of 1.25 M methanolic HCl (8.94 ml, 11.2 mmol), then heated to 85 °C for an additional 1 h. The mixture was cooled to rt and made basic with saturated NaHCO₃ solution (35 ml), and extracted three times with EtOAc (3 x 50 ml). The organic layers were combined, washed with brine (50 ml), dried over MgSO₄, filtered, and solvents removed *in vacuo*. The product was isolated by chromatography on silica gel (hexane/EtOAc) followed by removal of solvents to afford the product as a white solid (196 mg, 53%). Mp: 96 – 98 °C (literature: 100 °C).²⁶² Preparation of the Mosher's acid derivatives **96r** and **96s** confirmed the product to be racemic.

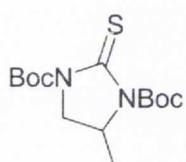
$^1\text{H NMR}$ (400 MHz, CDCl_3): δ 6.40 (br s, 1H, NH), 6.30 (br s, 1H, NH), 4.17 (m, 1H, CHCH_3), 3.86 (t, $J = 9.5$ Hz, 1H, CH_2), 3.32 (t, $J = 9.5$ Hz, 1H, CH_2), 1.32 (d, $J = 6.5$ Hz, 3H, CHCH_3).

$^{13}\text{C NMR}$ (100 MHz, CDCl_3): δ 182.4 (C=S), 52.7 (CH), 51.5 (CH_2), 20.3 (CH_3).

IR (neat, cm^{-1}): ν_{max} 3207, 2972, 2887, 1737, 1526, 1487, 1470, 1371, 1300, 1269, 1197, 1047, 1019.

HRMS (m/z ES): Found: 117.0487 ($\text{M}^+ + \text{H}$. $\text{C}_4\text{H}_9\text{N}_2\text{S}$ Requires: 117.0486).

1,3-Di(*tert*-butoxycarbonyl)-4-methylimidazolidine-2-thione (91)



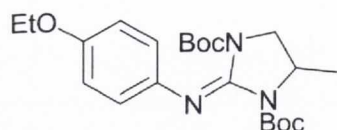
Following Method F, to a cooled solution of **90** (205 mg, 1.77 mmol) in tetrahydrofuran (20 ml) was added NaH as a 60% suspension in mineral oil (318 mg, 7.95 mmol). After 15 min, di-*tert*-butyldicarbonate was added neat (848 mg, 3.89 mmol). After 2.5 h, usual work up followed by chromatography over silica, eluting with hexane:EtOAc, afforded the title compound as a viscous yellow oil, which crystallised over several days to form a bright yellow solid (452 mg, 81%). Mp: 80 - 82 °C.

$^1\text{H NMR}$ (400 MHz, CDCl_3): δ 4.35 (m, 1H, CHCH_3), 3.94 (t, $J = 9.8$ Hz, 1H, CH_2), 3.57 (dd, $J = 9.8, 2.5$ Hz, 1H, CH_2), 1.55 (br s, 18H, Boc), 1.38 (d, $J = 6.0$ Hz, 3H, CHCH_3).

$^{13}\text{C NMR}$ (100 MHz, CDCl_3): δ 174.6 (C=S), 150.1 (C=O Boc), 149.7 (C=O Boc), 83.5 (Cq Boc), 83.4 (Cq Boc), 51.6 (CHCH_3), 51.4 (CH_2), 27.6 (2 x CH_3 Boc), 19.5 (CHCH_3).

IR (neat, cm^{-1}): ν_{max} 2980, 2935, 1753, 1737, 1366, 1271, 1249, 1142, 1047, 1004.

HRMS (m/z ES): Found: 339.1349 ($\text{M}^+ + \text{Na}$. $\text{C}_{14}\text{H}_{24}\text{N}_2\text{O}_4\text{NaS}$ Requires: 339.1354).

2-[(4-Ethoxyphenyl)imino]-5-methyl-1,3-di(*tert*-butoxycarbonyl)imidazolidine (92a)

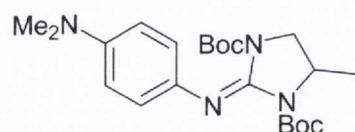
Following Method A, HgCl_2 (221 mg, 0.82 mmol) was added over a solution of **91** (215 mg, 0.68 mmol), 4-ethoxyaniline (96 μl , 0.75 mmol) and triethylamine (426 μl , 3.06 mmol) in methylene chloride (3.0 ml) at 0 °C. The resulting mixture was stirred for 1 h at 0° C and a further 16 h at room temperature. Usual work up followed by chromatography over aluminium oxide, eluting with hexane:EtOAc, afforded the title compound as a white solid (184 mg, 65%). Mp: 96 °C.

^1H NMR (400 MHz, CDCl_3): δ 6.91 (d, $J = 8.6$ Hz, 2H, CH Ar.), 6.74 (d, $J = 8.6$ Hz, 2H, CH Ar.), 4.23 (m, 1H, CHCH_3), 3.94 (q, $J = 6.0$ Hz, 2H, CH_2CH_3), 3.76 (dd, $J = 10.5, 7.8$ Hz, 1H, CHCH_2), 3.53 (d, $J = 10.5$ Hz, 1H, CHCH_2), 1.35 – 1.22 (m, 24H, CH_2CH_3 , CHCH_3 , 2 x Boc).

^{13}C NMR (100 MHz, CDCl_3): δ 154.2 (Cq Ar.), 150.3 (C=O), 149.6 (C=O), 141.2 (C=N), 138.2 (Cq Ar.), 121.9 (CH Ar.), 114.2 (CH Ar.), 82.0 (Cq Boc), 81.9 (Cq Boc), 63.2 (CH_2CH_3) 50.1 (CHCH_2) 49.3 (CHCH_2), 27.5 (CH_3 Boc), 27.4 (CH_3 Boc), 19.6 (CHCH_3) 14.4 (CH_2CH_3).

IR (neat, cm^{-1}): ν_{max} 2978 (CH), 2929 (CH), 1755 (C=O), 1694 (C=O), 1504 (C=N), 1479, 1396, 1326, 1298, 1236, 1149 (C-O), 1115, 1018, 961.

HRMS (m/z ES): Found: 420.2492 ($\text{M}^+ + \text{H}$. $\text{C}_{22}\text{H}_{34}\text{N}_3\text{O}_5$ Requires: 420.2498).

2-[(4-Dimethylaminophenyl)imino]-5-methyl-1,3-di(*tert*-butoxycarbonyl)imidazolidine (92b)

Following Method A, HgCl_2 (208 mg, 0.77 mmol) was added over a solution of **91** (202 mg, 0.64 mmol), 4-(dimethylamino)aniline (96 mg, 0.70 mmol) and triethylamine (401 μl , 2.88 mmol) in methylene chloride (3.0 ml) at 0 °C. The resulting mixture was stirred for 1 h at 0° C and a further 16 h at room temperature. Usual work up followed by

chromatography over aluminium oxide, eluting with hexane:EtOAc, afforded the title compound as a brown solid (209 mg, 78%). Mp: 134 - 136 °C.

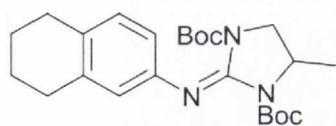
¹H NMR (400 MHz, CDCl₃): δ6.93 (d, J = 9.0 Hz, 2H, CH Ar.), 6.67 (d, J = 9.0 Hz, 2H, CH Ar.), 4.26 (m, 1H, CHCH₃), 3.77 (dd, J = 10.5, 7.5 Hz, 1H, CHCH₂), 3.56 (d, J = 10.5 Hz, 1H, CHCH₂), 2.85 (s, 6H, N(CH₃)₂), 1.37 – 1.27 (m, 21H, CHCH₃, 2 x Boc).

¹³C NMR (100 MHz, CDCl₃): δ150.5 (C=O), 149.8 (C=O), 146.7 (C=N), 138.6 (Cq Ar.), 137.5 (Cq Ar.), 121.9 (CH Ar.), 113.6 (CH Ar.), 81.9 (Cq Boc), 81.8 (Cq Boc), 50.0 (CHCH₂) 49.2 (CHCH₂), 41.1 (N(CH₃)₂), 27.5 (CH₃ Boc), 27.4 (CH₃ Boc), 19.7 (CHCH₃).

IR (neat, cm⁻¹): ν_{max} 2978 (CH), 2933 (CH), 1752 (C=O), 1693 (C=O), 1513 (C=N), 1366, 1325, 1299, 1018, 961, 947.

HRMS (*m/z* ES): Found: 419.2647 (M⁺ + H. C₂₂H₃₅N₄O₄ Requires: 419.2558).

1,3-Di(*tert*-butoxycarbonyl)-5-methyl-2-(5,6,7,8-tetrahydronaphth-2-yl)iminoimidazolidine (92c)



Following Method A, HgCl₂ (236 mg, 0.87 mmol) was added over a solution of **91** (220 mg, 0.70 mmol), 2-amino-5,6,7,8-tetrahydronaphthalene (128 mg, 0.87 mmol) and triethylamine (340 μl, 2.47 mmol) in methylene chloride (3.0 ml) at 0 °C. The resulting mixture was stirred for 1 h at 0° C and a further 16 h at room temperature. Usual work up followed by chromatography over aluminium oxide, eluting with hexane:EtOAc, afforded the title compound as an off-white solid (263 mg, 88%). Mp: 50 – 52 °C.

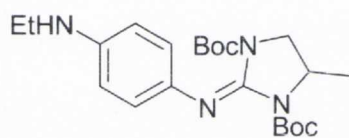
¹H NMR (400 MHz, CDCl₃): δ6.88 (d, J = 8.0 Hz, 1H, CH Ar.), 6.69 (d, J = 8.0 Hz, 1H, CH Ar.), 6.66 (s, 1H, CH Ar.), 4.23 (m, 1H, CHCH₂), 3.77 (dd, J = 10.5, 7.0 Hz, 1H, CHCH₂), 3.52 (d, J = 10.5 Hz, 1H, CHCH₂), 2.64 (br s, 4H, 2 x CH₂), 1.71 (br s, 4H, 2 x CH₂), 1.36 (d, J = 7.0 Hz, 3H, CHCH₃), 1.34 (s, 9H, Boc), 1.24 (s, 9H, Boc).

¹³C NMR (100 MHz, CDCl₃): δ150.3 (C=O), 149.7 (C=O), 145.1 (C=N), 138.1 (Cq Ar.), 136.3 (Cq Ar.), 130.8 (Cq Ar.), 128.6 (CH Ar.), 121.4 (CH Ar.), 118.3 (CH Ar.), 82.1 (Cq Boc), 81.9 (Cq Boc), 50.1 (CHCH₂), 49.2 (CHCH₂), 29.1 (CqCH₂CH₂), 28.4 (CqCH₂CH₂), 27.5 (CH₃ Boc), 27.3 (CH₃ Boc), 23.1 (CqCH₂CH₂), 22.9 (CqCH₂CH₂), 19.6 (CHCH₃).

IR (neat, cm⁻¹): ν_{max} 2980 (CH), 2931 (CH), 1752 (C=O), 1698 (C=O), 1367, 1302, 1252, 1147, 1020, 964, 909, 726.

HRMS (*m/z* ES): Found: 430.2721 (M⁺ + H. C₂₄H₃₆N₃O₄ Requires: 430.2706).

2-[(4-Ethylaminophenyl)imino]-5-methyl-1,3-di(*tert*-butoxycarbonyl)imidazolidine (92d)



Following Method A, HgCl₂ (311 mg, 1.15 mmol) was added over a solution of **91** (303 mg, 0.96 mmol), **105** (140 μl, 1.05 mmol) and triethylamine (726 μl, 4.30 mmol) in methylene chloride (4.0 ml) at 0 °C. The resulting mixture was stirred for 1 h at 0° C and a further 16 h at room temperature. Usual work up followed by chromatography over aluminium oxide, eluting with hexane:EtOAc, afforded the title compound as an amorphous brown tar (261 mg, 65%).

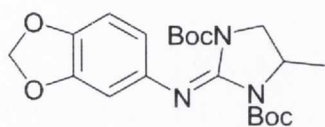
¹H NMR (400 MHz, CDCl₃): δ6.87 (d, J = 8.5 Hz, 2H, CH Ar.), 6.51 (d, J = 8.5 Hz, 2H, CH Ar.), 4.25 (m, 1H, CHCH₃), 3.77 (dd, J = 10.5, 7.5 Hz, 1H, CHCH₂), 3.53 (d, J = 10.5 Hz, 1H, CHCH₂), 3.16 (br s, 1H, NH), 3.09 (q, J = 7.0 Hz, 2H, CH₂CH₃), 1.37 – 1.26 (m, 21H, CHCH₃, 2 x Boc), 1.20 (t, J = 7.0 Hz, 3H, CH₂CH₃).

¹³C NMR (100 MHz, CDCl₃): δ150.4 (C=O), 149.7 (C=O), 143.9 (Cq Ar.), 138.4 (C=N), 137.2 (Cq Ar.), 122.0 (CH Ar.), 112 .8 (CH Ar.), 81.8 (Cq Boc), 81.7 (Cq Boc), 49.9 (CHCH₂) 49.1 (CHCH₂), 38.6 (CH₂CH₃), 27.4 (CH₃ Boc), 27.3 (CH₃ Boc), 19.5 (CHCH₃) 14.3 (CH₂CH₃).

IR (neat, cm⁻¹): ν_{max} 3384 (NH), 2975 (CH), 2931 (CH), 1745 (C=O), 1691 (C=O), 1512 (C=N), 1479, 1366, 1324, 1299, 1248, 1147 (C-O), 1018, 961.

HRMS (m/z ES): Found: 419.2657 ($M^+ + H$, $C_{22}H_{35}N_4O_4$ Requires: 419.2658).

2-(Benzo[*d*][1,3]dioxol-5-imino)-5-methyl-1,3-di(*tert*-butoxycarbonyl)imidazolidine (92e)



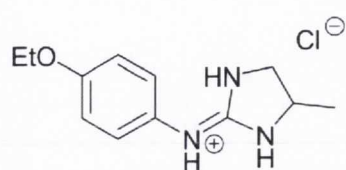
Following Method A, $HgCl_2$ (221 mg, 0.82 mmol) was added over a solution of **91** (215 mg, 0.68 mmol), 3,4-methylenedioxyaniline (102 mg, 0.75 mmol) and triethylamine (426 μ l, 3.06 mmol) in methylene chloride (3.0 ml) at 0 °C. The resulting mixture was stirred for 1 h at 0° C and a further 16 h at room temperature. Usual work up followed by chromatography over aluminium oxide, eluting with hexane:EtOAc, afforded the title compound as a white solid (196 mg, 69%). Mp: 54 - 56 °C.

1H NMR (400 MHz, $CDCl_3$): δ 6.64 (d, $J = 8.5$ Hz, 1H, CH Ar.), 6.52 (s, 1H, CH Ar.), 6.43 (d, $J = 8.5$ Hz, 1H, CH Ar.), 5.83 (app d, $J = 11.6$ Hz, 2H, OCH_2O), 4.22 (m, 1H, $CHCH_3$), 3.76 (dd, $J = 10.6, 7.5$ Hz, 1H, $CHCH_2$), 3.51 (d, $J = 10.6$ Hz, 1H, $CHCH_2$), 1.36 – 1.28 (m, 21H, $CHCH_3$, 2 x Boc).

^{13}C NMR (100 MHz, $CDCl_3$): δ 150.1 (C=O), 149.5 (C=O), 147.1 (C=N), 142.5 (Cq Ar.), 142.4 (Cq Ar.), 138.6 (Cq Ar.), 113.6 (CH Ar.), 107.5 (CH Ar.), 102.6 (CH Ar.), 100.2 (OCH_2O), 82.1 (Cq Boc), 82.0 (Cq Boc), 50.1 ($CHCH_2$), 49.3 ($CHCH_2$), 27.5 (CH_3 Boc), 27.4 (CH_3 Boc), 19.6 ($CHCH_3$).

IR (neat, cm^{-1}): ν_{max} 2979 (CH), 2933 (CH), 1753 (C=O), 1697 (C=O), 1502 (C=N), 1484, 1396, 1324, 1276, 1244, 1147 (C-O), 1036, 1018, 963, 928.

HRMS (m/z ES): Found: 420.2154 ($M^+ + H$, $C_{21}H_{30}N_3O_6$ Requires: 420.2135).

4-Ethoxy-*N*-(4-methylimidazolidin-2-ylidene)aniline hydrochloride (93a)

Following Method G, **92a** (170 mg, 0.41 mmol) was treated with 25 equivalents of a 4 M solution of HCl in dioxane (2.53 ml, 10.13 mmol). After 3.5 h stirring at 55 °C, the reaction was adjudged complete (TLC, MS), solvents were evaporated, and the residue was purified by reverse phase chromatography (C-8 silica using a 100% H₂O mobile phase). Removal of solvents under vacuum afforded the title compound as a clear hygroscopic gum (79 mg, 76%).

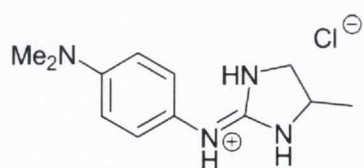
¹H NMR (400 MHz, D₂O): δ7.20 (d, J = 9.0 Hz, 2H, CH Ar.), 6.99 (d, J = 9.0 Hz, 2H, CH Ar.), 4.15 (m, 1H, CHCH₃), 4.08 (q, J = 7.0 Hz, 2H, CH₂CH₃), 3.81 (t, J = 9.5 Hz, 1H, CHCH₂), 3.28 (dd, J = 9.5, 7.0 Hz, 1H, CHCH₂), 1.34 (t, J = 7.0 Hz, 3H, CH₂CH₃), 1.27 (d, J = 6.0 Hz, 3H, CHCH₃).

¹³C NMR (100 MHz, D₂O): δ157.6 (C_q Ar.), 156.8 (C=N), 127.4 (C_q Ar.), 126.2 (CH Ar.), 115.1 (CH Ar.), 64.1 (CH₂CH₃), 51.0 (CHCH₂), 49.0 (CHCH₂), 19.1 (CHCH₃), 13.4 (CH₂CH₃).

IR (neat, cm⁻¹): ν_{max} 3138 (NH), 2976 (CH), 2931, 1646, 1606, 1586 (C=N), 1511, 1477, 1240, 1175, 1115, 1043, 1011, 922.

HRMS: (*m/z* ES): Found: 220.1443 (M⁺. C₁₂H₁₈N₃O Requires: 220.1450).

Purity by HPLC: 99.3% (*t_R* 23.91 min).

4-Dimethylamino-*N*-(4-methylimidazolidin-2-ylidene)aniline hydrochloride (93b)

Following Method G, **92b** (201 mg, 0.48 mmol) was treated with 22 equivalents of a 4 M solution of HCl in dioxane (2.64 ml, 10.57 mmol). After 3.5 h stirring at 55 °C, the reaction was adjudged complete (TLC, MS), solvents were evaporated, and the residue was purified by silica chromatography (gradient elution from

100% methylene chloride to 1:1 methylene chloride/CMA). Solvents were removed under vacuum and the residue was dissolved in 1.25 M methanolic HCl. Solvents were once more evaporated *in vacuo*, followed by reverse phase chromatography (C-8 silica using a 100% H₂O mobile phase). Removal of solvents under vacuum afforded the title compound as an off-white hygroscopic gum (99 mg, 71%).

¹H NMR (400 MHz, D₂O): δ 7.66 (d, J = 9.0 Hz, 2H, CH Ar.), 7.45 (d, J = 9.0 Hz, 2H, CH Ar.), 4.20 (m, 1H, CHCH₃), 3.85 (t, J = 10.0 Hz, 1H, CHCH₂), 3.25 (dd, J = 10.0, 7.0 Hz, 1H, CHCH₂), 3.27 (s, 6H, N(CH₃)₂), 1.27 (d, J = 6.0 Hz, 3H, CHCH₃).

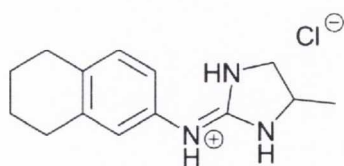
¹³C NMR (100 MHz, D₂O): δ 156.7 (C=N), 139.7 (C_q Ar.), 136.4 (C_q Ar.), 125.1 (CH Ar.), 121.7 (CH Ar.), 51.1 (CHCH₂), 49.1 (CHCH₂), 46.0 (N(CH₃)₂), 19.3 (CHCH₃).

IR (neat, cm⁻¹): ν_{max} 3127 (NH), 2971 (CH), 1643, 1600, 1517 (C=N), 1380, 1134, 1063, 996.

HRMS: (*m/z* ES): Found: 219.1600 (M⁺. C₁₂H₁₉N₄ Requires: 219.1610).

Purity by HPLC: 99.0% (*t_R* 18.83 min).

2-Amino-*N*-(4-methylimidazolidin-2-ylidene)-5,6,7,8-tetrahydronaphthalene hydrochloride (93c)



Following Method G, **92c** (125 mg, 0.29 mmol) was treated with 25 equivalents of a 4 M solution of HCl in dioxane (1.82 ml, 7.27 mmol). After 3.5 h stirring at 55 °C, the reaction was adjudged complete (TLC, MS), solvents were evaporated, and the residue was purified by reverse phase chromatography (C-8 silica using a 100% H₂O mobile phase). Removal of solvents under vacuum afforded the title compound as a white solid (57 mg, 73%). Mp: 78 – 82 °C.

¹H NMR (400 MHz, D₂O): δ 7.12 (d, J = 8.5 Hz, 1H, CH Ar.), 6.93 (d, J = 8.5 Hz, 1H, CH Ar.), 6.92 (s, 1H, CH Ar.), 4.16 (m, 1H, CHCH₃), 3.81 (t, J = 9.6 Hz, 1H, CHCH₂), 3.29 (dd,

$J = 9.5$ Hz, 7.0 Hz, 1H , CHCH_2), 2.69 (s, 4H , 2CH_2), 1.71 (s, 4H , 2CH_2), 1.27 (d, $J = 6.0$ Hz, 3H , CHCH_3).

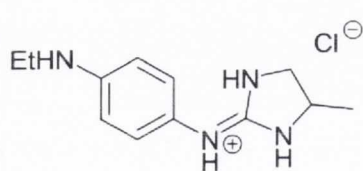
^{13}C NMR (100 MHz, D_2O): $\delta 156.9$ (C=N), 138.6 (Cq Ar.), 136.2 (Cq Ar.), 131.6 (Cq Ar.), 129.8 (CH Ar.), 123.7 (CH Ar.), 120.5 (CH Ar.), 50.9 (CHCH_3), 49.0 (CHCH_2), 28.3 (Cq CH_2CH_2), 27.9 (Cq CH_2CH_2), 22.0 (Cq CH_2CH_2), 21.9 (Cq CH_2CH_2), 19.2 (CHCH_3).

IR (neat, cm^{-1}): ν_{max} 3148 (NH), 2927 (CH), 1648 , 1607 , 1581 , 1505 , 1379 , 1338 , 1266 , 1247 , 1135 , 1065 .

HRMS: (m/z ES): Found: 230.1651 (M^+ . $\text{C}_{14}\text{H}_{20}\text{N}_3$ Requires: 230.1657).

Purity by HPLC: 98.3% (t_R 26.92 min).

4-Ethylamino-*N*-(4-methylimidazolidin-2-ylidene)aniline hydrochloride (93d)



Following Method G, **92d** (258 mg, 0.62 mmol) was treated with 25 equivalents of a 4 M solution of HCl in dioxane (3.84 ml, 15.38 mmol). After 4 h stirring at 55 °C, the reaction was adjudged complete (TLC, MS), solvents were evaporated, and the residue was purified by reverse phase chromatography (C-8 silica using a 100% H_2O mobile phase). Removal of solvents under vacuum afforded the title compound as a white hygroscopic gum (161 mg, 90%).

^1H NMR (400 MHz, D_2O): $\delta 7.47$ (d, $J = 8.6$ Hz, 2H , CH Ar.), 7.36 (d, $J = 8.6$ Hz, 2H , CH Ar.), 4.13 (m, 1H , CHCH_3), 3.78 (t, $J = 9.2$ Hz, 1H , CHCH_2), 3.39 (q, $J = 6.8$ Hz, 2H , CH_2CH_3), 3.25 (dd, $J = 9.2$, 6.8 Hz, 1H , CHCH_2), 1.21 (app t, $J = 6.8$ Hz, 6H , CHCH_3 + CH_2CH_3).

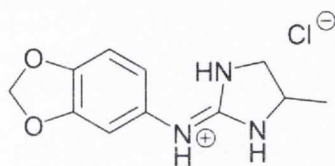
^{13}C NMR (100 MHz, D_2O): $\delta 156.6$ (Cq Ar.), 136.0 (C=N), 132.2 (Cq Ar.), 125.0 (CH Ar.), 123.9 (CH Ar.), 51.1 (CHCH_2), 49.0 (CHCH_2), 47.0 (CH_2CH_3), 19.2 (CHCH_3), 9.8 (CH_2CH_3).

IR (neat, cm^{-1}): ν_{max} 3146 (NH), 2975 (CH), 2891, 2639, 2464, 1639, 1600, 1514 (C=N), 1446, 1391, 1270.

HRMS: (m/z ES): Found: 219.1614 (M^+ . $\text{C}_{12}\text{H}_{19}\text{N}_4$ Requires: 219.1610).

Purity by HPLC: 97.9% (t_R 17.71 min).

5-Amino-*N*-(4-methylimidazolidin-2-ylidene)benzo[*d*][1,3]dioxole hydrochloride (93e)



Following Method G, **92e** (191 mg, 0.46 mmol) was treated with 25 equivalents of a 4 M solution of HCl in dioxane (2.85 ml, 11.40 mmol). After 3.5 h stirring at 55 °C, the reaction was adjudged complete (TLC, MS), solvents were

evaporated, and the residue was purified by reverse phase chromatography (C-8 silica using a 100% H_2O mobile phase). Removal of solvents under vacuum afforded the title compound as a white solid (90 mg, 78%). Mp: 220 – 222 °C.

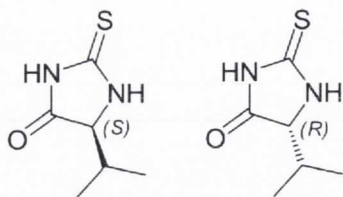
^1H NMR (400 MHz, D_2O): δ 6.86 (d, $J = 8.0$ Hz, 1H, CH Ar.), 6.76 (s, 1H, CH Ar.), 6.74 (d, $J = 8.0$ Hz, 1H, CH Ar.), 5.98 (s, 2H, OCH_2O), 4.16 (m, 1H, CHCH_3), 3.81 (t, $J = 9.5$ Hz, 1H, CHCH_2), 3.29 (t, $J = 7.5$ Hz, 1H, CH_2CH), 1.27 (d, $J = 6.0$ Hz, 3H, CHCH_3).

^{13}C NMR (100 MHz, D_2O): δ 157.5 (C=N), 147.4 (Cq Ar.), 146.1 (Cq Ar.), 128.0 (Cq Ar.), 118.3 (CH Ar.), 108.2 (CH Ar.), 105.9 (CH Ar.), 101.5 (OCH_2O), 51.0 (CHCH_2), 49.0 (CHCH_2), 19.2 (CHCH_3).

IR (neat, cm^{-1}): ν_{max} 3248 (NH), 2981 (CH), 2858, 1650, 1605, 1488 (C=N), 1449, 1248, 1198, 1130, 1104, 1032, 925, 809.

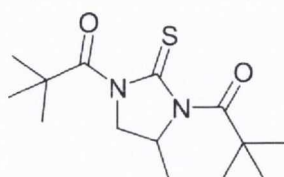
HRMS: (m/z ES): Found: 220.1082 (M^+ . $\text{C}_{11}\text{H}_{14}\text{N}_3\text{O}_2$ Requires: 220.1086).

Purity by HPLC: 96.7% (t_R 20.80 min).

(*S* and *R*)-5-Isopropyl-2-thiohydantoin (94a and b, respectively)

For the preparation of the *S* enantiomer **94a**, L-valine (1.00 g, 8.55 mmol) and thiourea (1.95 g, 25.64 mmol) were ground together using a mortar and pestle. The mixed solid was transferred to a round-bottom flask and the vessel was heated with stirring at 190 °C until the mixture was molten. The reaction was heated at 190 °C in the molten state for a further 25 min, then allowed to cool to rt. Cold water was added (10 ml), and the reaction was agitated and refrigerated for 3 h. The whitish precipitate was filtered and collected as the pure product. The filtrate was extracted using EtOAc (200 ml), washed once with brine (100 ml), and the organic layer was dried over MgSO₄. Removal of solvents afforded a crude mixture which was purified by silica gel chromatography using hexane:EtOAc and the purified product was combined with the precipitate collected earlier to afford **94a** as a white solid (998 mg, 74%). Mp: 133 °C (literature: 138-140 °C).²⁶¹ The *R* enantiomer **94b** was prepared from D-valine using an identical procedure (905 mg, 67%). Spectral and characterisation data matched that of the *S* enantiomer within experimental limits. The enantiomeric excess was not established in these experiments.

¹H NMR (400 MHz, CD₃CN): δ9.31 (br s, 1H, NH), 7.93 (br s, 1H, NH), 4.04 (d, J = 3.8 Hz, 1H, COCH), 2.14 (m, 1H, CH iPr), 1.00 (d, J = 6.8 Hz, 3H, CH₃ iPr), 0.88 (d, J = 6.8 Hz, 3H, CH₃ iPr).

1,3-Di(pivaloyl)-4-methylimidazolidine-2-thione (95)

Pivaloyl chloride (45 μl) was added to a solution of **90** (20 mg, 0.16 mmol), pyridine (37 μl, 0.46 mmol) and 4-(dimethylamino)pyridine (1 mg, 0.01 mmol) in methylene chloride, and heated at 45 °C for 2 h. The reaction was washed with 1 M aq. HCl (0.5 ml) then with water (2 x 0.5 ml). The organic phase was dried over MgSO₄, filtered, and solvents removed under reduced pressure. The residue was purified by pipette-scale flash chromatography on

silica gel, eluting with ether:hexane to afford the product as an off-white solid (23 mg, 53%).
Mp: 66 – 72 °C.

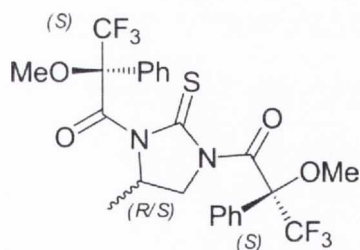
¹H NMR (400 MHz, CDCl₃): δ4.36 (m, 1H, CHCH₂), 4.11 (dd, J = 8.0, 9.6, Hz, 1H, CHCH₂), 3.58 (app t, J = 9.6 Hz, 1H, CHCH₂), 1.42 (s, 9H, CH₃ Piv), 1.41 (s, 9H, CH₃ Piv), 1.28 (d, J = 6.0 Hz, 3H, CHCH₃).

¹³C NMR (100 MHz, CDCl₃): δ187.3 (C=S), 182.7 (C=O), 179.9 (C=O), 54.7 (CHCH₂), 54.6 (CHCH₂), 43.7 (Cq Piv), 42.8 (Cq Piv), 27.4 (CH₃ Piv), 27.3 (CH₃ Piv), 17.4 (CHCH₃).

IR (neat, cm⁻¹): ν_{max} 2980 (CH), 2932, 1735, 1717, 1671, 1479, 1456, 1412, 1384, 1310, 1256, 1216, 1149 (C=S), 1109, 1007, 944, 933, 908.

HRMS (m/z ES): Found: 307.1465 (M⁺ + Na. C₁₄H₂₄N₂O₂ Requires: 307.1456).

(S,S,S/R) 1,3-Di(1-methoxy-1-trifluoromethyl-1-phenylacetyl)-4-methylimidazolidine-2-thione (96s and 96r, mixture of diastereomers)



(S)-α-Methoxy-α-trifluoromethylphenylacetyl chloride (32 μl) was added to a solution of **90** (10 mg, 0.08 mmol), pyridine (19 μl, 0.23 mmol) and 4-(dimethylamino)pyridine (1 mg, 0.01 mmol) in methylene chloride, and heated at 45 °C for 2 h. The organic layer was washed twice with water (2 x 0.5 ml), dried over MgSO₄, filtered, and solvents removed under reduced

pressure. The residue was purified by pipette-scale flash chromatography on silica gel, eluting with EtOAc:hexane to afford the product as an orange solid (35 mg, 85%, ~1:1 mixture of diastereomers). Mp: 176 °C.

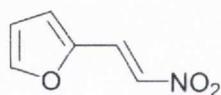
¹H NMR (600 MHz, CDCl₃): δ7.53 – 7.34 (m, 20H, CH Ar.), 4.48 (app. quintet, J = 6.5 Hz, 1H, CHCH₂), 3.73 – 3.61 (m, 11H, CHCH₂ + 3 x OMe), 3.55 (s, 3H, OMe), 3.13 (dd, J = 10.6, 6.5 Hz, 1H, CHCH₂), 3.01 (d, J = 10.6 Hz, 1H, CHCH₂), 2.71 (dd, J = 10.5, 6.5 Hz, 1H, CHCH₂), 0.71 (d, J = 6.5 Hz, 3H, CHCH₃), 0.43 (d, J = 6.5 Hz, 3H, CHCH₃).

^{13}C NMR (150 MHz, CDCl_3): δ 173.6 (C=S), 174.1 (C=S), 166.6 (C=O), 165.9 (C=O), 165.8 (C=O), 164.8 (C=O), 132.4 (Cq Ar.), 131.6 (Cq Ar.), 131.3 (Cq Ar.), 131.2 (Cq Ar.), 129.8 (CH Ar.), 129.7 (CH Ar.), 129.6 (CH Ar.), 129.5 (CH Ar.), 128.4 (2 x CH Ar.), 128.3 (CH Ar.), 128.2 (CH Ar.), 126.5 (CH Ar.), 126.3 (CH Ar.), 126.1 (CH Ar.), 125.9 (CH Ar.), 122.9 (q, $J = 296$ Hz, 4 x CF_3), 85.6 (q, $J = 30$ Hz, 4 x Cq), 56.3 (q, $J = 1.8$ Hz, OMe), 56.2 (q, $J = 1.8$ Hz, OMe), 55.9 (q, $J = 1.8$ Hz, OMe), 55.6 (q, $J = 1.8$ Hz, OMe), 54.0 ($\underline{\text{C}}\text{HCH}_2$), 53.0 ($\text{CH}\underline{\text{C}}\text{H}_2$), 52.9 ($\text{CH}\underline{\text{C}}\text{H}_2$), 52.6 ($\underline{\text{C}}\text{HCH}_2$), 17.7 ($\text{CH}\underline{\text{C}}\text{H}_3$), 17.3 ($\text{CH}\underline{\text{C}}\text{H}_3$).

IR (neat, cm^{-1}): ν_{max} 2988 (CH), 2952 (CH), 1726 (C=O), 1451, 1309, 1259, 1234, 1164 (C-F), 1124 (C-F), 1096, 1078.

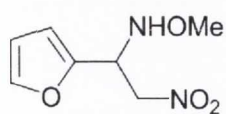
HRMS (m/z ES): Found: 571.1109 ($\text{M}^+ + \text{Na}$). $\text{C}_{24}\text{H}_{22}\text{N}_2\text{O}_4\text{SNaF}_6$ Requires: 571.1102).

(*E*)-2-(2-Nitrovinyl)furan (97)



An RBF was charged with furfural (388 μl , 4.69 mmol), nitromethane (251 μl , 4.69 mmol) and MeOH (15 ml) and cooled to -5 $^{\circ}\text{C}$ (salted ice-water bath). A solution of NaOH (192 mg, 4.80 mmol) in H_2O (10 ml) was added dropwise over 20 min. The mixture was poured into a cold stirring solution of conc. HCl (15 ml) in H_2O (20 ml) over 20 mins. After 30 min stirring at 0 $^{\circ}\text{C}$, the yellow solid precipitate was collected by filtration and washed with water (25 ml). The solid was dissolved in a minimal quantity of hot EtOH and treated with activated charcoal. The charcoal was removed by hot filtration, and the filtrate was refrigerated at 0 $^{\circ}\text{C}$ for 2 h. The resulting yellow precipitate was collected by filtration, the crystals were washed with 5 ml hexane, and air-dried to afford the product as bright yellow crystalline shards (396 mg, 61%). Mp: $68 - 70$ $^{\circ}\text{C}$ (literature: 70 $^{\circ}\text{C}$).²⁶³

^1H NMR (400 MHz, CDCl_3): δ 7.79 (d, $J = 13.3$ Hz, 1H, CH alkene), 7.61 (d, $J = 1.8$ Hz, 1H, CH-O Fur.), 7.55 (d, $J = 13.3$ Hz, 1H, CH alkene), 6.91 (d, $J = 3.5$ Hz, 1H, CH Fur.), 6.60 (dd, $J = 3.5, 1.8$ Hz, 1H, CH Fur.).

1-(Fur-2-yl)-2-nitro-*N*-methoxyethylamine (98)

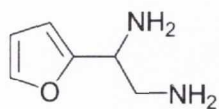
To a solution of **97** (300 mg, 2.16 mmol) in tetrahydrofuran (2 ml) were added *O*-methyl hydroxylamine hydrochloride (198 mg, 2.37 mmol) and sodium hydrogen carbonate (199 mg, 2.37 mmol). H₂O (0.5 mL) was added and the reaction was stirred at rt overnight under argon. The reaction was diluted with H₂O (1 ml) and extracted twice with EtOAc (2 x 3 ml). The combined organic fractions were washed with brine (2 ml), dried over MgSO₄, filtered and evaporated to afford the crude product as a yellow-brown oily residue (approximately 0.5 ml). The crude was purified using silica chromatography eluting with EtOAc/hexane (1:10) to afford the product as a bright yellow oil (395 mg, 91%). Spectroscopic data matches that in the literature.²⁴⁰

¹H NMR (400 MHz, CDCl₃): δ7.38 (d, *J* = 1.8 Hz, 1H, CH-O Fur.), 6.36 (dd, *J* = 3.3, 1.8 Hz, 1H, CH Fur.), 6.34 (d, *J* = 3.3 Hz, 1H, CH Fur.), 4.83 - 4.92 (m, 2H, CH₂), 4.72 (dd, *J* = 11.5, 3.5 Hz, CHNH), 3.48 (s, 3H, CH₃).

¹³C NMR (100 MHz, CDCl₃): δ148.7 (C_q Fur.), 142.3 (CHO Fur.), 110.1 (CH Fur.), 108.1 (CH Fur.), 74.3 (CH₂), 62.1 (CH₃), 56.1 (CHNH).

IR (neat, cm⁻¹): ν_{max} 3261, 2941, 2815, 1551 (NO), 1504, 1467, 1426, 1377 (NO), 1340, 1280, 1228, 1183, 1149, 1069, 1012, 973, 915.

HRMS (*m/z* ES): Found: 209.0541 (M⁺ + Na. C₇H₁₀N₂O₄Na Requires: 209.0538).

1-(Fur-2-yl)-1,2-ethylenediamine (99a)

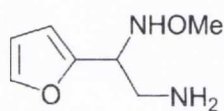
In an RBF fitted with a reflux condenser were placed **98** (1650 mg, 8.87 mmol) and acetic acid (31.5 ml). Zinc dust (6.96 g, 106.5 mmol) was slowly added over 15 min (six portions) with cooling. The reaction mixture was heated to 55 °C for 2.5 h (reaction progress was monitored by MS) and then allowed to cool to rt. The mixture was filtered and the zinc residue was washed with acetic acid (5 ml). The filtrate was concentrated *in vacuo* and then dissolved in methylene chloride (3 ml), to which was added slowly and with cooling a 20% solution of NaOH (5 ml). This

mixture was stirred for 15 min and then extracted with 25% isopropyl alcohol in methylene chloride (3 x 3 ml). The combined organic layer was washed first with 20% aqueous NaOH (2 ml), followed by brine (5 ml). The organic phase was filtered and solvents removed *in vacuo* to afford the product as a yellow oil, which used without further purification (875 mg, 78%). Spectroscopic data matches that in the literature.²⁴⁰

¹H NMR (400 MHz, CDCl₃): δ7.38 (app s, 1H, CH-O Fur.), 6.34 (app d, J = 2.5 Hz, 1H, CH Fur.), 6.19 (app d, J = 2.5 Hz, 1H, CH Fur.), 3.93 (t, J = 6.0 Hz, 1H, CHCH₂), 3.10 - 2.89 (m, 2H, CHCH₂), 1.67 (br s, 4H, 2 x NH₂).

HRMS (*m/z* ES): Found: 151.0843 (M⁺ + Na. C₆H₁₀N₂ONa Requires: 151.0847).

1-(Fur-2-yl)-N-(methoxy)ethylenediamine (99b)



The same procedure was followed as described for the preparation of **99a**, with the notable difference that the reaction time was 1 h and the temperature was 45 °C. The isolated material was purified by small scale vacuum distillation (Bp: *ca.* 150 °C, *ca.* 3 mbar) to afford the product as a yellow oil (640 mg, 46%).

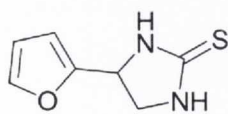
¹H NMR (400 MHz, CDCl₃): δ7.39 (app s, 1H, CH-O Fur.), 6.34 (app t, J = 2.0 Hz, 1H, CH Fur.), 6.27 (d, J = 2.0 Hz, 1H, CH Fur.), 4.05 (t, J = 6.0 Hz, 1H, CHCH₂), 3.51 (s, 3H, OMe), 3.06 (app d, J = 6.0 Hz, CHCH₂), 1.47 (br s, 3H, NH₂ + NH).

¹³C NMR (100 MHz, CDCl₃): δ152.8 (C_q Fur.), 141.5 (CH-O Fur.), 109.8 (CH Fur.), 106.9 (CH Fur.), 62.0 (CHCH₂), 60.7 (OMe), 41.9 (CHCH₂).

IR (neat, cm⁻¹): ν_{max} 3376, 2983, 1595, 1505 (NO), 1466, 1328, 1147 (NO), 1008, 808, 732 (very strong).

HRMS (*m/z* ES): Found: 179.0793 (M⁺ + Na. C₇H₁₂N₂O₂Na Requires: 179.0796).

4-(Fur-2-yl)imidazolidine-2-thione (100a)



To a stirring solution of **99a** (127 mg, 1 mmol) in methylene chloride (1.1 ml) under argon was added, dropwise over 30 min, a solution of 1,1'-thiocarbonyldiimidazole (188 mg, 1.06 mmol) in methylene chloride (1.1 ml). The reaction was stirred for 15 min after addition was complete (whitish precipitate observed), at which point methylene chloride was added (10 ml, just enough to dissolve the precipitate). The reaction was transferred to a separating funnel, washed three times with H₂O (3 x 5 ml) and then with brine (5 ml). The organic phase was filtered and evaporated to yield afford the crude product (brownish powder), which was triturated in 10 ml of 3:1 hexane:EtOAc, respectively. The solid was recovered by filtration, washed with 3:1 hexane:EtOAc (1 ml), and air dried to afford the product as an off-white solid (75 mg, 44%). Mp: 166 °C. Spectroscopic data matches that in the literature.²⁴⁰

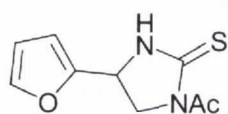
¹H NMR (400 MHz, DMSO): δ8.61 (br s, 1H, NH), 8.24 (br s, 1H, NH), 7.65 (d, J = 1.6 Hz, 1H, CH-O Fur.), 6.43 (dd, J = 3.1, 1.6 Hz, 1H, CH Fur.), 6.36 (d, J = 3.1 Hz, 1H, CH Fur.), 5.02 (dd, J = 10.1, 7.1 Hz, 1H, CHCH₂), 3.83 (t, J = 10.1 Hz, 1H, CHCH₂), 3.51 (d, J = 7.1 Hz, 1H, CH₂).

¹³C NMR (100 MHz, DMSO): δ182.5 (C=S), 153.1 (C_q Fur.), 142.9 (CHO Fur.), 110.5 (CH Fur.), 107.1 (CH Fur.), 53.1 (CHCH₂), 49.0 (CH₂).

IR (neat, cm⁻¹): ν_{max} 3221 (NH), 2896, 2884, 1535, 1509, 1485, 1466, 1393, 1372, 1342, 1266, 1203, 1142 (C=S), 1078, 1063, 1008, 989, 936.

HRMS (*m/z* ES): Found: 167.0284 (M⁻ - H. C₇H₇N₂OS Requires: 167.0279).

1-Acetyl-4-(fur-2-yl)imidazolidine-2-thione (100b)



The same procedure was followed as described for the preparation of **100a**, with the notable difference that the starting material **99a** was used as the crude diacetate salt instead of the free diamine, and the reaction was performed in the presence of 5 molar equivalents of triethylamine. The isolated material

was purified by flash chromatography (hexane:EtOAc) to afford the product as a white solid (41 mg, 24%). Mp: 142 - 144 °C.

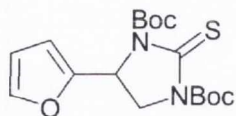
¹H NMR (400 MHz, CDCl₃): δ7.45 (dd, J = 1.8, 0.8 Hz, 1H, CH-O Fur.), 7.07 (br s, 1H, NH), 6.39 (dd, J = 3.3, 1.8 Hz, CH Fur.), 6.38 (d, J = 3.3 Hz, 1H, CH Fur.), 4.97 (dd, J = 9.8, 6.3 Hz, 1H, CHCH₂), 4.45 (dd, J = 12.0, 9.8 Hz, 1H, CHCH₂), 4.31 (dd, J = 12.0, 6.3 Hz, 1H, CHCH₂), 2.88 (s, 3H, Ac).

¹³C NMR (100 MHz, CDCl₃): δ180.5 (C=O), 171.8 (C=S), 150.4 (Cq Fur.), 143.6 (CH-O Fur.), 110.6 (CH Fur.), 108.1 (CH Fur.), 51.9 (CH₂), 49.6 (CHCH₂), 26.1 (CH₃).

IR (neat, cm⁻¹): ν_{max} 3135 (NH), 2988, 1690 (C=O), 1516, 1472, 1407, 1366, 1321, 1264, 1252, 1226, 1148 (C=S), 1078, 1040, 1015, 1063, 1015, 953, 915, 882.

HRMS (*m/z* ES): Found: 233.0358 (M⁺ + Na. C₉H₁₀N₂O₂SNa Requires: 233.0361).

1,3-Di(*tert*-butoxycarbonyl)-4-(fur-2-yl)imidazolidine-2-thione (101)



Following Method F, to a cooled solution of **100a** (210 mg, 1.25 mmol) in tetrahydrofuran (11 ml) was added NaH as a 60% suspension in mineral oil (225 mg, 5.63 mmol). After 15 min, di-*tert*-butyldicarbonate was added neat (600 mg, 2.75 mmol). After 3 h, usual work up followed by chromatography over silica, eluting with hexane:EtOAc, afforded the title compound as a pale yellow solid (385 mg, 84%). Mp: 106 - 108 °C.

¹H NMR (400 MHz, CDCl₃): δ7.39 (s, 1H, CH-O Fur.), 6.35 (d, J = 3.5 Hz, 1H, CH Fur.), 6.31 (d, J = 3.5 Hz, 1H, CH Fur.), 5.36 (dd, J = 4.0, 1.5 Hz, 1H, CHCH₂), 4.14 (dd, J = 9.6, 1.5 Hz, 1H, CHCH₂), 4.03 (dd, J = 9.6, 4.0 Hz, 1H, CHCH₂), 1.55 (s, 9H, Boc), 1.44 (s, 9H, Boc).

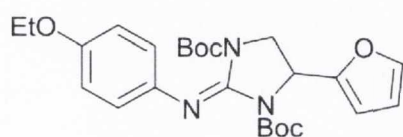
¹³C NMR (100 MHz, CDCl₃): δ174.3 (C=S), 150.9 (Cq Fur.), 149.6 (C=O Boc), 149.0 (C=O Boc), 142.2 (CH-O Fur.), 110.1 (CH Fur.), 107.3 (CH Fur.), 83.7 (2 x Cq Boc), 52.7 (CHCH₂), 49.6 (CHCH₂), 27.6 (CH₃ Boc), 27.4 (CH₃ Boc).

IR (neat, cm^{-1}): ν_{max} 2980 (CH), 2934, 1758, 1717, 1368, 1321, 1268, 1242, 1138.

HRMS (m/z ES): Found: 391.1317 ($M^+ + \text{Na}$. $\text{C}_{17}\text{H}_{24}\text{N}_2\text{O}_2\text{SNa}$ Requires: 391.1304).

4-Ethoxy-*N*-[1,3-di(*tert*-butoxycarbonyl)-4-(fur-2-yl)imidazolidin-2-ylidene]aniline

(102a)



Following Method A, HgCl_2 (111 mg, 0.41 mmol) was added over a solution of **101** (125 mg, 0.34 mmol), 4-ethoxyaniline (48 μl , 0.37 mmol) and triethylamine (213 μl ,

1.53 mmol) in methylene chloride (1.5 ml) at 0 °C. The resulting mixture was stirred for 1 h at 0 °C and a further 16 h at room temperature. Usual work up followed by chromatography over aluminium oxide, eluting with hexane:EtOAc, afforded the title compound as an off-white solid (147 mg, 62%). Mp: 48 - 50 °C.

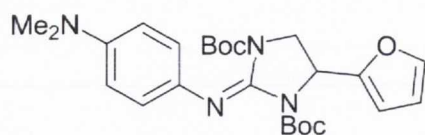
^1H NMR (400 MHz, CDCl_3): δ 7.38 (app s, 1H, CH-O Fur.), 6.96 (d, $J = 8.0$ Hz, 2H, CH Ar.), 6.77 (d, $J = 8.0$ Hz, 2H, CH Ar.), 6.35 (app d, $J = 5.5$ Hz, 2H, 2 x CH Fur.), 5.25 (app d, $J = 7.0$ Hz, 1H, CHCH_2), 4.12 (d, $J = 10.5$ Hz, 1H, CHCH_2), 3.97 (m, 3H, $\text{CHCH}_2 + \text{CH}_2\text{CH}_3$), 1.38 (t, $J = 7.3$ Hz, 3H, CH_2CH_3), 1.32 (s, 18H, 2 x Boc).

^{13}C NMR (100 MHz, CDCl_3): δ 154.4 (Cq Ar.), 151.8 (Cq Fur.), 150.2 (C=O), 149.3 (C=O), 142.1 (CH-O Fur.), 140.9 (C=N), 138.1 (Cq Ar.), 122.3 (CH Ar.), 114.2 (CH Ar.), 109.9 (CH Fur.), 106.9 (CH Fur.), 82.5 (Cq Boc), 82.2 (Cq Boc), 63.2 (CH_2CH_3) 51.2 (CHCH_2) 47.7 (CHCH_2), 27.4 (2 x CH_3 Boc), 14.4 (CH_2CH_3).

IR (neat, cm^{-1}): ν_{max} 2979 (CH), 2932 (CH), 1756 (C=O), 1699 (C=O), 1505 (C=N), 1478, 1366, 1299, 1236, 1145 (C-O), 1042.

HRMS (m/z ES): Found: 472.2450 ($M^+ + \text{H}$. $\text{C}_{25}\text{H}_{34}\text{N}_3\text{O}_6$ Requires: 472.2448).

4-(Dimethylamino)-*N*-[1,3-di(*tert*-butoxycarbonyl)-4-(fur-2-yl)imidazolidin-2-ylidene]-aniline (102b)



Following Method A, HgCl₂ (184 mg, 0.68 mmol) was added over a solution of **101** (200 mg, 0.54 mmol), 4-(dimethylamino)aniline (93 mg, 0.68 mmol) and triethylamine (265 μl, 1.90 mmol) in methylene chloride (3.0 ml) at 0 °C. The resulting mixture was stirred for 1 h at 0° C and a further 16 h at room temperature. Usual work up followed by chromatography over aluminium oxide, eluting with hexane:EtOAc, afforded the title compound as an off-white solid (185 mg, 72%). Mp: 46 - 48 °C.

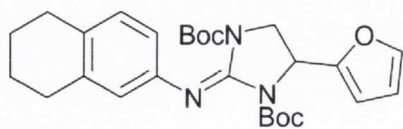
¹H NMR (400 MHz, CDCl₃): δ7.38 (app s, 1H, CH-O Fur.), 6.96 (d, J = 7.0 Hz, 2H, CH Ar.), 6.68 (d, J = 7.0 Hz, 2H, CH Ar.), 6.36 (app s, 2H, 2 x CH Fur.), 5.25 (d, J = 7.0 Hz, 1H, CHCH₂), 4.12 (d, J = 10.5 Hz, 1H, CHCH₂), 3.97 (dd, J = 10.5, 7.0 Hz, 1H, CHCH₂), 2.87 (s, 6H, N(CH₃)₂), 1.32 (s, 18H, 2 x Boc).

¹³C NMR (100 MHz, CDCl₃): δ152.0 (Cq Fur.), 150.5 (C=O), 149.5 (C=O), 146.9 (C=N), 142.0 (CH-O Fur.), 138.3 (Cq Ar.), 137.3 (Cq Ar.), 122.2 (CH Ar.), 113.5 (CH Ar.), 109.9 (CH Fur.), 106.8 (CH Fur.), 82.4 (Cq Boc), 82.1 (Cq Boc), 51.2 (CHCH₂) 47.6 (CHCH₂), 41.1 (N(CH₃)₂), 27.4 (2 x CH₃ Boc).

IR (neat, cm⁻¹): ν_{max} 2965 (CH), 2929, 1753 (C=O), 1696 (C=O), 1610 (C=N), 1513, 1365, 1300, 1251, 1146 (C-O).

HRMS (*m/z* ES): Found: 471.2614 (M⁺ + H. C₂₅H₃₅N₄O₅ Requires: 471.2607).

2-Amino-*N*-[1,3-di(*tert*-butoxycarbonyl)-4-(fur-2-yl)imidazolidin-2-ylidene]-5,6,7,8-tetrahydronaphthalene (102c)



Following Method A, HgCl₂ (184 mg, 0.68 mmol) was added over a solution of **101** (200 mg, 0.54 mmol), 2-amino-5,6,7,8-tetrahydronaphthalene (100 mg, 0.68 mmol) and triethylamine (265 μl, 1.90 mmol) in methylene chloride (3.0 ml) at 0 °C. The resulting

mixture was stirred for 1 h at 0° C and a further 16 h at room temperature. Usual work up followed by chromatography over aluminium oxide, eluting with hexane:EtOAc, afforded the title compound as an off-white solid (194 mg, 74%). Mp: 60 - 62 °C.

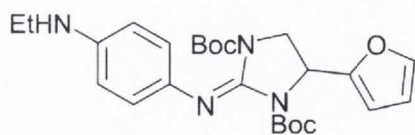
¹H NMR (400 MHz, CDCl₃): δ7.36 (s, 1H, CH Fur.), 6.88 (d, J = 8.0 Hz, 1H, CH Ar.), 6.72 (d, J = 8.0 Hz, 1H, CH Ar.), 6.68 (s, 1H, CH Ar.), 6.33 (s, 2H, 2 x CH Fur.), 5.22 (d, J = 7.6 Hz, 1H, CHCH₂), 4.08 (d, J = 11.0 Hz, 1H, CHCH₂), 3.96 (dd, J = 11.0, 7.6 Hz, 1H, CHCH₂), 2.66 (app d, J = 5.5 Hz, 4H, 2 x CH₂), 1.72 (br s, 4H, 2 x CH₂), 1.29 (s, 18H, 2 x Boc).

¹³C NMR (100 MHz, CDCl₃): δ151.9 (Cq Fur.), 150.3 (C=O), 149.3 (C=O), 144.9 (C=N), 142.0 (CH-O Fur.), 138.0 (Cq Ar.), 136.3 (Cq Ar.), 131.0 (Cq Ar.), 128.6 (CH Ar.), 121.7 (CH Ar.), 118.5 (CH Ar.), 109.9 (CH Fur.), 106.8 (CH Fur.), 82.4 (Cq Boc), 82.1 (Cq Boc), 51.1 (CHCH₂) 47.6 (CHCH₂), 29.0 (CqCH₂CH₂), 28.4 (CqCH₂CH₂), 27.3 (CH₃ Boc), 23.1 (CqCH₂CH₂), 22.9 (CqCH₂CH₂).

IR (neat liquid, cm⁻¹): ν_{max} 2978 (CH), 2930, 1754 (C=O), 1702 (C=O), 1606 (C=N), 1366, 1301, 1147 (C-O), 989, 968, 730.

HRMS (*m/z* ES): Found: 482.2640 (M⁺ + H. C₂₇H₃₆N₃O₅ Requires: 482.2655).

N-[1,3-Di(*tert*-butoxycarbonyl)-4-(fur-2-yl)imidazolidin-2-ylidene]-4-ethylaminoaniline (102d)



Following Method A, HgCl₂ (199 mg, 0.73 mmol) was added over a solution of **101** (225 mg, 0.61 mmol), **105** (90 μl, 0.67 mmol) and triethylamine (384 μl, 2.75 mmol)

in methylene chloride (3.0 ml) at 0 °C. The resulting mixture was stirred for 1 h at 0° C and a further 16 h at room temperature. Usual work up followed by chromatography over aluminium oxide, eluting with hexane:EtOAc, afforded the title compound as an off-white solid (244 mg, 85%). Mp: 58 - 60 °C.

¹H NMR (400 MHz, CDCl₃): δ7.34 (s, 1H, CH Fur.), 6.88 (d, J = 6.5 Hz, 2H, CH Ar.), 6.49 (d, J = 6.5 Hz, 2H, CH Ar.), 6.32 (s, 2H, 2 x CH Fur.), 5.22 (d, J = 7.0 Hz, 1H, CHCH₂), 4.08

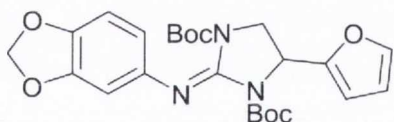
(d, $J = 10.6$ Hz, 1H, CHCH₂), 3.92 (dd, $J = 10.6, 7.0$ Hz, 1H, CHCH₂), 3.21 (br s, 1H, NH), 3.08 (q, $J = 7.0$ Hz, 2H, CH₂CH₃), 1.29 (s, 18H, 2 x Boc), 1.19 (t, $J = 7.0$ Hz, 3H, CH₂CH₃).

¹³C NMR (100 MHz, CDCl₃): δ152.0 (Cq Fur.), 150.5 (C=O), 149.4 (C=O), 144.1 (C=N), 142.0 (CH-O Fur.), 138.2 (Cq Ar.), 137.2 (Cq Ar.), 122.4 (CH Ar.), 112.8 (CH Ar.), 109.9 (CH Fur.), 106.7 (CH Fur.), 82.3 (Cq Boc), 82.0 (Cq Boc), 51.1 (CHCH₂) 47.6 (CHCH₂), 38.6 (CH₂CH₃), 27.4 (CH₃ Boc), 14.4 (CH₂CH₃).

IR (neat liquid, cm⁻¹): ν_{\max} 3387 (NH), 2975 (CH), 2932 (CH), 1752 (C=O), 1692 (C=O), 1611, 1512 (C=N), 1365, 1298, 1247, 1144 (C-O), 1101, 987, 964.

HRMS (m/z ES): Found: 471.2597 (M⁺ + H. C₂₅H₃₅N₄O₅ Requires: 471.2607).

5-Amino-*N*-[1,3-di(*tert*-butoxycarbonyl)-4-(fur-2-yl)imidazolidin-2-ylidene]benzo[*d*][1,3]dioxole (102e)



Following Method A, HgCl₂ (171 mg, 0.63 mmol) was added over a solution of **101** (185 mg, 0.50 mmol), 3,4-methylenedioxyaniline (86 mg, 0.63 mmol) and triethylamine (245 μ l, 1.76 mmol) in methylene chloride (3.0 ml) at 0 °C. The resulting mixture was stirred for 1 h at 0 °C and a further 16 h at room temperature. Usual work up followed by chromatography over aluminium oxide, eluting with hexane:EtOAc, afforded the product as an off-white solid (121 mg, 51%). Mp: 60 - 62 °C.

¹H NMR (400 MHz, CDCl₃): δ7.36 (s, 1H, CH-O Fur.), 6.66 (d, $J = 8.6$ Hz, 1H, CH Ar.), 6.55 (s, 1H, CH Ar.), 6.48 (d, $J = 8.6$ Hz, 1H, CH Ar.), 6.33 (app d, $J = 5.5$ Hz, 2H, 2 x CH Fur.), 5.84 (app d, $J = 10.0$ Hz, 2H, OCH₂O), 5.22 (d, $J = 7.5$ Hz, 1H, CHCH₂), 4.09 (d, $J = 11.0$ Hz, 1H, CHCH₂), 3.96 (dd, $J = 11.0, 7.5$ Hz, 1H, CHCH₂), 1.35 (s, 9H, Boc), 1.32 (s, 9H, Boc).

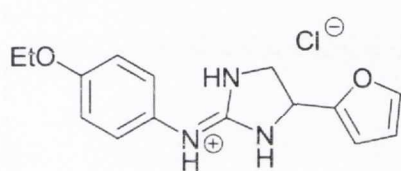
¹³C NMR (100 MHz, CDCl₃): δ151.7 (Cq Fur.), 150.1 (C=O), 149.2 (C=O), 147.1 (C=N), 142.6 (Cq Ar.), 142.3 (Cq Ar.), 142.1 (CH-O Fur.), 138.4 (Cq Ar.), 114.1 (CH Ar.), 110.0

(CH Fur.), 107.5 (CH Ar.), 106.9 (CH Fur.), 102.8 (CH Ar.), 100.2 (OCH₂O), 82.6 (Cq Boc), 82.3 (Cq Boc), 51.2 (CHCH₂) 47.7 (CHCH₂), 27.4 (CH₃ Boc).

IR (neat liquid, cm⁻¹): ν_{\max} 2978 (CH), 2928 (CH), 1754 (C=O), 1702 (C=O), 1502 (C=N), 1479, 1365, 1298, 1246, 1146 (C-O), 1075, 1035.

HRMS (*m/z* ES): Found: 472.2078 (M⁺ + H. C₂₄H₃₀N₃O₇ Requires: 472.2084).

4-Ethoxy-*N*-[4-(fur-2-yl)imidazolidin-2-ylidene]aniline hydrochloride (**103a**)



Following Method G, a solution of **102a** (140 mg, 0.30 mmol) in methylene chloride (0.40 ml) was treated with 15 equivalents of a 4 M solution of HCl in dioxane (1.12 ml, 4.45 mmol). After 3 h stirring at 55 °C, the reaction was

adjudged complete (TLC, MS), solvents were evaporated, and the residue was purified by silica chromatography, eluting with methylene chloride/CMA. Solvents were removed *in vacuo* and the residue was dissolved in 1.25 M methanolic HCl (2 ml). Solvents and excess HCl were removed under vacuum to afford the title compound as a clear hygroscopic gum (64 mg, 70%).

¹H NMR (400 MHz, D₂O): δ 7.51 (s, 1H, CH-O Fur.), 7.21 (d, J = 8.5 Hz, 2H, CH Ar.), 6.98 (d, J = 8.5 Hz, 2H, CH Ar.), 6.43 (s, 2H, 2 x CH Fur.), 5.21 (dd, J = 9.5, 6.5 Hz, 1H, CHCH₂), 4.06 (q, J = 7.0 Hz, 2H, CH₂CH₃), 4.04 (app t, J = 9.5 Hz, 1H, CHCH₂), 3.81 (dd, J = 9.5, 6.5 Hz, 1H, CHCH₂), 1.33 (t, J = 7.0 Hz, 3H, CH₂CH₃).

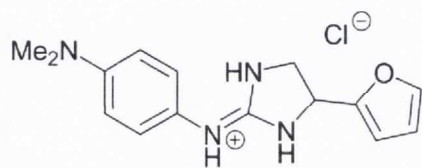
¹³C NMR (100 MHz, D₂O): δ 157.6 (Cq Ar.), 157.0 (C=N), 150.7 (Cq Fur.), 143.2 (CH-O Fur.), 127.1 (Cq Ar.), 126.3 (CH Ar.), 115.2 (CH Ar.), 110.1 (CH Fur.), 107.5 (CH Fur.), 64.0 (CH₂CH₃), 51.5 (CHCH₂), 46.9 (CHCH₂ + CH₂CH₃), 13.4 (CH₂CH₃).

IR (neat, cm⁻¹): ν_{\max} 3119 (NH), 2979 (CH), 1651, 1606, 1586 (C=N), 1512, 1477, 1244, 1043, 1010.

HRMS (*m/z* ES): Found: 272.1397 (M⁺. C₁₅H₁₈N₃O₂ Requires: 272.1399).

Purity by HPLC: 97.9% (t_R 25.99 min).

4-Dimethylamino-*N*-[4-(fur-2-yl)imidazolidin-2-ylidene]aniline dihydrochloride (103b)



Following Method G, **102b** (80 mg, 0.18 mmol) was treated with 12 equivalents of a 4 M solution of HCl in dioxane (0.57 ml, 2.29 mmol). After 3 h stirring at 55 °C, the reaction was adjudged complete (TLC, MS), solvents were evaporated, and the residue was purified by reverse phase chromatography over C-8 silica, eluting with 9:1 H₂O:acetonitrile, respectively. Solvents were removed under vacuum to afford the title compound as a hygroscopic off-white gum (33 mg, 58%). Mp: 114 -118 °C.

¹H NMR (400 MHz, D₂O): δ7.67 (d, *J* = 8.5 Hz, 2H, CH Ar.), 7.52 (s, 1H, CH-O Fur.), 7.49 (d, *J* = 8.5 Hz, 2H, CH Ar.), 6.45 (app d, *J* = 10.0 Hz, 2H, 2 x CH Fur.), 5.28 (dd, *J* = 10.0, 7.0 Hz, 1H, CHCH₂), 4.07 (t, *J* = 10.0 Hz, 1H, CHCH₂), 3.87 (dd, *J* = 10.0, 7.0 Hz, 1H, CHCH₂), 3.27 (s, 6H, N(CH₃)₂).

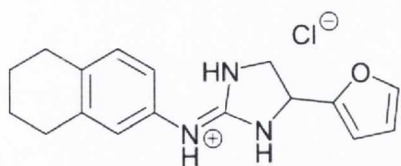
¹³C NMR (100 MHz, D₂O): δ156.7 (C=N), 150.5 (Cq Fur.), 143.2 (CH-O Fur.), 139.9 (Cq Ar.), 136.2 (Cq Ar.), 125.4 (CH Ar.), 121.7 (CH Ar.), 110.2 (CH Fur.), 107.7 (CH Fur.), 51.6 (CHCH₂), 47.0 (CHCH₂), 45.9 (N(CH₃)₂).

IR (neat, cm⁻¹): ν_{\max} 3120 (NH), 2450 (CH), 1645, 1602 (C=N), 1517, 1332, 1247, 1134, 1015, 902.

HRMS (*m/z* ES): Found: 271.1546 (M⁺. C₁₅H₁₉N₄O Requires: 271.1559).

Purity by HPLC: 98.7% (t_R 24.13 min).

2-Amino-*N*-[4-(fur-2-yl)imidazolidin-2-ylidene]-5,6,7,8-tetrahydronaphthalene hydrochloride (103c)



Following Method G, a solution of **102c** (98 mg, 0.20 mmol) in methylene chloride (0.35 ml) was treated with 12 equivalents of a 4 M solution of HCl in dioxane (0.60 ml, 2.40 mmol). After 3 h stirring at 55 °C, the reaction

was adjudged complete (TLC, MS), solvents were evaporated, and the residue was purified by reverse phase chromatography over C-8 silica, eluting with 9:1 H₂O:acetonitrile, respectively. Solvents were evaporated to afford the title compound as a white solid (39 mg, 60%). Mp: 76 – 78 °C.

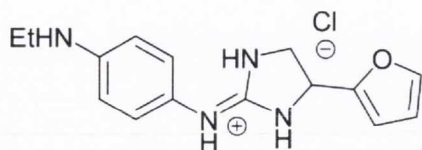
¹H NMR (400 MHz, D₂O): δ7.51 (s, 1H, CH-O Fur.), 7.15 (d, J = 8.0 Hz, 1H, CH Ar.), 7.00 (s, 1H, CH Ar.), 6.99 (d, J = 8.0 Hz, 1H, CH Ar.), 6.43 (s, 2H, 2 x CH Fur.), 5.22 (dd, J = 10.0, 6.5 Hz, 1H, CHCH₂), 4.02 (t, J = 10.0 Hz, 1H, CHCH₂), 3.82 (dd, J = 10.0, 6.5 Hz, 1H, CHCH₂), 2.71 (s, 4H, 2 x CH₂), 1.72 (s, 4H, 2 x CH₂).

¹³C NMR (100 MHz, D₂O): δ157.3 (C=N), 150.7 (Cq Fur.), 143.2 (CH-O Fur.), 138.7 (Cq Ar.), 136.7 (Cq Ar.), 131.4 (Cq Ar.), 129.9 (CH Ar.), 124.3 (CH Ar.), 121.1 (CH Ar.), 110.1 (CH Fur.), 107.5 (CH Fur.), 51.5 (CHCH₂), 46.9 (CHCH₂), 28.3 (CqCH₂CH₂), 27.9 (CqCH₂CH₂), 22.0 (CqCH₂CH₂), 21.8 (CqCH₂CH₂).

IR (neat, cm⁻¹): ν_{max} 2928 (CH), 1645, 1608 (C=N), 1504, 1435, 1330, 1247, 1193, 1148, 1076, 1011, 907.

HRMS (*m/z* ES): Found: 282.1599 (M⁺. C₁₇H₂₀N₃O Requires: 282.1606).

Purity by HPLC: 95.2% (*t*_R 28.83 min).

4-Ethylamino-*N*-[4-(fur-2-yl)imidazolidin-2-ylidene]aniline hydrochloride (103d)

Following Method G, a solution of **102d** (122 mg, 0.26 mmol) in methylene chloride (0.50 ml) was treated with 14 equivalents of a 4 M solution of HCl in dioxane (0.91 ml, 3.63 mmol). After 3 h stirring at 55 °C, the reaction was adjudged complete (TLC, MS), solvents were evaporated, and the residue was purified by silica chromatography, eluting with methylene chloride/CMA. Solvents were removed *in vacuo* and the residue was dissolved in 1.25 M methanolic HCl (2 ml). Solvents and excess HCl were removed under vacuum to afford the title compound as a peach-coloured solid (78 mg, 77%). Mp: 94 – 98 °C.

¹H NMR (400 MHz, D₂O): δ7.52 (m, 3H, CH Fur. + CH Ar.), 7.46 (d, J = 8.5 Hz, 2H, CH Ar.), 6.42 (app d, J = 12.5 Hz, 2H, CH Fur.), 5.26 (dd, J = 10.0, 6.5 Hz, 1H, CHCH₂), 4.04 (t, J = 10.0 Hz, 1H, CHCH₂), 3.85 (dd, J = 10.0, 6.5 Hz, 1H, CHCH₂), 3.45 (q, J = 7.5 Hz, 2H, CH₂CH₃), 1.28 (t, J = 7.5 Hz, 3H, CH₂CH₃).

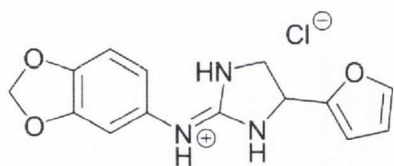
¹³C NMR (100 MHz, D₂O): δ156.9 (C=N), 150.5 (Cq Fur.), 143.3 (CH-O Fur.), 135.8 (Cq Ar.), 132.6 (Cq Ar.), 125.4 (CH Ar.), 123.9 (CH Ar.), 110.2 (CH Fur.), 107.7 (CH Fur.), 51.5 (CHCH₂), 46.9 (CHCH₂ + CH₂CH₃), 9.7 (CH₂CH₃).

IR (neat liquid, cm⁻¹): ν_{max} 3113 (NH), 2940 (CH), 2653, 1637, 1599 (C=N), 1514, 1335, 1247, 1148, 1075, 1014.

HRMS (*m/z* ES): Found: 271.1557 (M⁺. C₁₅H₁₉N₄O Requires: 271.1559).

Purity by HPLC: 95.4% (*t*_R 22.63 min).

5-Amino-*N*-[4-(fur-2-yl)imidazolidin-2-ylidene]benzo[*d*][1,3]dioxole hydrochloride (103e)



Following Method G, a solution of **102e** (120 mg, 0.25 mmol) in methylene chloride (0.80 ml) was treated with 12 equivalents of a 4 M solution of HCl in dioxane (0.76 ml, 3.06 mmol). After 4.5 h stirring at 55 °C, the reaction was adjudged complete (TLC, MS), solvents were evaporated, and the residue was purified by reverse phase chromatography over C-8 silica, eluting with 98:2 H₂O:acetonitrile, respectively. Solvents were evaporated to afford the title compound as a white solid (56 mg, 72%). Mp: 64 – 68 °C.

¹H NMR (400 MHz, D₂O): δ7.52 (s, 1H, CH Fur.), 6.87 (d, *J* = 8.0 Hz, 1H, CH Ar.), 6.80 (s, 1H, CH Ar.), 6.78 (d, *J* = 8.0 Hz, 1H, CH Ar.), 6.43 (app d, *J* = 1.0 Hz, 2H, 2 x CH Fur.), 5.99 (s, 2H, OCH₂O), 5.22 (dd, *J* = 9.5, 6.5 Hz, 1H, CHCH₂), 4.02 (t, *J* = 9.5 Hz, 1H, CHCH₂), 3.82 (dd, *J* = 9.5, 6.5 Hz, 1H, CHCH₂).

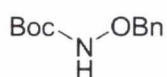
¹³C NMR (100 MHz, D₂O): δ157.7 (C=N), 150.7 (Cq Fur.), 147.5 (Cq Ar.), 146.3 (Cq Ar.), 143.2 (CH-O Fur.), 127.7 (Cq Ar.), 118.7 (CH Ar.), 110.1 (CH Fur.), 108.3 (CH Ar.), 107.5 (CH Fur.), 106.2 (CH Ar.), 101.5 (OCH₂O), 51.5 (CHCH₂), 46.9 (CHCH₂).

IR (neat, cm⁻¹): ν_{max} 3113 (NH), 2898 (CH), 1654, 1626, 1607 (C=N), 1502, 1485, 1450, 1243, 1196, 1033, 926.

HRMS (*m/z* ES): Found: 272.1029 (M⁺. C₁₄H₁₄N₃O₃ Requires: 272.1035).

Purity by HPLC: 99.6% (*t_R* 23.57 min).

***N*-Tert-butoxycarbonyl-*O*-benzylhydroxylamine (104a)**

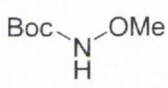


To a stirred solution of *O*-benzylhydroxylamine hydrochloride (200 mg, 1.25 mmol) in a 1:1 mixture of tetrahydrofuran and H₂O (2.5 ml total) was added

triethylamine (174 μ l, 1.25 mmol). A solution of di-*tert*-butyl dicarbonate (273 mg, 1.25 mmol) in tetrahydrofuran (1.5 ml) was added dropwise. The solution was stirred for 2.5 h at rt and then partially evaporated in vacuo. The residue was taken up in EtOAc (10 ml) and washed twice with 0.5 M formic acid (5 ml) and once with water (5 ml). The organic layer was dried over MgSO₄ and solvents were evaporated to afford the product as a clear viscous oil which crystallised slowly under high vacuum to afford a white solid (213 mg, 77%). Mp: 40 - 42 °C (literature: 45 - 46 °C).²⁶⁴

¹H NMR (400 MHz, CDCl₃): δ 7.39 (m, 5H, CH Ar.), 4.89 (s, 2H, CH₂), 1.51 (s, 9H, Boc).

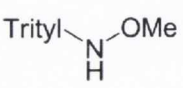
N-Tert-butoxycarbonyl-O-methylhydroxylamine (104b)

 To a stirred solution of di-*tert*-butyl dicarbonate (311 mg, 1.43 mmol) in methylene chloride (2.0 ml) was added a solution of Na₂CO₃ (379 mg, 3.57 mmol) in H₂O. To this mixture was added dropwise a solution of methoxyamine hydrochloride (300 mg, 3.57 mmol) in H₂O (1.5 ml). After stirring at rt for 18 h, the organic layer was washed with water, dried over MgSO₄, filtered and concentrated under reduced pressure to provide the product as a clear oil (202 mg, 96%).²⁶⁵

¹H NMR (400 MHz, CDCl₃): δ 7.40 (br s, 1H, NH), 3.68 (s, 3H, CH₃), 1.48 (s, 9H, Boc).

MS (*m/z* ES): Found: 148.1 (M⁺ + H. C₆H₁₄N Requires: 148.1).

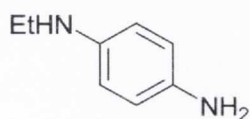
N-Triphenylmethyl-O-methylhydroxylamine (104c)

 To a stirred solution of methoxyamine hydrochloride (108 mg, 1.29 mmol) in pyridine (0.75 ml) was added, dropwise over 5 min, a solution of trityl chloride (300 mg, 1.08 mmol) in pyridine (1.0 ml). After 15 h stirring at rt, H₂O was added (15 ml) and the reaction was extracted three times with methylene chloride (3 x 3 ml). The combined organic phase was dried over Na₂SO₄, filtered and concentrated under reduced pressure. Column chromatography over silica gel (petroleum ether:EtOAc) followed by

recrystallization from petroleum ether:EtOAc afforded the product as a white solid (86 mg, 27%). Mp: 89 - 91 °C (literature: 90 - 91 °C).²⁶⁶

¹H NMR (400 MHz, CDCl₃): δ7.30 - 7.18 (m, 15H, CH Ar.), 3.51 (s, 3H, CH₃), 1.58 (br s, 1H, NH).

N-Ethyl-1,4-diaminobenzene (105)



To a suspension of lithium aluminium hydride (1833 mg, 45.83 mmol) in dry tetrahydrofuran (40 ml) under an atmosphere of argon and cooled to 0 °C (ice-water bath) was added dropwise a suspension of 4-aminoacetanilide (1250 mg, 8.33 mmol) in dry tetrahydrofuran (40 ml). The reaction was stirred 16 h at 55°C using a reflux condenser under a mild positive pressure of argon. After cooling to rt, stirring was continued for 1 h more and the reaction was cooled to 0 °C prior to the dropwise addition of water (3 ml) followed by 15% NaOH (5 ml). The reaction mixture was filtered through celite, the pad was washed with ether (100 ml), and the filtrate was washed with brine (80 ml). The pink-coloured organic layer was dried over MgSO₄ and filtered. The filtrate was concentrated under reduced pressure to afford the product as a dark red oil (879 mg, 95%).

¹H NMR (400 MHz, CDCl₃): δ6.62 (d, J = 8.5 Hz, 2H, CH Ar.), 6.53 (d, J = 8.5 Hz, 2H, CH Ar.), 2.85 - 3.19 (m, 5H, NH₂ + NH + CH₂CH₃), 1.24 (t, J = 7.0 Hz, 3H, CH₂CH₃).

¹³C NMR (100 MHz, CDCl₃): δ141.6 (Cq. Ar), 137.6 (Cq. Ar), 116.8 (CH. Ar), 114.5 (CH Ar.), 39.6 (CH₂CH₃), 15.0 (CH₂CH₃).

IR (neat, cm⁻¹): ν_{max} 3378, 3335, 3217.

MS (*m/z* ES): Found: 137.1 (M⁺ + H. C₈H₁₃N₂ Requires: 137.1).

References

- 1 *Diagnostic and Statistical Manual of Mental Disorders*, 4th ed. text revision, American Psychiatric Association, Washington DC, U.S.A., 2000.
- 2 N. D. Volkow, *Biol. Psychiat.*, 2004, **56**, 714-717.
- 3 L. D. Grandin, L. J. Yan, S. M. Gray, K. R. Jamison, G. S. Sachs, *J. Clin. Psychiat.*, 2001, **62**, 12-16.
- 4 S. R. Fordwood, J. R. Asarnow, D. P. Huizar, S. P. Reise, *J. Clin. Child Adolesc. Psychol.*, 2007, **36**, 392-404.
- 5 L. Brådvik, M. Berglund, *BMC Psychiatry*, 2011, **11**, 5.
- 6 L. R. Wulsin, *Arch. Intern. Med.*, 2000, **160**, 1731-1732.
- 7 *The Global Burden of Disease: 2004 update*, WHO Press, Geneva, 2008.
- 8 R. C. Kessler, T. B. Ustun, *Brit. J. Psychiat.*, 2002, **181**, 181-183.
- 9 *Mental health: facing the challenges, building solutions: Report from the WHO European ministerial conference*, WHO Press, Geneva, 2005.
- 10 R. C. Kessler, K. A. McGonagle, S. Zhao, C. B. Nelson, M. Hughes M, S. Eshleman, H-U. Wittchen, K. S. Kendler, *Arch. Gen. Psychiat.*, 1994, **51**, 8-19.
- 11 *National Disability Survey 2006 - First Results*, Central Statistics Office, Government of Ireland, Dublin, 2008.
- 12 V. Patel, M. Abas, J. Broadhead, C. Todd, A. Reeler, *Brit. Med. J.*, 2001, **322**, 482-484.
- 13 *Culture and common mental disorders in Sub-Saharan Africa: Studies in primary care in Zimbabwe*, V. Patel, Psychology Press, Hove, UK, 1998.
- 14 V. Patel, *Lancet*, 1996, **347**, 742-744.
- 15 R. Gater, M. Tansella, A. Korten, B. G. Tiemens, V. G. Mavreas, M. O. Olatawura, *Arch. Gen. Psychiat.*, 1998, **55**, 405-413.
- 16 A. G. Bulloch, J. V. Williams, D. H. Lavorato, S. B. Patten, *Depress. Anxiety*, 2009, **26**, 1172-1177.
- 17 G. Thornicroft, O. Margolius and D. Jones, *Brit. J. Psychiat.*, 1992, **161**, 621-624.
- 18 D. D. Dunlop, J. Song, J. S. Lyons, L. M. Manheim, R. W. Chang, *Am. J. Public Health*, 2003, **93**, 1945-1952.
- 19 S. A. Riolo, T. A. Nguyen, J. F. Greden, C. A. King, *Am. J. Public Health*, 2005, **95**, 998-1000.
- 20 C. Duggan, P. Sham, C. Minne, A. Lee, R. Murray, *Brit. J. Psychiat.*, 1998, **173**, 527-530.
- 21 P.S. Wang, G. Simon, R. C. Kessler, *Int. J. Meth. Psych. Res.*, 2003, **12**, 22-33
- 22 J. P. Lepine, M. Gastpar, J. Mendlewicz, A. Tylee, *Int. Clin. Psychopharm.*, 1997, **12**, 19-29.
- 23 *Mental Health Global Action Programme. Close the gap, dare to care*, WHO Press,

References

- Geneva, 2002.
- 24 P. Berto, D. D'Ilario, R. Di Virgilio, F. Rizzo, *J. Ment. Health Policy*, 2000, **3**, 3-10.
- 25 B. Barraclough, *Soc. Sci. Med.*, 1972, **6**, 661-667.
- 26 G. Isacsson, *Acta Psychiat. Scand.*, 2000, **102**, 113-117.
- 27 J. A. Bridge, S. Iyengar, C. B. Salary, R. P. Barbe, B. Birmaher, H. A. Pincus, L. Ren, D. A. Brent, *JAMA-J. Am. Med. Assoc.*, 2007, **297**, 1683-1696.
- 28 C. B. Nemeroff, A. Kalali, M. D. Keller, D. S. Charney, S. E. Lenderts, E. F. Cascade, H. Stephenson, A. F. Schatzberg, *Arch. Gen. Psychiat.*, 2007, **64**, 466-472.
- 29 R. M. Hirschfeld, *J. Clin. Psychiat.*, 1999, **60**, 326-335.
- 30 *Of the Epidemics*, Hippocrates.
- 31 K. S. Kendler, M. C. Neale, R. C. Kessler, A. C. Heath, L. J. Eaves, *Brit. J. Psychiat.*, 1994, **165**, 66-72.
- 32 *On Airs, Waters, Places*, Hippocrates.
- 33 *The Canon of Medicine*, Avicenna.
- 34 *Summa Theologica*, Thomas of Aquinas.
- 35 *A history of psychiatry: from the era of the asylum to the age of Prozac*, Edward Shorter, Wiley and Sons, New York, U.S.A., 1997.
- 36 *Psychiatrie: Ein Lehrbuch für Studierende und Aerzte.*, 2nd Ed., Emil Kraepelin, Leipzig, Germany, 1899.
- 37 *Classification of Endogenous Psychoses and their Differentiated Etiology*, 2nd Ed., ed. Helmut Beckmann. Springer-Verlag, New York/Wien, U.S.A., 1999.
- 38 Adapted with permission from media available through Wikimedia Commons.
- 39 <http://www.rci.rutgers.edu/~uzwiak/NBSummer11/NBSummerLect2.html>.
- 40 R. Remie, R. P. Coppes, H. Meurs, A.F. Roffel, J. Zaagsma, *Brit. J. Pharmacol.*, 1990, **99**, 223-226.
- 41 R. Aldunate, J. C. Casar, E. Brandan, N. C. Inestrosa, *Brain Res. Rev.*, 2004, **47**, 96-104.
- 42 S. G. Hormuzdi, M. A. Filippov, G. Mitropoulou, H. Monyer, R. Bruzzone, *Biochim. Biophys. Acta*, 2004, **1662**, 113-137.
- 43 S. Hidaka, Y. Akahori, Y. Kurosawa, *J. Neurosci.*, 2004, **24**, 10553-10567.
- 44 P. E. Chen, M. T. Geballe, P. J. Stansfeld, A. R. Johnston, H. Yuan, A. L. Jacob, J. P. Snyder, S. F. Traynelis, *Mol. Pharmacol.*, 2005, **67**, 1470-1484.
- 45 A. Contractor, G. T. Swanson, *The Glutamate Receptors*, in *The Receptors*, 99-158, Humana Press, Totowa, U.S.A., 2008.
- 46 M. J. Bakker, J. G. van Dijk, A. M. J. M. van den Maagdenberg, M. A. J. Tijssen, *Lancet Neurol.*, 2006, **5**, 513-524.
- 47 *Neurotransmitters, Drugs and Brain Function*, ed. R. A. Webster, Wiley, Hoboken, U.S.A., 2001.

References

- 48 J. M. Gaillard, *Ann. Clin. Res.*, 1985, **17**, 175-184.
- 49 Y. M. Hickling, N. S. Cheung, J. A. Larm, M. S. Cowen, A. Shulkes, P. M. Beart, *Neurochem. Int.*, 1997, **30**, 171-179.
- 50 J. Y. Xie, D. S. Herman, C.-O. Stiller, L. R. Gardell, M. H. Ossipov, J. Lai, F. Porreca, T. W. Vanderah, *J. Neurosci.*, 2005, **25**, 409-416.
- 51 R. Leurs, P. Blandina, C. Tedford, H. Timmerman, *Trends Pharmacol. Sci.*, 1998, **19**, 177-184.
- 52 F. S. Wu, T. T. Gibbs, D. H. Farb, *Mol. Pharmacol.*, 1991, **40**, 333-336.
- 53 E. P. Monaghan, L. A. Navalta, L. Shum, D. W. Ashbrook, D. A. Lee, *Epilepsia*, 1997, **38**, 1026-1031.
- 54 A. Kalda, L. Yu, E. Oztas, J. F. Chen, *J. Neurol. Sci.*, 2006, **248**, 9-15.
- 55 F. X. Guix, I. Uribesalgo, M. Coma, F. J. Muñoz, *Prog. Neurobiol.*, 2005, **76**, 126-152.
- 56 S. F. Tzeng, H. Y. Hsiao, O. T. Mak, *Curr. Drug Targets - Inflamm. Allergy*, 2005, **4**, 335-340.
- 57 M. Berger, J. A. Gray, B. L. Roth, *Annu. Rev. Med.*, 2009, **60**, 355-366.
- 58 K. Shaw, J. Turner, C. Del Mar, *Cochrane Db. Syst. Rev.*, 2002, **1**, CD003198.
- 59 A. L. Schultz, *5-Hydroxyindoleacetic Acid*, in *Methods in Clinical Chemistry*, ed. A. J. Pesce, L. A. Kaplan, Mosby-Year Book Inc., St. Louis, U.S.A., 1987.
- 60 I. B. Hickie, N. L. Rogers, *Lancet*, 2011, **378**, 621-631.
- 61 R. Hardeland, *Curr. Neuropharmacol.*, 2010, **8**, 168-181.
- 62 J. Yamada, Y. Sugimoto, I. Kimura, N. Takeuchi, K. Horisaka, *Eur. J. Pharmacol.*, 1990, **181**, 319-322.
- 63 B. Borowsky, N. Adham, K. A. Jones, R. Raddatz, R. Artymyshyn, K. L. Ogozalek, M. M. Durkin, P. P. Lakhani, J. A. Bonini, S. Pathirana, N. Boyle, X. Pu, E. Kouranova, H. Lichtblau, F. Y. Ochoa, T. A. Branchek, C. Gerald, *P. Natl. Acad. Sci. USA.*, 2001, **31**, 8966-8971.
- 64 G. M. Miller, *J. Neurochem.*, 2011, **116**, 164-176.
- 65 J. J. Schildkraut, *Am. J. Psychiat.*, 1965, **122**, 509-522
- 66 W. E. Bunney, J. M. Davis, *Arch. Gen. Psychiat.*, 1965, **13**(6), 483-494
- 67 F. A. Whitlock, L. E. Evans, *Drugs*, 1978, **15**, 53-71.
- 68 A. Carlsson, H. Corrodi, K. Fuxe, T. Hokfelt, *Eur. J. Pharmacol.*, 1969, **5**, 357-373.
- 69 A. Glassman, *Psychosom. Med.*, 1969, **31**, 107-114
- 70 A. Caspi, K. Sugden, T. E. Moffitt, A. Taylor, I. W. Craig, H. Harrington, J. McClay, J. Mill, J. Martin, A. Braithwaite, R. Poulton, *Science*, 2003, **301**, 386-389.
- 71 C. Gross, X. Zhuang, K. Stark, S. Ramboz, R. Oosting, L. Kirby, L. Santarelli, S. Beck, R. Hen, *Nature*, 2002, **28**, 396-400.
- 72 D. J. Nutt, *J. Clin. Psychiat.*, 2008, **69**, 4-7.

References

- 73 M. J. Owens, *Depress. Anxiety*, 1998, **4**, 153-159.
- 74 G. R. Heninger, P. L. Delgado, D. S. Charney, *Pharmacopsychiatry*, 1996, **29**, 2-11.
- 75 T. Mennini, E. Mocaer, S. Garattini, *N-S Arch. Pharmacol.* 1987, **336**, 478-482.
- 76 P. Rakic, *Nat. Rev. Neurosci.*, 2002, **3**, 65-71.
- 77 R. M. Sapolsky, *P. Natl. Acad. Sci. USA*, 2001, **98**, 12320-12322.
- 78 G. Kempermann, G. Kronenberg, *Biol. Psychiat.*, 2003, **54**, 499-503.
- 79 R. M. Thomas, D. A. Peterson, *Mol. Interv.*, 2003, **3**, 441-444.
- 80 J. A. Siuciak, D. R. Lewis, S. J. Wiegand, R. M. Lindsay, *Pharmacol. Biochem. Be.*, 1997, **56**, 131-137.
- 81 M. Nibuya, S. Morinobu, R. S. Duman, *J. Neurosci.*, 1995, **15**, 7539-7547.
- 82 Y. Li, B. W. Luikart, S. Birnbaum, J. Chen, C. H. Kwon, S. G. Kernie, R. Bassel-Duby, L. F. Parada, *Neuron*, 2008, **59**, 399-412.
- 83 B. S. McEwen, S. Chattarji, D. M. Diamond, T. M. Jay, L. P. Reagan, P. Svenningsson, E. Fuchs, *Mol. Psychiatr.*, 2010, **15**, 237-249.
- 84 P. J. Lucassen, E. Fuchs, B. Czéh, *Biol. Psych.*, 2004, **55**, 789-796.
- 85 L. P. Reagan, R. M. Hendry, L. R. Reznikov, G. G. Piroli, G. E. Wood, B. S. McEwen, C. A. Grillo, *Eur. J. Pharmacol.*, 2007, **565**, 68-75.
- 86 M. H. Kole, L. Swan, E. Fuchs, *Eur. J. Neurosci.*, 2002, **16**, 807-816.
- 87 C. D'Sa, R. S. Duman, *Bipolar Disord.*, 2002, **4**, 183-194.
- 88 B. Leonard, *The Past, Present and Future of Antidepressants*, Werner Chemical Society Invited Lecture, Trinity College Dublin, 2010.
- 89 T. J. Connor, B. E. Leonard, *Life Sci.*, 1998, **62**, 583-606.
- 90 I. Hanin, *Nat. Med.*, 1996, **2**, 1307-1308.
- 91 C. C. Chao, S. Hu, K. Close, S. S. Choi, T. W. Molitor, W. J. Novick, P. K. Peterson, *J. Infect. Dis.*, 1992, **166**, 847-853.
- 92 N. Müller, A. M. Myint, M. J. Schwarz, *Dialogues Clin. Neurosci.*, 2009, **11**, 319-332.
- 93 O.J. Schiepers, M.C. Wichers, M. Maes, *Prog. Neuro-psychoph.*, 2005, **29**, 201-217.
- 94 M. Maes, M. Kubera, E. Obuchowiczwa, L. Goehler, J. Brzeszcz, *Neuroendocrinol. Lett.*, 2011, **32**, 7-24.
- 95 M. Maes, *Hum. Psychopharm. Clin.*, 2001, **16**, 95-103.
- 96 S. M. O'Brien, L. V. Scott, T. G. Dinan, *Hum. Psychopharm. Clin.*, 2004, **19**, 397-403.
- 97 J. L. Warner-Schmidt, K. E. Vanover, E. Y. Chen, J. J. Marshall, P. Greengard, *P. Natl. Acad. Sci USA*, 2011, **108**, 9262-9267.
- 98 H. Vargas-Perez, K. R. Ting-A, C. H. Walton, D. M. Hansen, R. Razavi, L. Clarke, M. R. Bufalino, D. W. Allison, S. C. Steffensen, D. van der Kooy, *Science*, 2009, **324**, 1732-1734.
- 99 A. F. Leuchter, I. A. Cook, L. B. Marangell, W. S. Gilmer, K. S. Burgoyne, R. H. Howland, M. H. Trivedi, S. Zisook, R. Jain, J. T. McCracken, M. Fava, D. Iosifescu,

References

- S. Greenwald, *Psychiat. Res.*, 2009, **169**, 124-131.
- 100 D. Healy, *The Antidepressant Drama*, in *The treatment of depression: bridging the 21st century*, Weissman MM., Arlington, U.S.A., 2001, pp. 10-11.
- 101 R. Kuhn, *Am. J. Psychiat.*, 1958, **115**, 459-464.
- 102 T. A. Ban, *J. Neural Transm.*, 2001, **108**, 707-716.
- 103 F. J. Ayd Jr., *Psychosomatics*, 1960, **1**, 320-325.
- 104 A. Frazer, *J. Clin. Psychopharm.*, 1997, **17**, 2S-18S.
- 105 A. D. Woolf, A. R. Erdman, L. S. Nelson, E. M. Caravati, D. J. Cobaugh, L. L. Booze, P. M. Wax, A. S. Manoguerra, E. J. Scharman, K. R. Olson, P. A. Chyka, G. Christianson, W. G. Troutman, *Clin. Toxicol. (Phila.)*, 2007, **45**, 203-233.
- 106 A. Carlsson, M. Linqvist, *J. Pharm. Pharmacol.*, 1969, **21**, 460-464.
- 107 *Let them eat Prozac*, D. Healy, NYU Press, New York, U.S.A., 2004.
- 108 A. L. Iversen, *Neuroscience and drug development*, in *The Psychopharmacologists*, D. Healy, Arnold, London, U.K., 1998.
- 109 Y. G. Ni, R. Miledi, *P. Natl. Acad. Sci. U.S.A.*, 1997, **94**, 2036-2040.
- 110 *Manufacturer's Patient Information Leaflet*, Fluoxetine Capsules, Actavis UK Ltd., 2007.
- 111 S. Kasper, C. Spadone, P. Verpillat, J. Angst, *Int. Clin. Psychopharm.*, 2006, **21**, 105-110.
- 112 G. I. Papakostas, M. E. Thase, M. Fava, J. C. Nelson, R. C. Shelton, *Biol. Psychiat.*, 2007, **62**, 1217-1227.
- 113 M. Bartholow, *Top 200 Prescription Drugs of 2009*, in *Pharmacy Times*, Intellisphere LLC, Plainsboro, U.S.A, 2010.
- 114 A. Rubino, N. Roskell, P. Tennis, D. Mines, S. Weich, E. Andrews, *Brit. Med. J.*, 2007, **334**, 242-245.
- 115 M. Fava, R. Mulroy, J. Alpert, A. A. Nierenberg, J. F. Rosenbaum, *Am. J. Psychiat.*, 1997, **154**, 1760-1762.
- 116 *Wo. Pat.*, 072 608, 2006.
- 117 D. K. Vassilatis, J. G. Hohmann, H. Zeng, F. Li, J. E. Ranchalis, M. T. Mortrud, A. Brown, S. S. Rodriguez, J. R. Weller, A. C. Wright, J. E. Bergmann, G. A. Gaitanaris, *P. Natl. Acad. Sci. USA*, 2003, **100**, 4903-4908.
- 118 J. O. Ruuskanen, H. Xhaard, A. Marjamäki, E. Salaneck, T. Salminen, Y. L. Yan, J. H. Postlethwait, M. S. Johnson, D. Larhammar, M. Scheinin, *Mol. Biol. Evol.*, 2004, **21**, 14-28.
- 119 R. Aantaa, A. Marjamaeki, M. Scheinin, *Ann. Med.*, 1995, **27**, 439-449.
- 120 M. Raiteri, G. Bonanno, G. Maura, M. Pende, G. C. Andrioli, A. Ruelle, *Brit. J. Pharmacol.*, 1992, **107**, 1146-1151.
- 121 L. F. Callado, J. J. Meana, B. Grijalba, A. Pazos, M. Sastre, J. A. García-Sevilla, *J. Neurochem.*, 1998, **70**, 1114-1123.

References

- 122 M. Philipp, M. Brede, L. Hein, *Am. J. Physiol.-Reg. I.*, 2002, **283**, R287-R295.
- 123 E. MacDonald, B. K. Kobilka, M. Scheinin, *Trends Pharmacol. Sci.*, 1997, **18**, 211-219.
- 124 K. Gyires, Z. S. Zádori, T. Török, P. Mátyus, *Neurochem. Int.*, 2009, **55**, 447-453.
- 125 S. G. Rasmussen, H. J. Choi, D. M. Rosenbaum, T. S. Kobilka, F. S. Thian, P. C. Edwards, M. Burghammer, V. R. Ratnala, R. Sanishvili, R. F. Fischetti, G. F. Schertler, W. I. Weis, B. K. Kobilka, *Nature*, 2007, **450**, 383-387.
- 126 U. Gether, *Endocr. Rev.*, 2000, **21**, 90-113.
- 127 S. F. Altschul, W. Gish, W. Miller, E. W. Myers, D. J. Lipman, *J. Mol. Biol.*, 1990, **215**, 403-410.
- 128 M. A. Hanson, V. Cherezov, M. T. Griffith, C. B. Roth, V. P. Jaakola, E. Y. Chien, J. Velasquez, P. Kuhn, R. C. Stevens, *Structure*, 2008, **16**, 897-905.
- 129 C. D. Wang, M. A. Buck, C. M. Fraser, *Mol. Pharmacol.*, 1991, **40**, 168-179.
- 130 F. Gentili, F. Ghelfi, M. Giannella, A. Piergentili, M. Pignini, W. Quaglia, C. Vesprini, P. A. Crassous, H. Paris, A. Carrieri, *J. Med. Chem.*, 2004, **47**, 6160-6173.
- 131 J. M. Peltonen, T. Nyronen, S. Wurster, M. Pihlavisto, A. M. Hoffren, A. Marjamaki, H. Xhaard, L. Kanerva, J. M. Savola, M. S. Johnson, *Brit. J. Pharmacol.*, 2003, **140**, 347-358.
- 132 J. P. Hieble, A. Hehr, Y. O. Li, R. R. Robert Jr., *P. W. Pharmacol. Soc.*, 1998, **41**, 225-228.
- 133 A. U. Trendelenburg, M. Philipp, A. Meyer, W. Klebroff, L. Hein, K. Starke, *N-S Arch. Pharmacol.*, 2003 **368**, 504-12.
- 134 A. M. González, J. Pascual, J. J. Meana, F. Barturen, C. del Arco, A. Pazos, *J. Neurochem.*, 1994, **63**, 256-265.
- 135 R. W. Invernizzi, S. Garattini, *Prog. Neuro-Psychoph.*, 2004, **28**, 819-827.
- 136 A. Jäättelä, *Brit. J. Clin. Pharmacol.*, 1980, **10**, 67S-70S.
- 137 Goodlet I., S. E. Mireylees, M. F. Sugrue, *Brit. J. Pharmacol.*, 1977, **61**, 307-313.
- 138 N. Kakui, F. Yokoyama, M. Yamauchi, K. Kitamura, T. Imanishi, T. Inoue, T. Koyama, *Pharmacol. Biochem. Be.*, 2009, **92**, 393-398.
- 139 A.F.T. Arnsten, J.X. Cai, *Neurobiol. Aging*, 1993, **14**, 597-603.
- 140 H-T. Zhang, L. R Whisler, Y. Huang, Y. Xiang, J. M. O'Donnell, *Neuropsychopharmacol.*, 2009, **34**, 1067-1077.
- 141 M. Bourin, M. Poncelet, R. Chermat, P. Simon, *Arznei.-Forschung*, 1983, **33**, 1173-1176.
- 142 *The Antidepressant Era*, D. Healy, Harvard University Press, London, U.K., 1998.
- 143 R. D. Robson, M. J. Antonaccio, J. K. Saelens, J. Liebman, *Eur. J. Pharmacol.*, 1978, **47**, 431-442.
- 144 K. Yamada, T. Furukawa, *Folia Pharmacol. Jpn.*, 1991, **97**, 31-39.
- 145 P. Mayer, T. Imbert, *iDrugs*, 2001, **4**, 662-676.

References

- 146 E. H. Kang, I. S. Lee, S. K. Chung, S. Y. Lee, E. J. Kim, J. P. Hong, K. S. Oh, J. M. Woo, S. Kim, J. E. Park, B. H. Yu, *Psychiat. Res.*, 2009, 30, **169**, 118-123.
- 147 S. A. Anttila, E. V. Leinonen, *CNS Drug Rev.*, 2001, **7**, 249-264.
- 148 J. D. Guelfi, M. Ansseau, L. Timmerman, S. Kørsgaard, *J. Clin. Psychopharm.* 2001, **21**, 425-431.
- 149 M. Versiani, R. Moreno, C. J. Ramakers-van Moorsel, A. J. Schutte, *CNS Drugs*, 2005, **19**, 137-146.
- 150 M. J. Millan, A. Newman-Tancredi, V. Audinot, *Synapse*, 2000, **35**, 79-95.
- 151 M. M'Harzi, F. Willig, C. Bardelay, A. M. Palou, C. Oberlander, *Pharmacol. Biochem. Behav.*, 1997, **56**, 649-655.
- 152 A. A. Cordi, M. P. Snyers, D. Giraud-Mangin, C. Van der Maesen, J. P. Van Hoeck, S. Beuze, E. Ellens, F. Naporá, C. L. Gillet, H. Gorissen, P. Calderon, M. D. Remacle, P. J. de Varebeke, W. Van Dorsser, J. Roba, *Eur. J. Med. Chem.*, 1990, **25**, 557-568.
- 153 A. Cordi, I. Berque-Bestel, T. Persigand, J. M. Lacoste, A. Newman-Tancredi, V. Audinot, M. J. Millan, *J. Med. Chem.*, 2001, **44**, 787-805.
- 154 C. B. Chapleo, P. L. Myers, R. C. Butler, J. C. Doxey, A. G. Roach, C. F. Smith, *J. Med. Chem.*, 1983, **26**, 823-831.
- 155 J. C. Doxey, A. G. Roach, D. A. Strachan, N. K. Virdee, *Brit. J. Pharmacol.*, 1984, **83**, 713-722.
- 156 C. A. Halliday, B. J. Jones, M. Skingle, D. M. Walsh, H. Wise, M. B. Tyres, *Brit. J. Pharmacol.*, 1991, **102**, 887-895.
- 157 P. Mayer, P. Brunel, P. Pauwels, M. Marien, T. Imbert, *Intl. Symp. Med. Chem. Neurodegen. Dis.*, 1997, **3**, Poster 9. See also Reference 145.
- 158 F. Rodriguez, I. Rozas, J. E. Ortega, J. J. Meana, L. F. Callado, *J. Med. Chem.*, 2007, **50**, 4516-4527.
- 159 F. Rodriguez, I. Rozas, J. E. Ortega, A. M. Erdozain, J. J. Meana, L. F. Callado, *J. Med. Chem.*, 2008, **51**, 3304-3312.
- 160 F. Rodriguez, I. Rozas, J. E. Ortega, A. M. Erdozain, J. J. Meana, L. F. Callado, *J. Med. Chem.*, 2009, **52**, 601-609.
- 161 L. Steru, R. Chermat, B. Thierry, P. Simon, *Psychopharmacology*, 1985, **85**, 367-370.
- 162 T. A. Halgren, *J. Comput. Chem.*, 1996, **17**, 490-519.
- 163 R. R. Mittal, L. Harris, R. A. McKinnon, M. J. Sorch, *J. Chem. Inf. Model.*, 2009, **49**, 704-709.
- 164 J. E. Lennard-Jones, *P. Roy. Soc. Lond. A.*, 1924, **106**, 463-477.
- 165 H. Kubinyi, *Drug Discov. Today*, 1997, **2**, 457-467.
- 166 M. Haenlein, A. M. Kaplan, *Understanding Statistics*, 2004, **3**, 283-297.
- 167 A. K. Gupta, A. K. Saxena, *Med. Chem. Res.*, 2010, in press, DOI: 10.1007/s00044-010-9379-1.
- 168 A. Nowaczyk, K. Kulig, B. Malawska, *QSAR Comb. Sci.*, 2009, **28**, 979-988.

References

- 169 K. Jozwiak, A. Yiu-Ho Woo, M. J. Tanga, L. Toll, L. Jimenez, J. A. Kozocas, A. Plazinska, R-P. Xiao, I. W. Wainer, *Bioorgan. Med. Chem.*, 2010, **18**, 728-736.
- 170 G. L. Grunewald, V. H. Dahanukar, R. K. Jalluri, K. R. Criscione, *J. Med. Chem.*, 1999, **42**, 118-134.
- 171 G. L. Grunewald, T. M. Caldwell, Q. Li, V. H. Dahanukar, B. McNeil, K. R. Criscione, *J. Med. Chem.*, 1999, **42**, 4351-4361.
- 172 G. L. Grunewald, T. M. Caldwell, V. H. Dahanukar, R. K. Jalluri, K. R. Criscione, *Bioorg. Med. Chem. Lett.*, 1999, **9**, 481-486.
- 173 Laboratory of Prof. J. J. Meana and Dr. L. F. Callado, Department of Pharmacology, University of the Basque Country, *Leioa*, Bizkaia, Spain.
- 174 M. Clark, R. D. Cramer III, N. Van Opdenbosch, *J. Comput. Chem.*, 1989, **10**, 982-1012.
- 175 The SYBYL 8.0 molecular modelling environment is available from Tripos Inc., 1699 S. Hanley Road, St. Louis, MO 63144-2913.
- 176 P. R. Andrews, D. J. Craik, J. L. Martin, *J. Med. Chem.*, 1984, **27**, 1648-1657.
- 177 C. Abad-Zapateroa, J. T. Metza, *Drug Discov. Today*, 2005, **10**, 464-469.
- 178 C. H. Reynolds, B. A. Tounge, S. D. Bembenek, *J. Med. Chem.*, 2008, **51**, 2432-2438.
- 179 A. D. Harpalani, S. W. Snyder, B. Subramanyam, M. J. Egorin, P. S. Callery, *Cancer Res.*, 1993, **53**, 766-771.
- 180 R. Morphy, *J. Med. Chem.*, 2006, **49**, 2969-2978.
- 181 E. Malta, J. S. Ong, C. Raper, P. E. Tawa, G. N. Vaughan, *Brit. J. Pharmacol.*, 1980, **69**, 679-688.
- 182 M. J. Millan, A. Newman-Tancredi, V. Audinot, D. Cussac, F. Lejeune, J. P. Nicolas, F. Cogé, J. P. Galizzi, J. A. Boutin, J. M. Rivet, A. Dekeyne, A. Gobert, *Synapse*, 2000, **35**, 79-95.
- 183 H. Xhaard, T. Nyrönen, V. V. Rantanen, J. O. Ruuskanen, J. Laurila, T. Salminen, M. Scheinin, M. S. Johnson, *J. Struct. Biol.*, 2005, **150**, 126-143.
- 184 For a recent description of anion- π interactions, see: D. Quiñonero, C. Garau, C. Rotger, A. Frontera, P. Ballester, A. Costa, P. M. Deyà, *Angew. Chem. Intl. Ed.*, 2002, **41**, 3389-3392.
- 185 G. Ambady, G. Kartha, *J. Chem. Crystallogr.*, 1973, **3**, 37-45.
- 186 *US pat.*, 049 63563, 1990.
- 187 J. I. Andrés, J. Alcázar, J. M. Alonso, R. M. Alvarez, J. M. Cid, A. I. De Lucas, J. Fernández, S. Martínez, C. Nieto, J. Pastor, M. H. Bakker, I. Biesmans, L. I. Heylen, A. A. Megens, *Bioorg. Med. Chem. Lett.*, 2003, **13**, 2719-2725.
- 188 J. M. Caroon, R. D. Clark, A. F. Kluge, R. Olah, D. B. Repke, S. H. Unger, A. D. Michel, R. L. Whiting, *J. Med. Chem.*, 1982, **25**, 666-670.
- 189 S.A. Munk, D. Harcourt, P. Arasasingham, C. Gluchowski, H. Wong, J. Burke, A. Kharlamb, C. Manlapaz, E. Padillo, L. Williams, L. Wheeler, M. Garst, *Bioorg. Med. Chem. Lett.*, 1995, **5**, 1745-1750.

References

- 190 R. D. Cramer III, *J. Comput. Aid. Mol. Des.*, 2011, **25**, 197-201.
- 191 R. D. Clark, *J. Comput. Aid. Mol. Des.*, 2007, **22**, 507-521.
- 192 A. Vedani, M. Dobler, in *Progress in Drug Research.*, Birkhäuser Basel, Switzerland, 2000, **55**, pp. 105-135.
- 193 J. Ortega, J. J. Meana, L. F. Callado, F. Rodriguez, I. Rozas, unpublished work, 2011.
- 194 K. S. Kim, L. Qian, *Tetrahedron Lett.*, 1993, **34**, 7677-7680.
- 195 C. Dardonville, P. Goya, I. Rozas, A. Alsasua, I. Martín, J. Borrego, *Bioorgan. Med. Chem.*, 2000, **8**, 1567-1577.
- 196 V. Cody, G. T. DeTitta, *J. Cryst. Mol. Struct.*, 1980, **9**, 33-43.
- 197 B. Kelly, D. H. O' Donovan, J. O' Brien, F. Blanco, I Rozas, *J. Org. Chem.*, 2011, submitted.
- 198 S. Cunha, M. T. Rodrigues Jr., C. C. da Silva, H. B. Napolitano, I. Vencato, C. Lariucci, *Tetrahedron*, 2005, **61**, 10536-10540.
- 199 K. Wermann, M. Walther, W. Günther, H. Görls, E. Anders, *Tetrahedron*, 2005, **61**, 673-685.
- 200 T. S. Lobana, R. Sharma, R. Sharma, R. Sultana, R. J. Butcher, *Z. Anorg. Allg. Chem.*, 2008, **634**, 718-723.
- 201 A. C. Hiremath, A. S. R. Murthy, *Indian J. Chem. A.*, 1977, **15**, 55-56.
- 202 D. Castagnolo, S. Schenone, M. Botta, *Chem. Rev.*, 2011, in press, DOI: 10.1021/cr100423x.
- 203 M.A. Poss, E. Iwanowicz, J.A. Reid, J. Lin, Z. Gu, *Tetrahedron Lett.*, 1992, **33**, 5933-5936.
- 204 At the time of writing, Kim and Qian's paper has 156 citations, while the paper of Poss and Iwanowicz has 102.
- 205 M. Cortes-Salva, B-L. Nguyen, C. Javier, K. R. Pennypacker, J. C. Antilla, *Org. Lett.*, 2010, **12**, 1316-1319.
- 206 C. W. Zapf, C. J. Creighton, M. Tomioka, M. Goodman, *Org. Lett.*, 2001, **3**, 1133-1136.
- 207 Y. Wang, D. R. Sauer, S. W. Djuric, *Tetrahedron Lett.*, 2009, **50**, 5145-5148.
- 208 B. R. Linton, A. J. Carr, B. P. Orner, A. D. Hamilton, *J. Org. Chem.*, 2000, **65**, 1566-1568.
- 209 S-Ethyl chlorothioformate costs 122.50 euro per 5 gram quantity at the time of writing. *Source*: <http://www.sigmaaldrich.com>.
- 210 D. H. O'Donovan, I. Rozas, *Tetrahedron Lett.*, 2011, **52**, 4117-4119.
- 211 B. Yin, Z. Liu, M. Yi, J. Zhang, *Tetrahedron Lett.*, 2008, **49**, 3687-3690.
- 212 B. Yin, Z. Liu, J. Zhang, Z. Li, *Synthesis*, 2010, **6**, 991-999.
- 213 *N,N'*-bis-Boc-thiourea costs 394.50 euro per 5 gram quantity at the time of writing. *Source*: <http://www.sigmaaldrich.com>.
- 214 *Handbook of Heterocyclic Chemistry*, 2nd Ed., A. R. Katritzky and A. F. Pozharskii,

References

- 2000, Elsevier Science, Oxford, U.K.
- 215 M. R. Barvian, H. D. H. Showalter, A. M. Doherty, *Tetrahedron Lett.*, 1997, **38**, 6799–6802.
- 216 Modelled using Gaussian03, 6-31+G** basis set, zero imaginary frequencies recorded. Gaussian03: M. J. Frisch, G. W. Trucks, H. B. Schlegel, G. E. Scuseria, M. A. Robb, J. R. Cheeseman, J. A. Montgomery, T. Vreven, K. N. Kudin, J. C. Burant, J. M. Millam, S. S. Iyengar, J. Tomasi, V. Barone, B. Mennucci, M. Cossi, G. Scalmani, N. Rega, G. A. Petersson, H. Nakatsuji, M. Hada, M. Ehara, K. Toyota, R. Fukuda, J. Hasegawa, M. Ishida, T. Nakajima, Y. Honda, O. Kitao, H. Nakai, M. Klene, X. Li, J. E. Knox, H. P. Hratchian, J. B. Cross, V. Bakken, C. Adamo, J. Jaramillo, R. Gomperts, R. E. Stratmann, O. Yazyev, A. J. Austin, R. Cammi, C. Pomelli, J. W. Ochterski, P. Y. Ayala, K. Morokuma, G. A. Voth, P. Salvador, J. J. Dannenberg, V. G. Zakrzewski, S. Dapprich, A. D. Daniels, M. C. Strain, O. Farkas, D. K. Malick, A. D. Rabuck, K. Raghavachari, J. B. Foresman, J. V. Ortiz, Q. Cui, A. G. Baboul, S. Clifford, J. Cioslowski, B. B. Stefanov, G. Liu, A. Liashenko, P. Piskorz, I. Komaromi, R. L. Martin, D. J. Fox, T. Keith, M. A. Al-Laham, C. Y. Peng, A. Nanayakkara, M. Challacombe, P. M. W. Gill, B. Johnson, W. Chen, M. W. Wong, C. Gonzalez, J. A. Pople, Gaussian-03 ed.; Gaussian, Inc.: Wallingford CT, **2003**.
- 217 B. Adcock, A. Lawson, D. H. Miles, *J. Chem. Soc.*, 1961, 5120-5127.
- 218 B. Adcock, A. Lawson, *J. Chem. Soc.*, 1965, 474-479.
- 219 N. Neureiter, *J. Org. Chem.*, 1959, **24**, 2044–2046.
- 220 W. M. Kan, S.-H. Lin, C.-Y. Chern, *Synthetic Commun.*, 2005, **35**, 2633-2639.
- 221 S. Servi, M. Genc, *Synthetic Commun.*, 2007, **37**, 3173–3179.
- 222 F.-L. Hsu, A. Hamada, M. E. Booher, P. N. Patil, D. D. Miller, *J. Med. Chem.*, 1980, **23**, 1232-1235.
- 223 D. Huber, G. Leclerc, J.D. Ehrhardt, G. Andermann, *Tetrahedron Lett.*, 1987, **28**, 6453-6456.
- 224 D. Huber, J. D. Ehrhardt, N. Decker, J. Himber, G. Andermann, G. Leclerc, *J. Med. Chem.*, 1991, **34**, 3197-3204.
- 225 Y. T. Jeon, C. Luo, C. Forray, P. J.-J. Vaysse, T. A. Brancheck, C. Gluchowski, *Bioorg. Med. Chem. Lett.*, 1995, **5**, 2255-2258.
- 226 A. P. Treder, R. Andruszkiewicz, W. Zgoda, A. Walkowiak, C. Ford, A. L. Hudson, *Bioorgan. Med. Chem.*, 2011, **19**, 156-167.
- 227 D. J. Reis, S. Regunathan, *Trends Pharmacol. Sci.*, 2000, **21**, 187-193.
- 228 S. Reyes, K. Burgess, *J. Org. Chem.*, 2006, **71**, 2507-2509.
- 229 *Wo. Pat.*, 041 048, 2007.
- 230 T. B. Johnson, B. H. Nicolet, *J. Am. Chem. Soc.*, 1911, **33**, 1973–1978.
- 231 B. M. Duggan, R. L. Laslett, J. F. K. Wilshire, *Aust. J. Chem.*, 1996, **49**, 541-550.
- 232 C. Quirosa-Guillou, D. Z. Renko, C. Thal, *Tetrahedron*, 1992, **48**, 6385-6392.
- 233 J.-D. Zhou, F. Cao, H.-L. Wu, P. Wei, *Chinese J. Org. Chem.*, 2008, **28**, 228-233.

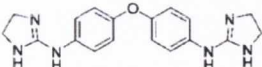
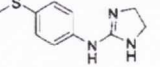
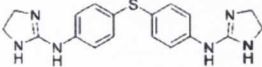
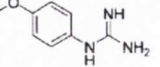
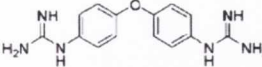
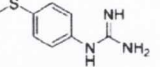
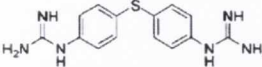
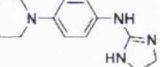
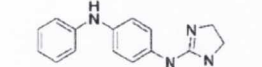
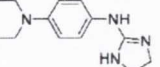
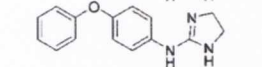
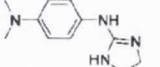
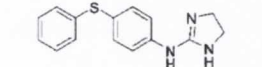
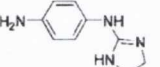
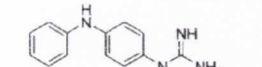
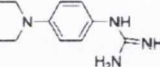
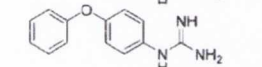
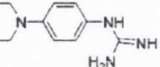
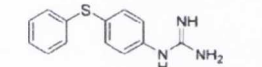
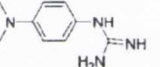
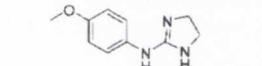
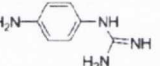
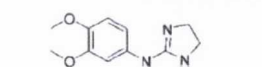
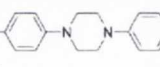

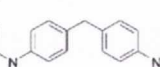
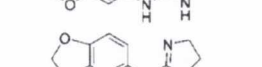
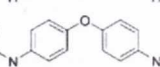
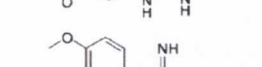
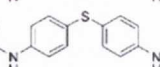
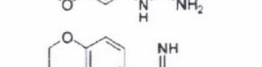
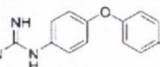
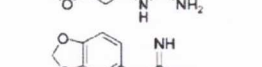
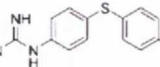
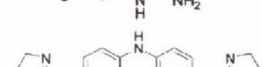
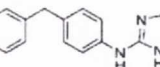
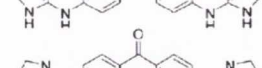
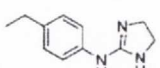
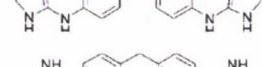
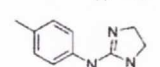
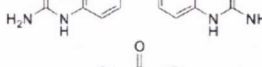
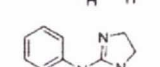
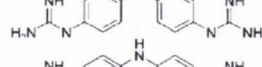
References

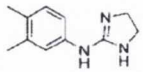
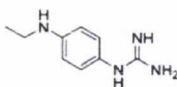
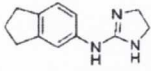
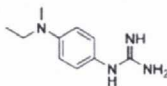
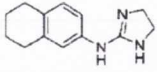
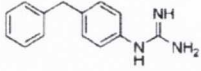
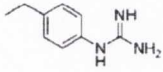
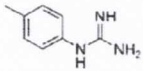
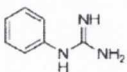
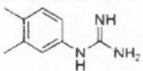
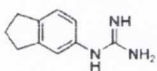
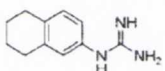
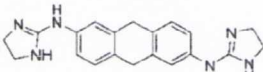
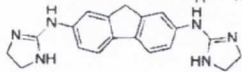
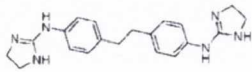
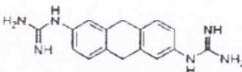
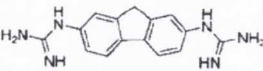
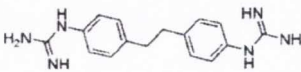
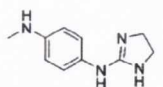
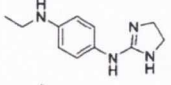
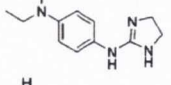
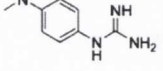
- 234 H. C. Brown, Y. M. Choi, S. Narasimhan, *J. Org. Chem.*, 1982, **47**, 3153-3163.
- 235 Z. D. Wang, S. O. Sheikh, Y. Zhang, *Molecules*, 2006, **11**, 739-750.
- 236 L. M. Sweeting, D. C. Crans, G. M. Whitesides, *J. Org. Chem.*, 1987, **52**, 2273-2276.
- 237 T. J. Wenzel, J. M. Ciak, in *Encyclopedia of Reagents for Organic Synthesis*, Wiley, 2001.
- 238 J. A. Dale, D. L. Dull, H. S. Mosher, *J. Org. Chem.*, 1969, **34**, 2543-2549.
- 239 2-(2-furyl)glycine costs 67.20 euro per 50 milligram quantity at the time of writing. *Source*: <http://www.sigmaaldrich.com>.
- 240 *Wo. Pat.*, 062 890, 2006.
- 241 H. Hiemstra, H. Wynberg, *J. Am. Chem. Soc.*, 1981, **103**, 417-430.
- 242 P. R. Schreiner, A. Wittkopp, *Org. Lett.*, 2002, **4**, 217-220.
- 243 B. Vakulya, S. Varga, A. Csámpai, T. Soós, *Org. Lett.*, 2005, **7**, 1967-1969.
- 244 S. H. McCooey, S. J. Connon, *Angew. Chem. Intl. Ed.*, 2005, **44**, 6367-6370.
- 245 X. Lu, L. Deng, *Angew. Chem. Intl. Ed.*, 2008, **47**, 7710-7713.
- 246 The authors are immensely grateful to the laboratory of Prof. S. J. Connon for their assistance in these studies; in particular thanks must be given to Cormac Quigley for carrying out several test reactions and providing many key insights into the reaction; to Oliver Gleeson for a sample of 9-*epi*-DHQT, and to Sean Tallon for providing a sample of the squaramide catalysts.
- 247 L. Wang, S. Shirakawa, K. Maruoka, *Angew. Chem. Intl. Ed.*, 2011, **50**, 5327-5330.
- 248 E. Costa, S. Garattini, L. Valzelli, *Experientia*, 1960, **16**, 461-463.
- 249 R. D. Porsolt, A. Bertin, M. Jalfre, *Arch. Int. Pharmacod. T.*, 1977, **229**, 327-336.
- 250 B. Petit-Demouliere, F. Chenu, M. Bourin, *Psychopharmacology*, 2005, **177**, 245-255.
- 251 A. P. Davenport, F. D. Russell, *Radioligand binding assays: theory and practice*, in *Current Directions in Radiopharmaceutical Research*, Ed. S.J. Mather, Kluwer Academic Publishers, Dordrecht, The Netherlands, 1996, pp. 169-179.
- 252 Y.-C. Cheng, W. H. Prusoff, *Biochem. Pharmacol.*, 1973, **22**, 3099-3108.
- 253 For a review of [³⁵S]GTPγS binding assays, see: C. Harrison and J. R. Traynor, *Life Sci.*, 2003, **74**, 489-508.
- 254 J. Gonzalez-Maeso, R. Rodriguez-Puertas, A. M. Gabilondo, J. J. Meana, *Eur. J. Pharmacol.*, 2000, **390**, 25-36.
- 255 H. Benveniste, P.C. Hüttemeier, *Prog. Neurobiol.*, 1990, **35**, 195-215.
- 256 C. E. Beyer, S. Boikess, B. Luo, L. A. Dawson, *J. Psychopharmacol.*, 2002, **16**, 297-304.
- 257 We are very thankful to the laboratory of Prof. Callado of the Universidad del Pais Vasco (Leioa, Spain) for their collaboration in performing these pharmacological studies, particularly to Carolina Muguruza Millan who carried out the majority of these experiments.

References

- 258 W. Kiemstedt, W. Sundermeyer, *Chem. Ber.*, 1982, **115**, 919-925.
- 259 Y. Sun, *Heterocycl. Commun.*, 2006, **12**, 25-28.
- 260 F. A. Csonka, B. H. Nicolet, *J. Biol. Chem.*, 1932, **99**, 213-216.
- 261 M. Jackman, *J. Am. Chem. Soc.*, 1948, **70**, 2884-2886.
- 262 Y. Robbe, *Eur. J. Med. Chem.*, 1982, **17**, 235-243.
- 263 P. Knochel, *Synthesis*, 1982, **12**, 1017-1018.
- 264 R. Sulsky, *Tetrahedron Lett.*, 1989, **30**, 31-34.
- 265 *Wo. Pat.*, 042 928 (A2), 2008.
- 266 M. L. Canle, W. Clegg, I. Demirtas, M. R. J. Elsegood, J. Haider, H. Maskill, P. C. Miatt, *J. Chem. Soc., Perk. T. 2*, 2001, **2**, 1742-1747.

Table A.1 α_2 -AR pK_i values of compounds described in our previous publications^a

| Structure | pK _i | Reference ^a | Structure | pK _i | Reference ^a |
|---|-----------------|------------------------|---|-----------------|------------------------|
|  | 7.00 | 158 |  | 7.07 | 158 |
|  | 7.74 | 158 |  | 6.39 | 158 |
|  | 5.78 | 158 |  | 6.40 | 158 |
|  | 6.57 | 158 |  | 5.93 | 158 |
|  | 6.56 | 158 |  | 7.09 | 158 |
|  | 6.58 | 158 |  | 7.42 | 158 |
|  | 6.62 | 158 |  | 6.92 | 158 |
|  | 6.83 | 158 |  | 5.52 | 158 |
|  | 6.05 | 158 |  | 6.34 | 158 |
|  | 6.30 | 158 |  | 7.06 | 158 |
|  | 7.77 | 158 |  | 5.58 | 158 |
|  | 6.66 | 158 |  | 5.97 | 158 |
|  | 7.85 | 158 |  | 8.80 | 158 |
|  | 7.33 | 158 |  | 7.00 | 158 |
|  | 5.84 | 158 |  | 7.74 | 158 |
|  | 8.21 | 158 |  | 5.78 | 158 |
|  | 6.40 | 158 |  | 5.97 | 158 |
|  | 7.24 | 158 |  | 6.85 | 159 |
|  | 5.80 | 158 |  | 6.68 | 159 |
|  | 6.38 | 158 |  | 7.82 | 159 |
|  | 5.20 | 158 |  | 6.48 | 159 |
|  | 6.00 | 158 | | | |

| Structure | pK _i | Reference ^a | Structure | pK _i | Reference ^a |
|---|-----------------|------------------------|--|-----------------|------------------------|
|  | 7.68 | 159 |  | 6.58 | 160 |
|  | 8.26 | 159 |  | 7.12 | 160 |
|  | 8.26 | 159 | | | |
|  | 5.55 | 159 | | | |
|  | 6.41 | 159 | | | |
|  | 6.53 | 159 | | | |
|  | 6.19 | 159 | | | |
|  | 7.12 | 159 | | | |
|  | 6.51 | 159 | | | |
|  | 7.11 | 159 | | | |
|  | 7.58 | 159 | | | |
|  | 6.32 | 159 | | | |
|  | 7.02 | 159 | | | |
|  | 7.96 | 159 | | | |
|  | 6.12 | 159 | | | |
|  | 5.88 | 159 | | | |
|  | 7.27 | 160 | | | |
|  | 6.75 | 160 | | | |
|  | 7.38 | 160 | | | |
|  | 6.95 | 160 | | | |

^aSee references 158, 159 and 160 in this text.

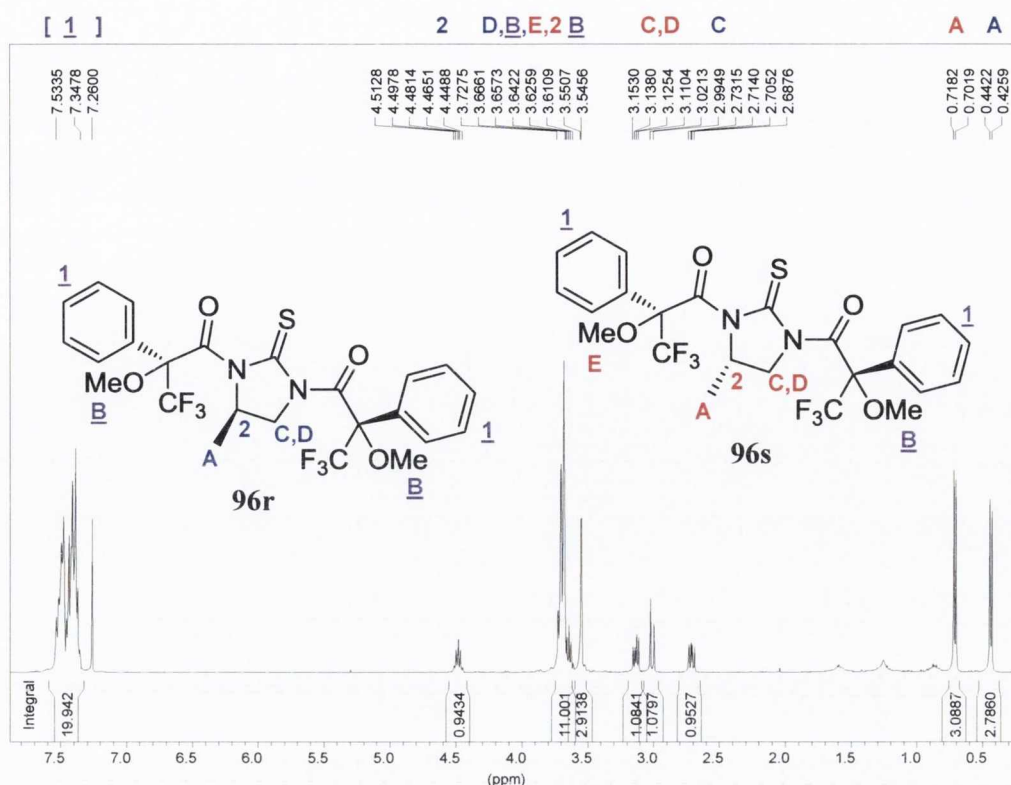


Fig. B.1. ^1H NMR spectrum of the diastereomeric mixture **96s** and **96r** in CDCl_3 (600 MHz). Signals corresponding to **96r** and **96s** are labelled in blue and red, respectively; signals which could not be definitively assigned are underlined and labelled in purple.

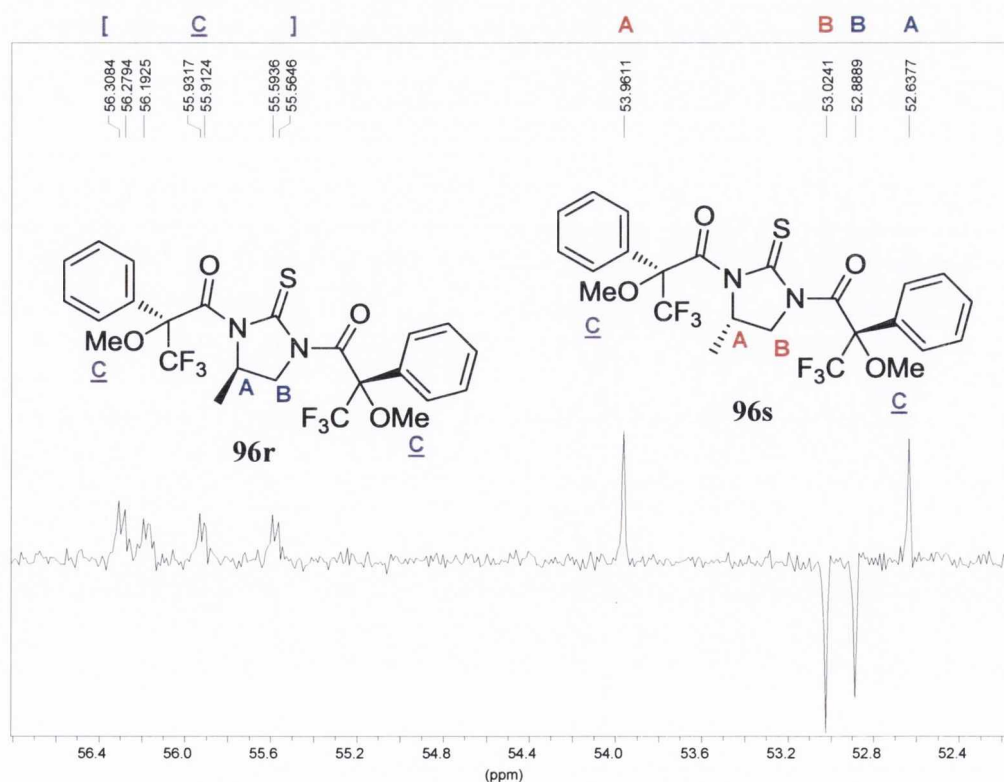


Fig. B.2. Partial DEPT-135 spectrum of **96s** and **96r** in CDCl_3 (150 MHz). The labelling scheme is as per Fig. B.1.